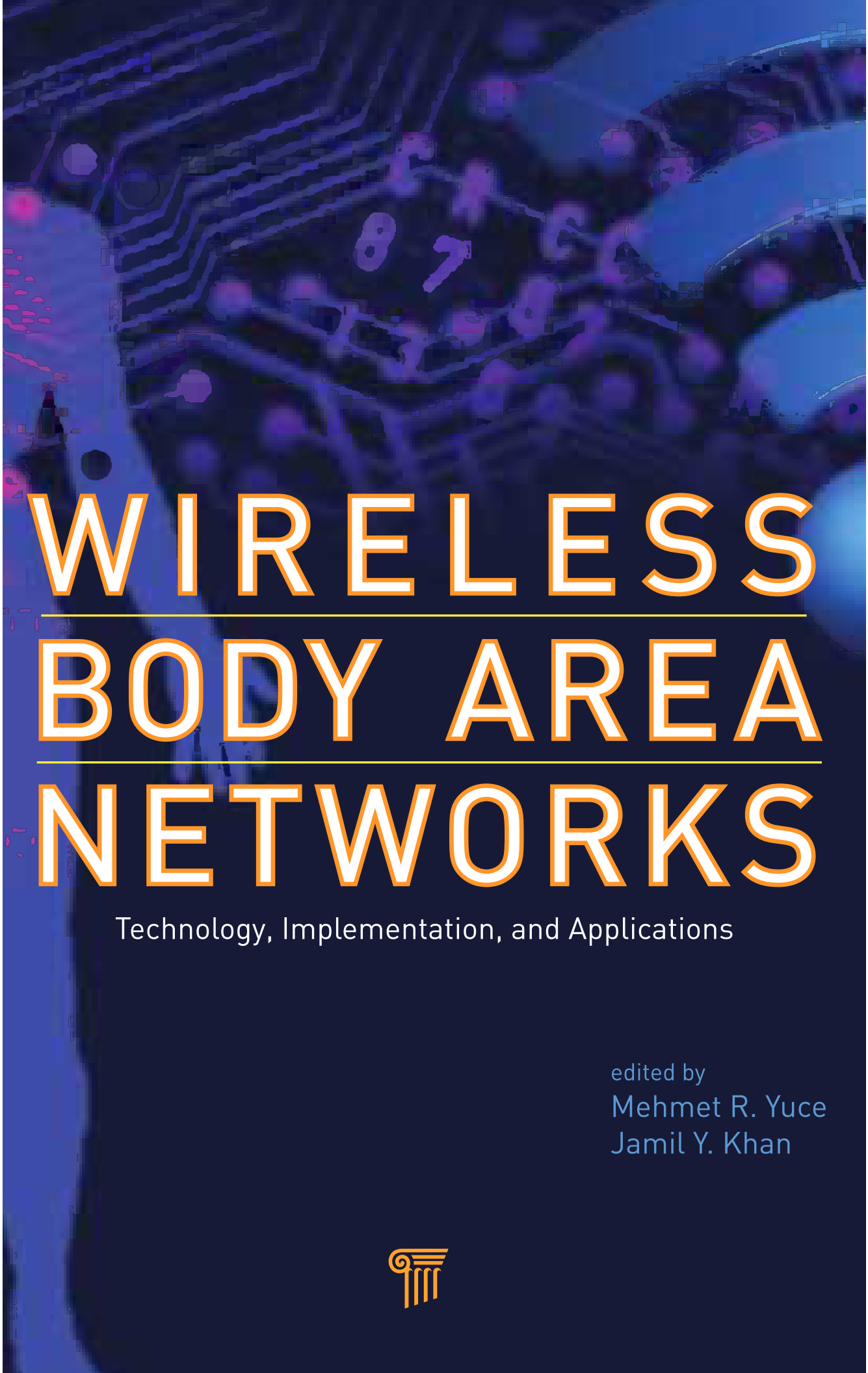

WIRELESS BODY AREA NETWORKS

Technology, Implementation, and Applications

edited by
Mehmet R. Yuce
Jamil Y. Khan

WIRELESS BODY AREA NETWORKS

This page intentionally left blank

edited by
Mehmet R. Yuce
Jamil Y. Khan

WIRELESS BODY AREA NETWORKS

Technology, Implementation, and Applications

PAN STANFORD PUBLISHING

CRC Press
Taylor & Francis Group
6000 Broken Sound Parkway NW, Suite 300
Boca Raton, FL 33487-2742

Version Date: 20111202

International Standard Book Number-13: 978-9-81424-157-1 (eBook - PDF)

Contents

This page intentionally left blank

Preface

Sensor-based measurements and monitoring techniques have been widely used in electronic patient care systems for a long time. The concept of wireless-sensor-based patient monitoring using wireless body area network (WBAN) will bring revolutionary changes in health care systems. WBAN allows flexibility in providing location-independent and seamless patient monitoring without affecting the lifestyle of patients. A WBAN system can be deployed at care centers for elderly people or at homes to look after elderly citizens without affecting their mobility or activities, thus improving the quality of life. The WBAN technology has advanced significantly in the last decade and gradually moved from the research laboratories to clinical trials and test environments. In future, WBAN applications will not remain restricted to the field of medicine. They will register their presence in other areas such as sports and training, military applications, and human safety. This book covers a range of topics on the WBAN technology, introduced in a manner that will be suitable for a broad range of readers. The book will be a key resource for medical ICT (information and communication technology) professionals, biomedical engineers, and graduate and senior undergraduate students in computer, electronic, and biomedical engineering.

This book discusses the current state of the art by focusing on the latest research and new design and development methodologies related to the WBAN technology. The book systematically introduces basic concepts, hardware, software and system design techniques, and various WBAN algorithms for wearable and implantable sensor applications. It also discusses some potential applications of WBAN in the field of e-health. Low-cost electronics and off-the-shelf consumer electronics-based wireless embedded systems are

introduced, which can be used to design basic low-cost wireless body area networks.

The book offers a comprehensive review of WBAN design, development, and deployment techniques. All chapters are written by leading experts in their fields. The contributions by the authors focus on applications of wireless body area networks, implementation, channel modeling, signal transmission around and in the body, antenna design, in-body communication, and hardware implementation of body sensors and nodes. Chapter 1 starts with an introduction to the WBAN to help readers understand the topic and the associated basic techniques. The next three chapters concentrate on the implementation of WBAN in clinical environments. Chapter 2 discusses clinical applications of WBAN, followed by discussions on the cardiac arrhythmias monitoring in Chapter 3. Human bio-kinematic monitoring using body area networks is described in Chapter 4. Ambulatory health monitoring applications are presented in Chapter 5. Hardware design, developments, and architectures are given in Chapter 6. Chapter 7 presents an overview of hardware implementation for the ambulatory health monitoring systems.

The design of sensor front-end circuits to detect biological signals is described in detail in Chapter 8. Network architecture and medium access control techniques used to design sensor networks are discussed in Chapter 9. Chapter 10 discusses the power management techniques for wireless body area networks. Chapter 11 concentrates on the radio transmission channel modeling for body-centric wireless communications**.** Chapter 12 focuses on antenna design and signal propagation techniques for WBAN applications. The effect of interference from other electronic systems such as Wi-Fi and microwave ovens could influence the performance of WBAN; these issues are discussed in Chapter 13. Implanted communication systems have been dealt with in Chapter 14. Chapter 15 describes the design of implantable devices that could form a sensor network by connecting with the on-body wireless nodes. The ultra-wideband (UWB) technology for both wearable and implantable WBAN applications is studied in the last chapter, Chapter 16.

We hope that this book will be a key resource for researchers and students who are working in this emerging area of the medical technology. Considering the rapid progress in the area, we firmly

believe that the wireless body area network technology will play important roles in future health care and associated areas. Finally we would like to thank all the authors for their excellent contributions, which enabled us to develop a key book on wireless body area network. We also thank the publisher for delivering an important book in a timely manner for one of the most important technologies in this century.

Mehmet R. Yuce
Jamil Y. Khan

This page intentionally left blank

Chapter 1

Introduction to Wireless Body Area Network

Mehmet Rasit Yuce[a] and Jamil Y. Khan[b]

[a] *Department of Electrical and Computer Systems Engineering, Monash University, Clayton, VIC 3800, Australia*
[b] *School of Electrical Engineering and Computer Science, The University of Newcastle, Callaghan, NSW 2308, Australia*
Mehmet.Yuce@monash.edu; Jamil.Khan@newcastle.edu.au

1.1 Introduction

Recent advances in wireless technologies and ICT (information and communication technology) systems are enabling the health care sector to efficiently administer and deliver a range of health care services. Advanced ICT systems will be able to deliver health care services to patients not only in hospitals and medical centers, but also in their homes and workplaces, thus offering cost savings and improving the quality of life of patients. For example, Internet is currently available almost everywhere in different forms, using either cable or wireless networking technologies. With the advancement of mobile and satellite communication technologies along with broadband communication techniques, e-health services can be delivered anywhere at any time. Especially, when wireless devices are

Wireless Body Area Networks: Technology, Implementation, and Applications
Edited by Mehmet R. Yuce and Jamil Y. Khan

ISBN 978-981-4316-71-2 (Hardcover), ISBN 978-981-4241-57-1 (eBook)
www.panstanford.com

integrated with sensors, it is possible to acquire and monitor human signals at any environment at any time. Hence, Internet can be used as a major tool to deliver e-health services to both developing and developed countries. E-health services can take advantages of wireless body area network (WBAN), which can act as an enabling technology. WBAN systems could offer great advancement for a ubiquitous health care, which has the potential to improve many aspects of everyday living leading to improved quality of life of many patients. Telemedicine and e-health services could offer several significant advantages, including speedup of diagnosis, therapeutic care for emergencies, offering specialist services to remote and rural locations, and supporting patients' mobility and lifestyles [1].

A WBAN monitors physiological signals from some tiny sensors with wireless transmission capability placed either inside or around a person's body, which are used to collect important health data of a person during a particular activity — medical or sport or training-related activities. These nodes form a network between the sensors and a control device. Figure 1.1 shows a generic WBAN application scenario. Basically, a WBAN system consists of a number of tiny sensor nodes and a gateway node used to connect them to remote locations (i.e., hospital, call center) as shown in Fig. 1.1. In literature, a number of different terminologies or names have been used for the gateway device; mainly terminologies such as body control unit (BCU) or central control unit (CCU) or personnel control unit (PCU) are used. The gateway device can be a smart phone or any portable device that can aggregate collected sensor data and forward them to remote stations. The gateway node can connect the sensor nodes to a range of communication networks. These communication networks can be either a standard telecommunication network, mobile/wireless network, a dedicated medical center/hospital LAN (local area network) or a public WLAN (wireless local area network) hotspot, commonly known as the Wi-Fi.

A WBAN allows a user to store collected data in his/her PDA (personal digital assistant) or iPod or any other portable devices and then transfer those information to a suitable computer when a communication link is available. Future applications of WBAN could

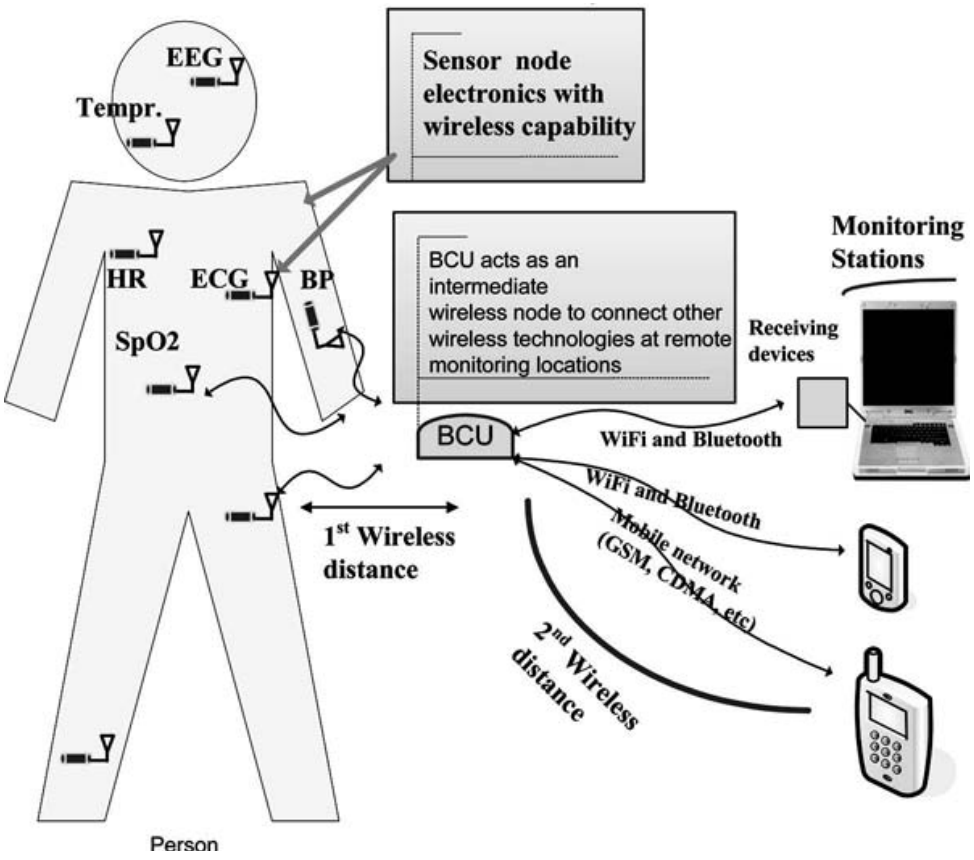

Figure 1.1. A wireless body area network scheme.

introduce numerous possibilities to improve health care and sports training facilities. In recent years, the WBAN concept has attracted the attention of medical and ICT researchers. Standard ICT systems are already in use in medical areas mostly related to patient record keeping and scheduling tasks. Some ICT systems or equipment are used to collect patient physiological data for treatments mainly using on-site wired equipment. The main drawback of the current system is the location specific nature of the system due to the use of fixed/wired systems. Introduction of WBANs opens up new possibilities in patient care and monitoring using e-health and tele-health systems. Another major area of health care where the WBAN will find its application is the aged care, where the quality of life of elderly people can be significantly improved if the health of older people is invasively monitored and appropriate health care is provided.

1.2 Applications

With the widespread use of portable devices such as mobile phones, pagers, PDAs, MP3 players, etc., the concept of collecting personal data in those devices becomes more realistic. In 1996, T. G. Zimmerman studied how such electronic devices operate on and near the human body**.** He used the term wireless personal area network (PAN) [2]. He characterized the human body and used it as a communication channel for intra-body communications. Later around 2001, the term PAN was modified to body area network (BAN) to represent all the applications and communications on, in, and near the body [3]. One of the most attractive applications of BAN is in medical environment to monitor physiological signals from patients [4].

In recent years, interest in the application of WBAN has grown significantly. According to ABIresearch (Allied Business Intelligence Inc.), "*The market for wireless devices that monitor patients' condition and report that data to health care providers is on the verge of explosive growth, according to a new study from ABI Research. Over the next few years, it will show a remarkable 77% compound annual growth rate (CAGR) resulting in global revenue of almost* $*950 million in 2014*" [5]. A WBAN based on low-cost wireless sensor network technology can significantly enhance patient monitoring systems in hospital, residential, and work environments. A WBAN system allows easy internetworking with other devices and networks, thus offering health care workers easy access to a patient's critical as well as non-critical data without or minimal manual intervention.

Currently many service providers use very basic manual/semi-automatic remote patient monitoring systems. Most of the current systems use the standard telephone network where a patient could send some medical data by manually connecting a medical sensor to its body that sends information via telephone networks. Various companies or service providers offer these services. AMAC (American Medical Alert Corp.) provides a system called health buddy, which allows patients to send medical data to health care professionals remotely [6]. Such a system requires manual intervention. According to the leading technology company Frost & Sullivan,

it is expected that the remote patient monitoring technology will be deployed in the near future to provide the following medical services [7]:

- Cardiac care
- Diabetes
- Pulmonary diseases
- Pharmaceutical compliance
- Mental health
- Co-morbidities and others

Various medical equipment vendors have started to produce remote tele-health equipment to support remote patient monitoring services. One of the examples of such equipment is the TeleStation produced by Philips [8]. The TeleStation unit acts as a hub that connects to other physiological data collection devices such as weighting scale, blood pressure and pulse cuff, ECG/rhythm strip recorder and the pulse oximeter. The TeleStation collects all the measurements from different units and sends those data over the telephone line to a Philips database server. The TeleStation can also receive instructions from physicians and/or health care workers. Physicians or health care workers can request more data from patients to study or analyze their condition. The TeleStation can be seen as a gateway of a basic WBAN, which comprises measurement devices. The TeleStation solution is still not a true WBAN because in this case, patients have to carry out manual measurements using standard equipment, whereas in a true WBAN we would expect sensors attached to a human body to automatically collect physiological data and transmit them over communication interfaces. Also, the TeleStation is only capable of transmitting data over a phone line only and doesn't support mobility because of the use of bulky measurement equipment.

Recently a European vendor Broek op Langedijk of the Netherlands has developed the RS TechMedic, a portable cardiac monitor [9]. The unit has an internal GSM mobile phone interface as well as Bluetooth class I and USB connections. Such devices and systems are yet to conform to WBAN requirements; however, the trend in the tele-health/e-health sector is moving towards WBAN applications.

Aged care is one of the prime areas of WBAN applications. Aging population, shortage of medical staff, and high demand of hospital resources are problems faced in many countries around the world. A wireless medical sensor network facilitates remote monitoring system, which allows the medical and health staff to detect early symptoms of any illness or even they can use those medical data to alter medications or care pattern. Timely medical intervention significantly improves a patient's chances of recovery. WBAN-based solution will provide invasive, mobile, and cost effective services for the above applications.

A WBAN-based monitoring system can also be extended to monitor athletes' performance to assist them in their training activities. Using sensor nodes, a trainer can get both on and off the track performance data. For example, for a cricketer or a tennis player, movement of arms and body postures are very important for their success. In this case, a trainer can obtain data from a player via a WBAN and store those data in computers for further analysis.

Another exciting application of WBAN is in space and military applications. With wireless and wearable sensors, the conditions and status of astronauts and soldiers can also be monitored. Military applications of WBAN have different operating environments. In the case of military application, a WBAN will be formed around a soldier's body by interconnecting various sensors, equipment, and perhaps with different communication devices [10]. In future, deployment of WBAN may not only be limited to medical applications but may also be extended to many other applications, including training, industrial safety, military and other logistic applications. Applications of WBANs to help disabled persons could be another major application. It is worthwhile to mention here that a WBAN is a special purpose sensor network; hence, it is possible for a WBAN to accomplish a range of tasks. Further research and development work is necessary to develop future WBAN applications.

1.3 Wireless Personal Area Network (WPAN)/Wireless Local Area Network (WLAN)

Wireless personal and local area networks are low power, short range wireless networks used to establish small size networks

Table 1.1. Wireless technologies for short-range data communications

	Frequency Band	DataRate	Range	Standard	Transmission Power
Bluetooth	2.4 GHz	Up to 1 Mbps	1–100 m	IEEE 802. 15.1, WPAN	1–100 mW
ZigBee	2.4 GHz Worldwide 868/915 Europe/US	Up to 250 kbps	0–10 m	IEEE 802. 15.4 WPAN	1–10 mW
Wi-Fi	2.4 GHz , 5 GHz	Up to 400 Mbps	300 m	IEEE802.11(b/g/n)	250–1000 mW
6LoWPAN	2.4 GHz	250 kbps	∼ 30m	IEEE802.15.4/IETF	∼ 10mW

to exchange data. Using these technologies, it is possible to develop low-cost, small-size communication networks to support many applications, including WBAN applications. Table 1.1 lists some of the current available wireless technologies that could be used to develop small-scale wireless sensor networks for various applications. Bluetooth, ZigBee, and 6LoWPAN systems have mainly been optimized for short range (10 m) communication transmitting at low power to connect sensors and control nodes. Wi-Fi devices are generally used for long-range applications and thus consume more energy due to higher transmission power. In addition, board dimensions of the wireless platform for Wi-Fi links are larger.

Most of the current WBAN systems tend to use commercially available WPAN platforms such as ZigBee and Bluetooth as sensor nodes of a WBAN system. Bluetooth technology can be used to communicate with new smart phones. It will be important for future systems to evaluate their designs for multi-patient environment, especially devices using a wireless platform at 2.4 GHz ISM band due to the massive presence of other wireless devices and equipment operating in the same frequency band. Interference from other devices operating in the ISM band could reduce the reliability of WBANs.

With the arrival of new smart phones (e.g., iPhones), PDAs , and other pervasive wireless devices (iPods, iPads), it is now possible to use many wireless connections to transmit data from anywhere to the IT unit of a medical center. Smart phones generally have multiple wireless links, which could be either 2G/3G mobile links or satellite links or Wi-Fi connections to transfer data. Smart phones

can select the most appropriate link based on availability, quality, or user preferences.

1.4 Wireless Body Area Network

A body area network is a collection of wireless sensors (i.e., sensor nodes) placed around or in a human body that are used to exchange important information from a human body to remote stations. Although WPAN devices have been used for WBAN applications, WBAN is a very small-scale network requiring a communication distance of a few meters between sensors and the control unit. For most applications, a WBAN node requires a low data transmission rate as each sensor node will transmit only one physiological signal. Physiological signals usually occupy small frequency components. Table 1.2 lists the biological signals that will most likely be the source of sensors for WBAN applications. Current WPAN standards are optimized for industrial applications. As an example, ZigBee is optimized for sensor network applications and Wi-Fi is optimized for data network with longer transmission ranges. Thus WBAN systems should be based on a different standard, which should be developed and optimized specifically for a short-range low power sensor network around a body [11]. Figure 1.2 shows the standing of WBAN among other wireless standards.

In addition to wearable vital signal monitoring sensors (ECG, temperature, heart rate, etc.), the use of implanted sensors is also

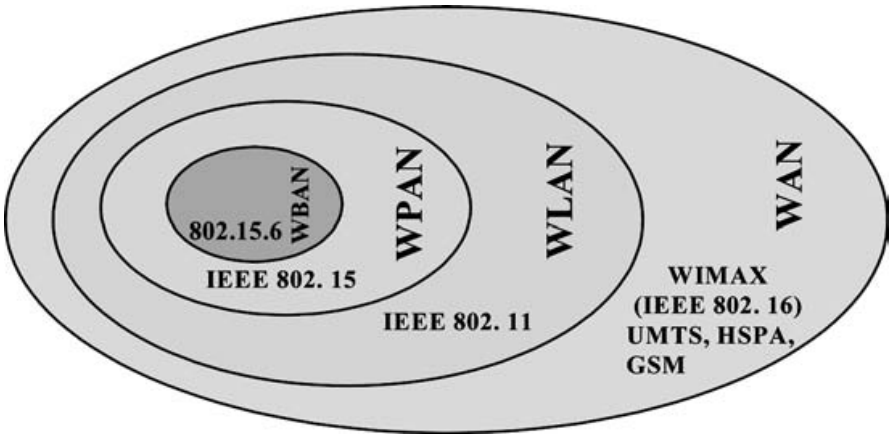

Figure 1.2. Wireless standards. See also Color Insert.

Table 1.2. List of biosensors

Wearable Sensors	Implantable
Electrocardiogram (ECG)	Pacemaker
Heart Rate	Cochlear Implants
Electromyography (EMG)	Implantable defibrillators
Electroencephalogram (EEG)	Wireless capsule endoscope (Electronic Pill)
Temperature	Electronic pill for drug delivery
Pulse oximeter	Deep brain stimulator
Blood pressure	Retina implants
Oxygen, pH value	
Glucose sensor	
Movement (accelerometer)	

increasing. Some examples are wireless capsule endoscope, cochlear implant, and implantable defibrillators. Among the biosensors listed in Table 1.2, except for retina implants and electronic pills, the remaining sensors require low data transmission rates. The electronic pill requires the highest data transmission rate, around 10 Mbps, to transmit good quality video from inside the body to a monitoring device.

In order to monitor the inner organs as well as the status of medical implants such as pacemakers and defibrillators, a frequency around 400 MHz has been used as a popular transmission band for recent systems [12]. To treat a large number of patients wearing implanted systems in the same environment (e.g., hospital), a reliable wireless networking is required to monitor and differentiate each individual implanted device and patient. Thus implanted wireless nodes in a patient's body should form a wireless body area network so that one or more implanted devices inserted in the bodies of a number of patients in a hospital environment can be controlled with minimum complexity. It is quite possible that for some applications both implantable and wearable sensors form a WBAN system.

A WBAN is mostly likely to incorporate wearable and implantable nodes operating in two different frequencies. An implantable node is most likely to operate at 400 MHz using the MICS (Medical Implantable Communication Service) band, whereas the wearable node could operate in ISM/UWB (Instrumentation Scientific Medical/Ultra Wide Band) or some other specific bands [13].

Both implantable and wearable sensor nodes require the use of a gateway-body control unit (BCU) to communicate with remote monitoring stations as depicted in Fig. 1.1.

A WBAN system can interface with or accommodate different wireless platforms. As an example, a multilink WBAN can have multiple wireless links. Multiple wireless links could consist of the standard ZigBee or Bluetooth to cover WPAN areas and a 802.11 based Wi-Fi link to cover a larger transmission range possibly to connect to a remote station or a database server [14, 15]. Different configurations of WBAN nodes are illustrated in Fig. 1.3.

Using WBAN nodes after obtaining raw data from a human body, sensor nodes transmit those data to the control device — BCU

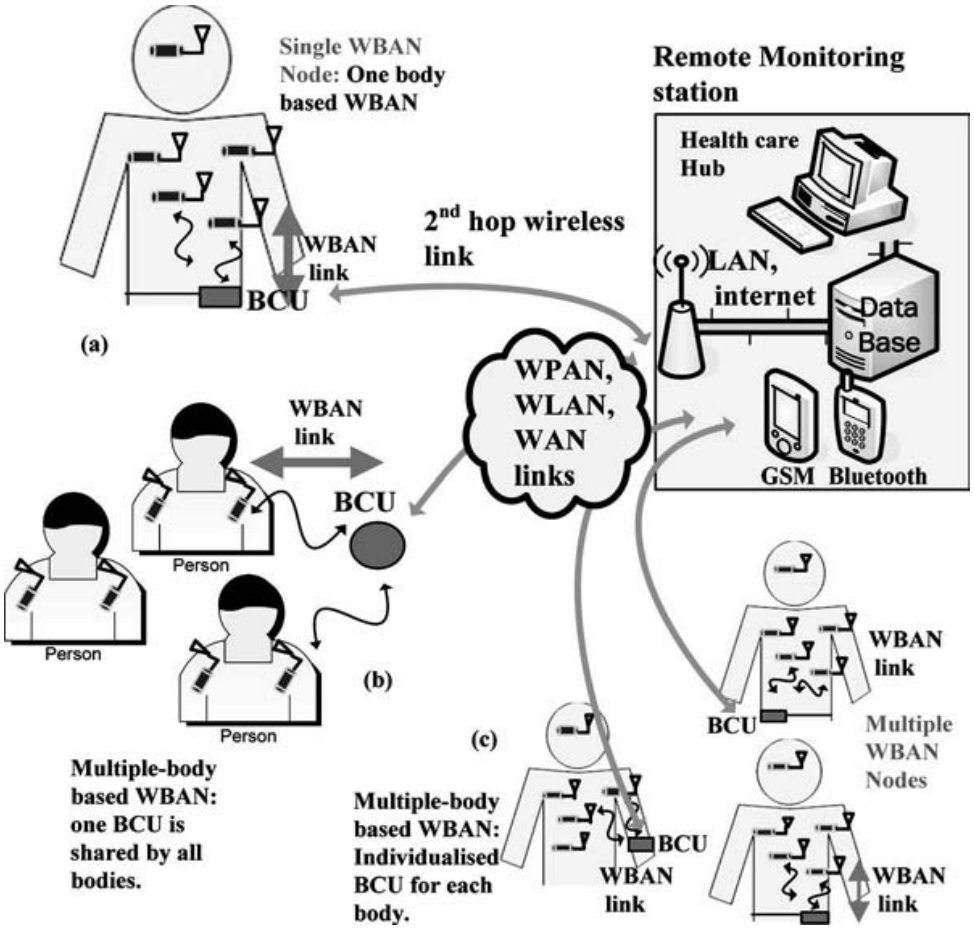

Figure 1.3. Wireless body area network implementation scenarios: (a) single WBAN node, (b) a WBAN node with multiple bodies, and (c) multiple WBAN nodes. See also Color Insert.

— over a short-distance wirelessly using one of the short-range wireless systems. The control device can be placed on the body like a mobile phone as shown in Fig. 1.3a, or it can be placed at an accessible location. Most suitable technologies for this link are ZigBee, Bluetooth, 6loWPAN, and WMTS. The main task of the BCU is to transfer data to a PC or to a smart phone. Wireless technologies used on this segment (BCU to PC or to an Internet device) could be a mobile communication network, a satellite link, or a Wi-Fi link. When the Internet is used, the data collected at this PC can be transferred to remote stations in remote medical centers across the network.

As described in Fig. 1.3, the collected sensor data can easily be transferred to remote stations (i.e., medical centers) with the existing wireless and information technology infrastructures such as satellite, mobile communication system, Internet, etc. Accessing the medical data of injured people through Internet is an effective solution at the moment, which will allow medical professionals at the hospital to collect and evaluate data while patients are being transferred to the hospital in an emergency vehicle. If provisioned, these data can also be accessed outside the emergency areas as they will be made available online.

The control device will be similar to smart phones we use in our daily life to receive and monitor the data obtained from sensors. They will be like minicomputers, which will most likely be connected via a wireless technology such as Bluetooth, Wi-Fi, 3G/2G networks or the satellite (VSAT: very small aperture terminal). These technologies offer flexible communication links that can be configured to send data from medical sensors to remote medical centers (second wireless link in Fig. 1.1 and Fig. 1.3), which can be accessed by medical professions at any time. The BCU can be attached to the body as a wristwatch or around belt.

The first scenario sharing a single WBAN node can be used for home care where there is need for only one body monitoring. Scenarios presented in Fig. 1.3a,b can be used at a disaster area, in emergency rooms in hospitals, and in ambulance while patients are taken to the hospital.

Above discussion shows that WBAN is a specialized sensor network with definite application requirements. For the commercial

deployment of WBANs, it is necessary to develop an industrial standard by considering its different application scenarios and requirements.

1.5 Design Requirements

Design of miniaturized, low-power, reliable, and wearable sensor node devices is the key requirement of a WBAN design. A WBAN is a special purpose wireless sensor network designed to transmit data within a very short distance. The quality of service (QoS) of a WBAN will depend on applications, which are primarily medical applications. As discussed earlier, WBANs could be used in other applications such as sports training, rehabilitation purposes, or military applications where the QoS will be dictated by the nature of those applications. For medical applications where the source of information is physiological signals such as heart rate, blood pressure, ECG, etc., the system generally demands low latency and high reliability. Also, most of the physiological signal sources produce shorter data bursts at a regular sampling frequency. Hence, a WBAN transmission data rate requirement is low to medium for each connection. However, one should keep in mind that a WBAN will comprise multiple sensor nodes where data transmission should be coordinated by using a reliable and efficient medium access control protocol [4]. Whatever may be the application of a WBAN, the main design requirement of a WBAN is to develop a short-range and reliable wireless sensor network.

A WBAN may need to send data over a longer distance or may need to support mobility. The range of a WBAN can be extended by using a multi-hop network using a gateway or a router, which could connect a WBAN to external networks. The range of a WBAN network should not affect the sensor node designs because the gateway will be responsible for seamless long distance services; hence, a modular design approach should be taken when a long distance WBAN application design is developed. Similarly, the mobility feature of a WBAN will be taken care by the gateway or a router, thus reducing the design complexity of sensor nodes. The gateway should be able to detect movement of a WBAN or a

person and connect itself to available external networks to exchange information with the WBAN. The mobility speed support will be determined by the external network. For example, a Wi-Fi can only support very low speed mobility up to 5 km/h, whereas a 2G/3G network could support mobility up to 240 km/h. If we are looking for mobility within a hospital or inside a home, then a Wi-Fi-type connection could be sufficient, whereas for a sport training application, it may be necessary to use a 2G/3G network to obtain data from the sensors located at an athlete's body. So the WBAN design requirements can be classified into basic and advanced requirements. Advance design requirements will be influenced by the design requirements of the applications that a WBAN is used. The basic WBAN design attributes are summarized below:

- WBAN sensor nodes should be able to transfer data over a distance of a few meters using a single hop connection.
- Sensor nodes should be miniaturized so that they can be easily wearable.
- Suitable frequency bands should be selected to reduce interference and thus increase the coexistence possibility of sensor node devices with other network devices available at medical centers or in homes.
- WBAN nodes should consume low power so that battery could last for a very long time. Also, WBAN nodes should use small size batteries so that light-weight nodes can be used.
- A WBAN should be designed in a fail-safe manner so that failure of a node can be automatically detected or failure of a node should not affect the operation of the network.
- A WBAN should be scalable so that health care workers can increase or decrease the number of nodes on a patient's body without any manual intervention of IT personnel.

To achieve the above design attributes, WBAN designers should consider the following points in their design work:

Wireless sensors: A transmitter circuit can be designed with a few components, which may consume extremely low power when designed with an integrated circuit technology. Appropriate sleep

and wake-up cycles should be incorporated with the designed hardware to reduce the power consumption to a minimum level.

Reliable data communication: Reliable, error free, and robust information should be received from sensors. A WBAN will use a wireless channel to transmit data, which is inherently unreliable. Error checking and correction mechanisms should be incorporated so that the unreliability of the transmission channels can be countered. The wireless technologies used in a medical environment should operate in the frequency bands that are **immune to interference and thus increase the coexistence of** sensor node devices with other network devices available at the same location. The wireless technology used should have less interference effect on other medical equipment. Any network outage should be automatically detected, and the sensor data should be delivered in a fail-safe manner, which could be a critical requirement for a patient monitoring system.

Wireless network security and privacy: Key software components should be defined and developed to accommodate secure and effective wireless networking. Protocols should be designed in such a manner that a WBAN data cannot be collected by intruders. A WBAN will use a wireless transmission channel, which opens up the possibility of external intrusion while transmitting data. Data encryption techniques could be used, but designers should keep in their mind that undue complexities should not be introduced at the sensor node level to avoid higher battery power and larger physical size.

Handover mechanism: Handover mechanism should be integrated in a WBAN using the gateway or a router. Handover features should not overload the sensor node design.

Miniaturized antenna: Unobtrusive small antenna design should be used, which will operate at high frequencies. Directional or narrow beam antenna design could be considered for specific medical applications.

Gateway devices: A WBAN node may have a wearable or implantable node. Gateway devices should be developed to interface with the existing wireless networks used in health care systems. Gateway devices should implement advanced algorithms, which are more power hungry so that sensor node design and requirements remain simple.

Alarm option: An alarm option should be included when an outage occurs or a sensor node fails.

Comfort: Sensor node electronics could be designed using flexible and stretchable technology so that sensor nodes can easily be embedded in textiles (i.e., patient's clothes). It can be attached to the human body using a plaster to eliminate movements.

1.6 Scope of the Book

This book addresses the applications, hardware, and software design of WBANs. It informs readers about some of the current and possible future applications of WBAN-based monitoring systems. A number of chapters have been devoted to WBAN applications as mentioned in the preface of the book. Following the application chapters, readers are presented with hardware and software design techniques, which can be utilized to develop WBAN systems for medical applications. Hardware design techniques and system level developments are discussed in detail. An important component of the WBAN is the antenna design, which is also introduced in a separate chapter. Protocol and network design techniques are discussed in several chapters, which will provide readers clear understanding of WBAN network requirements. It is important to understand protocol and network design issues because the efficiency and the performance of a WBAN system could be largely determined by them. The book also introduces various current industrial standards, which will inform readers about possible choice of hardware and software system selections. As mentioned in this chapter, a number of industrial wireless standards exist, which could be followed to develop a WBAN by procuring and configuring them in a suitable manner. Signal transmission around

and in-body, in-body communication techniques, and the design of implantable sensor nodes are also described in individual chapters. The book also presents a chapter on coexistence issues. This is an important issue because nowadays many other wireless devices are used in many locations in hospitals and homes; hence, it is necessary to understand the impact of other wireless devices and choice of appropriate frequency bands. In conclusion, the book provides a comprehensive coverage of WBAN applications, design, and deployment techniques.

References

1. ETHEL, http://www.e-wwg.com/Publications/eHealth/EHTEL%20Briefing%20Paper%20Sustainable%20Telemedicine.pdf.
2. Zimmerman, T. G. (1996) Personal Area Networks: Near-Field Intrabody Communication, *IBM Systems Journal*, 35(3–4), 609–617.
3. Dam, K. V., Pitchers, S., and Barnard, M. (May, 10–11, 2001) From PAN to BAN: Why Body Area Networks?, in *Proceedings of the Wireless World Research Forum (WWRF) Second Meeting*, Nokia Research Centre, Helsinki, Finland.
4. Khan, J. Y., and Yuce, M. R. (2010). Wireless Body Area Network (WBAN) for Medical Applications, New Developments, in *Biomedical Engineering* (ed. Domenico Campolo), ISBN: 978-953-7619-57-2, InTech.
5. http://www.abiresearch.com/press/3244-Healthcare.
6. Health Buddy, http://www.amac.com/remote_patient_monitoring.cfm.
7. http://www.frost.com/prod/servlet/market-insight-top.pag?docid=18086184.
8. TeleStation, http://www.healthcare.philips.com/in/products/telehealth/products/telestation.wpd.
9. RSTechMedic, http://www.rstechmedic.com/.
10. Cotton, S. L., Scanlon, W. G. and Madahar, B.K. (2009) Millimeter-Wave Soldier-to-Soldier Communications for Covert Battlefield Operations, *IEEE Communications Magazine*, 47(10), 72–81.
11. http://www.ieee802.org/15/pub/TG6.html.
12. Bradley, P. D. (2007) Implantable Ultralow-Power Radio Chip Facilitates In-Body Communications, *RF Design,* 20–24.

13. Hanna, S. (2009) Regulations and Standards for Wireless Medical Applications, *ISMICT*.
14. Istepanian, R. S. H., Jovanov, E., and Zhang, Y.T., (December 2004) Guest Editorial Introduction to the Special Section on M-Health: Beyond Seamless Mobility and Global Wireless Health-Care Connectivity, *IEEE Transactions on Information Technology in Biomedicine*, 8(4), 405–414.
15. Jovanov, E., Milenkovic, A., Otto, C., and de Groen, P.C., (March 2005) A Wireless Body Area Network of Intelligent Motion Sensors for Computer Assisted Physical Rehabilitation, *Journal of NeuroEngineering and Rehabilitation*, 2 (6), doi: 10.1186/1743-0003-2-6.

This page intentionally left blank

Chapter 2

Wireless Patient Monitoring in a Clinical Setting

Esteban J. Pino[a], Dorothy Curtis[b], Tom O. Stair[c], John V. Guttag[b], and Lucila Ohno-Machado[d]

[a] *Electrical Engineering Department, Universidad de Concepción, Concepción, Chile*
[b] *Computer Science and Artificial Intelligence Laboratory, Massachusetts Institute of Technology, Cambridge, Massachusetts, USA*
[c] *Department of Emergency Medicine, Brigham and Womens Hospital, Boston, Massachusetts, USA*
[d] *Division of Biomedical Informatics, Department of Medicine, University of California San Diego, La Jolla, California, USA*
estebanpino@udec.cl

This chapter presents the technology, implementation, and application of a wireless patient monitoring system for triage support. The SMART project was developed jointly at Brigham and Women's Hospital in Boston, MA and at the Massachusetts Institute of Technology, Cambridge, MA. It was deployed and evaluated at the Brigham and Women's Hospital over an 18-month period. We present a discussion of similar projects, all involving wireless patient monitoring, and then describe the SMART system design and the results of our experience with its deployment in the waiting area of the Emergency Department of the Brigham and Women's Hospital.

Wireless Body Area Networks: Technology, Implementation, and Applications
Edited by Mehmet R. Yuce and Jamil Y. Khan

ISBN 978-981-4316-71-2 (Hardcover), ISBN 978-981-4241-57-1 (eBook)
www.panstanford.com

2.1 Introduction

According to World Health Organization data, globally there are about 1.4 physicians per 1000 inhabitants [1]. In most developed countries, the ratio is only slightly better: 2 to 4 physicians per 1000 inhabitants. It is only natural that patients far outnumber care providers, particularly during peak demands. In large overcrowded settings, patient oversight becomes increasingly difficult, such as in waiting rooms during seasonal outbreaks, at improvised first-care centers or in other nonstandard settings. To manage a large concentration of patients, a monitoring system is key for ensuring high quality of care.

In health care settings, a wireless body area network (WBAN) can be used to collect patient-relevant information instead of having a caregiver constantly monitoring a group of patients. A wireless, automated data collection system provides several benefits:

- Ease of data collection with minimum patient discomfort
- Scalability to a large number of patients
- Real-time monitoring and assessment of changing physiological conditions
- Higher patient-to-caregiver ratio possible, while maintaining the same quality of care (better human resource utilization)

In current scenarios, caregivers are forced to collect patient data on a case-by-case basis. Bedside data collection is only used after patients have been admitted to the hospital. Collecting data is essential to support good medical decisions. In emergency departments, the first set of data is collected during triage, where an initial assessment of the patient status is performed. However, a single snapshot of the patient vitals may lead to misprioritization. Furthermore, it is very difficult to notice any changes in patient status after the triage process has been completed.

In terms of scalability, caregiver–centered systems can easily collapse during peak demand. A patient–centered system has obvious advantages. Such a system scales naturally as more nodes are added to monitor more patients. The only constraint is an eventual

overload at the network layer or at the monitoring station. To this end, as much computation as possible should be programmed into the WBAN components.

In order to assist in the monitoring of multiple patients, we developed SMART (Scalable Medical Alert and Response Technology). [2–4] SMART implements a patient-based wireless monitoring system as an aid for multiple patient scenarios. It can help first responders in emergency situations by providing a fast on–line triage system requiring little set-up time. In overloaded waiting rooms, it can help in re-prioritization of patients. In nursing homes, it can facilitate the supervision of a large number of people, without degrading their quality of life. SMART provides a steady flow of data from the patients and a real-time alarm system to prompt re-triage in the case where a patient's condition deteriorates.

Physiological signals such as electrocardiogram (ECG) and pulse oximetry (SpO_2) are simultaneously acquired from different patients and processed at a central server where a single operator can oversee a large number of patients. Location information is also collected wirelessly to facilitate locating a particular patient who needs attention.

Similar projects originate from the military. The Artemis project [5] uses a WBAN to evaluate the physiological state of soldiers in the field. A fuzzy logic based algorithm [6] gathers information from the SpO_2 sensor to trigger a distress signal or it can be initiated by a fellow team member. The distress signal is forwarded to medical personnel, along with location information provided by GPS, to guide the caregivers to the injured soldier. Konoske et al. present an evaluation of a Mobile Medical Monitor (M3) [7] for soldier care. The mobile unit is very complete, incorporating an assortment of physiological sensors. However, its main drawback and complaint among users is its inability to supervise multiple patients and save the data in relational databases, features SMART can support.

There are many proposals from academic institutions [8] for pervasive, wireless response systems. They all implement solutions for multiple patient monitoring. In the WIISARD project, a different solution is proposed for mass casualty incident response [9], with a clear focus on logistics. Mobile caregivers are equipped with wireless PDAs to evaluate patients in the field and relay that

information to a central command post. Patients only had basic online physiological monitoring, unlike SMART, preventing adequate detection of adverse events. An intelligent triage tag is proposed for WIISARD [10] as a replacement for the paper tag, mainly for notification and prioritization in the field. The wireless infrastructure [11] is provided using commercially available equipment.

AID-N project, [12] an extension of CodeBlue, [13] presents a mobile patient monitoring prototype for an electronic triage system. The sensors are similar to SMART: SpO_2, blood pressure, ECG and GPS/MoteTrack for outdoors/indoors location. The primary goal is triage management for mass casualty events. [14, 15] To this end, a central station collects data from mobile units, caregivers carry wireless PDAs to communicate with the server, and patients are equipped with physiological sensors and visual and audible alarms to alert caregivers to emergent conditions. A survey conducted after preliminary usability tests shows that the most important feature for caregivers is triaging support. SMART also provides triaging support in the main server, alerts and location information. A difference between AID-N and SMART is that our system is easily extensible to regular settings, such as a waiting room, helping ease the learning curve involved in using a new system.

Another application of WBAN systems is concerned with patient monitoring during transport [16] among units in a hospital. In this case, ECG and SpO_2 sensors are used, but no location information is necessary. The patient equipment is similar to SMART, based on an iPaq H5450. Another pre-hospital patient monitoring system [17] shows that body sensor networks can also prevent over- or under-triage of trauma patients. The authors propose an iPaq–based system that records eight different vital signs during transport to improve triage. They finally conclude that SpO_2 and ECG heart rate (HR) are a better predictors of the need for abdominal surgery than reports from pre-hospital clinicians. A low SpO_2 and high HR combination is a good predictor for internal bleeding injury. A smart vest can also be used as support for WBAN. [18] In this case, sensors are embedded into a vest or T-shirt. Wires are woven into the fabric and data and power are transmitted to and from a main processing hardware with wireless capability. Sensors used in the smart vest acquire ECG, photoplethysmogram (PPG), blood pressure (BP), skin temperature, galvanic skin response (GSR), and ECG–derived HR.

A project conducted at Pennsylvania Hospital [19] evaluated an ECG-based alarm system. Using a commercially available wireless ECG, the authors were able to assess the validity of ventricular fibrillation, asystole, tachycardia, or bradycardia alarms. The authors reported high patient and clinician satisfaction, even though there were more false alarms than useful alarms, in line with SMART's findings. Their system did not provide an automated location system, although the authors acknowledge its importance.

A complete survey of wearable medical monitors is discussed by Raskovic et al. [20] Issues, current proposed systems, and a general description of different systems and mobile monitoring implementations are presented by these authors.

2.2 Smart System

SMART is designed as a mass casualty response system, but is also easily used in everyday environments. The rationale is that a system that is used regularly by physicians and nurses will have a much easier transition into use in a disaster situation. In SMART, the wireless component allows the subject to move freely, and has little negative impact on their regular behavior. Furthermore, the patients perceive a higher sense of care as shown by our post-study survey. In terms of medical performance, the system helped detect several cases that would have otherwise gone undetected.

The SMART patient monitoring system was deployed in the waiting room of the Emergency Department at the Brigham and Women's Hospital in Boston, MA. The system was operational from June 2006 to December 2007, collecting 6815 minutes of data from 145 patients.

2.2.1 *Architecture*

2.2.1.1 Hardware

On the patient, physiological and location data are collected and wirelessly sent to a central server. The physiological sensors measure ECG and SpO_2 and are wired to a PDA that acts as a sensor hub and transmits the data via standard 802.11b Wi-Fi network. Location is implemented via ultrasound tags and detectors that can

pinpoint a particular patient to a predetermined area. Privacy issues are considered and patient-sensitive data is encrypted prior to transmission to caregiver PDAs. Physiological data transmitted from the patients to the server is not encrypted because it contains no identifying information.

The ECG sensor's printed circuit board is the only custom-made hardware in the project. It implements an instrumentation amplifier with fixed gain and filters. An 8-bit analog-to-digital converter (ADC) samples the signal at 200 Hz and sends the data using RS-232 serial communication. For SpO_2 sensing, a commercial sensor from Nonin Medical Inc. [21] is used. This sensor reports status, SpO_2 level, and heart rate every second, also via serial interface. As shown in Fig. 2.1, both sensors arrive at a sensor box, connected to a standard PDA acting as a wireless node. The HP iPaq 5500 is chosen because it provides Wi-Fi connectivity, extended battery life, and serial ports. Having a PDA as the basic building block was useful in configuration and debugging tasks.

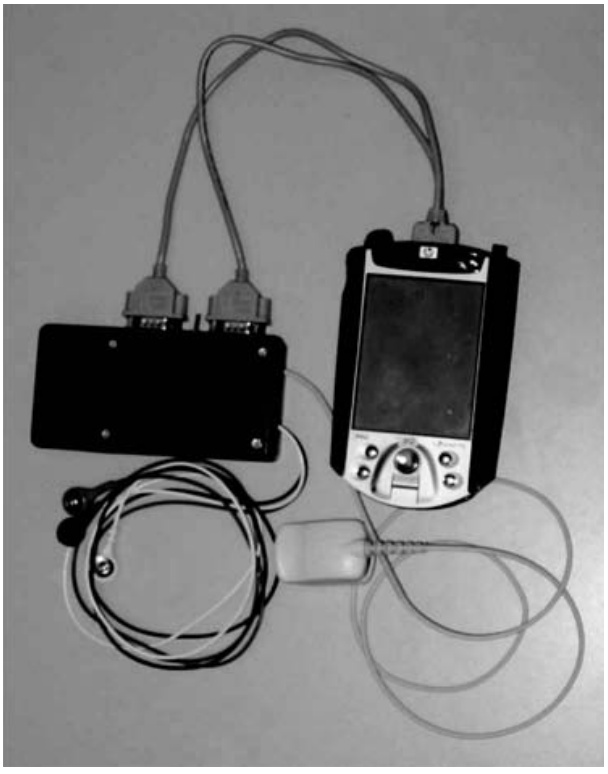

Figure 2.1. Patient PDA with ECG leads and SpO_2 sensor. See also Color Insert.

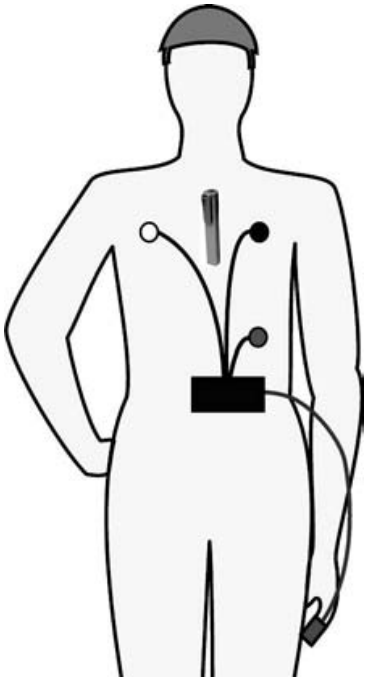

Figure 2.2. Patient with ECG, SpO_2 and location sensor.

Location data is provided by an ultrasonic (US) system from Sonitor Technologies. [22] US tags attached to patients transmit a unique code that is read by US receivers mounted on the walls. A simple signal strength algorithm assigns a tag to its closest receiver. The advantage of the US system is that the signal is confined by walls. This way, there is absolute certainty that a patient is in a given room. Large rooms can be subdivided by properly placing the receivers. The tags are pen-like and are usually worn on a lanyard around the neck. Figure 2.2 shows a diagram of the complete gear worn by the monitored patients.

Fourteen US detectors are installed covering the complete waiting area and the overflow area. By having detectors outside the waiting area, we can infer when a patient has left the waiting room and their general direction.

SMART also implements a caregiver wireless node. Caregivers can be equipped with a hand-held PDA and a location sensor. This way they can receive and respond to alarms forwarded to their PDA, check the status of a patient, and the server can know their location.

The server hardware is a standard PC with dual monitors, wired to a wireless router. ECG and SpO_2 data arrive wirelessly from the patients to the router. Location information is also received from the US detectors via wireless adapters. Only three detectors are wired to the router, due to their close proximity to the server. All wireless communications use the IEEE 802.11b standard.

The maximum bandwidth provided by the 802.11b network is 11 Mbps, which was enough for our needs. A simple calculation sets the requirements for 10 wireless nodes (patients and caregivers) at under 0.5 Mbps. [4] There are some other technical aspects to consider when using wireless networks. First, the available bandwidth is reduced as the distance to the wireless router or access point increases. Proper placement of the wireless router can minimize the number of nodes with reduced data rate, while serving the majority of the nodes at higher data rates. Second, wiring the server to the router reduces by half the number of wireless data packets on the network. Finally, radio interference can be avoided by proper coordination of channel usage in the hospital. In our particular case, our wireless network used a different channel than the existing network, and we did not experience any problems on either network.

2.2.1.2 Software

Different programming languages are used in SMART according to the task and platform, as shown in Fig. 2.3 For the mobile nodes, the

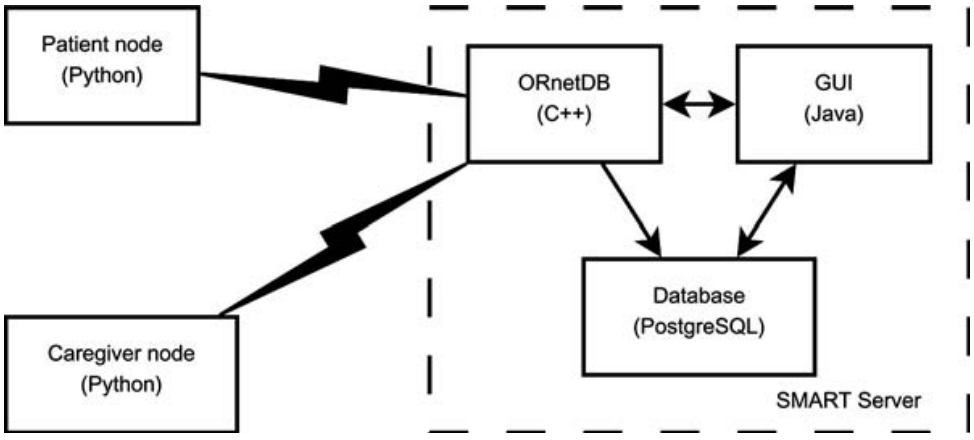

Figure 2.3. Software and data flow in SMART.

language of choice was Python. The PDA was running a linux-based OS, Familiar Linux, that provided better control over the hardware, and an open source platform. There are two Python programs, the data-collecting and forwarding program running on the patient PDA, and the data-fetching program running on the caregiver PDA. The patient PDA program is not intended to be used by patients. It provides a simple configuration screen to specify serial port usage and a "live" data screen used in the early stages of the project for debugging. Data are identified as ECG or SpO_2, timestamped and sent via TCP to the server. To reduce the wireless traffic, 20 samples of ECG data are packed together and sent every 0.1 s. Individual patient data streams are identified according to their originating PDA identification number. The caregiver PDA program displays a roster of patients being monitored and their main vital signs. It also has the ability to query the server for data for a particular patient and show live or retrospective ECG and SpO_2 data. This communication is encrypted to protect patient privacy, since at this point patient names are associated with the data. Both programs present a simple user interface (UI) programmed using Glade and GTK+ for configuration and monitoring.

At the server, data first arrive at ORnetDB. ORnetDB was developed in a previous project as an operating room streaming database. [23] This database is able to log and perform computations on live feeds of incoming data. Raw data and computed data such as QRS positions are then saved into a standard relational database, implemented in PostgreSQL. [24] Finally, the main UI for the operator is programmed in Java. The operator has an overview of all patients being monitored and can select one in particular to view detailed information (Fig. 2.4). There is also a list of issued alarms for all patients being monitored. The patient roster on the top of the screen shows: patient number, in/out status, name, SpO_2 and HR from the finger sensor, calculated HR from the ECG data, the Emergency Severity Index (ESI) [25, 26] assigned upon admission, the algorithm's proposed diagnosis, location and current alarm. Patient management (enrolling in monitoring, and completion of monitoring) is handled via web page forms. Location information is shown on a secondary monitor (Fig. 2.5) with colored tags for the patients and the caregivers, displayed over a map of the waiting area.

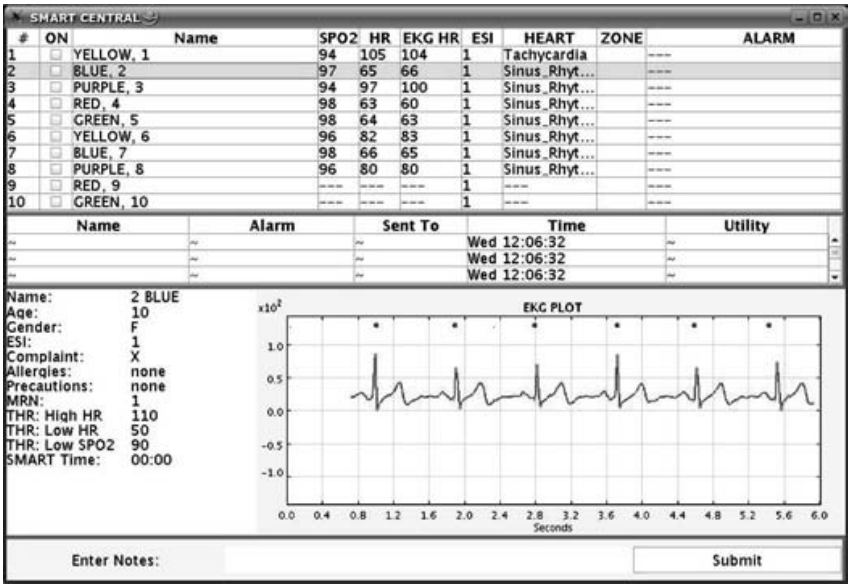

Figure 2.4. SMART central main GUI. See also Color Insert.

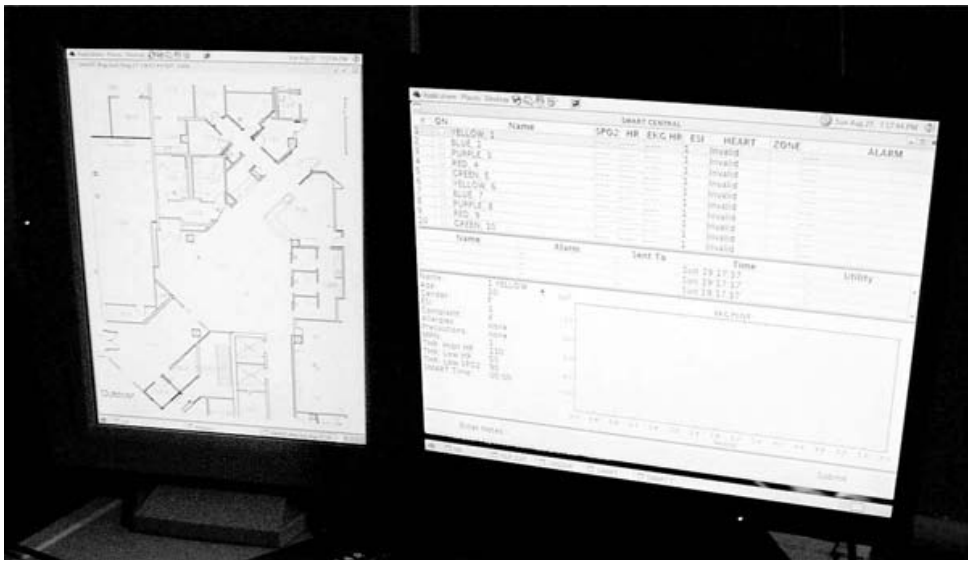

Figure 2.5. SMART dual monitor display. Left: location data. Right: main GUI.

2.2.2 *Clinical Implementation*

The goal of SMART is to enhance response in the presence of a high number of patients. Introducing a large number of wireless monitoring nodes requires that the system assist in the detection

of critical cases. This approach allows scalability with minimal requirements of extra-trained personnel. To this end, SMART implements a set of parameter computations and a decision tree to assist in alarm generation and diagnosis suggestion. To produce a diagnosis algorithm that will feed the alarming system, several steps were necessary. [3] We selected an ECG processing algorithm based on its ability to handle noisy data. 2) The algorithm was tested against standard ECG databases publicly available from Physionet. [27] We conducted tests on healthy volunteers to gain experience handling live and untethered patients. 4) We conducted tests on patient simulators to get feedback on how the system responded to different health conditions.

The final algorithm is programmed based on all the tests and preliminary results. [3] The ECG algorithm is based on the SQRS algorithm available on the Physionet website. The modifications introduced include an auto-calibration interval to account for differences in electrode placement and patient variability, an adaptive threshold to handle noisy segments, and a “no beat” output after 3 s of inactivity. The diagnosis suggestion is based on detected QRS positions and raw ECG statistical properties, sensor integration with SpO_2, and noise detection. All possible diagnoses and alarms generated are shown in Table 2.1.

Sinus rhythm, bradycardia, and tachycardia are determined by simple HR comparison to patient specific thresholds. By default, the low HR threshold is 60 beats per minute (BPM) and the

Table 2.1. Diagnosis suggestions and alarm generation

Diagnosis	Source	Validation	Alarm
Sinus rhythm	ECG or SpO_2	-	None
Bradycardia	ECG or SpO_2	-	Medical
Tachycardia	ECG or SpO_2	-	Medical
Ventricular tachycardia	ECG	-	Medical
Ventricular fibrillation	ECG	SpO_2	Medical
Irregular rhythm	ECG	-	Medical
Asystole	ECG	SpO_2	Medical
Leads off	ECG	-	Technical
Noise	ECG	-	Technical
Mismatch	ECG & SpO_2	-	Technical

high HR threshold is 100 BPM. The HR is either calculated from the detected QRS waves in the ECG or reported by the SpO_2 sensor. Ventricular tachycardia, fibrillation, and irregular rhythm can only be computed from the ECG data, since they depend on QRS width, ECG waveform, and QRS periodicity, respectively. Asystole status is determined when no QRS complexes can be found in the ECG.

Technical alarms are generated when an abnormal situation most likely related to the PDA or sensors (and not the patient) is detected. Leads off is easily detected from the ECG waveform. Noise is indicated by the QRS algorithm when a series of QRS-like peaks are detected in a short period. Finally, the mismatch technical alarm is issued when the ECG and SpO_2 data are contradictory.

The final decision tree programmed in SMART is shown in Fig. 2.6 The diagnosis with the most votes in the preceding 15 s is used as the final suggested diagnosis and alarms are issued for abnormal conditions.

Sensor integration is fundamental for alarm generation. While SpO_2 data proved to be extremely stable, it can't detect certain conditions of interest. ECG provides a quicker response time and better diagnosis capability. However, ECG is highly affected by noise from electrode movements and muscle activity. The solution is to validate preliminary ECG findings with SpO_2 information. For instance, an ECG finding of asystole is not possible with a normal O_2 saturation and reported HR greater than zero.

No major problems were found during the clinical implementation. However, it is clear that if the number of patients were to increase considerably, the load on the main server might become unsustainable. One proposed solution is to push most of the load to the mobile units. This was tested in the early stages of the project but later discarded in favor of a simpler, centralized system. However, all signal processing and alarm generation can run on the patient PDAs. This way, the main server is responsible for only minor tasks. Alternatively, SMART Central could be implemented using multiple computers that share the load as the number of patient nodes increases.

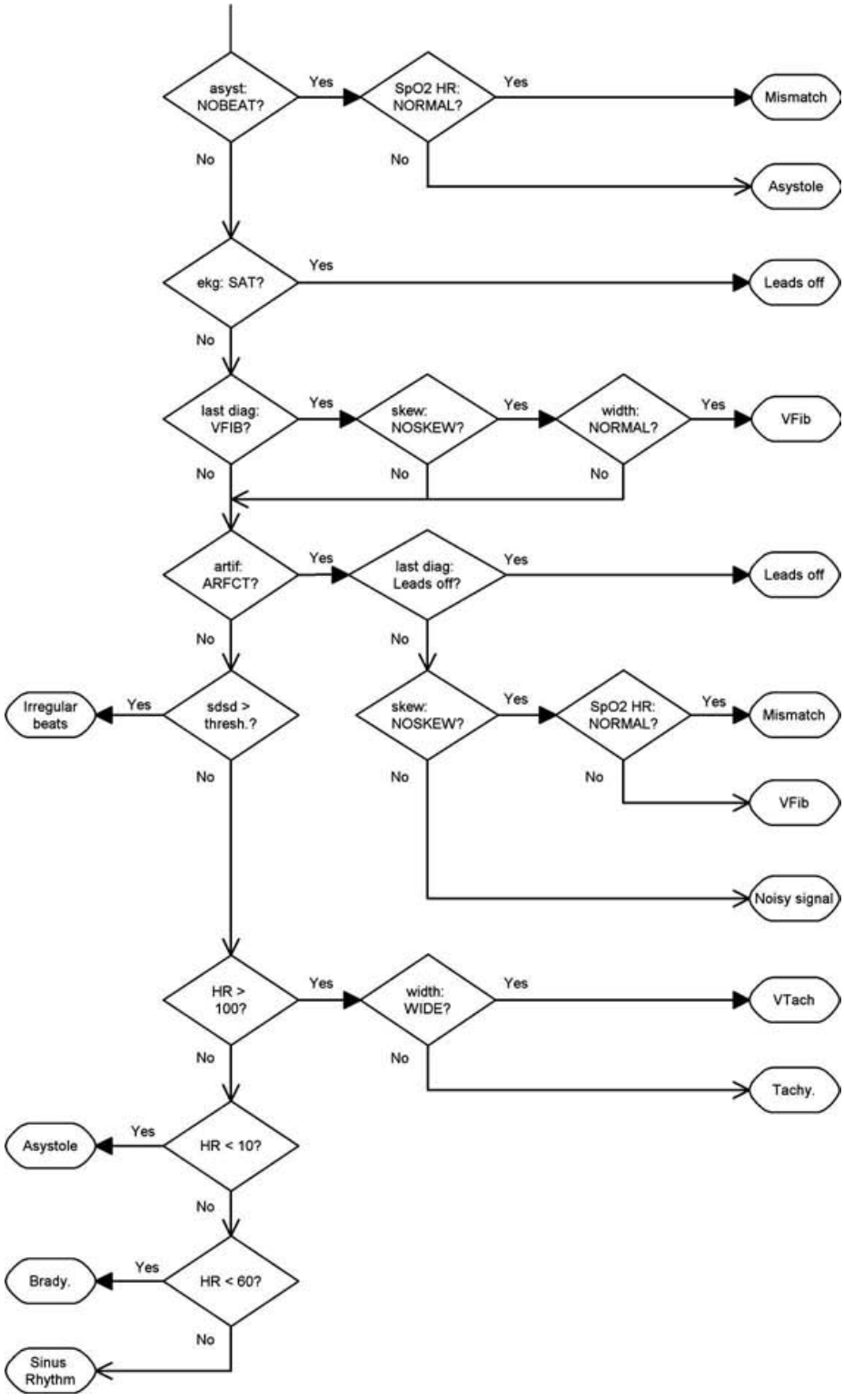

Figure 2.6. Decision tree programmed in SMART for diagnosis suggestion and alarm generation.

2.3 Results

During the implementation in the Emergency Department (ED), some important lessons were learned. Signal quality was worse than in the healthy volunteer training session data. Wireless, nonintrusive systems must be prepared to deal with bad quality data. Despite this, several patients and the system as a whole benefited from SMART. It was possible to detect unnoticed medical conditions and to dismiss a medical complaint sooner by using the data collected from patients in the waiting room. The critical cases were detected by SMART Central and reported to the SMART Operator (whose presence was required by the hospital's Institutional Review Board) and ED personnel were alerted when necessary.

2.3.1 *Medical Usefulness*

ECG, SpO_2, and location data were collected from 145 patients during 18 months. The amount of data collected per patient depends how long the patient was in the waiting room, prior to being seen by a physician. This time ranges from 5 min to slightly over 3 h. Only patients presenting with symptoms of shortness of breath and chest pain were approached for enrollment in the study. This selection was based on which symptoms might deteriorate quickly, resulting in a negative outcome for the patient, which determined the set of physiological sensors available in SMART.

The physiological data collected show that in normal conditions the system works. However, there is an important difference between real patients and simulators or healthy volunteers. The noise level encountered on real patients is much higher than expected, but relatively short-lived. This produces a significant number of false alarms that quickly become annoying to the operator. This usually happens on particular patients for different reasons, the most recurring one being restlessness. However, most patients present a normal, quiet ECG tracing with minimal number of alarms. Setting up and removing the equipment from the patients also causes false alarms. To alleviate this problem, an option is provided in the main GUI to disable alarms for particular patients.

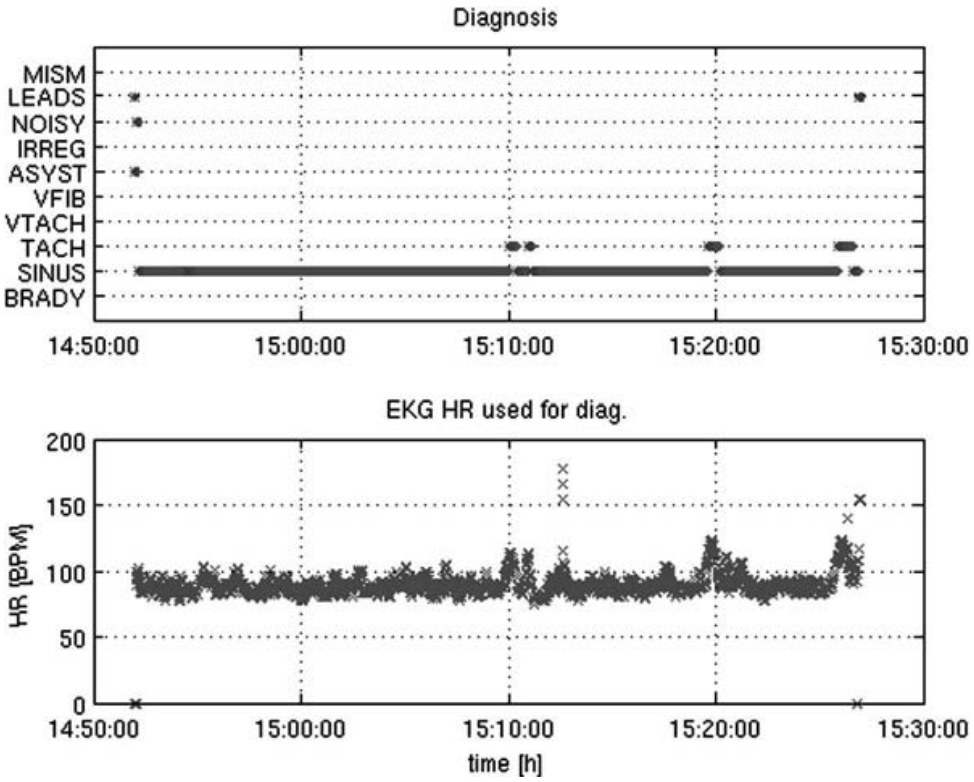

Figure 2.7. Diagnosis estimation and ECG-computed HR of an average patient. See also Color Insert.

This way, the alarm system is not enabled until the patient has settled. Figure 2.7 shows a typical tracing and its accompanying diagnosis suggestion.

During the evaluation period, three patients presented health problems detected by SMART that required re-prioritization. The first case was a patient with premature ventricular contractions that SMART detected as irregular rhythm and tachycardia. The second case presented a severe bradycardia. In the third case, the ECG-reported HR was significantly different than the SpO_2- reported HR. Upon closer examination of the live ECG acquired by SMART, the patient was admitted sooner to the ED, presenting with junctional tachycardia.

The last case worth mentioning is a patient who complained that her pacemaker wasn't working properly. Figure 2.8 shows the ECG HR and SpO_2 HR and the ECG tracing on the bottom. Every time the HR dropped below 60 BPM, the pacemaker is engaged and produces

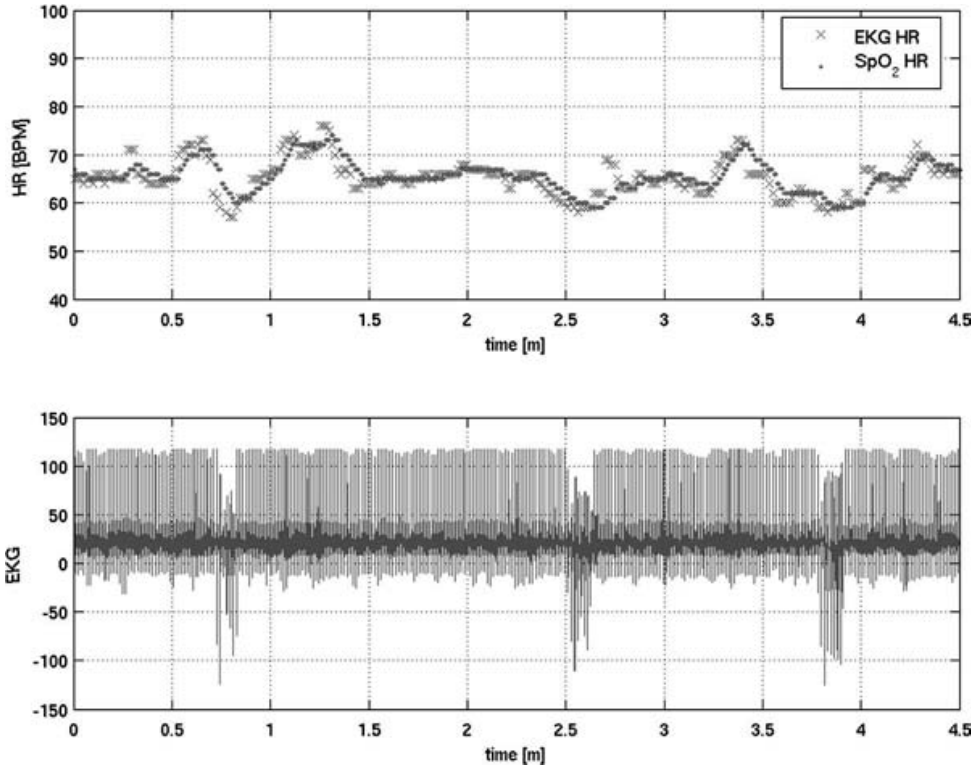

Figure 2.8. ECG – SpO_2 HR comparison and ECG pacemaker activity when patient HR dropped below 60 BPM. See also Color Insert.

a different tracing on the ECG. An added benefit of SMART is that the physicians are presented with valuable information by the time they get to see the patient for the first time, helping their diagnosis.

2.3.2 *User Acceptance*

Acceptance among the patients was very good. Most patients felt safer as they knew they were being monitored. For them, it was a large improvement over just waiting to be seen by a physician. Knowing that their location was known also helped build confidence in case they needed prompt care.

A survey was conducted among the patients right after they were admitted into the ED. Seventy patients completed the survey that evaluated their perception of the system. Figure 2.9 shows that 51% of the patients would definitively wear the system again. Another 41% would be inclined to do so. Only 7% are against or did not respond to the question. To the question "Did the monitoring system

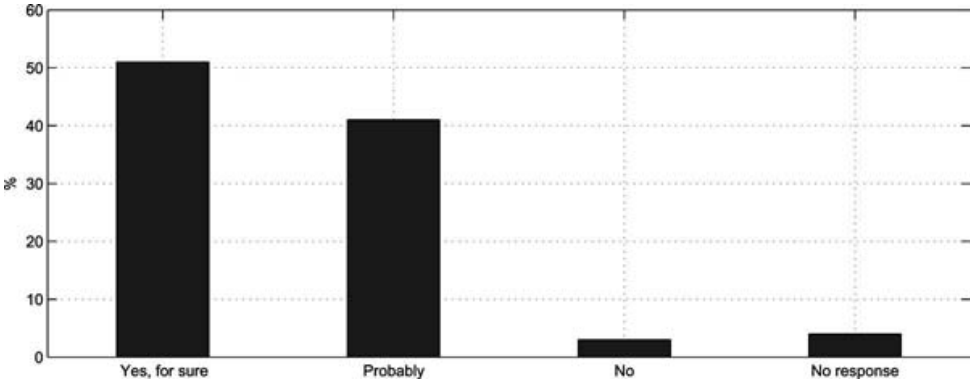

Figure 2.9. Response to survey question: Would you wear a SMART pouch again?

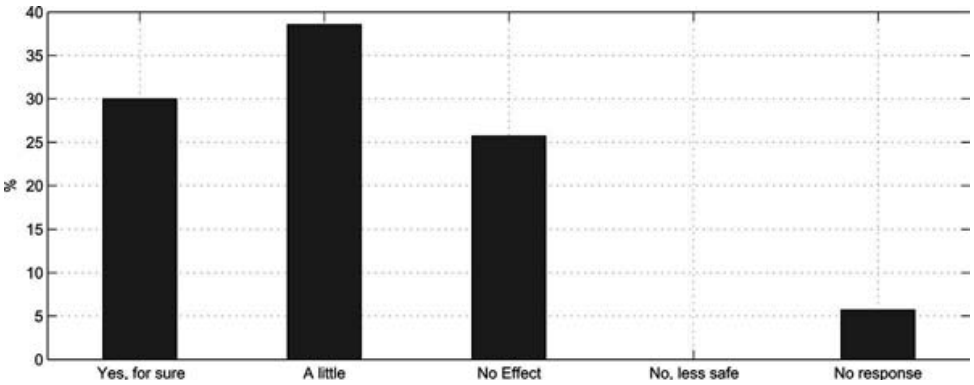

Figure 2.10. Response to survey question: Did the monitoring system make you feel safer?

make you feel safer?," over 69% of the patients answered positively, as shown in Fig. 2.10

Even though the patients who participated in this study were told that the system would not change the attention provided by the hospital, Table 2.2 shows that most of them felt that they were getting a higher level of care.

We also asked the patients about their perception of the value of having their location and their vital signs being monitored. We were concerned that they might find the location sensor too intrusive. However, 84.3% considered the location information valuable and 94.3% considered vital sign monitoring valuable (Table 2.3).

Finally, a majority of the patients found the system acceptably comfortable to wear (Table 2.4).

Table 2.2. Perceived effect on care

Effect of SMART monitoring on care	Preferences
Improved it a lot	17%
Improved it a little	24%
No effect	49%
Impaired it a little	0%
Impaired it a lot	0%

Table 2.3. Perceived value of monitoring

Category	Location	Vitals
Very important	68.6%	78.6%
A little	15.7%	15.7%
Not important	12.9%	5.7%
Not important and actually annoying	0.0%	0.0%
No response	2.8%	0.0%

Table 2.4. Patient evaluation of system comfort

Was the monitoring system comfortable?	Preferences
Didn't bother at all	82.9%
A little uncomfortable	14.3%
Very uncomfortable	1.4%
No response	1.4%

2.4 Conclusion

The SMART system facilitates the collection, storage, review, and detection of events that otherwise may go unnoticed regarding the patients' medical conditions. To accomplish this, the set of sensors on each patient in conjunction with the patient's PDA send their data wirelessly to a central station where individual care needs are evaluated.

SMART addresses the need to provide better care to multiple patients. It can extend care to nonstandard settings such as nursing homes for the elderly, improvised care facilities in case of mass

casualty events, locations designed for patients such as hospital waiting rooms, and homes or offices for people at risk during their daily activities. As cited, there is concern among health care facilities regarding patients in unmonitored areas. [19] In standard care centers, a wireless monitoring system that provides alarms for critical cases can reduce the workload on the triage staff and provide a better quality of care for the patients. Initial triage assessment time can be reduced, and by the time a physician first contacts the patient, a considerable amount of physiological data is available.

One of the main advantages of wireless networks in medicine is the ability to provide an enhanced level of care without interfering with the patient's quality of life. Even though in SMART the sensors are wired to the PDA hub on the patient, the wireless transmission of the data to a central station allows patients be untethered. The survey conducted among patients after wearing the device shows with high satisfaction levels, both in terms of care and comfort.

Acknowledgements

This work was supported in part by the National Library of Medicine, NIH, N01LM33509.

References

1. World Health Organization data and statistics (April 2010), URL: http://www.who.int/research/en/.
2. J. Waterman, D. Curtis, M. Goraczko, E. Shih, P. Sarin, E. Pino, L. Ohno-Machado, R. Greenes, J. Guttag, and T. Stair (2005) Demonstration of SMART (Scalable Medical Alert Response Technology), in *AMIA 2005 Annual Symposium*, Washington, DC, American Medical Informatics Association, pp. 1182–1183.
3. E. Pino, L. Ohno-Machado, E. Wiechmann, and D. Curtis (2005) Real–Time ECG Algorithms for Ambulatory Patient Monitoring, in *Proceedings of the AMIA Annual Symposium,* pp. 604–608.
4. D. W. Curtis, E. J. Pino, J. M. Bailey, E. I. Shih, J. Waterman, S. A. Vinterbo, T. O. Stair, J. V. Guttag, R. A. Greenes, and L. Ohno-Machado (2008) SMART — An Integrated Wireless System for Monitoring Unattended Patients,

Journal of the American Medical Informatics Association, **15**(1), pp. 44–53. doi: 10.1197/jamia.M2016.

5. S. P. McGrath, E. Grigg, S. Wendelken, G. Blike, M. D. Rosa, A. Fiske, and R. Gray (2003) Artemis: A Vision for Remote Triage and Emergency Management Information Integration, URL: <http://citeseerx.ist.psu.edu/viewdoc/summary? doi>= 10.1.1.128.4959.
6. S. M. Wendelken, S. P. McGrath, and G. T. Blike (2003) A Medical Assessment Algorithm for Automated Remote Triage, in *Proceedings of the 25th Annual Conference of the Engineering in Medicine and Biology Society,* Cancun, pp. 123–135.
7. P. Konoske, W. Deniston, R. Barker, and D. Moses (1998) Evaluation of the Mobile Medical Monitor (m3) in a Field Environment, in *Proceedings of the Medical Technology Symposium,* Pacific, pp. 83–92, doi: 10.1109/PACMED.1998.767929.
8. C. Orwat, A. Graefe, and T. Faulwasser (2008) Towards Pervasive Computing in Health Care — a Literature Review, *BMC Medical Informatics and Decision Making*, **8**(1), pp 26, ISSN 1472-6947, doi: 10.1186/1472-6947-8-26, URL: http://www.biomedcentral.com/1472-6947/8/26.
9. J. P. Killeen, T. C. Chan, C. Buono, W. G. Griswold, and L. A. Lenert (2006) A Wireless First Responder Hand-Held Device for Rapid Triage, Patient Assessment and Documentation During Mass Casualty Incidents, in *Proceedings of the AMIA Annual Symposium*, pp. 429–433.
10. L. Lenert, D. Palmer, T. Chan, and R. Rao (2005) An Intelligent 802.11 Triage Tag for Medical Response To Disasters, in *Proceedings of the AMIA Annual Symposium,* pp. 440–444.
11. M. Arisoylu, R. Mishra, R. Rao, and L. A. Lenert (2005) 802.11 Wireless Infrastructure To Enhance Medical Response to Disasters, in *Proceedings of the AMIA Annual Symposium*, pp. 1–5.
12. T. Massey, T. Gao, M. Welsh, J. H. Sharp, and M. Sarrafzadeh (2006) The Design of a Decentralized Electronic Triage System, in *Proceedings of the AMIA Annual Symposium*, pp. 544–548.
13. D. Malan, T. Fulford-Jones, M. Welsh, and S. Moulton (2004) CodeBlue: An Ad Hoc Sensor Network Infrastructure for Emergency Medical Care, in *International Workshop on Wearable and Implantable Body Sensor Networks*.
14. T. Gao, M. I. Kim, D. White, and A. M. Alm (2006) Iterative User-Centered Design of a Next Generation Patient Monitoring System for Emergency Medical Response, in *Proceedings of the AMIA Annual Symposium*, pp. 284–288.

15. T. Gao and D. White (August 2006) A Next Generation Electronic Triage To Aid Mass Casualty Emergency Medical Response, in *28th IEEE Annual International Conference of the Engineering in Medicine and Biology Society,* pp. 6501–6504, doi: 10.1109/IEMBS.2006.260881.
16. Y.-H. Lin, I.-C. Jan, P. C.-I. Ko, Y.-Y. Chen, J.-M. Wong, and G.-J. Jan (2004) A Wireless PDA-Based Physiological Monitoring System for Patient Transport, *IEEE Transactions on Information Technology in Biomedicine*. **8**(4), 439–447, ISSN 1089-7771.
17. C. F. Mackenzie, P. Hu, A. Sen, R. Dutton, S. Seebode, D. Floccare, and T. Scalea (2008) Automatic Pre-Hospital Vital Signs Waveform and Trend Data Capture Fills Quality Management, Triage and Outcome Prediction Gaps, in *Proceedings of the AMIA Annual Symposium,* pp. 318–322, URL: http://www.pubmedcentral.nih.gov/articlerender.fcgi? artid=2656089.
18. P. Pandian, K. Mohanavelu, K. Safeer, T. Kotresh, D. Shakunthala, P. Gopal, and V. Padaki (2008) Smart Vest: Wearable Multi-Parameter Remote Physiological Monitoring System, *Medical Engineering and Physics*, **30**(4), pp. 466 – 477, ISSN 1350-4533, doi: DOI:10.1016/j.medengphy.2007.05.014, URL: http://www.sciencedirect. com/science/article/B6T9K-4PNF2X4-1/2/733ffbd1f1553e04ed4fc73ef1331c40.
19. C. V. Pollack (March 2009) Wireless Cardiac Event Alert Monitoring Is Feasible and Effective in the Emergency Department and Adjacent Waiting Areas, *Crit Pathw Cardiol*, **8**(1), pp. 7–11, doi: 10.1097/HPC.0b013e3181980f8b, URL: http://dx.doi.org/10.1097/HPC.0b013e3181980f8b.
20. D. Raskovic, T. Martin, and E. Jovanov (2004) Medical Monitoring Applications for Wearable Computing, *The Computer Journal*, **47**(4), pp. 495–504, doi: 10.1093/comjnl/47.4.495, URL: http://comjnl.oxfordjournals.org/cgi/content/abstract/47/4/495.
21. Nonin Medical Inc. Nonin Medical Inc., http://www.nonin.com/.
22. Sonitor R home page, Sonitor R Technologies Inc., URL: http://www.sonitor.com. Accessed April 30, 2010.
23. D. W. Curtis, ORNetDB software, Available on request from dcurtis@csail.mit.edu.
24. PostgreSQL open source database, URL: http://www.postgresql.org/.
25. P. Tanabe, D. Travers, N. Gilboy, A. Rosenau, G. Sierzega, V. Rupp, Z. Martinovich, and J. G. Adams (2005) Refining Emergency Severity Index Triage Criteria, *Academic Emergency Medicine*, **12**(6), pp. 497–501.

26. R. C. Wuerz, L. W. Milne, D. R. Eitel, D. Travers, and N. Gilboy (2000) Reliability and Validity of a New Five-Level Triage Instrument, *Academic Emergency Medicine*, **7**(3), pp. 236–242, doi: 10.1111/j.1553-2712.2000.tb01066.x.
27. A. L. Goldberger, L. A. N. Amaral, L. Glass, J. M. Hausdorff, P. C. Ivanov, R. G. Mark, J. E. Mietus, G. B. Moody, C. -K. Peng, and H. E. Stanley (2000) PhysioBank, PhysioToolkit, and PhysioNet: Components of a New Research Resource for Complex Physiologic Signals, *Circulation*, **101**(23), pp. 215–220, doi: http://circ.ahajournals.org/cgi/reprint/101/23/e215.pdf.

Chapter 3

Real-Time Cardiac Arrhythmias Monitoring for Pervasive Health Care

Zhou Haiying,[a] Hou Kun-Mean,[b] de Vaulx Christophe,[c] and Li Jian[d]

[a]*School of Computer Science and Technology, Harbin Institute of Technology, N.92, Xi DaZhi Jie, Harbin, China*
[b]*Laboratoire LIMOS UMR 6158 CNRS, ISIMA, University of Blaise Pascal Clermont-Ferrand II, France*
[c]*Polytech'Clermont-Ferrand, CUST, University of Blaise Pascal Clermont-Ferrand II, France*
[d]*School of software, Harbin Institute of Technology, N.92, Xi DaZhi Jie, Harbin, China*
haiyingzhou@hit.edu.cn; kun-mean.hou@isima.fr; christophe.devaulx@cust.univ-bpclermont.fr; lijian_susan@hit.edu.cn

Pervasive health care (PHC) is a new health care model that enables patient mobility, continuous health monitoring, and timely detection of anomalies. Comparing with the ideal PHC services, the current available (commercial) remote patient monitoring services such as portable monitoring equipment and prototype systems need to be improved in real-time capability, effectiveness, and reliability of context-sensitive anomaly detection. This chapter addresses the PHC system architecture and anomaly detection techniques for chronic diseases; a pervasive cardiac care (PCC) prototype that supports real-time indoor and outdoor continuous

Wireless Body Area Networks: Technology, Implementation, and Applications
Edited by Mehmet R. Yuce and Jamil Y. Khan

ISBN 978-981-4316-71-2 (Hardcover), ISBN 978-981-4241-57-1 (eBook)
www.panstanford.com

cardiac arrhythmias monitoring service health care models is presented. Moreover, this chapter explores key PHC technologies such as architecture model and system, including context-aware recognition, abnormal detection, and adaptive environment, etc.

3.1 Introduction

Health care, as an essential part of modern society, which contributes to social stability and government reputation, claims a remarkable percentage of national budgets. Due to global population aging in the 21st century, health care system worldwide is facing a serious shortage of financial and human resources [1, 2].

World Health Organization (WHO) reports that the world's aging population over the age of 65 is reaching 761 million in 2025. [3, 4] The white paper of "The Development of China's Undertakings for the Aged" declares that China is entering the aging society [5]. By the end of 2005, the aging population over 60 in China was more than 1.44 million, and will reach 400 million in 2037, ranking first in the world [6, 7]. Furthermore, China is suffering from a serious shortage and an extremely unbalanced distribution of health resources: China takes up 22% of world population, yet only 2% of world total health resources, among which the 80% of the health resources in China is concentrated in urban areas, and the 80% of the urban resources is concentrated in handful large hospitals. Therefore, in China, the severe contradiction between supply and demand of health care services is prominent [8, 9].

Many studies have shown that more than 80% elderly people have chronic diseases as well as lifestyle-related diseases, and more than 30% of them suffer from two or more types of chronic diseases [10, 11]. Further studies reveal that long-term continuous health care observations, rather than clinical care or treatment, are essential for patients suffering from several chronic diseases. Also according to epidemiological data and related research findings, we discover that successful prevention and reduction of acute attack of diseases depends on the improvement of health care quality, proactive management of chronic diseases, detection of abnormal symptoms, and healthy out-of-hospital lifestyles [12].

To cope with the rapid rise of medical cost and the growing shortage of health care capabilities, a personalized out-of-hospital healthcare model, which supports independent lifestyle, is highly demanded [3, 13]. The model is characterized by its: (1) excellent chronic disease management in 7×24 h, by assisting medical experts with technologies of pervasive biomedical sensing, computing and communication; (2) excellent abnormality detection ability, which effectively helps avoid emergencies (sudden death); (3) timely and accurate health care services and emergency handling capability, available anytime anywhere [14, 15].

PHC is designed to provide high-quality health care services for patients or elderly people with more than one chronic disease. By integrating and balancing health care resources and thus reducing medical cost, PHC is a strong complement for the existing health care system in China and developed countries. With the help of PHC model, health care providers can largely be relieved from physical and mental pressures, the quality of collaborate-treatment can be improved and the cost be lowered, and eventually a better and healthier out-of-hospital lifestyle can be established for the patients [8].

Patient health care service is a billion-dollar industry [16]. Yet, research on the key technologies of PHC system model and service provision is still rare [17]. Hence, the major research purposes of this chapter are: (1) to provide the designing rules of PHC services and to explore PHC service model; (2) to study the key technologies of PHC for chronic diseases, including context-aware computing, abnormal detection and environment adaptive technologies, etc. Health care is crucial not only to people's lives and physical health, but also to national security and harmony. PHC is the technical foundation of future health care system, particularly in China. The application of PHC service will help to solve the conflict between resources and needs, and eventually facilitate social stability. By adopting pervasive service and IT technology and integrating pervasive computing concept into health care services, this chapter proposes an innovative service model for public and private PHC services provision with no limitation in time and place.

3.2 History of PHC Research

PHC technology, as a cutting edge of its kind, demonstrates significant differences in research content, methods, and techniques from its counterparts such as biomedical engineering technology, medical informatics, and pervasive computing technology. Due to the complexity, diversity, and variability of PHC applications, how to build a ubiquitous ICT-based embedded biomedical technology health care environment, is a complicated interdisciplinary research issue [18]. This chapter provides a review of the state-of-the-art of research and development in the PHC field.

Today the progress in areas of wireless communication technology and medical telemetry equipment has set forth the rapid advancement of patients' clinical care and out-of-hospital care, and a variety of patient monitoring systems have thus been developed and applied. Thanks to the technology development in pervasive computing, medical engineering, medical telemetry, and other associated disciplines, it is now possible to extract, record, analyze, and transmit data concerning patients health symptoms (in the form of physical signal characterization) in a timely way via medical equipment worn by patients to the computer or PDA device of medical service providers. In this way, the time required for medical diagnosis and treatment is largely reduced [15, 19]. Lately, research institutions and organizations involved in health care studies have made a remarkable achievement in developing patient monitoring prototype system for accurate monitoring of patients' vital signs and timely detection of patients' abnormal signs [20]. Recognizing the importance of the aged health care market, a number of world-renowned medical equipment companies, including General Electric, Hewlett-Packard, Honeywell, and Intel, jointly set up Research Center for Aging Services Technology (CAST) in 2002 in Washington, so as to promote the application of wireless and remote patient monitoring service model and to encourage the joint efforts in technology development and cooperation of elderly people service.

The development of a health care prototype system has gone through three typical phases [17]. According to the patient monitoring scene, the prototype can be divided into three different

types: hospital clinical care, home care as well as outdoor mobile monitoring [21]. The first generation of monitoring systems, such as Micropaq [22], collects and transmits multi-parameter monitoring information via short-range wireless medium (such as Bluetooth) to the network infrastructures within the building framework in the hospital. The second generation of surveillance systems, such as Medtronic [23], supports patient monitoring at home and is able to make time-appointed collection and transmission of patients' information. Based on television and cable networks, Motiva system provides a secure, personalized health care communication platform, which supports the interaction between patients at home and remote service providers, so as to achieve monitoring and management of chronic diseases and to improve patients' quality of life [24]. Other second-generation systems, such as CardioNet [25] and Biotronik [26], provide short-term care for patients at home (7–14 days). The new generation of surveillance systems is designed for mobile patients with continuous collection and transmission of patients' vital signs via infrastructure-based wireless networks (WLAN, cellular PCS, satellite, etc.). Relative research includes smart wearable health care research [27], medical telemetry devices [28], PDA Mobile Gateway [29], smart clothing care [30] and so on. References [31–34] present recent researches of the medical decision-making research for PHC service. There are also some typical PHC systems for elderly people such as Gator Tech Smart Room [35], perception Room [36], and the elite care [37].

By now, a large number of health care prototype systems have been designed, but there is still not much study in the architecture model of PHC system. The existing literature also mainly addresses the requirements and challenges in PHC system design, but not the actual system modeling. Kafeza et al. [38] analyzed the demand model of warning messages delivery. From the point of view of ICT infrastructure, Haux et al. [39] defined four types of health care architectures: people-centered, family-centered, remote health care service-centered, service provider-centered. The main functions of health care service are classified as: emergency state detection and alarm, disease management, health status feedback and suggestions. It also proposes the main components of a 24 h medical care environment: indoor home

monitoring system, remote monitoring and location-based outdoor activities, emergency rescue system, and service support system. Koch et al. [40] investigated the relevant researches in the health care field in recent five years and classify them into five categories: decision support information systems, consumer health informatics, and remote home healthcare, emergency information technology, and informatics methods. According to the service controllability and application location, Doukas et al. [41] divided health care into two categories: health controlled environment (such as health care units and hospitals) and immediate health care services unavailable environment (such as at home or outdoor). Sneha et al. [17] proposed a component-based system framework of pervasive health care service and explore the design methods of major system components (sensing, reasoning, and transferring function). Based on the wireless sensor network technology, Daramolar et al. [42] presented a grid-based framework for PHC system. By analyzing the existing pervasive health care applications, Salvador et al. [43] attempted to define a general PHC system framework, which is compatible with its software and classify the PHC application into three types of typical environment: home, grid space, and mobile space.

Although some remarkable achievements in the field of patient care have been made, there are still some major limitations and constraints: 1) the majority of proposed solutions is not dedicated to PHC services, and there is no in-depth study of the application characteristics of PHC, such as patient mobility, continuous monitoring, and timely detection of anomalies; 2) most of the solutions do not make full use of mobile computing platforms for biomedical data analysis, which not only produces large amount of raw data that leads to high network traffics and more bandwidth requirements, but also brings huge mental and physical pressure on medical professionals when performing signal analysis and abnormalities monitoring.

Between the ideal PHC services and the current remote patient monitoring services with commercially available portable monitoring equipment and prototype systems, a huge gap still exists, especially in their real-time capability, effectiveness and reliability of context-sensitive anomaly detection. Partly because the existing solutions are lack of in-depth understanding, exploration of the

complicated processing mode, the relevant system parameters as well as reasoning and decision-making mechanisms of the PHC system.

To solve the above problems, this chapter addresses the PHC system architecture and anomaly detection techniques for chronic diseases. The objective of this chapter is 1) to provide timely anomaly detection, prevent sudden attack of illness, and reduce avoidable medical costs; 2) to provide a PHC service, which is based upon the mobile computing platform, with the capabilities of biomedical data analysis and medical intervention, and is able to reduce network traffics and bandwidth requirements. This chapter presents a WSN-based pervasive cardiac care prototype that supports clinical, home, and outdoor models to provide continuous cardiac arrhythmias monitoring service [44, 45]. Based on this prototype system, this chapter explores the system architecture technology [46, 47], context-aware recognition and abnormal detection technology [48, 49], adaptive environment technology [50], and so on.

3.3 Overview of PCC System

Heart disease ranks as the top threat to human health. Elderly people and middle-aged person in long-term sub-health state are among the high risk population of cardiac sudden death (CSD). Clinical experiences prove that the most efficient way to prevent CSD is to detect the cardiac abnormalities in time by making long-term regular cardiac monitoring. Traditional health care systems are not suitable for pervasive cardiac monitoring (PCC) due to the time and space constraints in health care applications, as well as the inability of real-time continuous ECG monitoring. In recent years, a new generation of cardiac monitoring system named pervasive cardiac monitoring is booming. By introducing ubiquitous computing into traditional healthcare, the PCC system provides a real-time continuous cardiac monitoring service for different subjects with no constraints of time or space.

3.3.1 *PCC System Architecture*

The PCC system integrates the advanced technologies of wireless communication, embedded system, automatic ECG diagnosis (AED),

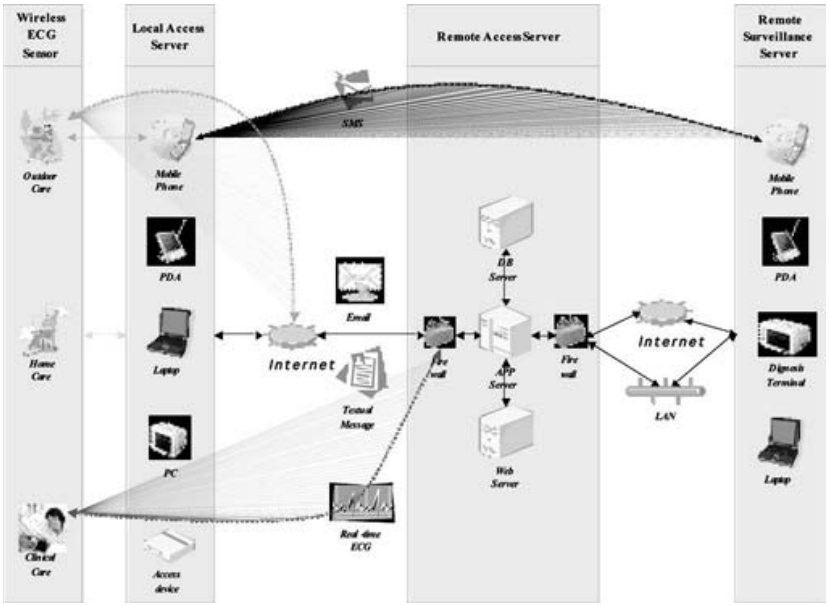

Figure 3.1. Architecture of PCC system. See also Color Insert.

and telemedicine, which consists of four main functional components: wireless ECG sensor (WES), local access server, remote access server, and remote surveillance terminal. Figure 3.1 shows the architecture and operation fashions of the PCC system.

3.3.1.1 Wireless ECG sensor

To minimize cost and to correspond to the latest AHA recommendations [51], an energy-efficient compact ECG collection device, named WES, is implemented. WES conforms to the basic characteristics of wireless sensor device: tiny resource, tiny power-consumption, and associated tiny cost. Furthermore, the basic embedded software such as a distributed real-time fault tolerant microkernel [52], dedicated hardware and firmware [53], and a TCP/IP protocol stack [54] are implemented and ported into WES.

The WES prototype (Fig. 3.2) is a real-time wireless embedded portable sensor (size $=$ 70 mm $\times$ 100 mm) based on TI MSP430 microcontroller. The key features of WES are

- Gain: 1000
- CMMR (min): 120 dB
- Bandwidth: 0.05 Hz to 125 Hz

Figure 3.2. Wireless ECG sensor. See also Color Insert.

- Programmable sample frequency more than 500 Hz
- Analogue to digital converter (ADC): 12 bit
- Leakage current: 10 μA

WES enables the capture of 4-leads ECG signals sampled at 500 Hz (sample frequency) in real-time. Note that the sample frequency is reprogrammable (100 Hz to 2000 Hz). The sample data is sent to the local server over a wireless medium such as Wi-Fi or Bluetooth. In offline mode, ECG signals can be stored in the flash memory card. The signal store duration depends on the flash card capacity, the sample frequency, and the number of ECG leads. For example, a 128 megabyte flash memory card can store 24 h data of continuous 4-leads ECG signals sampled at 500 Hz. In this way, the WES works as Holter or RTEST device.

3.3.1.2 Local access server

Local access server may be implemented on a standard PC, a PDA, a mobile phone, or a dedicated network access device. It provides two kinds of network connection services: connection with WES via a local wireless medium (Wi-Fi or Bluetooth) and connection with remote system via infrastructure network, such as cable modem, ADSL, 2G/3G, etc.

In view of the difference of network mediums, local servers, and transmission speeds caused by network traffics, the PCC system provides an adaptable communication mechanism to guarantee a reliable data transmission service between local server and remote server. Furthermore, in order to provide a real-time data transmission, it is important to minimize the amount of transmission data

to reduce network traffics over low-bandwidth connection links. A lossless ECG signals compression algorithm is thus implemented.

If the local access server is a high-performance machine, the ECG diagnostic module can be migrated from WES into the local server and the cost of WES will thus be reduced. In addition, patients' video information is necessary as an aided method for online diagnosis. Hence, a "webcam" can be installed in the local server to provide patients' images.

3.3.1.3 Remote access server

The remote access server provides the capability of network connection between local access server and remote surveillance server. In view of network types, it can support two types of access servers: PPP server and WAP server. The PPP server establishes connections between patients and cardiologists via PSTN, while the WAP server establishes the connections via wide wireless network. In addition, if the patients and the cardiologists are located in a same area (e.g., in hospital or at clinic) and share local network infrastructures (e.g., high-speed LAN), or they utilize the global network connection services provided by commercial ISPs (Internet service providers), this component is no more necessary and can be removed from the PCC system architecture.

Several function modules can be loaded in the remote access server, including database service and Web service. The medical history records of patients are important for the diagnosis of heart diseases. In the remote access server, the medical records with multimedia formats are stored in the patient database system, which include the ECG signals sequences, cardiologists' diagnostic reports, patients' video, voice and individual profile information, etc. The Web service provides the capacity of Internet access to the patients' database system.

3.3.1.4 Remote surveillance server

The remote surveillance server has an interactive visualization graphical user interface (GUI, see Fig. 3.3) which enables cardiologists to diagnose cardiac arrhythmias events in real-time and

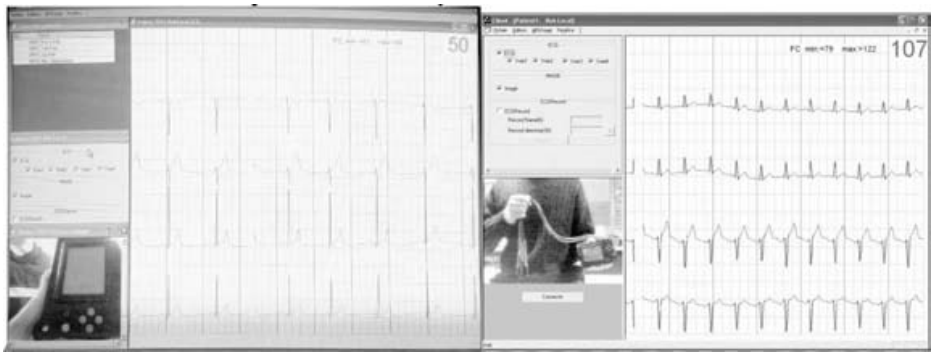

Figure 3.3. Remote surveillance server. See also Color Insert.

to respond to alarm messages by monitoring the ECG signals sequence and patients' images. This server supports multi-patients surveillances and one patient on-line diagnosis (by cardiologists) at one time. The 4-lead ECG signals and related diagnostic results (by the AED algorithm) are displayed on the screen and stored into data files with the format of WaveForm DataBase (WFDB) [55]. The diagnostic reports can be produced automatically and be printed with the ECG signals sequence and the related statistic results.

When a patient's number of a PCC application is few, e.g., an application of small clinic, the cardiologist of the remote surveillance server can directly connect with the patient in the local access server via the Internet. In this way, the database service and Web service can be implemented directly in the remote surveillance server.

3.3.2 *PCC Operation Modes*

This PCC system enables four operation modes which work together to make the system always adaptable to different application scenarios and requirements. Cardiologists can reset the operation mode by taking into account patients' physical status and network medium access bandwidth. The key features of the four operation modes are illuminated as follows:

- *Real-time continuous ECG signal*. For the sake of remote real-time displaying and diagnosing, the data including continuous ECG signals acquisition and its diagnosis report will be sent in real-time to the remote system. This

operation mode has the highest alarm level that enables on-line diagnosis in real-time. Note that this mode does not fit to monitor a large number of patients due to the limitations of network bandwidth, system resources and medical resources, but it has remarkable performance in monitoring the CSD high risk patient. In practice, each cardiologist can survey approximately four patients simultaneously. In this mode, to assure reliable cardiac arrhythmias diagnosis, a patient's image is required.

- *ECG signal sequence*. In order to satisfy remote real-time multi-patient detection and monitoring, WES is configured to send automatically a sequence of ECG signals (pre- and post-abnormality) to the remote system when a cardiac arrhythmia event defined by cardiologists is detected. This operation mode is suitable for long-term multi-patient (lower risk of sudden death than the previous class of patients) cardiac arrhythmias events surveillance.
- *Textual emergency message*. In this mode, only a short textual emergency message will be sent to cardiologists when a cardiac arrhythmia event is detected. According to the gravity of the symptom, the cardiologists can decide to intervene immediately or later. This mode may be operated on any access medium (wire or wireless).
- *Diagnosis report email*. It is the lowest level operation mode. The local server will send periodically a report (like HOLTER report) attached to an email to the remote server. The cardiologists predefined the reporting period. This mode is suitable to monitor a large number of patients.

It is to be noted that cardiologists can remotely reconfigure the operation mode to adapt to the changes of a patient's status and environments.

3.4 Key Technologies of PCC System

In this chapter, we present the key technologies developed for the PCC system, including the lossless signal compression technique,

adaptive real-time communication mechanism, and the adaptive ECG diagnosis (AED) algorithm.

3.4.1 *Lossless ECG Signal Compression*

Minimizing the amount of the data transmission is the most effective technique to reduce network traffics, and it is thus necessary to compress the ECG signals before data transferring. The 500 Hz sampling frequency in WES offers high quality ECG signals for the ECG diagnosis, but also increases network traffics for the data transmission. For example, a 4-lead ECG signals with 500 Hz sampling frequency and 12 bit sample data (ADC resolution), the size of its 5 s frame is 20 KB (4 leads * 500 Hz * 5 s * 2 byte). In order to support real-time data transmission through classical modem, the network bandwidth must be superior to 32 Kbps (20,000 * 8 bit/5 s) when PCC works in the level-I operation mode. This speed is obviously unfitted for the low bandwidth networks. The ECG signals with the high sampling frequency (500 Hz in WES) are absolutely necessary to guarantee the accuracy of the AED algorithm. Note that ECG signals with the low sampling rate (often 128 Hz) are acceptable for the purpose of the ECG observation in the remote visualization system. In general the ECG signals issued from HOLTER devices are sampling at 128 Hz. Hence, the sampling frequency of ECG signals can be sub-sampled to reduce network traffics.

On the other hand, the morphological features of ECG signals show that the signals have huge data redundancies. A good data compression algorithm can thus reduce network traffics. In fact, there are many high ratio data compression techniques such as MPEG3/4, etc., but they are lossless and CPU time consuming. Thus, to minimize energy consumption and ease VLSI integration of WES, we adopt a very simple no-loss compression algorithm: only the difference value between two consecutive samples is sent to the remote server. Since the potential amplitudes of the ECG signals in the cardiac cycle duration are almost equal to the zero isoelectric value, the difference value between the samples data of the cardiac cycle duration is thus almost equal to zero. According to the data sizes of the difference values, the sample compression format is defined in Fig. 3.4.

1 bit	2 bit	1 or 5 or 9 or 13 bit
+/-	type	data
	00	1
	01	5
	10	9
	11	13

Figure 3.4. Data format of signal compression algorithm.

Where the "$+/-$" field indicates the positive/negative property of the difference value: 1 — positive and 0 — negative; the "type" field indicates the type of data length, and the "data" field stores the difference data. The statistical results show that this compression algorithm has 50%–60% compression ratios. Hence, in case of a 4-lead ECG signals at 500 Hz sampling frequency and 12 bit ADC resolution, when adopting the sub-sampling frequency technique (to 125 Hz) and the signal compression algorithm, PCC can reduce 87.5% $\sim$ 90% network traffics.

3.4.2 *Adaptive Communication Mechanism*

In order to support a real-time data transmission, the UDP protocol is adopted in PCC to transmit ECG signals. Because the UDP protocol does not offer a guaranteed datagram delivery service, a reliable data transmission mechanism must be implemented in the application layer. In fact, the network bandwidth of the PCC communication system is normally fluctuated and affected by network traffics and some interference factors, an application layer communication mechanism dedicated to PCC is thus implemented, which enables reliable real-time data transmission in various healthcare environments.

3.4.2.1 PCC data frame

The transfer data unit between remote and local peers in PCC is named a *PCC frame*, which is used to establish/terminate connection, to deliver data (ECG signals or images), and to configure operation modes or other system parameters. Each frame consists

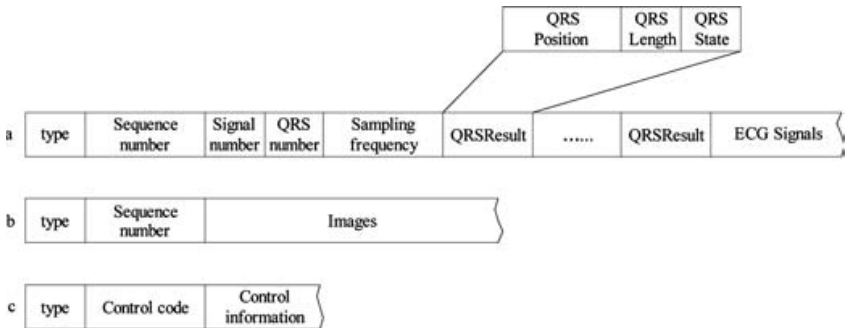

Figure 3.5. Frame format of PCC.

of two parts: a frame header followed by data. Figure 3.4 shows the PCC frame format.

The type field is used to identify the type of PCC frame. Three frame types are implemented in PCC: a value of 0×01 indicates a system control frame; a value of 0×02 indicates an ECG signal frame; and a value of 0x03 indicates an image frame. Each type of PCC frames has a unique system priority identified by the type value (1 to 3, from high to low).

Figure 3.5a shows the format of an ECG signal frame. Each ECG frame has a unique identifier specified by the sequence number. Every time when the local server sends an ECG frame, the sequence number increments automatically by one for next frame. Basing upon this value, PCC calculates the surveillance time of heart monitoring. The value of signal number field indicates the channel number of ECG signals and the default channel number is four in WES. The value of QRS number fields represents the number of QRS complexes detected by the AED algorithm in the ECG frame. The default sampling frequency of WES is 500 Hz, which is identified in the sampling frequency field. This value is alterable by the sub-sampling frequency operation because the signal compression algorithm changes the size of original ECG frame. Hence this frequency value is useful to define the length of the uncompressed original frame in the remote server.

The following area of the ECG frame stores the diagnostic results of the AED algorithm. It is a QRS structure queue, where the QRS member number is indicated in the QRS number field. Each QRS member named QRSResult consists of three elements: QRS position,

QRS length, and QRS state. The QRS position indicates the onset position of a QRS complex in the uncompressed ECG frame. The heart rate of each beat can be calculated basing on the positions of two consecutive QRS. The QRS length represents the time interval of a QRS. The QRS state shows the type of heart rhythm and its related heart statue classified by the AED algorithm. The ECG signals field stores the compressed ECG signals. In the PCC system, each ECG frame contains 5 s of ECG signals.

Figure 3.5b shows the format of the image frame. The sequence number field is unused for an image frame. The image field contains an image in the jpeg format. Figure 3.5c shows the format of the system control information frame. The value of control code field indicates the type of control code. The related control information is stored in the following control information field.

3.4.2.2 PCC communication mechanisms

Three kinds of UDP connections are established in PCC. They are responsible for the system control (udp_CMD), the ECG signal transmission (udp_SIG), and the image transmission (udp_IMG).

3.4.2.2.1 PCC system control PCC control frames are responsible for the system remote configuration, the patient online/offline notifications, and the ECG frames retransmission management. The control frame is transferred via the UDP_CMD connection. PCC defines nine types of control frames:

- REQ_Connect /ACK_Connect; REQ_Terminate /ACK_Terminate
- REQ_Configure /ACK_Configure; REQ_Restra
- ACK_5Frames; ACK_Image.

The control frames with the code of REQ_Connect and ACK_Connect are responsible for the connection establishment between patients and cardiologists. The control frames with the code of REQ_Terminate and ACK_Terminate are responsible for the connection termination. Both patients and cardiologists have a right to open and close the UDP_CMD connection. The control frames with the code of REQ_Configure and ACK_Configure are responsible for

the system configuration. Currently, PCC provides the configurations of the operation mode and the sampling frequency. The other control frames with the code of REQ_Restra, ACK_5Frames, and ACK_Image will be introduced in the following subsections.

3.4.2.2.2 Signal retransmission mechanism PCC guarantees a reliable ECG signal delivery service by providing a signal retransmission mechanism. Two ECG frame queues are defined, respectively, for the local access server (Hold_Queue) and the remote surveillance server peer (Wait_Queue). The standard length of the two queues is set to five. The retransmission mechanism is described in Fig. 3.6.

When an ECG frame with the sequence number k is lost during network transmission, the remote surveillance server sends a retransmission requirement frame with a control code of REQ_Restra

```
If (an ECG frame is recieved)
    If (Seq_cur == Seq_exp)
        Insert current frame to wait_queue; The position of current
        frame in wait_queue is decided by its Seq_cur;
        Seq_exp++;
    else if (Seq_cur < Seq_exp)
        drop it;
        Send Control Frame REQ_Restra to the local server;
    else if (Seq_cur > Seq_exp)
        Add current frame to the tail of wait_queue;
    end

    if (continuous Five frame is received)
        Send Control Frame ACK_5Frames to the local server;
    end
end
```

```
If (ACK_5Frames frame is received)
    Release the ECG frames whose Seq_fra <= Seq_ack from the
    hold_queue;
else if (REQ_Restra frame is received )
    Retransmit an ECG frame of Seq_req to the remote surveillance
    server;
    Release the ECG frames whose Seq_fra < Seq_req from the
    hold_queue;
end

if (an ECG frame is ready)
    Send an ECG frame of Seq_cur to remote surveillance
    server;
    Seq_cur++;
end
```

Figure 3.6. Signal Retransmission Mechanism: Remote Surveillance Peer (U) and Local Access Peer (D).

and the local access server responses to this requirement by retransmitting the ECG frame *k*. When five consecutive ECG frames are received by the remote surveillance server, a control frame containing the code of ACK_5Frames will be sent to the local server to inform the release of the remainder ECG frames in Hold_Queue.

3.4.2.2.3 Data competition mechanism Considering the network quality and communication cost, PCC employs a data competition mechanism to guarantee those important data (i.e., ECG signals) being transferred in a higher priority, so that in the remote surveillance peer, cardiologists can detect and diagnose the ECG signals in real time.

As mentioned above, PCC has three types of data frames. Each kind of data frame has a unique transmission priority. The system control frame has the highest priority in this system. Furthermore, since the ECG signals are more important than the images data for the diagnosis of cardiologists, the ECG frame has higher priority than the image frame. In order to guarantee a real-time ECG signal transmission service, a data competition mechanism is implemented in the PCC system, described in Fig. 3.7.

When the queue length of Wait_Queue is equal to or greater than 5, it means that there is at least 25 s of ECG signals stored in the remote surveillance server. Hence, it is acceptable to allow the local server to transmit images. Whereas, when the queue length of Wait_Queue is smaller than 5, it means that the network speed begins to fluctuate and the network quality is lowered; hence, the system will stop image transmission so as to reduce network traffics.

3.4.3 *AED Algorithm*

In recent years, the study of automatic ECG diagnosis (AED) techniques addressed mainly clinical applications, but rarely PHC applications, due to two reasons: 1) to be applied on various scenes, i.e., different objectives and environments, the system signals are ambulatory, easily being disturbed by interferences; 2) to meet the needs of portable, the system node has strict resource constraints, traditional AED techniques are resource-consumption in views

```
If (an Image frame is received)
    If(the length of wait_queue >= 5)   //25 seconds delays
        Send a Control frame ACK_Image to the local server;
        Set the Image_Enable = TRUE;
    else
        Set the Image_Enable = FALSE;
    end
end

if ( an ECG frame is received)
    If(the length of wait_queue > 5 && Image_Enable == FALSE )
        Send a Control frame ACK_Image to the local server;
        Set the Image_Enable = TRUE;
    end
end
```

```
If (Image_Enable == TRUE)
    Send an Image frame to the remote surveillance server;
    Set the Image_Enable = FALSE;
end

if ( a Control frame ACK_Image is received)
    Set the Image_Enable = TRUE;
end
```

Figure 3.7. System competition mechanism: remote surveillance peer (U) and local access peer (D).

of PCC services. A novel AED algorithm dedicated to the PCC applications has thus been developed. By offering the PCC service, this system can reduce the risk of cardiac sudden death by detecting cardiac arrhythmia events in time.

3.4.3.1 Signal preprocessing and conditioning

Due to the nonstationary and easy-to-be-disturbed features, the ambulatory ECG signals must be de-noised before decision-making. Most of artifacts, such as baseline drifts, electrical noises, and muscle tremor interferences, can be eliminated or restrained by adopting suitable filters.

3.4.3.1.1 ECG time series Three ECG signal series, i.e., $R(t)$, $AD(t)$, and $RC(t)$, are adopted in the AED algorithm. The $R(t)$ series is raw ECG signals acquired from electrodes. It is generally contaminated

by different kinds of noises. The $AD(t)$ series is the adaptive differential signals with the processing of the differential filter and the adaptive filter. The inferences of the baseline drift and the motion artifacts can be eliminated in the $AD(t)$ series; hence, this series is used to detect and localize the QRS complexes. The $RC(t)$ series is the de-noised ECG signals with the operations of the band-pass filter and the linear amplifier. Since electrical noises and muscle tremors have been removed from the $RC(t)$ series, the $RC(t)$ series is used to extract the characteristics of the QRS complexes.

3.4.3.1.2 Adaptive filter Classical filters for the ECG series, e.g., notch filter, low-pass filter, and high-pass filter, can effectively remove or reduce most of interferences. But for motion artifacts, because of their irregular occurrences and irregular morphological attributes, these filters cannot eliminate these disturbances. These artifacts can cause much trouble in QRS detection when encountering QRS-like artifacts. This algorithm adopts an adaptive filter (AT) to reduce motion artifacts. The resultant signal series, named $A(t)$, is generated by performing AT operation in the raw series $R(t)$. The AT expression is

$$\begin{cases} Aecg(0) = R(0) \\ \qquad\qquad\qquad 0 < \alpha < 1,\ t = 1 \cdots N \\ Aecg(t) = \alpha * Aecg(t-1) + (1-\alpha) * R(t) \end{cases} \tag{3.1}$$

where α is the balance coefficient of AT, which is a key factor to influence the performance of the AT filter. If the value of α is augmented, the previous estimated value $Aecg(t - 1)$ then gives more proportion in the estimation of current $Aecg(t)$. Thereby, the achieved $A(t)$ is stable but cannot reveal the changes of ECG signals. In contrast, if the value of α is diminished, the original value $R(t)$ then gives more proportion and the achieved $A(t)$ is thus more dynamic and adaptive to the changes of ECG signals. Hence, the value of α should be cautiously selected to make $A(t)$ both stable and adaptive to the changes in $R(t)$. The value of α is set to 0.95 by default in views of the ECG sample frequency in PCC (500 Hz). Figure 3.8 shows the QRS complex waveform after the adaptive filter operation with different impact factors.

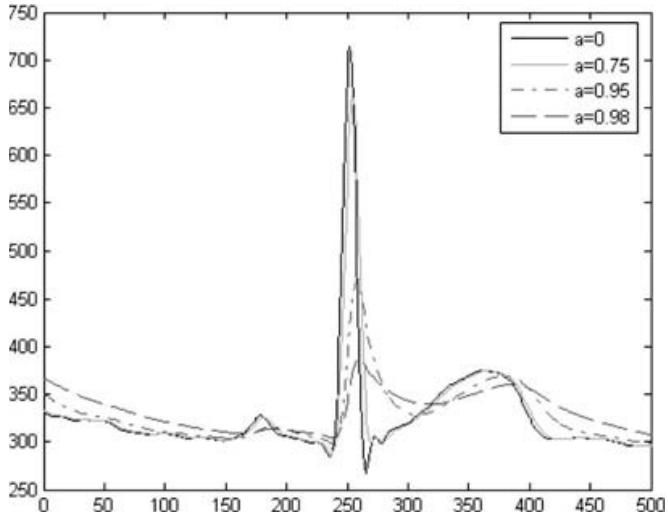

Figure 3.8. QRS complex waveform after different impact factor in the adaptive filters. See also Color Insert.

Figure 3.9 shows different ECG series: (a) is the raw signals $R(t)$, which are seriously polluted by noises. (b) represents the reconstructed series $RC(t)$ when filtering the $R(t)$ series by traditional filters, i.e., notch filter, low-pass filter, and high-pass filter. The $RC(t)$ series still contain the interferences generally caused by baseline wandering and motion artifacts. (c) is the adaptive filter signal $A(t)$ when filtering the $R(t)$ series by AT, which has

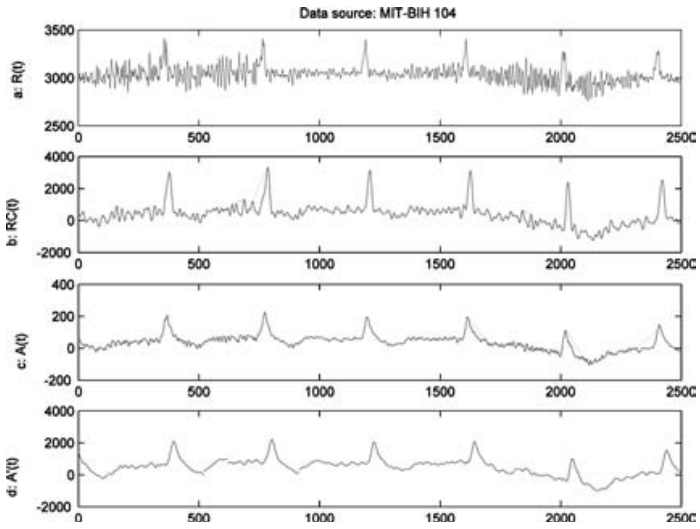

Figure 3.9. ECG series after different filters.

better signal quality than $RC(t)$. (d) is the reconstructed signal $RC^*(t)$ based on the adaptive filter signal $A(t)$. Obviously, in contrast to the previous reconstructed signal $RC(t)$, the signal $RC^*(t)$ has better signal quality in which the motion artifacts are effectively eliminated.

3.4.3.2 QRS complex detection

A new QRS detector has been developed to eliminate noises and artifacts by exploiting a self-adaptive threshold (SAT) method and designing state transition recognition (STR) procedure. The SAT method is used to estimate the peaks of ECG subsegments and the means of contextual thresholds, which allow estimating the optimum thresholds in a segment space. The STR procedure traces the waveform changes of signal series and identifies QRS complexes based on the optimum thresholds and the rules of state transition.

3.4.3.2.1 Diagnostic segment window (DSW) A short-term redundant data (default 5 s) is important in QRS detection. First, this short-term segment enables the complex contextual correlative analysis and reduces the interferences of baseline drift. In view of the low-frequency baseline drift, a short-term segment has fewer disturbances caused by baseline wandering than long-term signals. The redundant data enable the QRS detector to identify current QRS complex by comparing with fore-and-aft QRS complexes. Furthermore, in view of the unpredictability and variability of network quality, redundancy is necessary for data retransmission and network communication.

3.4.3.2.2 Self-adaptive threshold The QRS complexes of AECG have rapid changes and high potential amplitudes so that the differential series $D(t)$ can exactly represent the changes. The QRS signals have higher absolute amplitudes in a cardiac cycle of the $D(t)$ series. The solution to QRS detection is to search the optimum pair-peak for each QRS complex, i.e., the positive and negative peaks in a cardiac cycle. In Diagnostic Segment Window (DSW), there are generally multiple pair-peaks because several heartbeats will occur within 5 s. These pair-peaks make up of a pair-peak series in a DSW. Based on the pair-threshold extracting from the

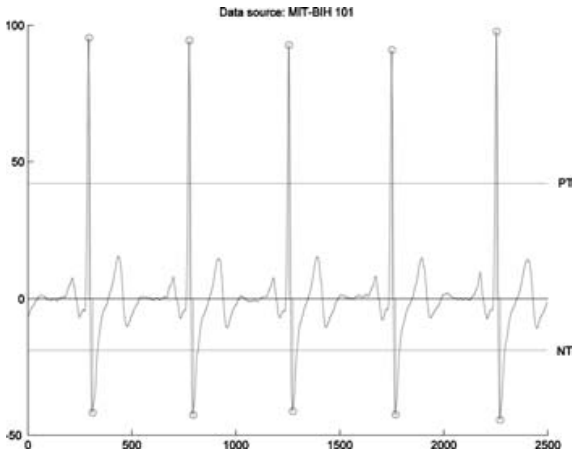

Figure 3.10. Mean of pair-peak series in a diagnostic window.

pair-peaks series in a DSW, the STR procedure is then able to locate QRS complexes. The absolute amplitude of each peak is generally greater than the associated absolute threshold in $D(t)$. Furthermore, since the position offset between the $D(t)$ series and the $A(t)$ series is constant, we can thus obtain the positions of QRS complexes in $A(t)$ by locating the complexes in $D(t)$.

The SAT method aims to determine the optimum pair-threshold, which is estimated from two aspects: the mean of the pair-peak series in a DSW and the pair-threshold of the previous DSW. The pair-threshold results from the means of the negative and positive pair-peaks series in a DSW. In order to accurately estimate these pair-peaks, the diagnostic segment window is divided into five subsegments with the length of 1 s (see Fig. 3.10). Because the normal heart rate of a healthy adult is 60–100 bmp, each subsegment thus contains one heartbeat. Since the differential signals of QRS complex have the maximum absolute amplitudes in a cardiac cycle, a pair-peak will indicate a QRS complex and then can be used to estimate the thresholds. Furthermore, the shorter the subsegment, the less interference of baseline drift the subsegment has. A subsegment with the length of 1 s can thus be regarded as a stationary series.

3.4.3.2.3 QRS location: State transition recognition In view of the QRS morphology properties in the $D(t)$ series, the complexes are categorized into two groups: positive and negative. Therefore,

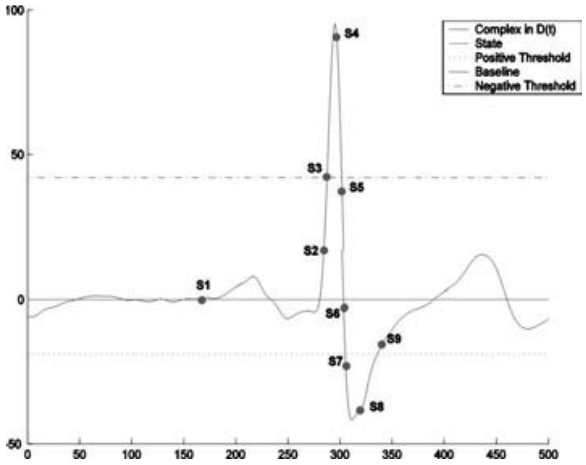

Figure 3.11. Positive states of a QRS complex in $D(t)$. See also Color Insert.

different states are defined to outline the phases of QRS complex in $D(t)$. $S2\sim\ S9$ represent the positive states of a QRS complex (see Fig. 3.11); corresponding $S20\sim\ S29$ represent negative states. An adaptive and self-corrected procedure, named STR, is developed to automatically track the changes of signal series, to correct error detection, and to record detected complexes. The states transitions are based on three basic reference lines: the baseline, the positive threshold, and the negative threshold.

3.4.3.2.4 Feature extraction: geometric analysis method QRS complex has triangular-alike or triangular-component morphological characteristics (see Fig. 3.12). This chapter thus adopts the geometric analysis method (GAM) to extract the features of QRS complexes. GAM has simple operations and low resource consumption, being able to predict and estimate the key points of QRS complexes under noisy situations, such as R wave peak, end point of Q wave (Q_t), and onset point of S wave (S_i). Therein, R wave peak can be obtained from $T_{peak\,1}$ or $T_{peak\,2}$, and it has mono-peak or poly-peaks. The measurement and detection phases of Q_t and S_i points are illuminated as follows.

- Defining two-level thresholds for left and right sides of R wave ($LH = (1/4) \times V_{peak\,1}$, $LL = (3/4) \times V_{peak\,1}$, $RH = (1/4) \times V_{peak\,2}$, $RL = (3/4) \times V_{peak\,2}$).

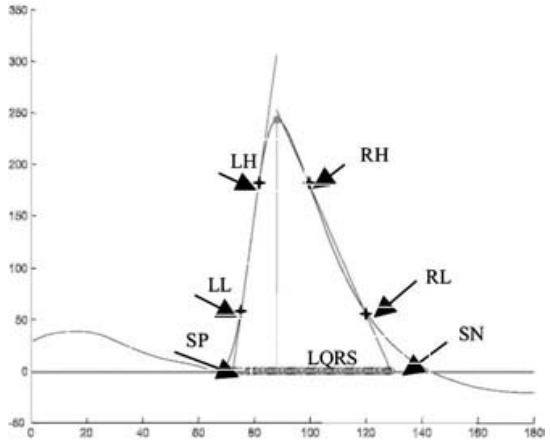

Figure 3.12. Illumination of geometric analysis method. See also Color Insert.

- Calculating the intersection points between the threshold values and complex signals. The slopes of two approaching lines represent two characteristics of QRS complex: SP (positive slope) and SN (negative slope).
- Obtaining the duration length of QRS (LQRS) which is the distance of two intersection points between the baseline and two approaching lines.

3.4.3.3 AED performance analysis

The AED algorithm has been evaluated on two ECG databases: MIT-BIH arrhythmia database [56] and CSD database (Clinic *STAR* Database). The former contains 48 half-hour excepts of two-channel ambulatory ECG recordings, and the latter is obtained from 30 patients of C.H.R.U. of Gabriel Montpied's hospital (Clermont-Ferrand, France) by using the PCC system named *STAR* [57]. The CSD signals are recorded by using WFDB format as the MIT-BIH Database one.

Dotsinsky et al. [58] defined four performance parameters to assess the algorithm efficiency (Se: sensitivity and Sp: specificity): TP (true positive), FP (false positive), FN (false negative), and shifted SH beats, shown as follows:

$$\mathrm{Se} = \frac{\mathrm{TP}}{\mathrm{TP} + \mathrm{FN} + \mathrm{SH}} \quad \mathrm{Sp} = 1 - \frac{\mathrm{FP}}{\mathrm{TP} + \mathrm{FP}} = \frac{\mathrm{TP}}{\mathrm{TP} + \mathrm{FP}} \tag{3.2}$$

Table 3.1. Performance evaluations of QRS detection algorithms

		Se (%)		Sp (%)	
Afonso *et al.* [59]		99.59		99.56	
Poli *et al.* [60]		99.60		99.51	
Dotsinsky *et al.* [58]		99.04		99.62	
Kaiser *et al.* [61]		99.68		99.72	
Datex-Ohmeda Corp. [62]		99.86		99.88	
Millet *et al.* [63]	Alg 1	94.6		98.0	
	Alg 2	97.3		98.0	
Our algorithm		99.43	99.25	98.55	97.94
		MIT	CSD	MIT	CSD

Comparing with the performance results of other algorithms listed in Table 3.1, the overall results of our detection algorithm, 99.37% sensitivity and 99.68% specificity on MIT-BIH database, 99.67% sensitivity and 99.74% specificity on CSD database, show the high sensitivity and specificity. This detection algorithm has minimal beat detection latency, low computational consumption, and fast detection ability.

3.5 Conclusion

Currently, the PCC system has been evaluated on 30 patients who had acute cardiac arrhythmia disturbances at the CHRU of Gabriel Montpied's hospital (Clermont-Ferrand, France), shown in Fig. 3.13. Since patients and cardiologists are located at the same area (at the hospital) in this application, the PCC system is thus configured as *clinical care* state. The local access server is a laptop on which the real-time cardiac arrhythmias program is installed. The remote access server and the remote surveillance server are installed in the same laptop or a standard PC, which connect with the local server via the local high-speed network. This system supports continuous remote cardiac arrhythmias monitoring, and the 4-lead ECG signals are sent directly to the remote surveillance terminal in real time with *real-time continuous ECG signal* operation mode.

The system has also been utilized to evaluate athletes' cardiac status during physical exercises, shown in Fig. 3.13. The obtained

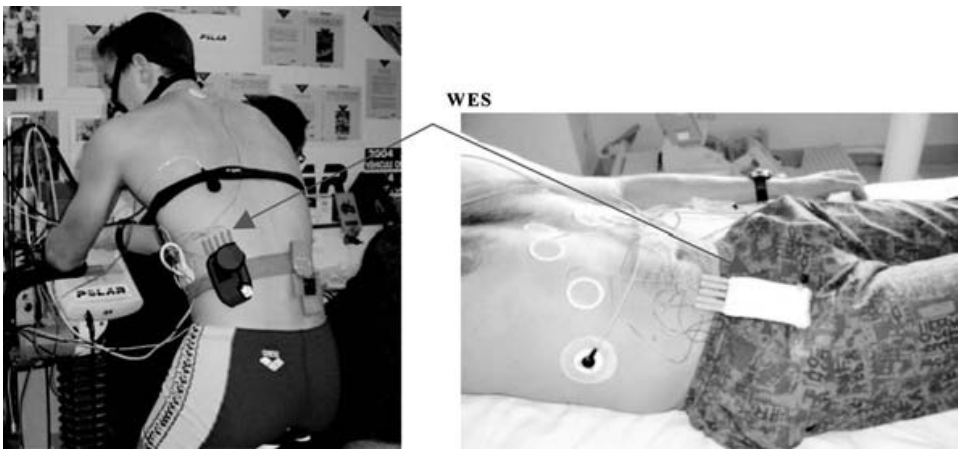

Figure 3.13. Application example of PCC system. See also Color Insert.

results show this system still provides high quality ECG signals and accurate QRS detection PCC is an efficient system for diagnosing cardiac arrhythmias. It provides a new clinical approach adapted to monitor accurately and efficiently large scale high-risk patients. Furthermore, it may be used by cardiologists to remotely monitor patients, to evaluate the efficiency of drugs and to discuss difficult cardiac pathology cases with other colleagues.

In order to compare with other system, the HP telemetry system has been applied during PCC evaluation. For each patient, the evaluation duration is 30 min. The evaluation results obtained by the PCC system and the HP telemetry system are compared, as shown in Fig. 3.14. Due to the higher sampling frequency, the ECG signals of our system have better quality than HP ones. Concerning the clinical off-line cardiac arrhythmia detection, the two systems have similar results. The evaluation results prove that the PCC system meets the requirements of real-time cardiac monitoring and diagnosing application.

In order to improve this system, the following techniques should be developed: (i) Embedded RTOS (i.e., HEROS [64]) adopts a full "modularity" design fashion. The system primitives and tasks of HEROS will be defined as a set of actions. Thus, it may be configured according to different applications. (ii) AED algorithm has been ported into the local access unit and the remote center server, but it can be integrated as an ECG diagnostic chip. We are working on the

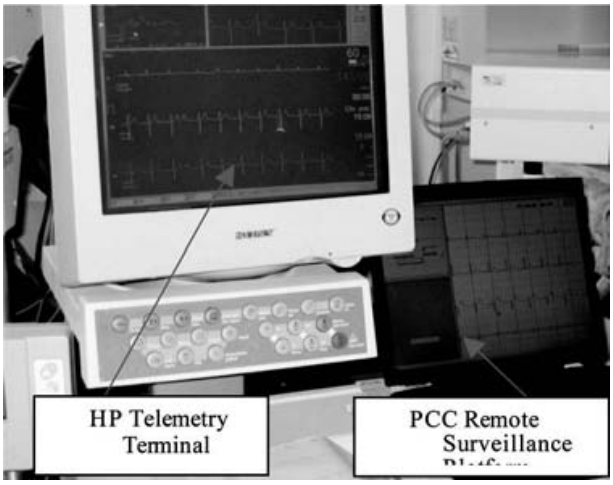

Figure 3.14. PCC test and comparision with HP telemetry.

implementation of an intelligent wireless ECG sensor (IWES) [65] by integrating the algorithm into a VLSI chip. This chip is currently under evaluation and test on an ALTERA FPGA board.

Acknowledgment

We would like to thank the MENRT, the ANVAR and the Conseil Regional d'AUVERGNE for their support, and also the colleagues of the SMIR group of LIMOS UMR 6158 CNRS for their help.

References

1. Goldberg, S. and Wickramasinghe N. (2003) 21st Century Healthcare: the Wireless Panacea in *Proceedings of the 36th Hawaii International Conference on Systems Sciences*.
2. Varshney, U. (2005) Pervasive Healthcare: Applications, Challenges and Wireless Solutions *Communications of the Association of Information Systems,* 16(3).
3. Tablado, A. Illarramendi, A., Bermudez, J., and Goni, A. (2003) Intelligent Monitoring of Elderly People, in *Proceedings of the 4th Annual IEEE Conference on Information Technology Applications in Biomedicine*.
4. World Health Organization (1999) Death by Cause, Sex and Mortality Stratum in WHO Regions, *WHO General Report*.

5. Chinese National Aging office (2006) Forecast Study of the Development Trend of China's Population Aging Issue, *General Report* (in Chinese).
6. Zou, N. J. (2007) Old-Age Security, Old-Age Home and Community Support: New Option for Old-Age Models, *Jiangsu Social Sciences*, 4 (in Chinese).
7. Chinese National Bureau of Statistics (2006) *China's Demographic Yearbook2006*, pp. 289 (in Chinese).
8. Zhu, Z. M. (2010) Health Ubiquitous Service: Exploring Pervasive Computing in Health/Medical Applications, http://www.bjkp.gov.cn/bjkpzc/kjqy/it/lsywl/ 250584.shtml (in Chinese).
9. Yang, T. Li, Z. G. and Shi, Y. C. (2007) Study Elderly Care Services by Integration With the Community Health Services in Rural China, *General Report* (in Chinese).
10. Yan, J. L. and Wei, S. (2009) The Health Education Problems and Countermeasures for Urban Elderly in Community, *Modern Nursing*, 35(6), pp. 122 (in Chinese).
11. Chronic Care Improvement (2004) A Product of the E-Health Committee, *ITAA E-Health White Paper*, pp. 5.
12. Sneha, S. (2008) Patient Monitoring via Mobile Ad Hoc Networks: Maximizing Reliability While Minimizing Power Usage and Delays, *Doctoral Dissertation*, Georgia State University.
13. Website (2010) US Administration on Aging Report on Demographic Changes, http://www.aoa.dhhs.gov/aoa /stats/aging21 /demography.html.
14. Chiasson, M. Davidson, E. Kaplan, B., et al. (2004) Strangers in a Strange Land: Can IS Meet the Challenges and Opportunities of Research in Healthcare? in P*roceedings of the 10*th *Americas Conference in Information Systems*.
15. Gouaux, F. Simon-Chautemps, L. Adami, S., et al. (2003) Smart Devices for the Early Detection and Interpretation of Cardiological Syndromes, in *Proceedings of the 4*th *International IEEE EMBS Conference on Information Technology Applications in Biomedicine*.
16. Website (2010) US Patient Monitoring Industry Overlook., http://www.frost.com/prod/servlet/report-homepage.pag ?repid=A369-01-00-00-00.
17. Sneha, S. and Varshney, U. (2009) Enabling Ubiquitous Patient Monitoring: Model, Decision Protocols, Opportunities and Challenges, *Decision Support Systems*, **46**, pp. 606–619.

18. Bardram, J. E. (2008) Pervasive Health Ccare as a Scientific Discipline, *Methods Information Medicine*, **47(3)**, pp. 178–185.
19. Hung, K. and Zhang, Y. (2003) Implementation of a WAP-Based Telemedicine System for Patient Monitoring, *IEEE Transactions on Information Technology in Biomedicine* **7(2)**, pp. 101–107.
20. Sneha, S. and Varshney, U. (2005) Wireless ECG Monitoring System for Pervasive Health Care, in *Proceedings of the 11th Americas Conference on Information Sys*tems.
21. Zhou, H. Y. and Hou, K. M. (2010) Pervasive Cardiac Monitoring System for Remote Continuous Heart Care, in *Proceedings of International Conference on Bioinformatics and Biomedical Engineering.*
22. Website (2010) Patient Monitoring by Welch Allyn, http:// www.monitoring. welchallyn. com/products/wireless.
23. Mendoza, G. G. and Tran, B. Q. (2002) In-Home Wireless Monitoring of Physiological Data for Heart Failure Patients, in *Proceedings of the 24th Joint IEEE EMBS/BMES Annual Conference*.
24. Website (2010) TV-Based Monitoring by Philips http:// www.medical.philips.com/main/ news/content/file_630.html.
25. Website (2010) Cardionet, http://www.cardionet.com/.
26. Website (2010) Biotronik, http://www.biotronik.com/.
27. Bonato, P. (2003) Wearable Sensors/Systems and Their Impact on Biomedical Engineering, *IEEE Engineering Medicine and Biology Magazine* **22(3)**, pp. 18–20.
28. Gieras, I. A. (2003) The Proliferation of Patient-Worn Wireless Telemetry Technologies Within the US Healthcare Environment, in *Proceedings of the 4th International IEEE EMBS Special Topic Conference on Information Technology Applications in Biomedicine*.
29. Jovanov, E. O'Donnell Lords, A. Raskovic, D., et al. (2003) Stress Monitoring Using a Distributed Wireless Intelligent Sensor System, *IEEE Engineering in Medicine and Biology Magazine* **22(3)**, pp. 49–55.
30. Website (2010) Smart Shirt, http://www.smartshirt.gatech.edu.
31. Brahnam, S. Chuang, C. F., Sexton, R. S. and Shih, F. Y. (2007) Machine Assessment of Neonatal Facial Expressions of Acute Pain, *Decision Support Systems* **43(4)**, pp. 1242–1254.
32. Hu, P. J. H., Wei, C. P. Cheng, T. H. and Chen, J. X. (2007) Predicting Adequacy of Vancomycin Regimens: a Learning-Based Classification Approach to Improving Clinical DecisionMaking, *Decision Support Systems* **43(4)**, pp. 1226–1241.

33. Lin, L. J-HHu, P. and Sheng, O. R. L. (2006) A Decision Support System for Lower Back Pain Diagnosis: Uncertainty Management and Clinical Evaluations, *Decision Support Systems*, **42(2)**, pp. 1152–1169.
34. Varshney, U. (2008) A Framework for Supporting Emergency Messages in Wireless Patient Monitoring, *Decision Support Systems,* **45(4)**, pp. 981–996.
35. Website (2010) Gator Tech Smart House, http://www.icta.ufl.edu/gt.html.
36. Website (2010) Aware Home Project, http://www.awarehome.gatech.edu/projects/ index.html.
37. Stanford, V. (2002) Using Pervasive Computing to Deliver Elder Care, *IEEE Pervasive Computing Magazine* **1(1)**, pp. 10–13.
38. Kafeza, E., Chiu, D. K. W., Cheung, S. C. and Kafeza, M. (2004) Alerts Immobile Health Care Applications: Requirements and Pilot Study, *IEEE Transactions on Information Technology in Biomedicine* **8(2)**, pp. 173–181.
39. Haux, R. Howe, J. Marschollek, M., Plischke M. and Wolf, K. H. (2008) Health-Enabling Technologies for Pervasive Health Care: on Services and ICT Architecture Paradigms, *Informatics for Health and Social Care* **33(2)**, pp. 77–89.
40. Koch, S. and Hägglund, M. (2009) Health Informatics and the Delivery of Care to Older People, *Maturitas* **63(3)**, pp. 195–199.
41. Doukas C. and Maglogiannis, I. (2008) Intelligent Pervasive Healthcare Systems, *Advanced Computational Intelligence Paradigms in Healthcare* (Springer Press), **107**, pp. 95–115.
42. Daramolar, J. O. Osamor, V. C., and Oluwagbemi, O. O. (2008) A Grid-based Framework for Pervasive Healthcare Using Wireless Sensor Networks: a Case for Developing Nations, *Asian Journal of Information Technology*, **7(6)**, pp. 260–267.
43. Salvador, Z. Larrea M. and Lafuente, A. (2007) Infrastructural Software Requirements of Pervasive Health Care, in *Proceedings of IADIS International Conference on Applied Computing*, pp. 557–562.
44. Zhou, H. Y. (2004) Wireless Sensor Networks Dedicated to Remote Continuous Real-Time Cardiac Arrhythmias Detection and Diagnosis, Ph.D Thesis, University of Blaise Pascal Clermont-Ferrand II (France).
45. Zhou, H. Y. et al. (2006) A New System Dedicated to Real-Time Cardiac Arrhythmias Tele-Assistance and Monitoring, *Special Issue of Journal of Universal Computer Science*, **12(1)**, pp. 30–44.

46. Zhou, H. Y. et al. (2004) Remote Continuous Cardiac Arrhythmias Detection and Monitoring, *Transformation of Healthcare With Information Technologies*, *Studies in Health Technology and Informatics* (IOS Press), **105**, pp. 112–120.
47. Zhou, H. Y. et al. (2005) A Real-Time Continuous Cardiac Arrhythmias Detection System: RECAD, in *Proceedings of the 27th Annual International Conference of the IEEE Engineering in Medicine and Biology* **(EMBC05)**, pp. 875–881.
48. Zhou, H. Y. Hou, K. -M. and Zuo, D. C. (2009) Real-Time Automatic ECG Diagnosis Method Dedicated to Pervasive Cardiac Care, *Wireless Sensor Network*, **1(4)**, pp. 276–283.
49. Zhou H. Y. and Hou, K. -M. (2008) Embedded Real-Time QRS Detection Algorithm for Pervasive Cardiac Care System, in *Proceedings of the 9th International Conference on Signal Processing*, pp. 2150–2153.
50. De Sousa, G. Zhou, H. Y., Hou, K. -M. et al. (2007) Adaptive System for Wireless Sensor Networks Applications, *Journal of Harbin Institute of Technology* **39**, pp. 153–157.
51. Bailey, J. J. Berson, A. S. Garson A. et al (1990) Recommendations for Standardization and Specifications in Automated Electrocardiography: Bandwidth and Digital Signal Processing, *Circulation* American Heart Association **81(2)**, pp. 730–739.
52. De Vaulx, C. and Hou, K. -M. (2002) DREAM: un micro noyau réparti, temps réel orienté pour la tolérance aux fautes, *Revue Informatique et santé*, Télémédecine et e-santé, **13**, pp. 63–69.
53. Gineste, L (2002) Plate-forme de suivi à distance d'arythmie cardiaques, *DEA CSTI report*, University of Blaise Pascal Clermont-Ferrand II, France.
54. Palau, P. Hou, K. -M. and Ponsonnaille, J. (2002) TelmedTCP: Protocole TCP/IP temps réel dédié à la télémédecine, *Revue Informatique et santé*, Télémédecine et e-santé, **13**, pp. 53–60.
55. PhysioNet (2002) The WFDB Software Package Software for Viewing, Analyzing, and Creating Recordings of Physiologic Signals, http://www.physionet.org/physiotools/ wfdb.shtml.
56. Moody G. B. and Mark, R. G. (1990) The MIT-BIH Arrhythmia Database on CD-ROM and Software for Use With It, *Computers in Cardiology* **17**, pp. 185–188.
57. Zhou, H. Y. Hou, K. -M. Ponsonnaille, J. et al. (2004) Remote Continuous Cardiac Arrhythmias Detection and Monitoring, in *Proceedings of the 2nd International Conference on E-health in Common Europe*.

58. Dotsinsky I. A., and Stoyanov, T. V. (2004) Ventricular Beat Detection in Single Channel Electrocardiograms, *BioMedical Engineering OnLine* 3(3), doi:10.1186/1475-925X-33.
59. Afonso, V. X. Tompkins, W. J. Nguyen T. Q. and Luo S. (1999) ECG Beat Detection Using Filter Banks, *IEEE Transactions on Biomedical Engineering*, **46**, pp. 192–202.
60. Poli, R. Cagnoni, S. and Valli G. (1995) Genetic Design of Optimum Linear and Nonlinear QRS Detectors, *IEEE Transactions on Biomedical Engineering* **42**, pp. 1137–1141.
61. Kaiser W. and Findeis M. (2000) Novel Signal Processing Methods for Exercise ECG, Special Issue on Electrocardiography in Ischemic Heart Disease, in *Proceedings of IJBEM*.
62. Datex-Ohmeda Corp. (2002) Bedside Arrhythmia Monitoring Quick Guide, Internal Web Journal for Medical Professionals, http://www.clinicalwindow.com.
63. Millet, J. Perez, M. Joseph, G. Mocholi A. and Chorro J. (1997) Previous Identification of QRS Onset and Offset Is Not Essential for Classifying QRS Complex in a Single Lead, *Computers in Cardiology*, **24**, pp. 299–302.
64. Zhou, H. Y. Hou, K. -M. de Vaulx C. and Zuo, D. C. (2009) A Hybrid Embedded Real-Time Operating System for Wireless Sensor Networks, *Journal of Networks*, **4(6)**, pp. 428–435.
65. Ding, H. Hou, K. M. Lecoq J. et al. (2009) Toward a Low Cost and Single Chip Holter: SoC-Holter, *in Proceedings of the 3rd International Conference on New Technology, Mobility, and Security-2009*.

This page intentionally left blank

Chapter 4

Human Bio-Kinematic Monitoring with Body Area Networks

Roozbeh Jafari, Hassan Ghasemzadeh, Eric Guenterberg, Vitali Loseu, and Sarah Ostadabas

Embedded Systems and Signal Processing Laboratory, Department of Electrical Engineering, University of Texas at Dallas
Richardson, TX, 75080, USA
rjafari@utdallas.edu; h.ghasemzadeh@utdallas.edu; mavpion@gmail.com; vitali.loseu@utdallas.edu; and sarahostad@student.utdallas.edu

Body Area Networks (BANs), known as enabling technology for many biomedical applications, are composed of body-worn sensor devices that can provide mobile and continuous monitoring of the human body. This chapter presents an overview of platform design strategies for BANs with applications in physical movement monitoring. First, an introduction to several compelling applications is given, which shows BAN versatility in both medical and recreational fields. Applications are important in the sense that they help in understanding design requirements of the BAN platform. An architecture of the system, including hardware and software components, is then described. It is followed by a description of typical signal processing for movement monitoring applications. While this type of signal processing flow can be generally used in movement monitoring applications, in order to take the most

Wireless Body Area Networks: Technology, Implementation, and Applications
Edited by Mehmet R. Yuce and Jamil Y. Khan

ISBN 978-981-4316-71-2 (Hardcover), ISBN 978-981-4241-57-1 (eBook)
www.panstanford.com

advantage of the system, the signal processing needs to be custom tailored for each individual application. An example of this process is shown based on the Hidden Markov Model (HMM) movement annotation applications. Finally, the chapter is concluded with discussion of possible BAN system optimizations. In particular, it is shown that the energy consumption of the system can be reduced by using buffers to decrease the number of transmissions.

4.1 Physical Movement Monitoring

A BAN system uses several sensor units each equipped with motion sensors, processing units, and wireless and memory components. The system aims to collect sensor readings and transform them into useful information. In order for a wearable system to be successful, it is required to be comfortable and not introduce any additional movement constraints. The main deployment objective of any BAN is to improve its wearability and the ease of use. This idea has a few consequences. First, it forces sensor units to be powered by a battery. Using a large energy source would hinder mobility and, therefore, is not acceptable. Second, wearability concerns rule out a wired communication scheme because a set of wires all over the body is not natural and may constrain some human movements. Finally, reducing the form factor of sensor units is crucial for wearability. It can be done via reducing the size of the sensor unit's components such as the processor, memories, sensors, and the battery. While technology made a wide leap in reducing the size of microprocessors, memories, and sensors, the progress in battery size reduction has not been as fertile [1]. It suggests that currently the battery size dominates the form factor of the wearable sensor units. The requirement of the extreme battery efficiency motivates the need for light-weight and highly efficient signal processing algorithms and optimization techniques. The signal processing, however, needs to exhibit sufficient reliability and sensitivity in extracting the relevant parameters.

BAN systems are desirable because they provide objective, quantitative measurements while not restricted to a laboratory environment. Furthermore, depending on the number and locations

of the sensing units, BAN systems can vary greatly in the scope of possible tasks from a general action recognition to extracting a very specific detail about a movement. This property makes BAN systems extremely useful in a large set of applications. In particular, they find applications in rehabilitation [2], sports medicine [3], geriatric care [4], gait analysis [5], balance evaluation, [6] and sports training [7, 8].

4.2 Applications

BANs can collect a wide range of information that monitor different aspects of human life from movement monitoring and emotion recognition [9, 10] to sports training and leisure applications. Applications can be divided into two categories, including medical and nonmedical applications. With traditional health care, patients are either observed by doctors who rely on personal experience to identify symptoms and the severity of a condition or have to be examined in a laboratory environment. With wearable mobile sensors, however, remote and continuous monitoring the patients is available. Sports training is another important application area of BANs. Quantitative feedback provided by wearable sensors can be used to provide atheletes with better instruction on improving their game without an involved participation from a human expert trainer.

4.2.1 *Medical Applications*

An emerging application for BANs involves their use in medical application. BAN area revolutionizes the health care system by allowing inexpensive, continuous, and ambulatory health monitoring with real-time capabilities. Using human bio-kinematic monitoring that provides sensor data as a biometric of body functionality is of increasing interest since it is noninvasive and can be measured without subject contact or knowledge. In clinical application, as therapists increase their emphasis on evidence-based practice, they must increase the use of objective, quantitative methods to demonstrate efficacy of their method. For instant, gait analysis is an proper method for demonstrating change from treatment or

from disease progression. Gait analysis by means of BANs for the person with Parkinsons disease (PD) can be used as a tool for determining the treatment efficacy of pharmacologic, surgical, or physical therapeutic interventions. In this section, we review some of the existence methods for gait analysis and Parkinson's disease assessment.

4.2.1.1 Gait analysis

In the human action recognition, gait analysis is the systematic measurement, description, and assessment of those quantities thought to characterize human locomotion. Through gait analysis, kinematic and kinetic data are acquired and analyzed to provide information, which describes fundamental gait characteristics and which is ultimately interpreted by clinicians to form a medical assessment.

For the purpose of gait analysis, wearable sensors of the BAN can be attached at the externor side of the thigh [11]. The hip angle is defined as the angle between the thigh and gravity direction. The swing velocity (angular velocity) of the thigh is defined as $v = \frac{d\theta}{dt}$. Kalman filter is applied to estimate θ and v, which are key features of the gait cycle. Another proposed method for gait analysis is a generic algorithm for temporal parameter extraction called the hidden Markov event model based on HMMs. This method constrains the state structure to facilitate location of key events of gait [12].

In the context of signal processing, gait recognition experiments using spectral features in terms of magnitude, phase, and phase-weighted magnitude show that both magnitude and phase spectra are effective gait signatures. In [13], authors proposed a gait recognition approach using spectral features of horizontal and vertical movement of ankles in a normal walk. They used an integration of magnitude and phase spectra for gait recognition using AdaBoost classifier. At each round, a weak classifier evaluates each magnitude and phase spectra of a motion signal as dependent subfeatures, then classification results of each subfeature are normalized and summed for the final hypothesis output. Authors in [14] investigate an ear- worn sensor for the development of a

gait analysis framework. Instead of explicitly defining gait features that indicate injury or impairment, an automatic method of feature extraction and selection is proposed.

4.2.1.2 Parkinson's disease assessment systems

Many efforts have been made to come up with objective measures for motor impairment and disability assessment in Parkinson's disease. Hoehn and Yahr Clinical staging [15], Webster Rating scale [16], Columbia University Rating scale [17], the short Parkinson's evaluation scale (SPES) [18] and the Unified Parkinson's Disease Rating Scale (UPDRS) [19] are a few of them. The UPDRS has become the gold standard of rating scales for PD detection and assessment [20], as it is one of the most evaluated and reliable, bearing close correlation to other widely accepted standards at the same time [21].

Systems have been designed for PD assessment as described in [22] and [23] albeit for specific activities like recording tremor and measuring sleep disorder [24]. In [25], Homann et al. examined a method to measure bradykinesia and akinesia using finger-tap test on a computer. Rajaraman et al. [26] demonstrated a 3D tremor measurement system for comparing tremor across patients and in measuring the efficacy of therapeutic interventions. Their system employed 3D electromagnetic position sensors to measure the actual and cumulative displacement of the tremoring finger. The tremor frequency and amplitude are estimated using spectral analysis on the data after low-pass filtering at 15 Hz. Systems for clinical measurement of tremor have also been demonstrated in [27] and [28], but unrelated to the assessment of any disease in particular.

The methods used for the measurements have varied from electromyography (EMG) [29, 30] to accelerometers [23, 31], electromagnetic sensors, [26] and custom transducers [22]. Hassan et al. [32] examines light-weight sensor devices which enable on-body and mobile health-care monitoring. Goetze et al. [20] employed an at-home testing device for testing motor impairment in PD, which consisted of a dedicated apparatus for conducting the tests. The device consisted of a testing panel on the base that contains

a two-key keyboard for finger tapping, two buttons for reaction time/movement time and repetitive hand tapping assessments, an eight-peg pegboard, control buttons, and a docking station for an actiwatch device measuring tremor.

4.2.2 *Sports Training Application*

Sport training represents the body's adaptation to conditions of certain exercises. One can achieve considerable progress in a sport with the aid of appropriate exercises and training methods [33]. The biggest challenges of sports training is the evaluation of a movement and an ability to provide feedback regarding movement's quality. Traditionally, these two tasks are performed by a human coach who uses personal expertise and experience to evaluate exercises and provide feedback. However, personal coaches are expensive and, to make training more affordable, often coach multiple students at the same time, thus diverting attention from detailed diagnosis of problems of individual students. An automated system that can assess the overall performance of a learner and pinpoint problem areas in the learners movements would facilitate performance assessment, increasing the effectiveness of unsupervised practice.

Traditionally, mechanical training systems [34, 35] have been used to provide movement feedback. However, these types of systems lack fine grain details of movements. Authors in [36] use a motion capture system to record and analyze tennis movements. They show that alternative forehand and backhand movements outperform discrete forehand or backhand practices due to the inertia of the trunk rotation movements between subsequent strokes. The approach in [37] tracks the movements in rugby football using close-range or long-range photography. Shoulder orientation and trunk flexion are demonstrated to be significantly different in experienced players and novices and, therefore, can be used to measure players' performance and training quality. A motion capture system is also used in [38] to design a virtual baseball training system. In the system, a batter swings a bat toward the virtual ball, and the trajectory of the swing is used to calculate the quality of the swing. While these systems tend to perform well, they require an expensive laboratory setup and, therefore, are not

desirable. A BAN-based solution to sports training is either based on a solution where sensors are placed in the environment [39] or embedded within the sports equipment [40].

Overall, there are two areas of interest in sports training. Training can focus on a precise execution of each movement individually. Training can also focus on coordination in execution of series of movements. While these two components are connected, they can be considered individually. Next two sections demonstrate how BAN systems can address both of these cases.

4.2.2.1 Golf swing training

The popular sport of golf requires a complicated sequence of motions to swing the golf club properly with the primary goal of propelling the golf ball a certain distance in a desired direction. A repeatable and consistent golf swing can dramatically improve a golfer's score. However, this single movement, which has such a major impact on the player's overall game, is difficult to master and execute consistently for players who are new to the sport or have little experience.

A full swing is a complex motion of the body aimed at accelerating the club at great speed. The motion starts at an initial position, referred to as the address position [41], followed by the swing. A golf swing can be divided into smaller segments. A general golf swing model considers a full swing composed of four major segments: takeaway, backswing, downswing, and follow-through [42]. *Takeaway* starts as the first movement after the address position and ends when the club is approximately parallel to the target line and at waist level. The *backswing* follows the takeaway and continues until the golf club is lifted to its highest point behind the player. Following this is the *downswing* in which the club is brought back down to hit the ball. After impact with the ball, the *follow-through* motion brings the club to its stopping point in front of the player. This model enables more precise analysis of the actions by reporting the quality of each individual part of the swing.

The goal in achieving a perfect swing is to hit the ball squarely and straight [43]. This would also give the golfer maximum distance. Consequently, it is important to investigate actions that prevent

development of a perfect swing. According to the literature, there are two kinds of common mistakes new players make, resulting in a poor shot [41]: *wrist rotation* and *out-of-plane* movements. To simplify the system, a virtual coach can address each one of the issues individually. For example, the system can focus on evaluating golf swing in terms of the angle of wrist rotation. This information can be obtained by placing sensing units on the upper body and arms to capture significant motions during the swing [44] and placing two sensing units on the golf club to capture its movements [7].

4.2.2.2 Baseball swing training

Baseball batting involves hitting a thrown ball with the primary objective of transferring maximum force to propel the ball as far as possible in a desired direction. Numerous baseball players and coaches have suggested methods for successful batting. A good swing is the result of a sequence of rotational movements including foot, knees, hips, shoulder, and hands movements. Generally, the action of the batter starts in the lower body and moves upward. Properly performed motions executed at the right time maximize the power of the swing. Major components of a good swing include bat speed, bat swing plane, and timing. Common mistakes include late rotation of lower body, back shoulder dip, and drifting of the front foot. Late movement of the foot and hips impairs the swing timing. Dropping the back shoulder affects the bat plane so as the bat does not pass through the strike zone horizontally, decreasing the chance of a successful hit. Drifting refers to improper weight transfer from the back foot to the front foot. One consequence is losing power in the hips, which decreases the bat speed at impact. Therefore, proper weight transfer necessitates coordination between different body segments during the swing.

The considered swing model emphasizes three major events: 1) Rotation of the lower body (feet, knees, hips) toward the pitcher, 2) rotation of the upper body into the swing, and 3) the swing of the arms and hands toward the pitcher. These key events should be executed in a specific and overlapping sequence. The coordination is extremely important as it ensures that the maximum power from arms, shoulders, and hips is delivered exactly as the bat crosses the

plate [45]. In order to recognize movement coordination, sensing units placed on the ankle, hip, upper body, and the bat have to identify body movements and their timings. It can be achieved with detailed body, choreography modeling with motion transcripts introduced in [8].

4.3 Hardware and Software Architecture

The purpose of an action recognition system is to classify transitional movements into pre-defined actions. Given a set of movements, the system must distinguish between every pair of motions. These sensors capture inertial information from physical movements. An example platform used to generate data and achieve results in this chapter is shown Fig. 4.1. The system consists of several sensor units; each has a tri-axial accelerometer, a bi-axial gyroscope, a microcontroller, and a radio. In this specific setup, the accelerometers are LIS3LV02DQ with 1024 LSb/g sensitivity. The IDG-300 gyroscopes have 2 mV/$^\circ$/s sensitivity. The processing unit of each node, or mote, can sample sensor readings at certain rate and transmit the data wirelessly to a base station. A common protocol

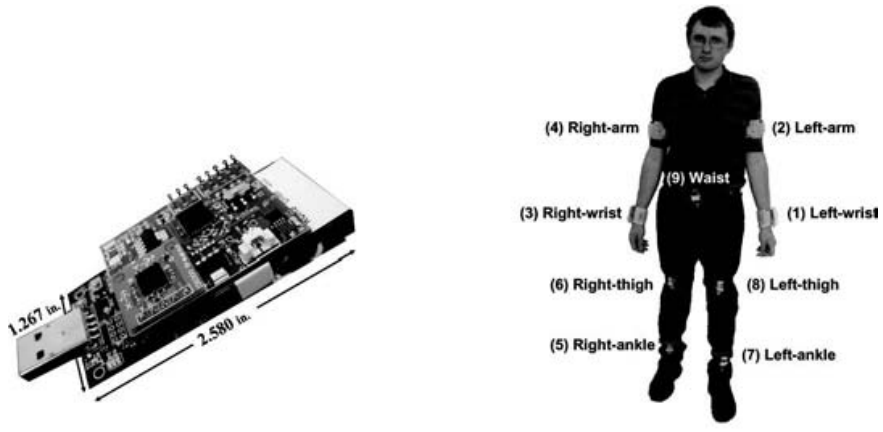

Figure 4.1. (a) A sensor node composed of processing unit and custom-designed sensor board. The motion sensor board has a triaxial accelerometer and a biaxial gyroscope Sensor node and subject (b) A subject wearing nine sensor nodes. See also Color Insert.

for this transmission is Time Division Multiple Access (TDMA). For the purpose of action recognition, authors of [46] use the TelosB motes [47], which are commercially available from XBow®. The sensor board they use is predominantly a custom designed with an integrated Li-Ion battery that powers both sensor board and mote as shown in Fig. 4.1a. The sensor nodes can be placed on different locations on the body to capture movements of their subjects. Figure 4.1b shows a subject with nine nodes placed on different body segments.

Signal processing for body sensor network usually comprises multiple levels of data abstraction, from raw sensor data to data calculated from processing steps. SPINE (Signal Processing in Node Environment) [48] is a software framework that aims to enable efficient implementations of signal processing on sensor nodes in BAN. SPINE is a framework for distributed signal processing founded on the following principles:

Open source: SPINE is developed as an open source project to establish a broad community of users and developers that contributes to extend the framework with new capabilities and applications.

Interoperability through APIs: SPINE provides local and remote applications with lightweight Java APIs that can be used by local and remote applications to manage the sensor nodes or issue service requests, and are easily portable to devices of various capabilities, such as PCs or mobile phones, that can be used as BAN coordinator.

High-level abstractions: SPINE provides libraries of protocols, utilities, and processing functions; hence, it simplifies the task of application developers by raising the level of abstraction. The layer defined by the SPINE libraries allows designers to focus on application-specific issues and program at a higher level of abstraction than TinyOS.

Distributed implementations of classification algorithms: SPINE simplifies the development of applications that require complex signal processing algorithms and classifiers. For example, SPINE supports distributed implementation of classification algorithms to reduce the amount of data to be transmitted and save energy.

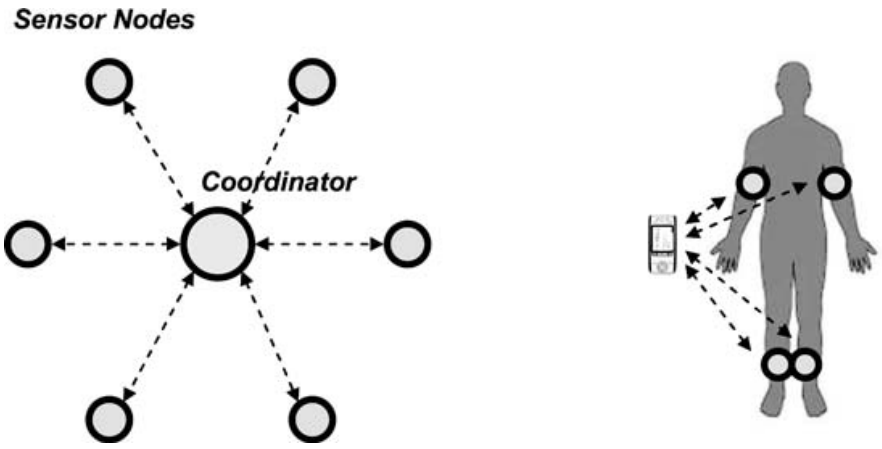

Figure 4.2. SPINE 1.0 Network Architecture [48].

SPINE relies on a BAN architecture with star topology, including one or more sensor nodes and a BAN coordinator node. The coordinator typically manages the BAN, collects and analyzes the data received from the sensor nodes, and acts as a gateway to connect the BAN with wide area networks for remote data access. Figure 4.2 visualizes a typical architecture with star topology.

4.4 Signal Processing for Body Area Networks

Figure 4.3 shows several processing tasks typically used for signal processing and action recognition in BANs. Each processing block is described as follows.

Sensor data collection: Data is collected from all of the sensors on each of the nodes at a specified frequency. The sampling rate can be empirically chosen to provide sufficient resolution while compensating for bandwidth constraints of the system [49], or it can be determined to satisfy the Nyquist criterion [50]. Usually, a 20 samples per seconds would provide fine details of human movements [51].

Preprocessing: Data is filtered with a small window moving average to remove high frequency noise. The number of points used to average the signal can be chosen by examining the power spectral density of the signals. The filter is required to remove unnecessary motions (e.g., tremors) while maintaining significant data. With

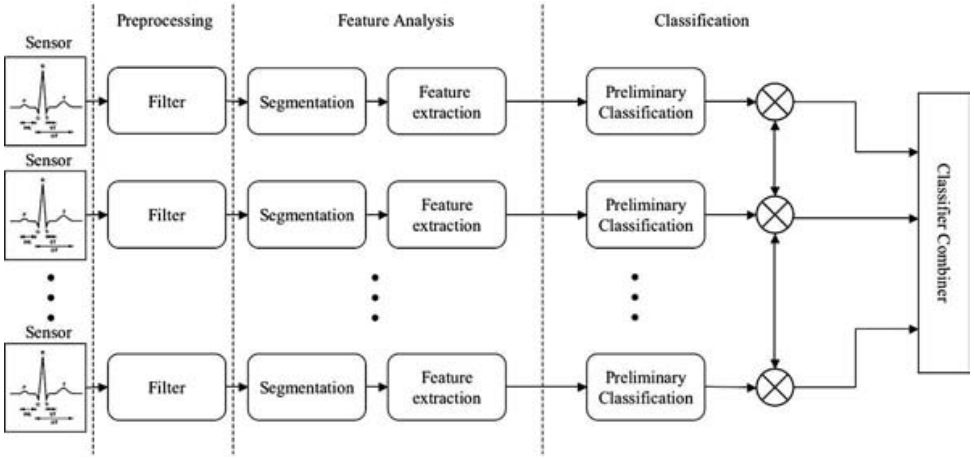

Figure 4.3. Signal processing flow.

these objectives, authors in [52] test several moving average filters with varying window sizes and choose the filter that best satisfies the aforementioned requirements.

Segmentation and annotation: Segmentation algorithms divide continuous data streams into discrete time intervals of the type expected by the information processing step, while annotation algorithms locate and label specific events. To enable real-time movement monitoring, an automated method is required.

Feature extraction: Statistical and morphological features are extracted from the signal segment. For example, sensor readings can be transformed into a set of informative attributes, including mean, start-to-end, standard deviation, peak-to-peak amplitude, RMS power, median, and maximum value.

Per-node classification: Each node uses the feature vector generated during feature extraction to determine the most likely action. Due to its simplicity and scalability, k-Nearest Neighbor (k-NN) [53] is a widely used classifier [54].

Final classification: The final decision can be made using either a data fusion or a decision fusion scheme. In the data fusion, features from all sensor nodes are fed into a central classifier. The classifier then combines the features to form a higher dimensional feature space and classifies movements using the obtained features. In the decision fusion, however, each sensor node makes a local

classification and transmits the result to a central classifier where a final decision is made according to the received labels.

In Section 4.5, we focus on the human movement annotation. Many movement models divide an action into several parts. In sports, many swings can be divided into phases. The golf swing is separated into takeaway, backswing, downswing, and follow-through portions [55]. In walking, the human stride is marked by several events such as initial stance (the foot placed on the ground), mid-stance, initial swing (the foot has just been lifted from the ground), and mid-swing, which repeat indefinitely [56]. These divisions can be used directly. For instance, high standard deviation of stride time during walking is indicative of Parkinson's disease or Huntington's disease and can be used to assess the risk of falling [57, 58]. We introduce a model based on HMMs that divides walking into aforementioned events. Inertial sensors provide movement data directly; therefore, these events can be found by looking for patterns in the sensor data.

4.5 An Automatic Parameter Extraction Method Based on HMM

Human movement models often divide movements into parts. These parts are often divided based on key events, also called temporal parameters. When analyzing a movement, it is important to correctly locate these key events, and so automated techniques are needed. There exist many methods for dividing specific actions using data from specific sensors, but for new sensors or sensing positions, new techniques must be developed. To address this problem, this section introduces a generic method for temporal parameter extraction called the Hidden Markov Event Model based on HMMs. This method can be quickly adapted to new movements and new sensors/sensor placements. This method is validated on a walking dataset using inertial sensors placed on various locations on a human body. The technique is designed to be computationally complex for training, but computationally simple at runtime to allow deployment on resource-constrained sensor nodes.

4.5.1 *HMEM Training and Use*

The Hidden Markov Event Model (HMEM) is the name of the introduced key event labeling system, which uses an HMM with a specific state structure and a modified training procedure designed to find key events. The model also adds a feature selection and model parametrization system based on Genetic Algorithms (GAs). The HMEM makes several assumptions about the underlying data: 1) there are a number of different event types, 2) the events always occur in a specific order and for cyclical movements they repeat, 3) every single event type is represented in every action, and 4) there are a number of unlabeled samples between two adjacent events.

A traditional pattern recognition technique used for time-varying signals is the Hidden Markov Model. A basic HMM describes a discrete-time Markov process. At a particular moment the process is in just one state. At fixed time intervals, the process produces an output and then transitions to another state (or remains in the current state). The transitions and outputs are probabilistic and based exclusively on the present state. The process generates a sequence of outputs, and a corresponding sequence of states. The states cannot be directly observed, and are thus hidden. An HMM is completely described by initial state probabilities, state transition probabilities, and output probabilities. Algorithms exist to 1) build an HMM to describe a given set of output sequences, 2) choose which of several models best describe an output sequence, 3) find the most likely current state of an HMM given the output sequence up until now, and 4) the most likely state sequence associated with a particular output sequence for a specified HMM [59, 60].

For a general HMM, it is possible for any state to transition to any other state. This is called an ergodic model. Another variant is to enforce a specific ordering for the states: each state can only transition to itself or state to the "right" of it in the ordering. This is called a left-right model [60].

Each key event can be represented by a unique state. Ideal events occur at a specific time but have no duration. However, given the idea that the key event might be associated with unique features in the

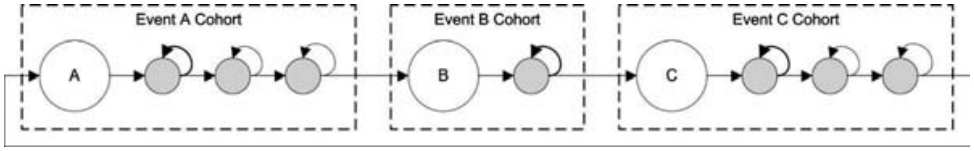

Figure 4.4. HMEM model and structure. See also Color Insert.

observation sequence, the key event state should have a one-sample duration. The HMEM encodes this concept into an HMM by removing the self-transition from states associated with key events, forcing a transition after one sample. The samples between key events are represented by transition states which support both self-transitions and forward-transitions, as seen in Fig. 4.4 states are grouped into cohorts, which start with a key event state and end with the last transition state before the next key event state. For any observation sequence in the training data, the positions of the key event states are known. This means that training each cohort independently is identical to training the whole system at once.

4.5.2 *Overview*

There are several stages required to train the HMEM as shown in Fig. 4.5.

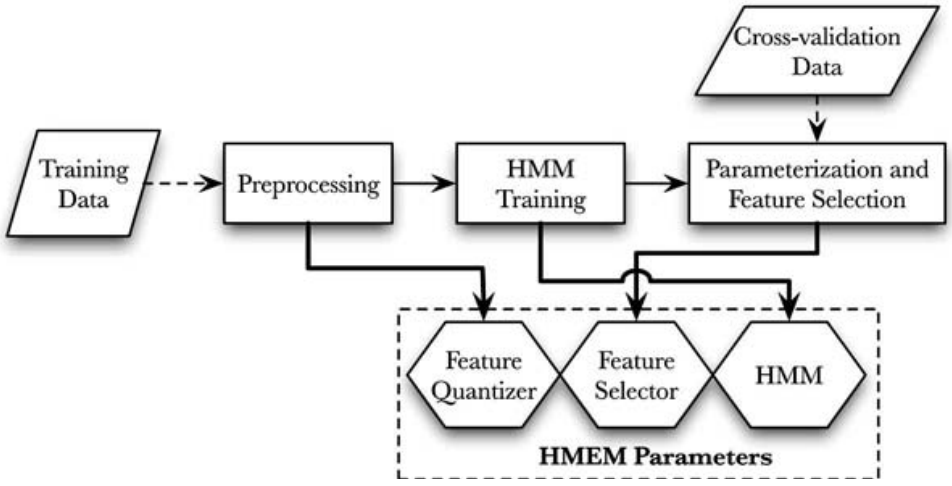

Figure 4.5. HMEM training procedure.

4.5.2.1 Preprocessing and feature extraction

The signal is filtered with a moving average filter to remove high frequency noise. Then it is normalized by subtracting a large-window mean and dividing by a large-window standard deviation. Several parameters representing the action data inside the signal, referred to as features, are extracted at each sample. These features are further quantized with a 10-level uniform quantizer based on the range of the features in the training data [10].

4.5.2.2 HMM training

The HMM is effectively a finite state machine with probabilistic transitions and certain emission probabilities. These probabilities must be specified as part of the mathematical model defining an HMM. The exact locations of all key event states and what observations they emit are known from the annotations in the training data. However, the number of transition states and their transition and emission probabilities are unknown and must be trained. There are several well-known techniques for training HMMs, including Baum-Welch and Viterbi Path Counting [59, 61].

The training data is segmented using the canonical annotations. Each cohort is trained independently using a set of segments that start with a sample that should be labeled with the cohorts event and end just before the next labeled event. According to this model, the first state must be the cohort's event state, and the last sample must be associated with the last transition state in the cohort. During training, it is important to make sure that all considered paths meet this constraint. Viterbi Path Counting produces a single path for each event that can be edited to meet the constraints if necessary, while Baum-Welch can also be constrained in this way, VPC is much faster, which is important given the already high training times. This feature is one of the primary reasons for choosing VPC over Baum-Welch. The details of the training process are discussed in Section 4.5.3.

4.5.2.3 Parametrization and feature selection

HMMs are trained to represent a process, not to minimize segmentation error. It is possible to explicitly attempt to increase

classification accuracy by choosing model parameters with that goal in mind. A genetic algorithm with uniform crossover is used to train the model. The population fitness is evaluated using the training model, and then at the end, the model that gives the best results for the cross-validation data is selected. Further discussion follows in Section 4.5.4.

4.5.3 *HMM Training and the Viterbi Algorithm*

A Markov process has N states $S = \{s_1, s_2, \cdots, s_N\}$, and can emit M observations $X = \{x_1, x_2, \cdots, x_M\}$. For a given observation sequence $O_T = (o_1, o_2, \cdots, o_T)$ with T observations, there is a corresponding state sequence $Q_{(T)} = (q_1, q_2, \cdots, q_T)$. The HMM $\lambda = \{\pi, A, B\}$ is defined by three sets of probabilities: initial state probabilities $\pi = \{\pi_i | \pi_i = P(q_o = s_i)\}$, state transition probabilities $A = \{a_{ij} | a_{ij} = P(q = s_j | q_{prev} = s_i)\}$, and observation probabilities $B = \{b_j(k) | b_j(k) = P(o = x_k | q = s_j)\}$.

The most common training algorithm is the Baum-Welch algorithm [59], however a newer algorithm, the Viterbi Path Counting (VPC) algorithm is more appropriate for this work [61]. Both algorithms follow the training procedure shown in Algorithm 4.1. They start with a fixed number of states and an initial set of model parameters, then extract probabilistically weighted state sequences

Algorithm 4.1 HMM Training Procedure

Require: $\lambda_0, \hat{} = \{O^1_{(T_1)}, O^2_{(T_2)}, \cdots, O^Y_{(T_Y)}\}$

1: $\lambda \leftarrow \lambda_0$
2: **for** $i \leftarrow 1$ to K **do** {estimates from ˜}
3: $\tilde{} \leftarrow \emptyset$
4: **for all** $O_{(T)} \in \hat{}$ **do**
5: $Q_{(T)} \leftarrow$ collect weighted state sequences using λ
6: $\tilde{} \leftarrow \tilde{} \cup Q_{(T)}$
7: **end for**
8: $\bar{\pi}_i = \frac{\text{number of times in state } s_i \text{ at time 1}}{\text{number of times at time 1}}$
9: $\bar{a}_{ij} = \frac{\text{number of transitions from state } s_i \text{ to state } s_j}{\text{number of transitions from state } s_i}$
10: $\bar{b}_j(k) = \frac{\text{number of times in state } s_j \text{ observing symbol } x_k}{\text{number of times in state } s_j}$
11: $\lambda \leftarrow \{\bar{\pi}, \bar{A}, \bar{B}\}$
12: **end for**

using the model parameters. Next, the transition and emission probabilities are updated based on the transitions and observations associated with each state sequence. The initial model is updated with these new probabilities. This process repeats until some desired level of convergence is reached. It will implicitly converge to a local minima.

The key to VPC is extracting the most likely state sequence.

$$Q_{(T)\max} = \arg \max_{Q_{(T)} \in S^T} P\left(Q_{(T)}, O_{(T)}\right) \tag{4.1}$$

A dynamic programing algorithm, called the Viterbi algorithm [59], solves this problem. Using the most likely state sequence extracted using the Viterbi algorithm, the transition and emission probabilities are found simply by counting the occurrences in all the most likely state sequences for each observation sequence in the training set. Since every conhort is trained individually, each observation sequence is a sequence starting on the key event and ending right before the next key event.

Maximizing the probability is equivalent to maximizing the log probability; therefore, we use log probabilities to prevent numerical underflow and facilitate faster computing. The order of the Viterbi algorithm for a left-right model with independent features is $O(\text{Viterbi}) = O(TxN) \cdot O(Pr_{est})$, where $O(Pr_{est})$ is the order of algorithm required to estimate probability. This order is constant time for the state transition probability, but based on the number of features for the observation probability estimation. This means $O(\text{Viterbi}) = O(TxNx|\vec{F}|)$.

4.5.4 *Feature Selection and Model Parametrization Using Genetic Algorithms*

The choice of whether or not to include each feature and the choice of the number of transition states for the cohorts are all tunable parameters of the HMEM. The feature selection $\Psi = \{\psi_k | \psi_k \in \{0, 1\}, i = 1, \ldots, |F|\}$ represents a choice of which features out of an exhaustive list are to be included and which are to be discarded. The number of selected features is $|\Psi| = \sum_k \psi_k$. Feature k is selected if $\psi_k = 1$ and is discarded if $\psi_k = 0$. The other parameter is

the number of transitions states for each cohort, $\Omega = \{\omega_e | \omega_e \in \{1, \ldots, 5\}, e = 1 \ldots E\}$, where E is the number of key events. The full HMEM model is represented by $\lambda_{HMEM} = \{\lambda_{HMM}, \Psi, \Omega\}$.

In essence, parametrization consists of choosing several good models based on one or more objective functions applied to the training set. These models are then compared against each other using the same objective function(s) applied to the cross-validation set. The best model on the cross-validation set is chosen. Because the cross-validation set exclusively contains data from subjects not in the training set, generalizability of the models to new subjects is improved. Genetic algorithms are used to generate the list of "good" models.

4.5.5 *HMEM Application Procedure*

After the HMEM is trained, it can be used to find key events in a data stream for the movement it has been trained on. The data flow for the algorithm is shown in Fig. 4.6. First, the data is filtered using the procedure described above, then features are extracted and quantized. Next, the feature selection is applied, and finally the most likely state sequence is extracted using the Viterbi algorithm. The annotation converter finds all the event states in this sequence and outputs an ordered set where each element consists of a time and event label.

4.5.6 *Experimental Analysis*

The results discussed in this section are based on an experiment reported in [62] and the node placement as described in Section 4.3.

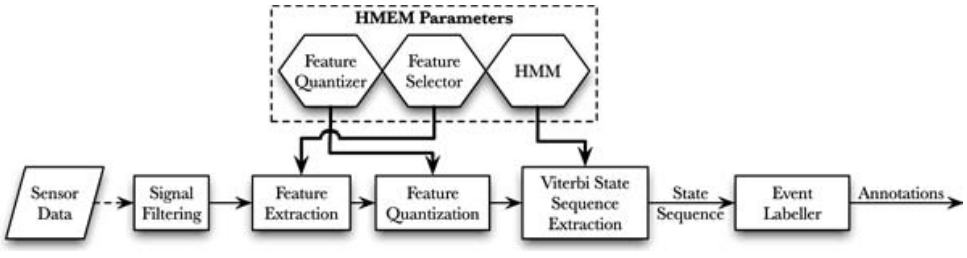

Figure 4.6. Application of the HMEM as described in Section 1.5.5.

The results are reported with precision (P), recall (R), Quality (RMSE). The first and last annotations were ignored because the algorithm needs context to determine annotations, and we are interested in the steady-state performance only. We show error for each mote using just the accelerometer readings, look at per-subject error for a poor performing sensor node, and a well-performing sensor node.

4.5.6.1 Examination of per-subject error

One of the goals of the HMEM system is good generalization to new subjects. Table 4.1 shows per-subject error for the sensor on the right thigh. Initially subjects two to four were in training, five to seven in cross validation, and eight and nine in test. However, subjects five and seven have walking patterns that differ significantly from the others, but are similar to each other. Therefore, subjects four and five were exchanged. It is likely that with a larger dataset the system could generalize better to such subjects. All the results are shown from the portion of the subjects' data that was in the test dataset.

The sensor on the right thigh, as shown in Table 4.1, performs well. Subjects eight and nine perform a little worse than subjects in the training and cross-validation sets. The worst per-subject error comes from subjects five and seven. The reason for this is not entirely clear. The use of the GA does not significantly reduce the discrepancy in per-subject error. Since the final selection criteria

Table 4.1. Subject error for R thigh with Accel and TP

	Default (132 Features)			GA (38 Features)		
Subject	P	R	RMSE	P	R	RMSE
Sub 2 Train	100	100	1.44	100	100	1.62
Sub 3 Train	100	100	1.33	100	100	1.11
Sub 4 Cross	100	100	1.36	100	100	1.38
Sub 5 Train	100	100	3.54	100	100	3.43
Sub 6 Cross	100	100	1.03	100	100	1.02
Sub 7 Cross	100	100	3.25	100	100	3.09
Sub 8 Test	100	100	1.74	100	100	1.76
Sub 9 Test	100	100	1.55	100	100	1.66

Table 4.2. Cross-validated subject error (R thigh)

Subject	P	R	RMSE	Fsel
Sub 2	100	100	1.47	6.7
Sub 3	100	100	1.38	8.7
Sub 4	100	100	1.68	4.7
Sub 5	99.8	99.8	3.55	4.7
Sub 6	100	100	1.20	6.7
Sub 7	100	100	3.09	28.7
Sub 8	100	100	1.52	10.7
Sub 9	100	100	1.59	16.0

for the solution is minimum total error, not minimum worst-case subject error, this is not surprising.

Manual partitioning of the data into training, cross-validation, and testing sets can artificially bias the results. Therefore, we performed an experiment for each subject where the subject was placed exclusively in the testing set, and the training and cross-validation sets were selected randomly from the remaining subjects. The results shown in Table 4.2 are the average of three tests after the GA. These results demonstrate that the model has good generalization to many subjects, but performs poorly on some.

4.6 System Optimizations

In Section 4.1 we discussed some of the constraints of the BAN systems. It was pointed out that energy constraint dominates the wearability of BAN systems. In general, energy can be used for local computation and communication. Previous studies of embedded sensor nodes have shown that data communication is expensive in terms of energy consumption, whereas data processing is relatively inexpensive [63].

The energy cost of the system can be improved in multiple ways. First, communication protocols used in embedded devices tend to be very general. Protocols, such as ZigBee [64], do not take advantage of the BAN specific features such as node proximity, data requirements, and signal processing flow. For example, due to proximity of the sensor units on the body, it may not be required for the radio to

operate at full range. Sensors nodes can be optimized to operate at the minimum required range to save energy. Second, not all of the sensor nodes may be required to contribute to a given computation. If that is the case, then the system can be optimized to select only required nodes at any given time. Finally, the signal processing technique can explicitly address the energy problem by selecting less expansive operations. In the following section, we describe how in the case of applications that do not have hard data deadlines it is possible to optimize energy expenditure of the communication system.

4.6.1 *Burst Communication*

Most BAN applications have specific signal processing requirements as can be seen in Section 4.2. The typical signal processing flow involves several processing blocks, which may require collaboration among the sensing units. Intensive signal processing may require a lot of inter-node communication. Frequent inter-node communication leads to increased energy consumption. Therefore, if an application does not have a strict deadline, transmissions in short bursts at a high bit rate can help minimize transmission energy per bit [65].

4.6.1.1 Task graph

The signal processing model described earlier is usually implemented in a distributed manner over a BAN. Information flow across the network can be represented with a task graph model. In a system of n sensor nodes, task graph is composed of n subgraphs connected through inter-node links. Each subgraph represents static information dependencies within a node as shown in Fig. 4.7, where u_i^R, u_i^S, u_i^F, and u_i^C denote sensor reading and

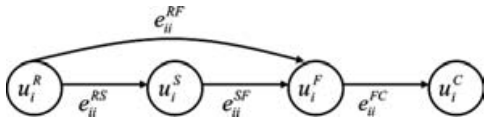

Figure 4.7. Intra-node task subgraph.

preprocessing, segmentation, feature extraction, and classification blocks, respectively.

Given a set of n sensor nodes, *intra-node task subgraph* for node s_i is defined by $G_i = (V_i, E_i)$, where V_i is the set of four vertices and E_i is the set of four edges. Each vertex, denoted by u_i^{μ}, corresponds to a processing unit, and each edge is denoted by $e_{ii}^{\mu\eta}$ $(\mu, \eta \in \{R, S, F, C\})$ representing intra-node dependencies. Inter-node links that represent dependencies across sensor nodes are used to connect subgraphs and form a task graph. An inter-node link is determined according to dependencies induced by application.

Given a set of n sensor nodes $s_1, \ldots, s_n$ and inter-node dependencies, *task graph* $G = (V, E)$ is formed by connecting n intra-node task subgraphs $G_1, \ldots, G_n$ through dependency links E_b defined by application criteria. The set of edges E is given by

$$E = E_w \cup E_b \tag{4.2}$$

where the set of intra-node edges E_w is given by

$$E_w = \bigcup_{i=1}^{n} E_i \qquad i = 1, \ldots, n \tag{4.3}$$

and the set of vertices V is defined by

$$V = \bigcup_{i=1}^{n} V_i \qquad i = 1, \ldots, n \tag{4.4}$$

where each V_i is the set of vertices within subgraph G_i.

As an abstract example, Fig. 4.8 shows a task graph for a network of two sensor nodes where processing units are connected through five inter-node dependency links.

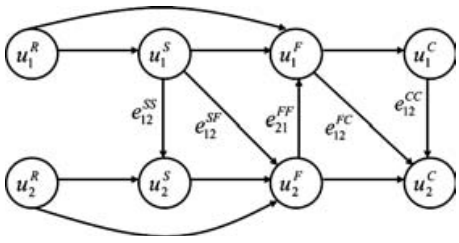

Figure 4.8. Sample task graph with five internode links.

In the context of the task graph, the idea behind using buffers is to transmit the maximum amount of data on the inter-node links in short time intervals. The large number of data blocks produced by each processing unit is stored locally and is transmitted using available bandwidth. This would conform to real situations of health care systems where physicians are interested in receiving reports on daily activities rather than immediate reports. By assuming no immediate deadlines in the system, individual buffers on each link are maintained and the data blocks are transmitted separately for each inter-node link. The optimization problem can be defined as follows:

Optimization Problem: Given task graph G, each inter-node link $e_{ij}^{\mu\eta}$ is associated with a number $x_{ij}^{\mu\eta}$ denoting the number of actions for which data blocks produced by the source unit u_i^{μ} are buffered prior to every transmission. The objective is to find values $x_{ij}^{\mu\eta}$ that minimize the number of transmissions subject to memory constraints on nodes.

4.6.1.2 Problem formulation

Given the task graph G as described earlier, let $a_{ij}^{\mu\eta}$ be a binary that represents existence of inter-node links and is given by

$$a_{ij}^{\mu\eta} = \begin{cases} 1, & \text{if } s_i \text{ and } s_j \text{ are dependent through } u_i^{\mu} \text{ and } u_j^{\eta} \\ 0, & \text{otherwise} \end{cases} \tag{4.5}$$

and let d_i^{μ} be another binary denoting whether or not a processing unit is slower than its predecessor.

$$d_i^{\mu} = \begin{cases} 1, \text{ if } r_i^{\mu} < r_i^{\mu-1} \\ 0, \text{ otherwise} \end{cases} \tag{4.6}$$

The number of actions A occurred at action rate k during time period T is given by

$$A = k \times T \tag{4.7}$$

and the number of transmissions can be calculated by

$$Z = \sum_{i,j} A \frac{a_{ij}^{\mu\eta}}{x_{ij}^{\mu\eta}} \tag{4.8}$$

The total size of the intra-node buffers W_i for node s_i is given by

$$W_i = \sum_{\mu} b_i^{\mu} \tag{4.9}$$

and the total size of the inter-node buffers for node s_i is determined by

$$B_i = \sum_{\mu} (\max_{j,\eta}(a_{ij}^{\mu\eta} b_i^{\mu} x_{ij}^{\mu\eta}) + \max_{j,\eta}(a_{ji}^{\eta\mu} b_j^{\eta} x_{ji}^{\eta\mu}) + \max_{j,\eta}(a_{ji}^{\eta\mu} b_j^{\mu-1} x_{ji}^{\eta\mu})) \tag{4.10}$$

and the total size of delay buffers for node s_i is given by

$$D_i = T \sum_{\mu} d_i^{\mu} ((r_i^{\mu-1} - r_i^{\mu}) b_i^{\mu-1} + \sum_{j,\eta} a_{ji}^{\eta\mu} b_j^{\eta}) \tag{4.11}$$

Let M_i be the size of the memory on node s_i. The problem of minimizing the number of transmissions can be formulated as a convex optimization problem as follows:

$$Min \ Z \tag{4.12}$$

subject to

$$W_i + B_i + D_i \leq M_i \qquad \forall i \in \{1, \ldots, n\} \tag{4.13}$$

$$x_{ij}^{\mu\eta} \in Z^{+} \quad \forall i, j, \mu, \eta \tag{4.14}$$

The non-linear constraints due to the *max* functions in Eq. (4.10) can be transformed into linear equations by expanding every function over all values taken by the function. The integrality condition (4.14) can be relaxed to solve the problem using common convex programming tools.

$$x_{ij}^{\mu\eta} > 0 \quad \forall i, j, \mu, \eta \tag{4.15}$$

The solution obtained due to integrality relaxation will not carry the optimality condition, but it is possible to find a lower bound on the size of memory for which the result is optimal. For each sensor node s_i, the integer relaxed convex optimization finds optimal solutions for memories of size

$$M_i - \sum_{\mu} (1 - \varepsilon) \alpha_i^{\mu} \beta_i^{\mu} \gamma_i^{\mu} \tag{4.16}$$

where

$$\begin{aligned} \alpha_i^{\mu} &= a_{ij}^{\mu\eta} b_i^{\mu} \quad \text{s.t.} \quad j,\eta = \arg\max_{j,\eta}(a_{ij}^{\mu\eta} b_i^{\mu} x_{ij}^{\mu\eta}) \\ \beta_i^{\mu} &= a_{ji}^{\eta\mu} b_j^{\eta} \quad \text{s.t.} \quad j,\eta = \arg\max_{j,\eta}(a_{ji}^{\eta\mu} b_j^{\eta} x_{ji}^{\eta\mu}) \\ \gamma_i^{\mu} &= a_{ji}^{\eta\mu} b_j^{\mu-1} \quad \text{s.t.} \quad j,\eta = \arg\max_{j,\eta}(a_{ji}^{\eta\mu} b_j^{\mu-1} x_{ji}^{\eta\mu}) \end{aligned} \tag{4.17}$$

Inter-node buffers assigned to each processing unit can have at most three components as given in Eq. (4.10). Integer relaxation would increase size of each optimal buffer associated with $x_{ij}^{\mu\eta}$ by factor $1-\varepsilon$ of the unit data (α_i^{μ},β_i^{μ},γ_i^{μ}).

4.6.1.3 Experimental results

The results discussed in this section are based on the experiment reported in [66]. During the experiment three communication networks are considered. Each network is based on a particular signal processing requirements, which define specific inter- and intra-connection networks. For each network, Table 4.3 shows the number of network transmissions required, including the number of packets exchanged with and without using the buffer approach and highlights the improvement of applying buffers.

Based on the results in Table 4.3, a few conclusions can be made. In addition to communication simplification, the approach can reduce the communication coordination and enhance the system lifetime. Since the considered metric is based on the number of packets, it is independent of the communication protocol. However, the choice of packet size is important for the system. A larger

Table 4.3. Number of transmissions for different communication networks

Configuration	Action Rate (Hz)	# Packets		Improvement
		Without Buffer	With Buffer	
1	1.8	185760	74485	59%
	0.0167	1440	80	94%
2	1.8	46440	31226	32%
	0.0167	1440	153	89%
3	1.8	69660	37297	46%
	0.0167	1440	17	98%

packet size would enhance energy per bit transmitted ratio. Finally, the discussed solution assumes that buffers are preallocated for a particular implementation. An approach that would dynamically update the buffer size to accommodate for the system requirements at any given time would be potentially more beneficial.

References

1. S. Park, A. Savvides, and M. Srivastava (2001) Battery capacity measurement and analysis using lithium coin cell battery, in *Proceedings of the 2001 international symposium on Low power electronics and design*, pp. 387, ACM.
2. V. Jones, R. Bults, D. Konstantas, and P. Vierhout (2001) Healthcare PANs: personal area networks for trauma care and home care, in *Proceedings of the Fourth International Symposium on Wireless Personal Multimedia Communications (WPMC)*, pp. 9–12.
3. O. Bott, M. Marschollek, J. Bergmann, K. Wolf, U. Tegtbur, and R. Haux (2007) Sensor-enhanced health information system architectures for home and telecare: concept and prototype, in *European Conference on eHealth*, **118**, pp. 193–203.
4. S. Po, G. Dagang, M. Hapipi, N. Naing, W. Shen, A. Ongkodjojo, and F. Hock (2006) Overview of MEMSWear II-incorporating MEMS technology into smart shirt for geriatric care, *Journal of Physics: Conference Series*, **34**, pp. 1079–1085, Institute of Physics Publishing.
5. E. Jovanov, A. Milenkovic, C. Otto, and P. De Groen (2005) A wireless body area network of intelligent motion sensors for computer assisted physical rehabilitation, *Journal of NeuroEngineering and Rehabilitation*, **2(1)**, pp. 6.
6. R. Ramachandran, L. Ramanna, H. Ghasemzadeh, G. Pradhan, R. Jafari, and B. Prabhakaran (2008) Body sensor networks to evaluate standing balance: interpreting muscular activities based on inertial sensors, in*Proceedings of the second International Workshop on Systems and Networking Support for Health Care and Assisted Living Environments*, pp. 4, ACM.
7. H. Ghasemzadeh and R. Jafari (2009) sport training using body sensor networks: a statistical approach to measure wrist rotation for golf swing, in *The Fourth International Conference on Body Area Networks (BodyNets 09)*, Los Angeles, CA.

8. H. Ghasemzadeh and R. Jafari (2010) Body sensor networks for baseball swing training: coordination analysis of human movements using motion transcripts, *in Proceedings of the Eight IEEE International Conference on Pervasive Computing and Communications Workshops*, pp. 792–795.
9. A. Van Halteren, R. Bults, K. Wac, D. Konstantas, I. Widya, N. Dokovsky, G. Koprinkov, V. Jones, and R. Herzog (2004) Mobile patient monitoring: The mobihealth system, *The Journal on Information Technology in Healthcare*, **2**(5), pp. 365–373.
10. K. Kim, S. Bang, and S. Kim (2004) Emotion recognition system using short-term monitoring of physiological signals, *Medical and Biological Engineering and Computing*, **42**(3), pp. 419–427.
11. L. Dong, J. Wu, X. Bao, and W. Xiao (2006) Extraction of gait features using a wireless body sensor network (BSN), in *Proceedings of the Sixth International Conference on ITS Telecommunications,* pp. 987–991.
12. E. Guenterberg, A. Yang, H. Ghasemzadeh, R. Jafari, R. Bajcsy, and S. Sastry (2009) A method for extracting temporal parameters based on hidden markov models in body sensor networks with inertial sensors, *IEEE Transactions on Information Technology in Biomedicine*, **13(6)**, pp. 1019, (2009).
13. A. Lie, R. Shimomoto, S. Sakaguchi, T. Ishimura, S. Enokida, T. Wada, and T. Ejima (2005) Gait recognition using spectral features of foot motion, *Lecture Notes in Computer Science*, **3546**, pp. 767–776.
14. L. Atallah, O. Aziz, B. Lo, and G. Yang (2009) Detecting walking gait impairment with an ear-worn sensor, in *Proceedings of the 2009 Sixth International Workshop on Wearable and Implantable Body Sensor Networks 00*, pp. 175–180, IEEE Computer Society.
15. M. Hoehn and M. Yahr (1967) Parkinsonism: onset, progression and mortality, *Neurology*, **17**(5), pp. 427–442.
16. D. Webster (1968) Critical analysis of the disability in Parkinson's disease, *Modern Treatment*, **5(2)**, pp. 257.
17. G. Montgomery, N. Reynolds Jr., and R. Warren (1985) Qualitative assessment of parkinson's disease: study of reliability and data reduction with an abbreviated columbia scale., *Clinical Neuropharmacology*, **8(1)**, pp. 83.
18. J. Rabey, H. Bass, U. Bonuccelli, D. Brooks, P. Klotz, A. Korczyn, P. Kraus, P. Martinez-Martin, P. Morrish, W. Van Sauten, et al. (1997) Evaluation of the short parkinson's evaluation scale: a new friendly scale for

the evaluation of Parkinson's disease in clinical drug trials, *Clinical Neuropharmacology*, **20**(4), pp. 322–337.

19. S. Fahn and R. Elton, Members of the UPDRS Development Committee (1987) Unified Parkinson's disease rating scale, *Recent Developments in Parkinson's Disease*, **2**, pp. 153–163.
20. C. Goetz, G. Stebbins, D. Wolff, W. DeLeeuw, H. Bronte-Stewart, R. Elble, M. Hallett, J. Nutt, L. Ramig, T. Sanger, et al. (2009) Testing objective measures of motor impairment in early Parkinson's disease: Feasibility study of an at-home testing device Potential conflict of interest: Nothing to report., *Movement Disorders*, **24(4)**, pp. 551–556.
21. C. Ramaker, J. Marinus, A. Stiggelbout, and B. Van Hilten (2002) Systematic evaluation of rating scales for impairment and disability in Parkinson's disease, *Movement Disorders*, **17(5)**, pp. 867–876.
22. J. Ackmann, A. Sances, S. Larson, and J. Baker (1977) Quantitative evaluation of long-term Parkinson tremor, *IEEE Transactions on Biomedical Engineering*, pp. 49–56.
23. E. Van Someren, B. Vonk, W. Thijssen, J. Speelman, P. Schuurman, M. Mirmiran, and D. Swaab (1998) A new actigraph for long-term registration of the duration and intensity of tremor and movement, *IEEE Transactions on Biomedical Engineering*, **45(3)**, pp. 386–395.
24. B. Van Hilten, J. Hoff, H. Middelkoop, E. Van der Velde, G. Kerkhof, A. Wauquier, H. Kamphuisen, and R. Roos (1994) Sleep disruption in Parkinson's disease. Assessment by continuous activity monitoring, *Archives of Neurology*, **51**(9), pp. 922–928.
25. C. Homann, K. Suppan, K. Wenzel, G. Giovannoni, G. Ivanic, S. Horner, E. Ott, and H. Hartung (2000) The bradykinesia akinesia incoordination test (BRAIN TEST©), an objective and user-friendly means to evaluate patients with Parkinsonism, *Movement Disorders*, **15(4)**, pp. 641–647.
26. V. Rajaraman, D. Jack, S. Adamovich, W. Hening, J. Sage, and H. Poizner, (2000) A novel quantitative method for 3D measurement of Parkinsonian tremor, *Clinical Neurophysiology*, **111**(2), pp. 338–343.
27. P. Bain, (1998) Clinical measurement of tremor, *Movement Disorders*, **13**, pp. 77–80.
28. J. Matsumoto, D. Dodick, L. Stevens, R. Newman, P. Caskey, and W. Fjerstad (1999) Three-dimensional measurement of essential tremor, *Movement Disorders*, **14(2)**, pp. 288-294.
29. G. Deuschl, P. Bain, and M. Brin (1998) Consensus statement of the Movement Disorder Society on tremor, *Movement Disorders*, **13**, pp. 2–23.

30. D. Wright, K. Nakamura, T. Maeda, K. Kutsuzawa, K. Miyawaki, and K. Nagata (2008) Research and development of a portable device to quantify muscle tone in patients with Parkinson's disease, in *Proceedings of the 30th IEEE Annual International Conference of the Engineering in Medicine and Biology Society*, pp. 2825–2827.
31. P. Bain, L. Findley, P. Atchison, M. Behari, M. Vidailhet, M. Gresty, J. Rothwell, P. Thompson, and C. Marsden (1993) Assessing tremor severity, *British Medical Journal*, **56(8)**, pp. 868–873.
32. H. Ghasemzadeh, E. Guenterberg, and R. Jafari (2009) Energy-efficient information-driven coverage for physical movement monitoring in body sensor networks, *IEEE Journal on Selected Areas in Communications*, **27(1)**, pp, 2.
33. A. Viru and M. Viru (2001) *Biochemical Monitoring of Sport Training*, Human Kinetics.
34. M. Rizzo (2001) Softball/baseball training machine, United States Patent, US 6,305,366 Bl (45).
35. Kuster (20 November 2003) Golf swing training device, US Patent App. 10/717,841.
36. Y. Yamamoto (2004) An alternative approach to the acquisition of a complex motor skill: Multiple movement training on tennis strokes, *International Journal of Sport and Health Science*, **2**, pp. 169–179.
37. A. Chong (March 2009) A photogrammetric application in virtual sport training, *The Photogrammetric Record*, **24**, pp. 51–65(15).
38. T. Komura, A. Kuroda, and Y. Shinagawa (2002) NiceMeetVR: facing professional baseball pitchers in the virtual batting cage, in *Proceedings of the 2002 ACM Symposium on Applied Computing*, pp. 1065. ACM.
39. I. Karliga and J. Hwang (2006) Analyzing human body 3-d motion of golf swing from single camera video sequences, in *Proceedings of the IEEE International Conference on Acoustics, Speech and Signal Processing (ICASSP 2006)*.
40. A. Baca and P. Kornfeind (2006) Rapid feedback systems for elite sports training, *IEEE Pervasive Computing*, **5**(4), pp. 70–76.
41. A. Cochran, J. Stobbs, and Golf Society of Great Britain (1968) *Search for the Perfect Swing*, Triumph Books.
42. P. A. Hume, J. Keogh, and D. Reid (2005) The role of biomechanics in maximising distance and accuracy of golf shots, *Sports Medicine*, **35**, pp. 429–449(21).

43. J. Tartagni and P. Schmid (6 January 2004) Putting stroke training aid, US Patent 6,672,974.
44. M. Bellagamba (18 June 1991) Athletic swing practice apparatus, US Patent 5,024,443.
45. C. Welch, S. Banks, F. Cook, and P. Draovitch (1995) Hitting a baseball: a biomechanical description, *The Journal of Orthopaedic and Sports Physical Therapy*, **22(5)**, pp. 193.
46. H. Ghasemzadeh, E. Guenterberg, and R. Jafari (2009) Energy-Efficient Information-Driven Coverage for Physical Movement Monitoring in Body Sensor Networks, *IEEE Journal on Selected Areas in Communications*, **27**, pp. 58–69.
47. J. Polastre, R. Szewczyk, and D. Culler (April 2005) Telos: enabling ultra-low power wireless research, in *Fourth International Symposium on Information Processing in Sensor Networks (IPSN 2005)*, pp. 364–369, doi: 10.1109/IPSN.2005.1440950.
48. R. Gravina, A. Guerrieri, G. Fortino, F. Bellifemine, R. Giannantonio, and M. Sgroi (2008) Development of body sensor network applications using SPINE, in *Proceedings of the IEEE International Conference on Systems, Man, and Cybernetics (SMC 2008)*, Singapore.
49. H. Ghasemzadeh, J. Barnes, E. Guenterberg, and R. Jafari (2008) A phonological expression for physical movement monitoring in body sensor networks, in *Fifth IEEE International Conference on Mobile Ad Hoc and Sensor Systems (MASS 2008)*, pp. 58–68.
50. N. Stergiou, (2003) *Innovative Analyses of Human Movement: Analytical Tools for Human Movement Research*, Human Kinetics.
51. H. Ghasemzadeh, E. Guenterberg, K. Gilani, and R. Jafari (2008) Action coverage formulation for power optimization in body sensor networks, in *Design Automation Conference, 2008 (ASPDAC 2008)*, Asia and South Pacific, pp. 446–451.
52. H. Ghasemzadeh, V. Loseu, and R. Jafari (2009) Structural action recognition in body sensor networks: Distributed classification based on string matching, *IEEE Transactions on Information Technology in Biomedicine*, **14(2)**, pp. 425 - 435.
53. R. Duda, P. Hart, and D. Stork (1973) *Pattern Classification and Scene Analysis*, Wiley, New York.
54. R. Jafari, R. Bajcsy, S. Glaser, B. Gnade, M. Sgroi, and S. Sastry (June 2007) Platform design for health care monitoring applications, in *Joint Workshop on High Confidence Medical Devices, Software, and Systems and Medical Device Plug-and-Play Interoperability*, pp. 88–94.

55. S. Newell and E. Els (2001) *The Golf Instruction Manual*, Dorling Kindersley.
56. J. Perry (1992) *Gait analysis: normal and pathological function*, 1st edn. SLACK incorporated.
57. J. Hausdorff, M. Cudkowicz, R. Firtion, J. Wei, and A. Goldberger (1998) Gait variability and basal ganglia disorders: stride-to-stride variations of gait cycle timing in Parkinson's disease and Huntington's disease, *Movement Disorders*, **13(3)**, pp. 428–437.
58. J. Hausdorff, D. Rios, and H. Edelberg (2001) Gait variability and fall risk in community-living older adults: a 1-year prospective study, *Archives of Physical Medicine and Rehabilitation*, **82(8)**, pp. 1050–1056.
59. L. Rabiner and B. Juang (1986) An introduction to hidden Markov models, *IEEE ASSP Magazine*, **3**(1 Part 1), pp. 4–16.
60. L. Rabiner (1989) A tutorial on hidden Markov models and selected applications in speech recognition, in *Proceedings of the IEEE*, **77(2)**, pp. 257–286.
61. N. Liu, B. Lovell, and P. Kootsookos (2003) Evaluation of HMM training algorithms for letter hand gesture recognition, in *Proceedings of the Third IEEE International Symposium on Signal Processing and Information Technology (ISSPIT 2003)*, pp. 648–651.
62. E. Guenterberg, H. Ghasemzadeh, and R. Jafari (2009) A distributed hidden Markov model for fine-grained annotation in body sensor networks, in *Proceedings of the 2009 Sixth International Workshop on Wearable and Implantable Body Sensor Networks*, 00, pp. 339–344, IEEE Computer Society.
63. V. Raghunathan, C. Schurgers, S. Park, and M. Srivastava (March 2002) Energy-aware wireless microsensor networks, *Signal Processing Magazine, IEEE*, **19(2)**, pp. 40–50, ISSN 1053-5888. doi: 10.1109/79.985679.
64. Z. Alliance, ZigBee specification, ZigBee Document 053474r06, Version **1**, 2005.
65. J. M. Kahn, R. H. Katz, and K. S. J. Pister (1999) Next century challenges: mobile networking for "smart dust," in *Proceedings of the Fifth Annual ACM/IEEE International Conference on Mobile Computing and Networking (MobiCom 1999)*, pp. 271–278, ISBN 1-58113-142-9.
66. H. Ghasemzadeh, N. Jain, M. Sgroi, and R. Jafari (2009) Communication minimization for in-network processing in body sensor networks: a buffer assignment technique, in *Proceedings of the ACM/IEEE Design, Automation and Test in Europe (DATE09)*.

Chapter 5

Signal Processing In-Node Frameworks for Wireless Body Area Networks: From Low-Level to High-Level Approaches

Francesco Aiello, Giancarlo Fortino, Stefano Galzarano, Raffaele Gravina, and Antonio Guerrieri

Department of Electronics, Informatics, and Systems (DEIS), University of Calabria, Via P. Bucci, cubo 41C, 87036 Rende (CS), Italy
faiello@si.deis.unical.it; g.fortino@unical.it; galzarano@si.deis.unical.it; rgravina@deis.unical.it; aguerrieri@deis.unical.it

To develop applications based on wireless body area networks (WBANs), either low-level or high-level programming approaches can be adopted. Low-level approaches are based on low-level APIs (application programming interfaces) offered by sensor platforms, whereas high-level approaches are based on high-level programming models and frameworks that facilitate programming and increase productivity. This chapter proposes a high-level approach based on the agent-oriented programming model to flexibly design and efficiently implement signal processing in-node environments supporting WBAN applications. The approach is exemplified through a case study concerning a real-time human

Wireless Body Area Networks: Technology, Implementation, and Applications
Edited by Mehmet R. Yuce and Jamil Y. Khan

ISBN 978-981-4316-71-2 (Hardcover), ISBN 978-981-4241-57-1 (eBook)
www.panstanford.com

activity monitoring system, which is developed through two different agent-based frameworks: MAPS (Mobile Agent Platform for Sun SPOT) and AFME (Agent Factory Micro Edition). A comparison of the effectiveness and efficiency of the developed systems is finally presented.

5.1 Introduction

Wireless sensor networks (WSNs) are currently emerging as one of the most disruptive technologies enabling and supporting next generation ubiquitous and pervasive computing scenarios [24]. WSNs are capable of supporting a broad array of high-impact applications in several domains such as disaster/crime prevention, military, environment, logistics, health care, and building/home automation. WSNs applied to human body monitoring are usually called wireless body area networks (WBANs) [29]. WBANs are conveying notable attention as their real-world applications aim at improving the quality of life of human beings by enabling continuous and real-time, non-invasive medical assistance at low cost. Health care applications where WBANs could be greatly useful include early detection or prevention of diseases, elderly assistance at home, e-fitness, rehabilitation after surgeries, motion and gestures detection, cognitive and emotional recognition, medical assistance in disaster events, etc.

However, programming WBAN applications is a complex task due to the hard constraints of wearable devices in terms of limited resources (computing power, memory, and communications) and due to the lack of proper and effective software abstractions. To deal with these issues, several software frameworks have been developed such as CodeBlue [18], Titan [16], and SPINE [12, 9]. They aim at decreasing development time and improving interoperability among signal processing intensive applications based on WBANs while fulfilling efficiency requirements. In particular, they basically rely on a star-based network architecture, which is organized into a coordinator node and a set of sensor nodes. Moreover, they are developed in TinyOS at the sensor node side and in Java at the coordinator node side.

Apart from the adoption of software frameworks, we believe that the exploitation of the agent-oriented programming paradigm to develop WSN applications could provide more effectiveness as demonstrated by the application of agent technology in several key application domains [8, 17]. In this chapter, we, therefore, propose high-level, agent-oriented design and agent-based implementation to support the development of WBAN applications. In particular, the approach is applied in the context of a real-time human activity monitoring system through two different Java-based agent platforms running on the Sun SPOT sensor platform: MAPS (Mobile Agent Platform for Sun SPOTs) [4, 2] and AFME (Agent Factory Micro Edition) framework [21]. The system architecture relies on a typical star-based WBAN composed of a coordinator node and two sensor nodes, which are located on the waist and the thigh of the monitored human being, respectively. The coordinator is based on an enhancement of the Java-based SPINE coordinator [12, 27] and allows configuring the sensing process, receiving sensed data features, and recognizing predefined human activities. Each sensor node executes either a MAPS-based agent or an AFME-based agent that performs sensing of the on-board 3-axial accelerometer sensor, computation of significant features on the acquired data, and aggregation and transmission of features to the coordinator. Finally, a comparison between the MAPS-based and the AFME-based implementations is discussed.

This chapter is organized as follows. Section 5.2 describes a reference architecture for WBAN applications from network and functional perspectives. Section 5.3 details and compares the state-of-the-art on signal processing in-node frameworks and applications based on TinyOS for the development of WBAN applications: CodeBlue, Titan, and two versions of SPINE. In Section 5.4, the most known available agent-oriented platforms for developing WSN-based applications are described. Section 5.5 presents an agent-oriented approach for the construction of WBAN applications, whereas Section 5.6 exemplifies it by describing the implementation and evaluation of an agent-based, real-time human activity monitoring system through aforementioned different agent platforms. Finally conclusions are drawn and future research delineated.

5.2 A WBAN Reference Architecture

The network architecture of the reference WBAN for signal processing is organized into multiple sensor nodes and one coordinator node according to the scheme reported in Fig. 5.1. The coordinator manages the network, collects, stores, and analyzes the data received from the sensor nodes, and also can act as a gateway to connect the WBAN with other networks (e.g., Internet) for remote data access. Sensor nodes measure local physical parameters and send raw or preprocessed data to the coordinator. In this system, sensor nodes only communicate with the coordinator according to the star network topology.

The software architecture of the system consists of two main components installed, respectively, on the coordinator (e.g., a PC or a smartphone) and on the sensor nodes. Figure 5.2 shows a schema of the software architecture from a functional point of view.

At the coordinator side, an interface to the WBAN, which is placed between user applications and the hardware and software host platform, is made available. User applications manage the WBAN through a *system API*. The top level of the software architecture at the coordinator allows registered applications being notified of the following events generated by the WBAN: discovery of new nodes, sensor data communication, node alarms, and system messages such as low battery warnings. Commands issued by user applications and network-generated events are, respectively, coded in lower-level messages and decoded in higher-level information by

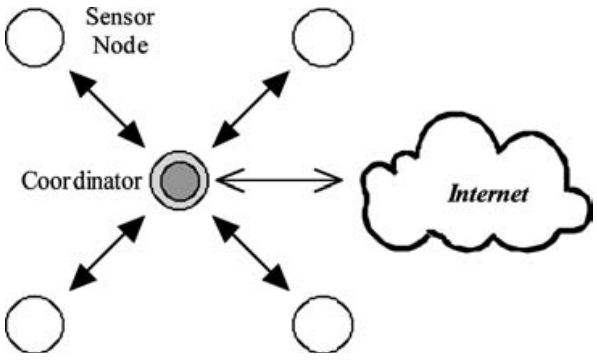

Figure 5.1. WBAN reference network architecture.

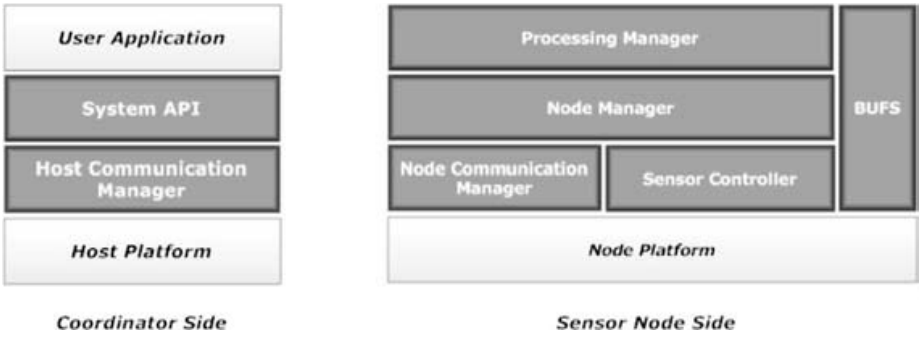

Figure 5.2. WBAN reference software architecture.

the *host communication manager* according to a specific over-the-air protocol. This component handles the generation and reception of messages and is interfaced with specific software components of the host platform to access the physical radio module to transmit/receive messages to/from the sensor nodes.

At the sensor node side, the software architecture provides: (i) abstractions of hardware resources such as sensors and the radio, (ii) a default set of ready-to-use common signal processing functions, and (iii) a flexible and modular architecture to be customized and extended to support new physical platforms and sensors and introduce new signal processing services. In particular, the *Node Communication Manager* acts as the counterpart of the *Host Communication Manager*. The *Sensor Controller* manages and abstracts the sensors on the node platform, providing a standard interface to the diverse sensor drivers. Specifically, it is responsible for sampling the sensors and storing the sensed data in properly defined *Buffers*. The *Node Manager* is the central component of the sensor node side, responsible of recognizing the coordinator requests and dispatching them to the proper components. Finally, the *Processing Manager* offers core processing services, which can be enriched by user-defined services.

5.3 Software Frameworks for Programming WBANs

WBAN applications can be mainly implemented according to the following approaches: (i) *application-specific code*, which aims at

Table 5.1. Comparison among different approaches for WBAN application development

Approaches/ Features	Application-specific code	Domain-specific framework	General-purpose middleware
Code Reusability		•	•
Rapid prototyping		•	•
Ease of debugging		•	•
Code efficiency	•	•	
System interoperability		•	•
Specific support to flexible sensing operations		•	
Specific support to in-node signal processing		•	

developing a WBAN application by using the low-level API provided by the sensor node platform; (ii) *general-purpose middleware*, which provides a high-level distributed framework for programming WSN applications for distributed signal processing; (iii) *domain-specific frameworks*, which aims at supporting specific development of WBAN applications according to a reference architecture. Table 5.1 reports the characteristics of the three approaches: code reusability, rapid prototyping, ease of debugging, code efficiency, system interoperability, specific support to flexible sensing operations, and specific support to in-node signal processing. In the following, specific applications and frameworks belonging to such approaches are described.

Most of the previous research efforts on WBANs were focused on proof-of-concept applications with the aim to demonstrate the feasibility of new context-aware algorithms and techniques, e.g., for recognition of physical activity or prompt detection of heart diseases, considering issues like power consumption and also radio channel usage but not taking into account code reusability and modularity. In reference [22], a method for physical activity monitoring is presented, which is able to detect body postures and periods of walking in elderly persons using one kinematic sensor attached to the chest. In reference [13], wearable motion sensors are used to guide post-stroke rehabilitation by models to predict clinical scores of motor abilities. In reference [23], activity recognition

is improved by integrating wearable sensors with ambient blob-based vision sensor data. Another physical activity recognition system based on wearable devices is presented in reference [19]. In reference [15], it is discussed in detail the interesting issue of developing a personal activity recognition system, which is based on data coming from a single body location regardless of the specific sensor location and able to work with different individuals. The system can be further personalized to enhance the activity recognition accuracy. Finally, the most exhaustive effort on activity recognition based on wearable sensors is presented in reference [5]. All these research efforts have been focused on efficient application-specific solutions rather than on the definition of reusable frameworks facilitating the development of WBAN applications.

The first important solution provided to define a general platform able to support various WBAN applications is CodeBlue [18]. CodeBlue is a framework running on TinyOS specifically designed for integrating wireless medical sensor nodes and other devices. CodeBlue allows these devices to discover each other, report events, and establish communications. CodeBlue is based on a publish/subscribe-based data routing framework in which sensors publish relevant data to a specific channel and end-user devices subscribe to channels of interest. It includes a naming scheme, a multi-hop communication protocol, authentication and encryption capabilities, location tracking, and in-network filtering and aggregation. CodeBlue provides end-user devices with a query interface for retrieving data from previously discovered sensor nodes. Although CodeBlue provides a sensor driver abstraction architecture, which allows an easy integration of new sensors within the system, selection of sensor types or physical node identifiers as data sources, tuning of the data rate, and definition of threshold-based filters to avoid unnecessary data being transmitted, it does not allow inserting complex signal processing functionalities into the sensor nodes. It supports just simple threshold-based triggers on the sensor readings that do not give enough flexibility for the variety of requirements of the WBAN applications.

A higher-level approach is adopted by Titan [16]. Titan is a general-purpose middleware implemented in TinyOS that supports

implementation and execution of context recognition algorithms in dynamic WSN environments. Titan represents data processing by a data flow from sensors to recognize result. The data are processed by tasks, which implement elementary computations. Tasks and their data flow interconnections define a task network, which runs on the sensor network as a whole. Tasks are mapped onto each sensor node according to the sensors and the processing resources they provide. Titan dynamically reprograms the WSN to exchange context recognition algorithms, handle defective nodes, variations in available processing power, or broken communication links. The architecture of Titan is composed of several software components, which enhance modularity. Although Titan raises the programming abstraction level by offering a middleware for effectively developing signal processing applications in WSNs, it is based on too generic mechanisms for providing efficient solutions in the specific BAN application domain. In fact, the programming of a feature extraction operation on the sensor node, which is often carried out in a BAN application, requires the creation of at least five tasks (sampling, buffering, loading, feature calculation, and transmission). Moreover, some overhead can be introduced due to the connections of the output and input ports among tasks through which data are exchanged.

The first example of domain-specific framework in the WBAN area is represented by SPINE (Signal Processing in Node Environment) [11, 12, 27]. SPINE is a software framework for the design of collaborative WBAN applications. It provides programming abstractions, APIs and libraries of protocols, utilities and data processing functions, which simplify development of distributed signal processing algorithms for the analysis and the classification of sensor data. SPINE [27] is distributed in open source under the LGPL (Lesser General Public License) license to facilitate establishing a broad community of users and developers that contribute to the scientific evolution of the framework with new capabilities and applications. The SPINE framework is composed of two distinctive parts: a node side runtime system residing on the sensor nodes and a Java application, the coordinator, residing on a PC and having functionalities such as nodes configuration and control, data gathering and data analysis. To date, two releases of SPINE are available:

- The TinyOS release (version 1.3), which supports different kinds of sensor platforms running the TinyOS [28] operating system (supported platforms are TelosB, MicaZ, Shimmer).
- The Z-Stack release (version 1.0), which allows the development of WBAN applications on the Z-Stack platform according to the ZigBee standard [30]. In particular, Z-Stack is the implementation of the ZigBee stack carried out by Texas Instruments.

The SPINE2 framework [10, 9] is an evolution of SPINE based on the C language for reaching a very high platform independency for C-like programmable sensor platforms (e.g., TinyOS, EmberZNet, Z-Stack) so raising the level of the provided programming abstractions from platform-specific to platform-independent. SPINE2 is founded on a software layering approach based on the C language, which is the language used for programming the majority of embedded systems. It embodies the following features: (i) execution on commercial resource-constrained sensor platforms each one having a different operating system; (ii) minimization of the amount of code that should be replicated for each specific implementation; (iii) enabling C developers (eventually C++) to extend the SPINE2 framework without having to learn low-level details of specific sensor platforms or without having to learn new programming languages; (iv) enabling, compiling, and simulating the code by using normal ANSI C tools.

While SPINE is centered on a programming model based on functions, SPINE2 is based on a task-oriented programming model in order to best fit the requirements of collaborative distributed applications in resource-constrained environments. Distributed and collaborative applications can then be programmed as a dynamically schedulable and reconfigurable set of tasks. Different tasks can be assigned to each node of the network, and tasks can be controlled at execution time via proper message exchange; in this way the network can overall adapt to changes in context, in overall goals, in the state of each single node, and it can better balance load and task types between each element of the network. Dynamic distribution of tasks also allows preprocessing of sensed data directly on the node, a significant reduction of data transmission and battery

consumption, and an overall increase in the network lifetime. Due to task-oriented programming, application developers do not need to program in tiny environments but only configure tasks on the WBAN coordinator.

To summarize, we promote the use of the domain-specific framework approach, which stands in the middle between application-specific code and general-purpose middleware approaches. It specifically addresses and standardizes the core challenges of WSN development within a particular application domain. While maintaining high efficiency, it allows for a more effective development of customized applications with little or no additional hardware configuration and with the provision of high-level programming abstractions tailored for the reference application domain. In particular, the SPINE and SPINE2 frameworks are domain-specific frameworks in the context of signal processing in-node intensive WBAN applications, whereas CodeBlue and Titan can be seen as general-purpose middleware solutions for WBAN applications. SPINE allows for both code efficiency similarly to an application-specific code approach, and code reusability, rapid prototyping, easy debugging, and system interoperability as CodeBlue and Titan. Moreover, it specifically supports functionalities for flexible sensing operations and easily programmable in-node signal processing. SPINE2 extends the functionalities of SPINE with the development of WBAN applications on heterogeneous sensor platforms based on C-like languages.

5.4 Agent-Oriented Platforms for Wireless Sensor Networks

In the context of WSNs, it is challenging to develop agent platforms (APs) for supporting (mobile) agent-based programming [8, 3]. Due to the currently available resource-constrained sensor nodes and related operating systems, building flexible and efficient agent platforms is a very complex task. Very few APs for WSNs have been to date proposed and actually implemented. An AP architecture (see Fig. 5.3) relies on the services offered by the hosting sensor node OS and support execution of agents by managing agent

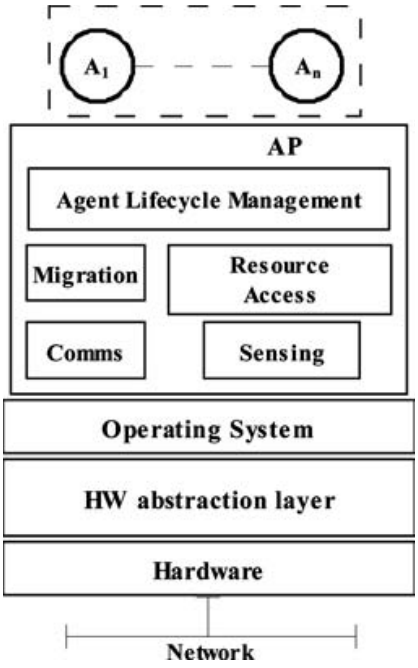

Figure 5.3. Reference architecture of a sensor node agent platform.

lifecycle, migration, communication, sensing capabilities, and sensor resource access. The most representative APs developed to date are SensorWare [7], Agilla [8], actorNet [14], MAPS [4], and AFME [21].

SensorWare [7] is a general middleware framework based on agent technology, where the mobile agent concept is exploited. Mobile control scripts in Tcl model network participants' functionalities and behaviors, and routing mechanisms to destination areas. Agents migrate to destination areas performing data aggregation reliably. The script can be very complex, and diffusion gets slower when it reaches destination areas. The replication and migration of such scripts in several sensor nodes allows the dynamic deployment of distributed algorithms into the network. SensorWare defines, creates, dynamically deploys, and supports such scripts. SensorWare is designed for iPAQ devices with megabytes of RAM. The verbose program representation and on-node Tcl interpreter can be acceptable overheads; however, they are not yet on a sensor node.

Agilla [8] is an agent-based middleware where each node supports multiple agents and maintains a tuple space and neighbors' list. The tuple space is local and shared by the agents residing on the

node. Special instructions allow agents to remotely access another node's tuple space. The neighbors' list contains the addresses of all one-hop nodes. Agents can migrate carrying their code and state, but do not carry their own tuple spaces. Agilla is currently implemented on MICA2, MICAZ, and TelosB motes.

While both Agilla and SensorWare rely on mobile agents, they employ a different communication model: Agilla's agent interaction is based on local tuple spaces, whereas SensorWare's agent interaction is based on direct communication based on network messages. In reference [26], another mobile agent framework is proposed. The framework is implemented on Crossbow MICA2DOT motes. In particular, it provides agent migration and agent interaction based both on locally shared memory and network messages. In reference [25], the authors propose an extension of Agilla to support direct communication based on messages. In particular, to establish direct communications, agents are mediated by a middle component (named landmark) that interact with agents through zone-based registration and discovery protocols.

In reference [14], actorNet, a mobile agent platform for WSNs based on the actor model, is proposed. In particular, it provides services such as virtual memory, context switching, and multitasking to support a highly expressive yet efficient agent functional language. Currently, the sensor node actorNet platform is specifically designed for TinyOS on MICA2 sensors.

The aforementioned mobile agent systems for WSNs are all implemented for TinyOS-based sensor platforms and use ad-hoc languages for agent programming (Agilla uses a micro-programming language, whereas actorNet employs a function-oriented language). Although some supported operations (e.g., migration) are very efficient, programming complex tasks is not so straightforward and, moreover, developers need to learn another very specific language. In the following, the available Java-based agent platforms are introduced.

The Mobile Agent Platform for Sun SPOT framework (MAPS) [4, 20] is an innovative Java-based framework for wireless sensor networks based on Sun SPOT technology, which enables agent-oriented programming of WSN applications. The MAPS architecture is based on components that interact through events. Each component offers

a minimal set of services to mobile agents, which are modelled as multi-plane state machines driven by ECA rules. In particular, the offered services include message transmission, agent creation, agent cloning, agent migration, timer handling, and easy access to the sensor node resources (sensors, actuators, input switches, flash memory, and battery).

The Agent Factory Micro Edition (AFME) [21, 1] is a lightweight version of the Agent Factory framework purposely designed for wireless pervasive systems and implemented in J2ME, recently ported onto Sun SPOT and purposely used for implementing agent communication and migration in WSNs. The AFME agents are based on a BDI (beliefs-desires-intentions)-like architecture and are programmed through a high-level logic-based language. AFME also provides a translator, which converts high-level agent specifications into Java code.

However, AFME was not specifically designed for WSNs and, particularly, for Java Sun SPOT. MAPS is conversely specifically designed for WSNs, and it fully exploits the release 5.0 red of the Sun SPOT library to provide advanced functionality of communication, migration, sensing/actuation, timing, and flash memory storage. Moreover, it allows developers to program agent-based applications in Java according to the rules of the MAPS framework so that no translator and/or interpreter need to be developed and no new language has to be learnt.

5.5 An Agent-Oriented Design of Signal Processing In-Node Environments

The exploitation of the agent-oriented programming paradigm to develop WBAN applications could provide more effectiveness as demonstrated by the application of agent technology in several key application domains [17]. In this section, we describe an agent-oriented design of SPINE (see Section 5.3), named ASPINE [6], which extends the functionalities provided by SPINE and allows for a more rapid development of signal processing intensive WBAN applications in terms of agent-based systems. The reference architecture defined in Section 5.2 was designed by using an

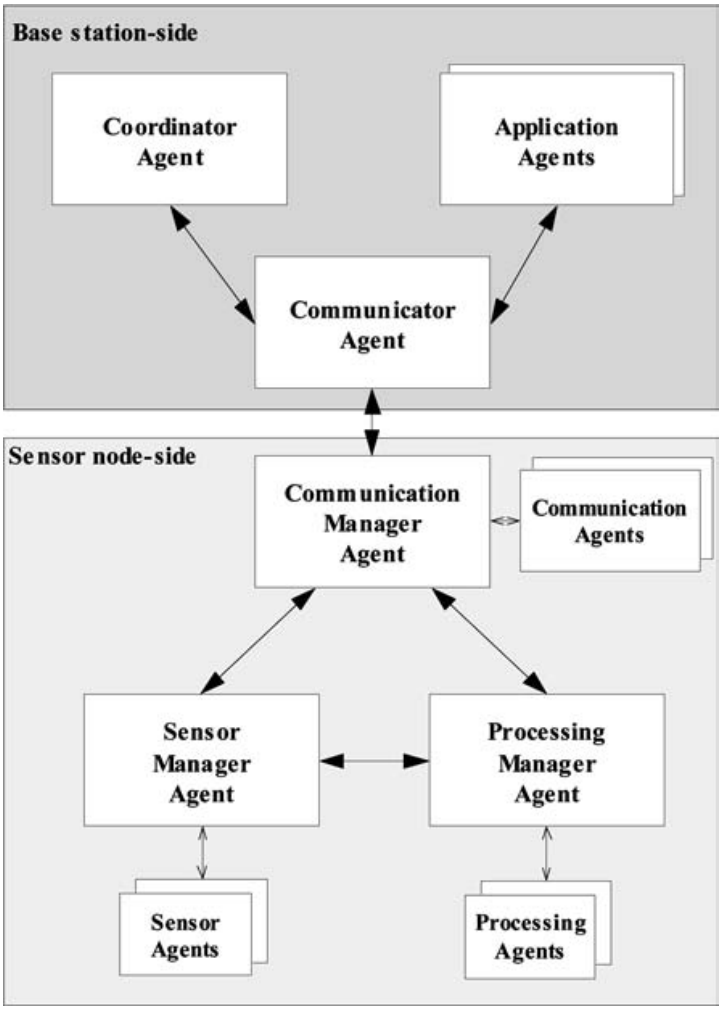

Figure 5.4. The ASPINE high-level architecture.

agent-based approach. Figure 5.4 shows the high-level architecture of ASPINE through a class diagram.
In particular, the following core agents are defined:

Base station-side

- The CoordinatorAgent is responsible for managing the set of nodes of the sensor network under control. Management involves configuring and monitoring nodes.
- The ApplicationAgents are agents implementing application-specific or domain-specific logics.

- The CommunicatorAgent allows the CoordinatorAgent and the ApplicationAgents to interact with the sensor nodes through an efficient over-the-air application-level protocol.

Sensor node-side

- The SensorManagerAgent manages the sensor/actuator resources of the node through specific SensorAgents able to interact with specific sensors (temperature, light, accelerometer, etc.), actuators (LEDs, actuation devices, etc.), and the battery.
- The CommunicationManagerAgent manages the communication with the communicator agent and with the other CommunicationManagerAgents, located at different sensor nodes, by means of specific CommunicationAgents. Moreover, such agent manages the radio settings (e.g., duty cycling, transmission power, etc.).
- The ProcessingManagerAgent supports one or more local processing tasks or parts of global processing tasks (spanning multiple sensor nodes) through processing agents. They are able to perform computation on sensed data (e.g., feature extraction, threshold functions, classification algorithms, etc.) and data aggregation.

An example of in-node signal processor is portrayed in Fig. 5.5 by means of a data-flow model based on tasks. The in-node signal processor aims at sampling the on-board 3-axial accelerometer, computing selected features on sample windows, and sending the results to the coordinator. In particular, the sensed data periodically produced by the sensing task acting on the three channels (X, Y, Z) of the accelerometer are split for the computation of the features Mean on all three axes (XYZ), and Min and Max on axis X. Each triple

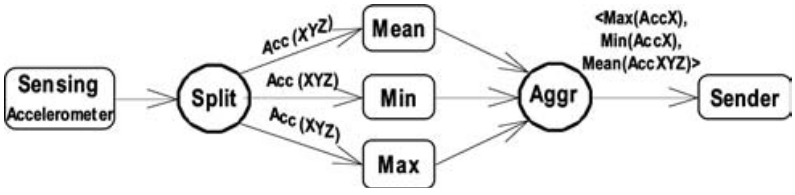

Figure 5.5. Data-flow-based model of an in-node signal processing task.

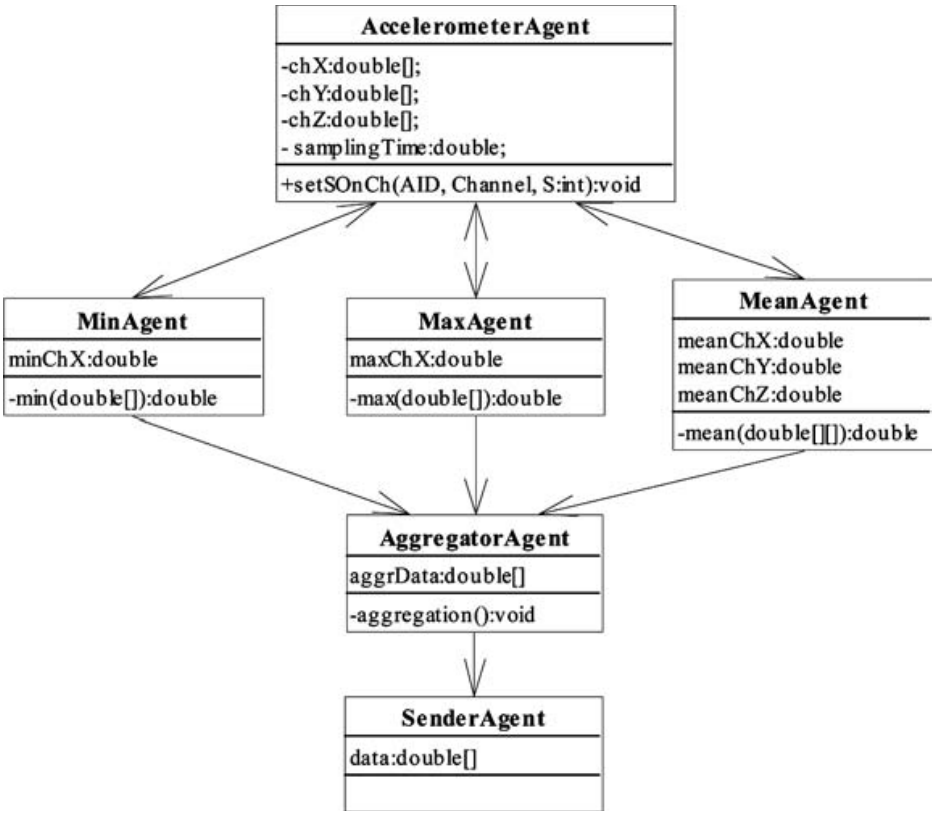

Figure 5.6. ASPINE-based design of the example in-node signal processing task.

of computed features (<Mean(AccXYZ), Min(AccX), Max(AccX)>) are aggregated by the aggregation task (Aggr) and sent to the coordinator node by the data transmission task (Sender) as soon as the aggregated data is available.

The ASPINE design of the data-flow-based model of Fig. 5.5 is shown in Fig. 5.6. The AccelerometerAgent interacts with the accelerometer sensor and, according to the set sampling time (samplingTime), acquires one sample per channel (X, Y, Z), and stores them into the corresponding buffers chX, chY, chZ. Once *S* samples are acquired, the AccelerometerAgent passes them to the MinAgent, MaxAgent, and MeanAgent. These relationships are created through the method setSOnCh(AID, Channel, *S*), where AID is the agent identifier, Channel refers to the channels to be considered, and *S* is the number of samples. In this case, all agents are based on the same *S* but on different channels. In particular,

MinAgent, MaxAgent, and MeanAgent receive the last acquired S samples, respectively, from the chX buffer, from the chX buffer, and from the chX, chY, and chZ buffers. Upon reception of such data, the agents compute their respective functions and pass the results to the AggregatorAgent. This waits for the aggregation of the data triple aggrData=<minChX, maxChX, <meanChX, meanChY, meanChZ≫ and passes it to the SenderAgent, a specific CommunicationAgent, which, in turn, transmits it to the CommunicatorAgent located at the base station.

5.6 An Analysis of Agent-Oriented Implementations of In-Node Signal Processors

A WBAN-based activity human monitoring system aims at recognizing postures and movements of assisted livings [22]. The developed prototype is able to recognize some postures (lying down, sitting, and standing still) and a movement (walking). The architecture of the system, shown in Fig. 5.7, is organized into a coordinator and two sensor nodes according to the reference WBAN architecture described in Section 5.2.

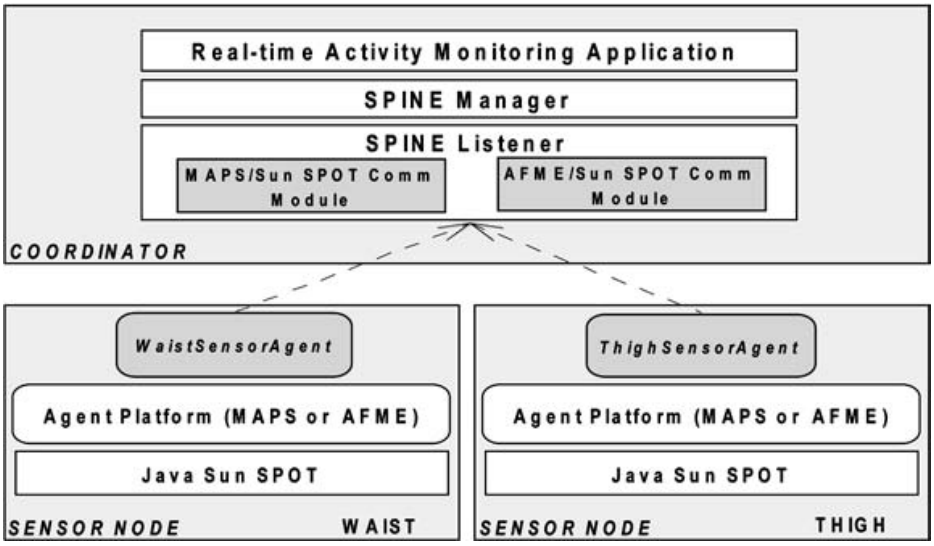

Figure 5.7. Architecture of the WBAN-based real-time activity monitoring system.

The coordinator is based on the Java-based SPINE coordinator developed in the context of the SPINE project [27]. In particular, the SPINE Manager is used by end-user applications (e.g., real-time activity monitoring application) for sending commands to the sensor nodes. Moreover, the SPINE Manager is responsible for capturing low-level messages and node events through the SPINE Listener, which integrates several sensor platform-specific SPINE communication modules (e.g., TinyOS, Z-Stack, etc.) to notify registered applications with higher-level events and message content. A SPINE communication module is composed of a send/receive interface and some components that implement such interface according to the specific sensor platform and that formalize the high-level SPINE messages in sensor platform-specific messages. The SPINE Listener is enhanced with MAPS/Sun SPOT and AFME/Sun SPOT communication modules to configure and communicate with MAPS-based and AFME-based sensor nodes, respectively. Such modules translate high-level SPINE messages formatted according to the SPINE OTA (over-the-air) protocol [27] into lower-level MAPS or AFME/Sun SPOT messages through its transmitter component and vice versa through its receiver component. Such modules also integrate an application-specific logic for synchronizing the operations of the two sensors. The SPINE-based real-time activity monitoring application was thus completely reused as well as the SPINE Manager; only the SPINE Listener was modified to account for such enhancement.

The sensor nodes are based on Java Sun SPOT sensors respectively positioned on the waist and the thigh of the monitored person. In particular, an agent platform (MAPS or AFME) is resident on the sensor nodes and supports the execution of the WaistSensorAgent and the ThighSensorAgent. Such sensor agents have the following similar step-wise cyclic behavior:

1. *Sensing* the 3-axial accelerometer sensor according to a given sampling time (ST).
2. *Computation* of specific features (Mean, Max, and Min functions) on the acquired raw data according to the window (W) and shift (S) parameters. In particular, W is the sample size on which features are computed, whereas S is the number of new

acquired sample data for calculating a new feature. Usually S is set to 50% of W.
3. Features *aggregation* and *transmission* to the coordinator.
4. Goto 1.

The agents differ in the specific computed features even though the W and S parameters are equally set. In particular, while the waist sensor agent computes the mean values for data sensed on the XYZ axes, the min and max values for data sensed on the X axis, the ThighSensorAgent calculates the min value for data sensed on the X axis.

In the following subsections, we describe the implementation of the WaistSensorAgent carried out with MAPS and AFME and, then, compare the implemented solutions.

5.6.1 *MAPS-Based and AFME-Based Implementation of Sensor Agents*

The architecture of the MAPS-based sensor agent (Fig. 5.8) is composed of two planes (*sensing* and *feature calculation and transmission*) modeled as finite state machines. Each plane is able to handle specific events, which are instances of system and user-defined event types. The *sensing plane* (see Fig. 5.9a) specifies the sensing process: the MSG.START event initiates the sensing of the three channels of the accelerometer; after the sensed data are returned through the ACC_CURRENT_ALL_AXES event, the sampling timer is scheduled for the next acquisition; if a MSG.RESYNCH, formalizing a re-synchronization operation among the sensor agents sent by the coordinator, is received, the sensing process is paused until a MSG.RESTART event arrives; finally, the MSG.STOP halts the sensing process. The *feature calculation and transmission* plane (see Fig. 5.9b) specifies the feature extraction process and the transmission of the computed features to the coordinator, which are triggered by the MSG.COMPFEATURES event.
The architecture of the AFME-based sensor agent (Fig. 5.10) is composed of:

- *Two perceptors*. MTSPerceptor checks for the arrival of a new message and SensingPerceptor checks for the feature

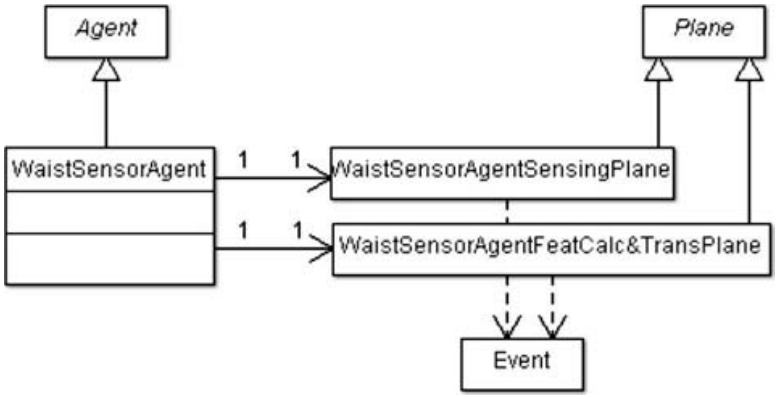

Figure 5.8. MAPS-based sensor agent.

computation and send the computation results to the coordinator if such results are available.

- *Three actuators*. ActivateSensorActuator allows activating the sensing operation, ResetActuator resets the data buffer after the reception of the resynch message, and RequestActuator is used to send a request message to the coordinator.
- *Rules*. TerImplication contains the rules of the agent behavior (see below).

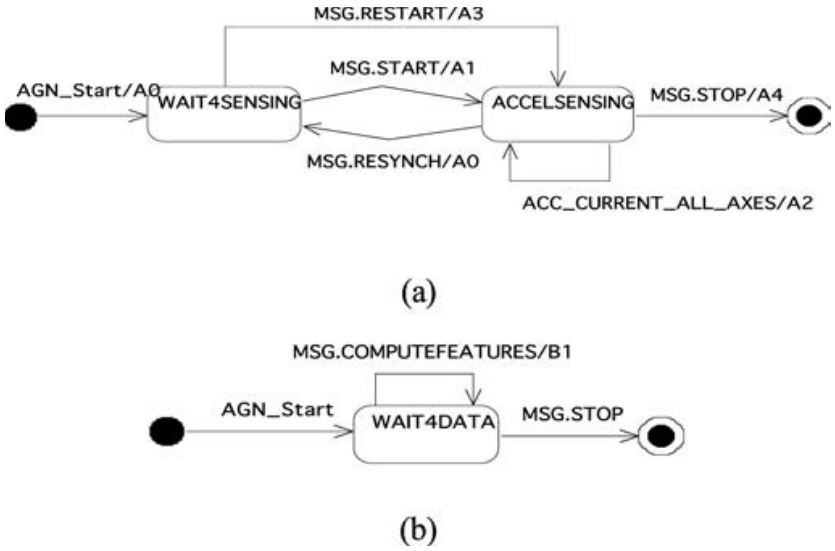

Figure 5.9. Planes of the MAPS-based sensor agent: (a) sensing plane; (b) feature calculation and transmission plane.

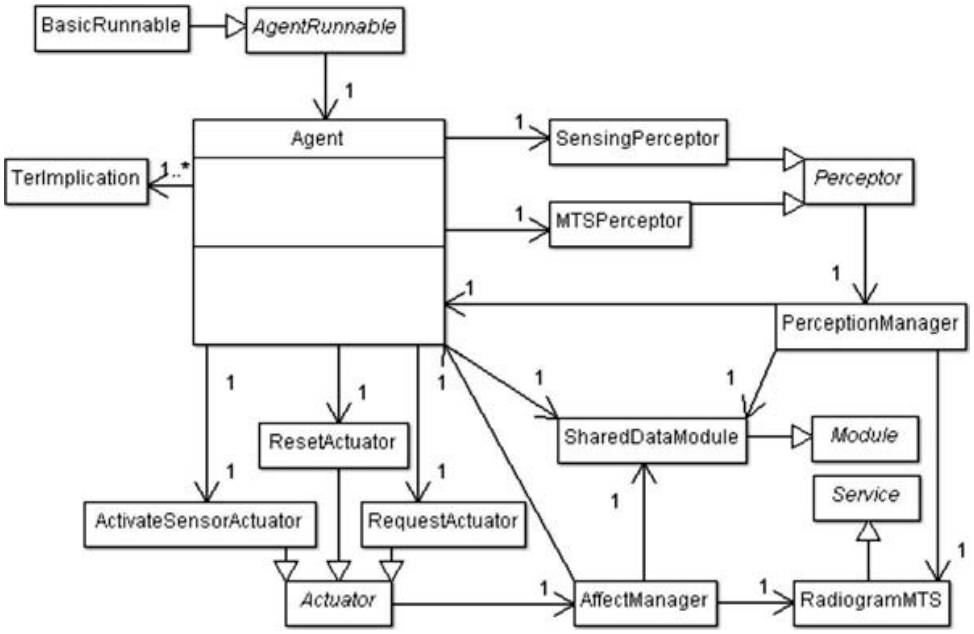

Figure 5.10. AFME-based sensor agent.

- *One Module*. SharedDataModule contains buffers storing the data sensed from the three accelerometer channels, the feature extraction parameters, the flag variable (*activation*) enabling the sensing process.
- *One Service*. RadiogramMTS represents the transport service for data transmission to the coordinator.

The agent behavior is modeled through the following three basic rules:

1. message(inform, sender(BaseStation, addresses(BSAddress)), begin) > activateSensors(1);
2. sense(?val), !message(inform, sender(BaseStation, addresses (BSAddress)), resynch) > request(agentID(BaseStation, addresses (”radiogram://”+BSAddress)), ?val);
3. message(inform, sender(BaseStation, addresses(BSAddress)), resynch) > reset;

Rule (1) enables the sensor reading operation on the sensor node. In particular, this rule states that the message belief, which is generated upon the reception of an inform message with “begin” content sent

by the coordinator with address BSAddress, triggers the action ActivateSensors(1), which will then set the *activation* flag on.

Rule (2) regulates the agent behavior during the sensing phase. If a new sense belief having the sensed data is generated and a message belief generated upon reception of the resynch message sent by the coordinator does not exist, the request action is carried out so that the new message containing the feature calculation is sent to the coordinator.

Finally, rule (3) allows re-synchronizing the sensor agent. In particular, it states that if the belief message is generated upon reception of the resynch message, the action reset, which re-initializes all the data structures in SharedDataModule, is executed.

5.6.2 *Agent Implementation Comparison*

The comparison of the two different agent implementations are carried out according to the following two aspects: (i) effectiveness in prototyping the agent-based solutions; (ii) timing and synchronization of the real-time monitoring.

The development of MAPS and AFME agents is based on different approaches. MAPS uses state machines to model the agent behavior and directly the Java language to program guards and actions. AFME uses a more complex model centered on perceptors, actuators, rules, modules, and services that define the agent behavior. They are both effective in modeling agent behavior even though MAPS is more straightforward as it relies on a programming style based on state machines widely known by programmers of embedded systems.

Two important issues to deal with are the timing of the sensing process in terms of admissible sampling rate and the synchronization between the operations of the two agents, which is to be maintained within a maximum skew for not affecting real-time monitoring. If such skew is overtaken, the two agents are to be re-synchronized. Indeed such two aspects are strictly correlated. In particular, as the sensor agents compute a different number of features, when the sampling rate is high, the agent computing more features (i.e., the WaistSensorAgent) takes more time to complete its operations for each S sample acquisition

than the ThighSensorAgent. Re-synchronization is driven by the synchronization logic included in the developed MAPS/Sun SPOT and AFME/Sun SPOT communication modules, which sends a re-synchronization message as soon as it detects that the synchronization skew is greater than a given threshold. Detection is based on the skew time between the receptions of two messages sent by the agents that contain features referring to the same interval of S sample acquisition: if $skew \geq P \times S \times ST$, then *resynchronize*, where P is a percentage, S = 0.5 W is the shift, W is the data sample window, ST is the sampling time. Thus, the evaluation aims at analyzing the synchronization of the sensor agents and their monitoring continuity. The defined metrics are:

- The *packet pair average time* (PPAT), which is the average reception time between two consecutive pairs of synchronized packets, having the same logical timestamp and containing the computed features sent by the sensor agents.
- The *synchronization packet percentage* (SPP), which is the percentage of resynchronization packets, which are sent by the coordinator for re-synchronizing the sensor agents, calculated with respect to the total number of received feature packets.

PPAT should be ideally equals to ST*S, i.e., the packet pair arrives each monitoring period and so there is no de-synchronization in the average. SPP should be as much as possible close to 0, i.e., a few or no re-synchronizations are carried out and so the monitoring can be continuous as a resynch operation usually takes 600 ms. Thus, system parameters (W, ST, and P) should be carefully set to optimize the monitoring process. To this purpose, a set of experiments was set up to tune the system parameters. In particular, the experiments were carried out by fixing ST (ms) = [25, 50, 100], W (samples) = [40, 20], and P (%) = [5, 15, 25]. Figures 5.11 and 5.12 show the obtained results.

As can be noticed, the system cannot support an ST = 25 ms because PPAT is always greater than the ideal value and SPP is too high. This leads to a non-continuous monitoring due to very frequent

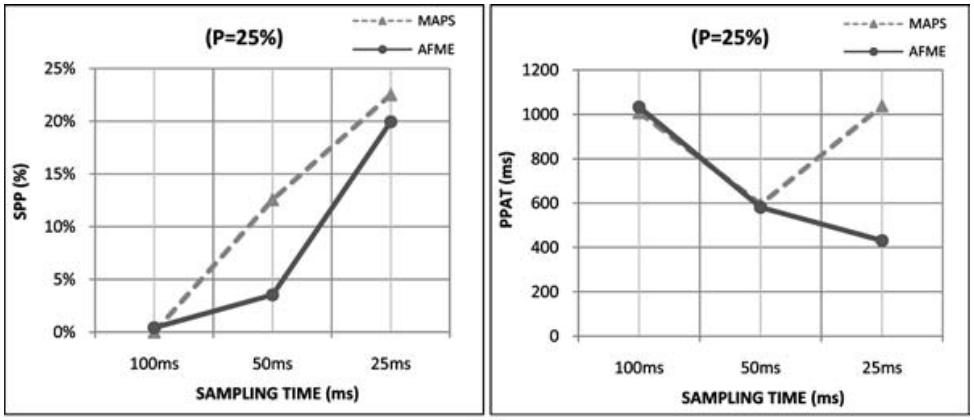

(a)

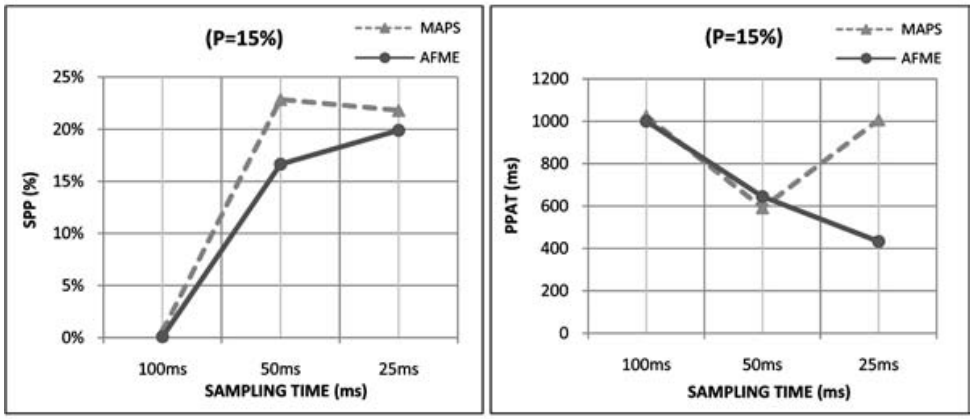

(b)

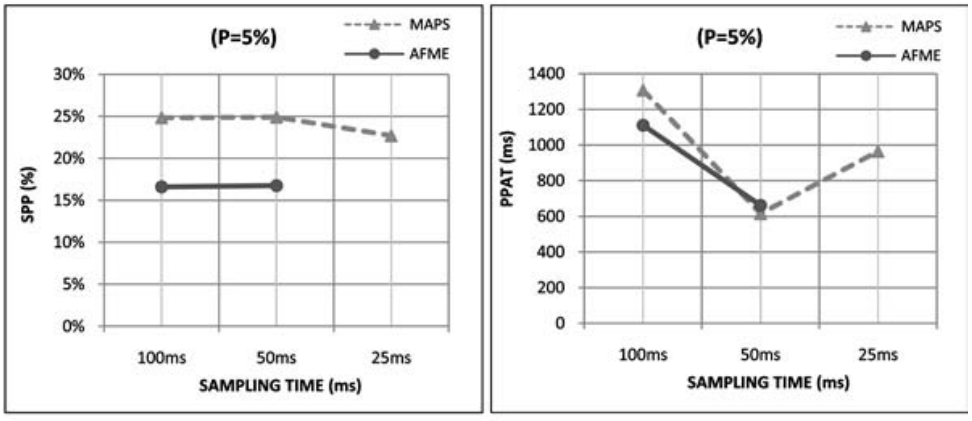

(c)

Figure 5.11. Analysis of PPAT and SPP of the sensor agents with W = 20, S = 10, and P = (a) 25%, (b) 15%, (c) 5%. See also Color Insert.

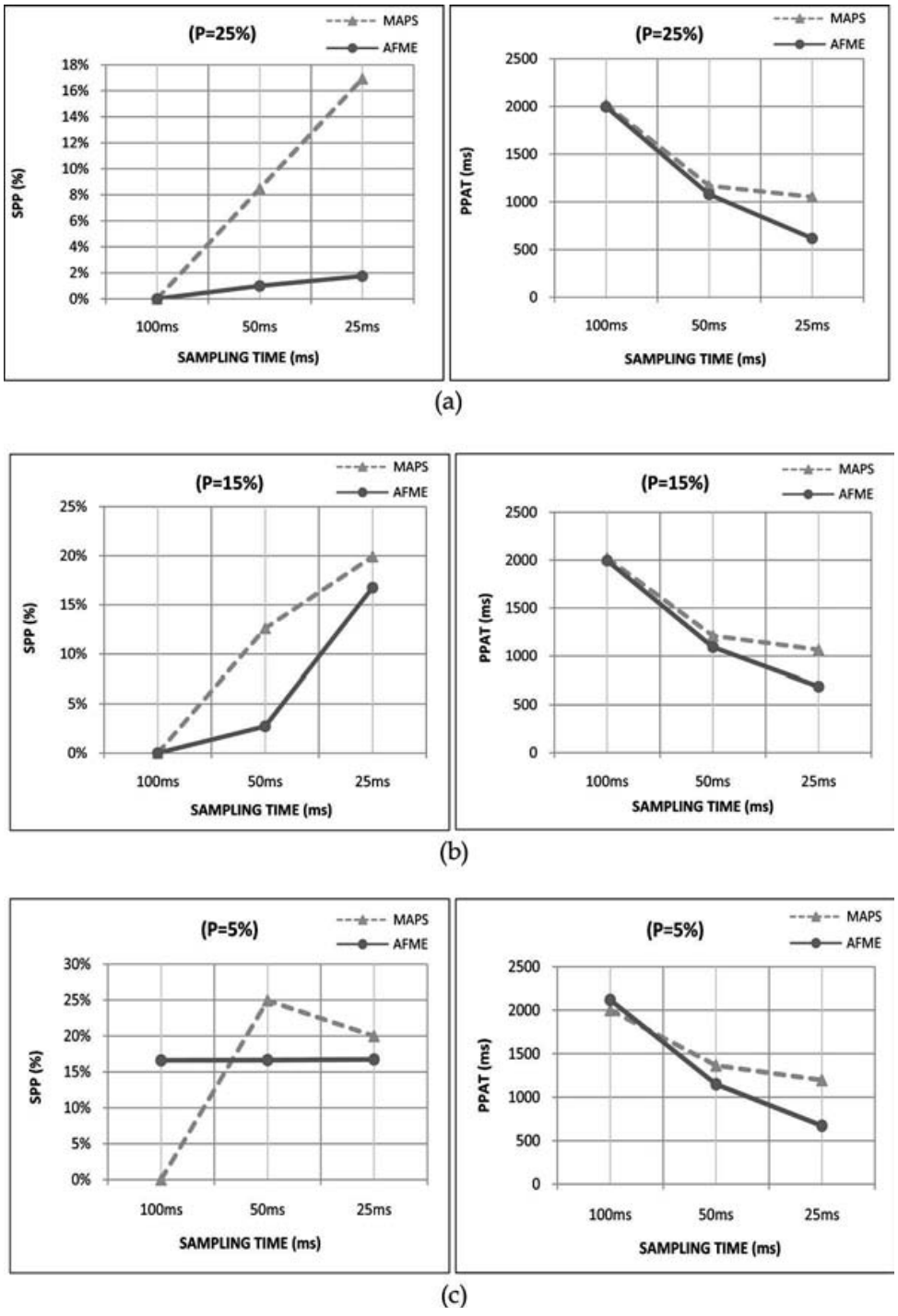

Figure 5.12. Analysis of PPAT and SPP of the sensor agents with W = 40, S = 20, and P = (a) 25%, (b) 15%, (c) 5%. See also Color Insert.

re-synchronizations (SPP >= 20% for W = 20 and S = 10). The best results are obtained with ST = 100 ms, P = 25% or 15% and W = 20; they guarantee monitoring continuity due to an SPP ≈ 0% and regularity as the experimented PPAT ≈ the ideal PPAT for W = 20. If W = 20 and P = 5%, ST = 100 ms is not a good value either because an out-of-limits skew frequently occurs. Although the AFME implementation performs better than the MAPS implementation, the AFME implementation collapses in the case W = 20, S = 10, and P = 5%. It is worth noting that even though a lower ST would allow a finer monitoring, the considered human activities can be well captured by an ST = 100 ms as demonstrated by the good accuracy results (95% in the average) obtained from the carried-out real-time human activity monitoring [12].

5.7 Conclusions and Future Work

In this chapter, we have presented an agent-oriented approach for high-level programming of WBAN applications. The agent approach is not only effective during the design of a WBAN application but also during the implementation phase. In particular, the presented frameworks MAPS and AFME allow for a more rapid prototyping of sensor node code than low-level APIs, which can be effectively used only by sensor node skilled programmers having knowledge of sensor drivers, data buffers, radio and energy mechanisms. The higher level software abstractions provided by MAPS and AFME are suitable for the development of real-time monitoring systems as demonstrated by the performance evaluation of the proposed case study concerning a real-time human activity monitoring system. Ongoing work is aimed at implementing ASPINE through MAPS to provide a full-fledged agent-based signal processing in-node environment.

References

1. *Agent Factory Micro Edition (AFME)*, documentation and software at http://sourceforge.net/projects/agentfactory/files/ (2011).

2. Aiello, F., Bellifemine, F., Fortino, G., Gravina, R., and Guerrieri, A. (10–14 May 2010) An agent-based signal processing in-node environment for real-time human activity monitoring based on wireless body sensor networks, in *Proceedings of the 1st International Workshop on Infrastructures and Tools for Multiagent Systems (ITMAS-2010),* jointly held with the9th *International Joint Conference on Autonomous Agents and Multiagent Systems (AAMAS-2010)*, Toronto, Canada.
3. Aiello, F., Fortino, G., and Guerrieri, A. (25–31 August 2008) Using mobile agents as an effective technology for wireless sensor networks, in *Proceedings of the 2nd IEEE/IARIA International Conference on Sensor Technologies and Applications (SENSORCOMM 2008)*, Cap Esterel, France.
4. Aiello, F., Fortino, G., Gravina, R., and Guerrieri, A. (2011) A Java-based agent platform for programming wireless sensor networks, *The Computer Journal,* 54(3), pp. 439–454.
5. Bao, L., and Intille, S. S. (2004) Activity recognition from user-annotated acceleration data, in *Proceedings of the 2nd International Conference on Pervasive Computing (PERVASIVE)*, pp. 1–17.
6. Bellifemine, F., and Fortino, G. (9–10 July 2009) ASPINE: an agent-oriented design of SPINE, in *Proceedings of the Workshop on Objects and Agents (WOA'09)*, Parma, Italy.
7. Boulis, A., Han, C. -C., and Srivastava, M. B. (2003) Design and implementation of a framework for efficient and programmable sensor networks, in *Proceedings of the 1st International Conference on Mobile systems, Applications and Services (MobiSys)*, pp. 1 87–200.
8. Fok, C. -L., Roman, G. -C., and Lu, C. (6–10 June 2005) Rapid development and flexible deployment of adaptive wireless sensor network applications, in *Proceedings of the 24th International Conference on Distributed Computing Systems (ICDCS'05)*, Columbus, Ohio, pp. 653–662.
9. Fortino, G., Guerrieri, A., Giannantonio, R., and Bellifemine, F. (11–14 October 2009) Platform-independent development of collaborative WBSN applications: SPINE2, in *Proceedings of the IEEE International Conference on Systems, Man, and Cybernetics (SMC 2009)*, San Antonio, Texas, USA.
10. Fortino, G., Galzarano, S., Giannantonio, R., Gravina, R., and Guerrieri, A. (2010) SPINE-based application development on heterogeneous wireless body sensor networks, *International Journal of Computing*, 9(1), pp. 80–89.

11. Gravina, R., Andreoli, A., Salmeri, A., Buondonno, L., Raveendranathank, N., Loseuk, V., Giannantonio, R., Seto, E., and Fortino, G. (7–9 June 2010) Enabling multiple BSN applications using the SPINE framework, in *Proceedings of the International Conference on Body Sensor Networks (BSN 2010),* Biopolis, Singapore.
12. Gravina, R., Guerrieri, A., Fortino, G., Bellifemine, F., Giannantonio, R., and Sgroi, M. (12–15 October 2008) Development of body sensor network applications using SPINE, in *Proceedings of the IEEE International Conference on Systems, Man, and Cybernetics (SMC 2008)*, Singapore.
13. Hester, T., Hughes, R., Sherrill, D. M., Knorr, B., Akay, M., Stein, J., and Bonato, P. (3–5 April 2006) Using wearable sensors to measure motor abilities following stroke, in *Proceedings of the 3rd International Workshop on Wearable and Implantable Body Sensor Networks, 2006 (BSN 2006)*, MIT, Boston (MA), USA, pp. 5–8.
14. Kwon, Y., Sundresh, S., Mechitov, K., and Agha, G. (2006) ActorNet: An actor platform for wireless sensor networks, in *Proceedings of the 5th International Joint Conference on Autonomous Agents and Multiagent Systems (AAMAS)*, pp. 1297–1300.
15. Lester, J., Choudhury, T., Borriello, G. (2006) A practical approach to recognizing physical activities, in *International Conference on Pervasive Computing (PERVASIVE)*, pp. 1–16.
16. Lombriser, C., Roggen, D., Stager, M., and Troster, G. (26 February–2 March 2007) Titan: a tiny task network for dynamically reconfigurable heterogeneous sensor Networks, in *Verteilten Systemen (KiVS 2007)*, Bern, Switzerland.
17. Luck, M., McBurney, P., and Preist, C. (2004) A manifesto for agent technology: towards next generation computing, *Autonomous Agents and Multi-Agent Systems,* 9(3), pp. 203–252.
18. Malan, D., Fulford-Jones, T., Welsh, M., and Moulton, S. (June 2004) CodeBlue: An ad hoc sensor network infrastructure for emergency medical care, in *Proceedings of MobiSys 2004 Workshop on Applications of Mobile Embedded Systems (WAMES 2004)*.
19. Maurer, U., Smailagic, A., Siewiorek, D. P., and Deisher, M. (2006) Activity recognition and monitoring using multiple sensors on different body positions, in *Proceedings of the 3rd International Workshop on Wearable and Implantable Body Sensor Networks (BSN 2006)*, MIT, Boston (MA), USA.
20. *Mobile Agent Platform for Sun SPOT (MAPS)*, documentation and software at http://maps.deis.unical.it/ (2011).

21. Muldoon, C., O'Hare, G. M. P., O'Grady, M. J., and Tynan, R. (2008) Agent migration and communication in WSNs, in *Proceedings of the 9th International Conference on Parallel and Distributed Computing, Applications, and Technologies*.
22. Najafi, B., Aminian, K., Ionescu, A., Loew, F., Büla, C. J., and Robert, P. (June 2003) Ambulatory system for human motion analysis using a kinematic sensor: monitoring of daily physical activity in the elderly, *IEEE Transactions on Biomedical Engineering*, 50(6), pp. 711–723.
23. Pansiot, J., Stoyanov, D., McIlwraith, D., Lo, B. P. L., and Yang, G. Z. (26–28 March 2007) Ambient and wearable sensor fusion for activity recognition in healthcare monitoring systems, in *Proceedings of the 4th International Workshop on Wearable and Implantable Body Sensor Networks (BSN 2007)*, RWTH Aachen University, Germany.
24. Sohraby, K., Minoli, D., and Znati, T. (2007) *Wireless Sensor Networks: Technology, Protocols, and Applications*, Wiley.
25. Suenaga, S., and Honiden, S. (14 May 2007) Enabling direct communication between mobile agents in wireless sensor networks, in *Proceedings of the 1st International Workshop on Agent Technology for Sensor Networks (ATSN 2007)*, jointly held with the6th *International Joint Conference on Autonomous Agents and Multiagent Systems (AAMAS 2007)*, Honolulu, Hawaii.
26. Szumel, L., LeBrun, J., Owens, J. D. (30–31 May 2005) Towards a mobile agent framework for sensor networks, in *Proceedings of the 2nd IEEE Workshop on Embedded Networked Sensors (EmNetS-TT)*, Sydney, Australia.
27. *Signal Processing In-Node Environment (SPINE)*, documentation and software at http://spine.tilab.com (2011).
28. *TinyOS website*, www.tinyos.net (2011).
29. Yang, G. -Z. (2006) *Body Sensor Networks*, Springer.
30. *ZigBee alliance*, technical documents and standard specifications at http://www.zigbee.org (2011).

This page intentionally left blank

Chapter 6

Hardware Development and Systems for Wireless Body Area Networks

Mehmet Rasit Yuce
Department of Electrical and Computer Systems Engineering, Monash University, Clayton, VIC 3800, Australia
mehmet.r.yuce@ieee.org

Miniaturized and wearable sensor nodes are required to form a wireless body area network (WBAN) to monitor physiological parameters from human bodies. In this part of the book, we will present the existing hardware solutions to realize a small wireless sensor for use in WBAN applications. Implementation issues are discussed, and details of techniques for the design of wireless sensors in WBAN applications are presented.

6.1 Introduction

A WBAN network aims to provide efficient and optimized wireless link for physiological signal monitoring from single or multiple human bodies. As shown in Fig. 6.1, the future WBAN-based sensor network requires miniaturized and wearable sensor nodes that can communicate with the receiving device. A WBAN system consists of individual wireless sensor nodes that can transfer a person's

Wireless Body Area Networks: Technology, Implementation, and Applications
Edited by Mehmet R. Yuce and Jamil Y. Khan

ISBN 978-981-4316-71-2 (Hardcover), ISBN 978-981-4241-57-1 (eBook)
www.panstanford.com

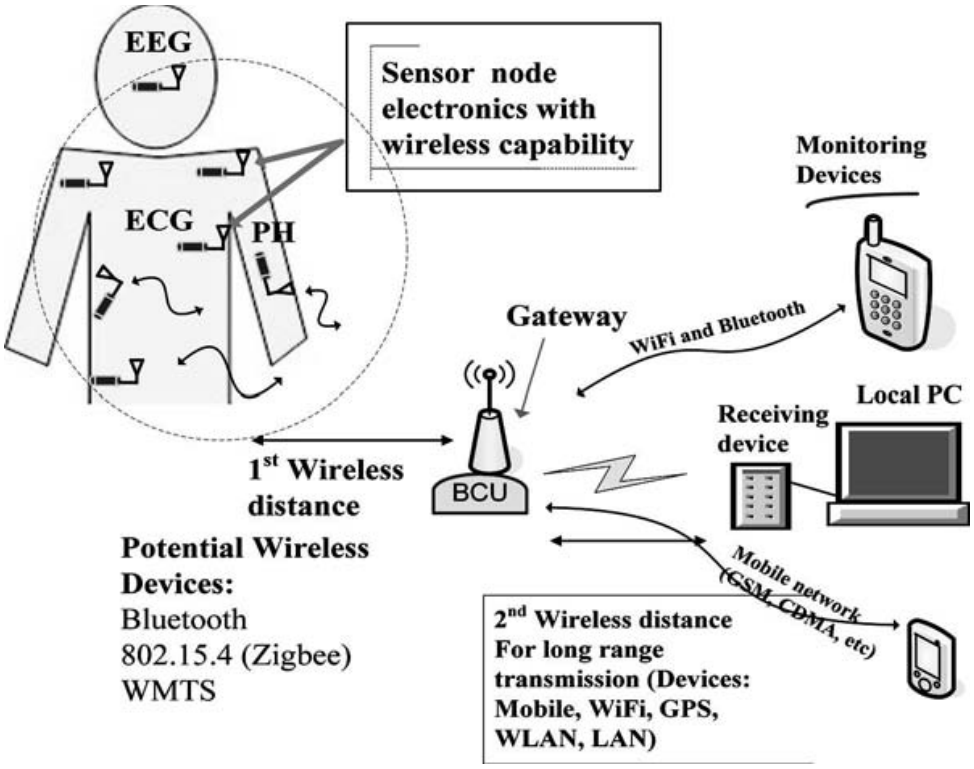

Figure 6.1. A wireless sensor network system detecting and transmitting signals from a human body.

physiological data such as heart rate, blood pressure, and ECG via a wireless link, without the need of any wired connection. Each sensor will have wireless capability and its design will be optimized in terms of the physical characteristic of the physiological signal. Having individual wireless nodes are also very beneficial since not all patients require all the physiological parameters for diagnosis. Each sensor can easily be plugged in and plugged out from a human body.

6.2 Wireless Body Sensors

Figure 6.1 shows a WBAN-based telemedicine system for collecting medical data from a human body using wireless sensors. This telemedicine system comprises sensor nodes, a body control unit (BCU) that transmits data to a receiver station (i.e., remote PC) that can have communication with remote stations at a medical center [1].

The BCU can be a smart phone or any portable device that will act as a gateway device to pass on the collected data from sensors to remote stations. The control device will be similar to smart phones we use in our daily life, which can also be used to monitor the data obtained from sensors. Such portable electronic devices will mostly contain Bluetooth, Wi-Fi, and GPS technologies built-in, which can be connected to medical sensors and to remote medical centers so that data can be accessed by medical professionals at any time. The BCU can be carried on the body as a wristwatch or can be placed on the belt.

For collecting data from a human body, usually short-range wireless technologies operating at MICS (medical implant communication service), WMTS (wireless medical telemetry service), 2.4 GHz ISM (industrial, scientific, and medical) bands have been developed by designers. However, it is necessary to connect the sensor nodes to remote stations using Wi-Fi and mobile communication links for longer range data transfer. In order to provide long-range remote monitoring, several gateway devices should be developed to interface with the existing ICT (information and communication technology) infrastructure in emergency vehicles or in medical centers. These gateway devices will mainly be used to provide communication between BCUs and remote computers or mobile devices.

6.2.1 *Sensor Nodes and Hardware Designs*

Low-power wireless technologies should be used to form small, light-weight, and wearable sensor nodes to collect and sense physiological data from a human body. Especially, when the number of sensors used on a single body increases, the weight of each sensor node becomes an important issue. Wireless sensor nodes are being developed by biomedical companies and researchers to make them safe, secure, and light weight so that they can be wearable. Key parameters of a wireless sensor node can be as follows:

- The wireless sensor nodes should be able to transfer data over a distance of a few meters.
- Sensor nodes should be miniaturized so that they can be easily wearable or attachable to a patient body.

Table 6.1. Physiological parameter range and signal frequencies

	Parameter	Range of parameter	Signal frequency
Continuous Signals	ECG signal	0.5–4 mV	0.01–250 Hz
	EMG (Electromyogram)	10–15 mV	10–500 Hz
	EEG	3–300 μV	0.5–70 Hz
Discrete Signal*	Body Temperature	32–40° C	0– 0.1 Hz
	Blood Pressure (BP)	10–400 mm Hg	0–50 Hz
	GSR (Galvanic Skin Reflex)	30–3 mV	0.03–20 Hz
	Respiratory rate	2–50 breaths/min	0.1–10 Hz

*Here the term "discrete" indicates large time intervals.

Alternatively, they can also be inserted in clothes using textile technology to improve the patient's comfort.

Wireless sensor nodes are developed specifically to detect and transmit the physiological signals listed in Table 6.1. These signals can be put in two categories: discrete and continuous. ECG/EEG signals are periodic signals, which require continuous monitoring. Body temperature is an example of discrete physiological data since it is taken usually at discrete times, e.g., every hour.

Most physiological signals are low frequency in nature and occupy a small information bandwidth. At such low frequencies and low amplitudes, some problems inherent to circuits need additional attention. For reliable information transfer, it is necessary that the interface electronic in the sensor nodes detect physiological signals in the presence of noise and increase the signal-to-noise ratio (SNR) of the detected signal for processing by the subsequent blocks of the sensor nodes.

Sensor nodes are designed to be small and power efficient so that their battery lasts for a long time. They collect weak, raw signals from a human body. Signals from a human body are usually weak and coupled with noise, and thus they need to go through amplification/filtering process to increase the signal strength and to remove unwanted signals and noise. Then an analog-to-digital conversion (ADC) stage is employed to convert the analog body signals into digital for digital processing. The digitized signal is processed and stored in the microprocessor. The microprocessor (i.e., microcontroller) will then pack the data and transmit over the

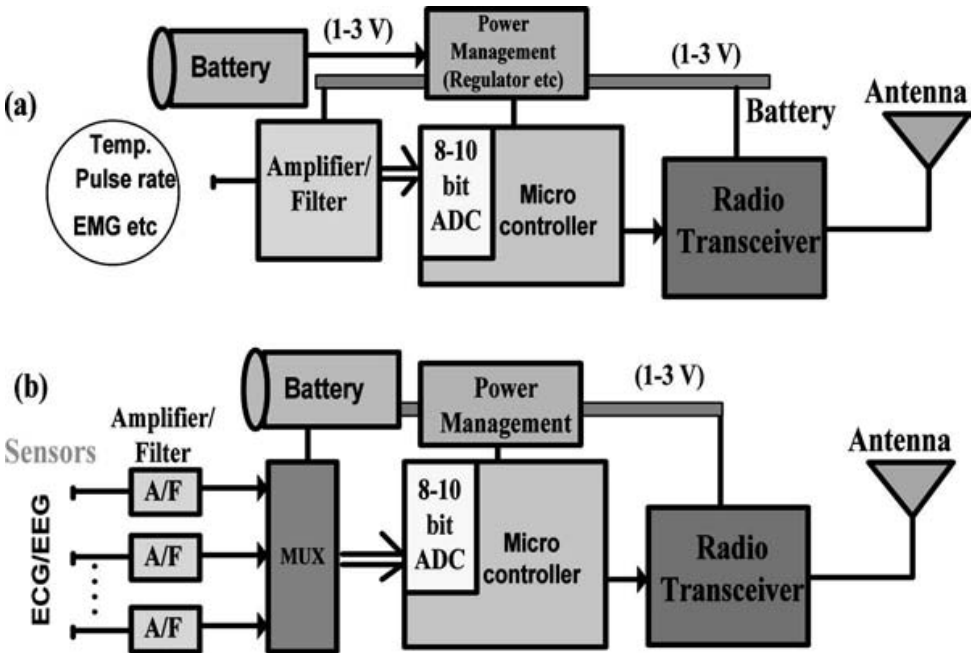

Figure 6.2. An example of sensor node hardware: (a) single wireless sensor node, (b) multi-channel wireless sensor node. See also Color Insert.

air via a wireless transceiver. Figure 6.2 shows two commonly used hardware implementations of sensor nodes.

A sensor node consists of three main blocks: the sensing front end, microcontroller, and the radio receiver to undertake the tasks mentioned above. In addition to these blocks, there is also a battery and its power management circuitry. The power management circuit is usually a regulator chip used to distribute the power source to the individual blocks. It is advised to keep all the sensor blocks' power supply level the same (e.g., all at 3 V) so that the regulator will not consume a large power.

Considering the signal attributes given in Table 6.1, a sampling rate of around 200–1000 Hz will be necessary for the ADC in the microcontroller (the sampling rate should be a minimum of twice the highest frequency in the signal that is digitized). Unlike other wireless sensor network applications, in a medical scenario, each sensor node has a different frequency and thus should be optimized according to its frequency band. The trade-off between the reduction in sampling rate and the total power consumption of the ADC is thus

determined by the choice of the specific physiological parameter used in the sensor node.

In case of emergency in a medical application, usually the monitoring and analyzing of critical physiological signals such as ECG and blood pressure (BP) will be the top priority. Thus, it is important if the signals in Table 6.1 are grouped into critical and noncritical data before attaching sensors on the injured people in a medical area. The wireless communication from sensors to the BCU should be designed such that priority should be given to the critical data. A WBAN-based telemedicine system will result in better data gathering process if data are prioritized according to the vital sign and patient situation.

The front end of a sensor node (i.e., interface electronics) is the first unit connected to sensors and electrodes. It is an analog electronics circuit that consists of amplifiers and filters. In case of detecting a continuous physiological signal such as EEG, ECG, or EMG, the front end should use an instrumental amplifier. An instrumental amplifier helps to amplify and detect noisy body signals at the presence of common mode noise (DC noise) at the input. By looking at Table 6.1 for amplitude and frequency information on continuous physiological signals, parameter values could be similar or different in some cases. It mainly depends on the quality of electrodes used to detect these signals. The same analog front end can be used to detect these continuous physiological signals. On the other hand, the required amplification and filtering can easily be adjusted for a specific signal by modifying capacitors and resistors in the front-end circuit.

Figure 6.3 shows a front-end circuit that can be used to detect ECG, EEG, and EMG signals. This circuit utilizes an instrumentation amplifier (INA321) to detect noisy body signals and a low-pass filter with an op-amp (LTC6081) [2]. The final stage is a 100 Hz LPF added for antialiasing. Typically the useful spectrums of ECG and EEG signals have amplitude of less than 500 μV with a frequency less than 100 Hz. In this example, the input medical signals are amplified by 60 dB; INA321 produces a gain of 14 dB, and the second amplification stage with low-pass filter characteristic-LTC6081 provides a gain of 46 dB with a cutoff frequency at 100 Hz. The circuit is running from a 3.3 V source with virtual ground set

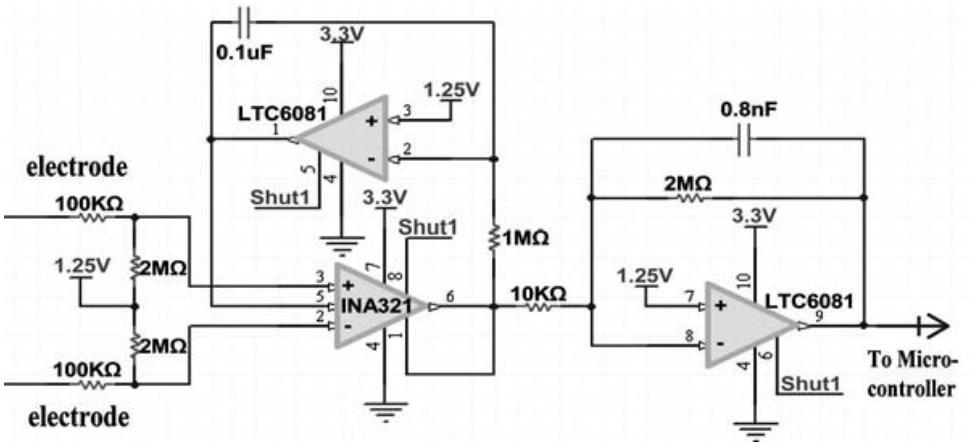

Figure 6.3. Schematic of analog front end for continuous physiological parameter detection.

at 1.25 V. Both components possess high common mode rejection ratio (CMRR) and low current consumption properties. INA321 has a CMRR of 94 dB, while LTC6081 has a CMRR of 100 dB. High CMRR values help obtain better quality signal. The active current consumption is 40 μA, and when operating in shutdown mode, it consumes less than 1 μA. The INA321 not only has extremely good CMRR and meets the low power need, but also has the ability to shut down when not in use. This is directly controlled by the microcontroller by connecting the shutdown pin to a CMOS I/O pin. The INA321 instrumental amplifier has 100 nV/$\sqrt{}$Hz, @ 1 kHz, input voltage noise and 3 fA/$\sqrt{}$Hz @ 1 kHz input current noise.

To eliminate DC drift caused by ICs, an integrator op-amp circuit is used as a negative feedback to the reference pin of the INA321. Any DC buildup is inverted and fed back into the system to cancel it out. This is only necessary for high gain circuits since any DC drift is multiplied just like any other signal. With a gain of 1000, a shift of 1 mV will cause the output to jump 1 V, which is close to saturation in this case. Apart from the integrator feedback, this circuit is relatively straight forward and has many common features to any other signal processing circuits.

The 2 MΩ and 100 kΩ resistors are used to limit the current to provide protection for the human body. In addition to this, it is also advised to use a safe power supply. Using a portable battery during

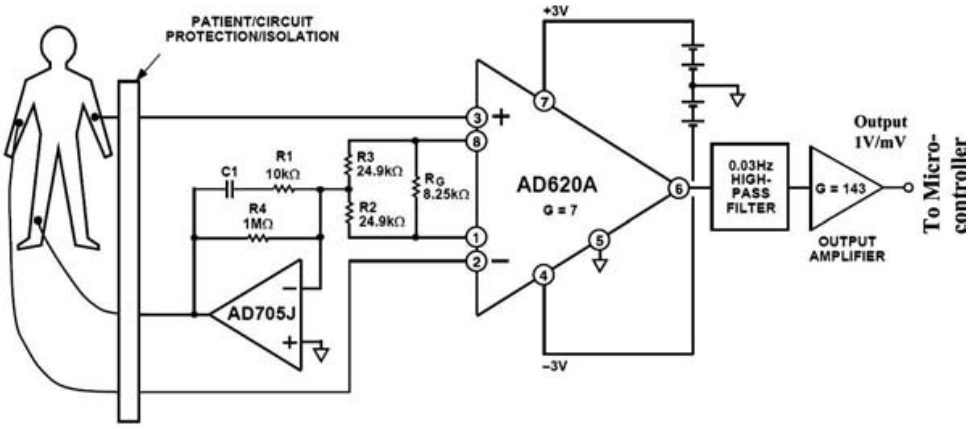

Figure 6.4. ECG detection with the AD620 instrumentation amplifier.

the design of this circuit is a better idea rather than using a direct source from a power line.

The AD620 is another well known low cost, high accuracy instrumentation amplifier (Analog Devices, USA), which can be used to detect body signals. It has 9 nV/$\sqrt{}$Hz, @ 1 kHz, input voltage noise and 0.1 pA/$\sqrt{}$Hz @ 1 kHz input current noise. Similar to INA321, the AD620 can be configured to have a CMRR value of 100 dB. The details of circuit configuration as a front end to detect sensor signals can be found in references [3] and [4]. Figure 6.4 shows a schematic for ECG detection designed with AD620. As explained before, the additional filter and a gain stage are added to make the detected signal ready for digitization at the micro-controller.

Another noise exists in detecting body signals, known as the power-line interference at 50 Hz (or 60 Hz in some countries). A notch filter (a combination of low-pass filter and high pass filter) can be designed at the front end to remove this noise. Alternatively, this can be done digitally at the microcontroller or at the remote computer after the continuous signal is received wirelessly [4]. An analogue notch filter works for most applications, but it requires more power and increases the board size and is, thus, avoided. Figure 6.5 shows an ECG signal obtained using the circuit given in Fig. 6.3. Figure 6.5b shows a clear ECG signal after using a notch filter to remove the 50/60 Hz noise.

Employing a digital–notch filter at the computer will make the sensor node less complex. It is also possible to use a combination

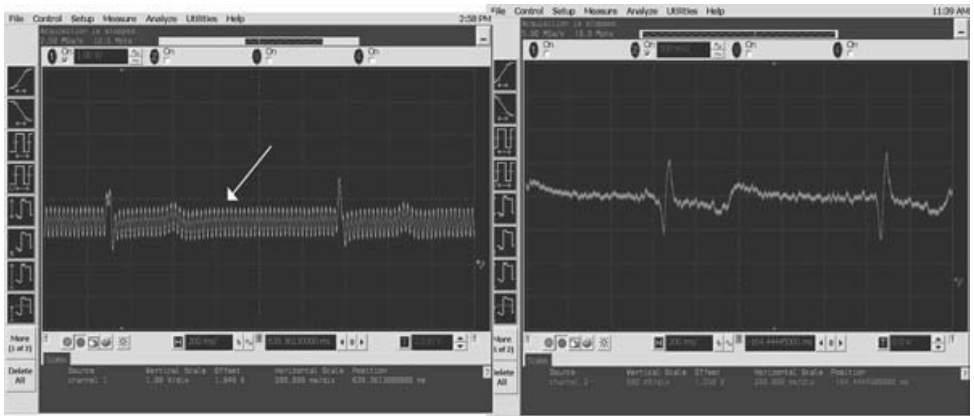

Figure 6.5. ECG with 60 Hz (or 50 Hz) noise (a) and without noise (b). See also Color Insert.

of an analog notch filter at the front end and then digitally via computation programs like MATLAB. The latter approach will increase the clarity of the signal further.

Some ECG projects use a "right leg drive" circuit, which is simply the inverse of the 50/60 Hz injected back into the patient to cancel the power line noise out. Similar to the above approach, this would require more op-amps and an extra electrode and is preferred not to be used. This method also requires a small amount of current, approximately 1–3 μA, to be passed through the patient.

In case of detecting discrete physiological signals such as body temperature and respiratory rate, a simple active low-pass filter (a filter together with a gain amplifier) is sufficient to bring the signal detected by a sensor to a level to be digitalized by a microcontroller.

Figure 6.2b shows a sensor node based on multichannel detection. A multiplexer is an array of analog switches operated with a clock that allows all the input signals to a single output to be digitized at the microcontroller. A multichannel sensor node requires the use of wires connected to electrodes for a single sensor node which should be avoided if possible for a WBAN application. The existing of wires will restrict human movements and thus comfort.

Having said that, for some clinical applications, a multichannel sensor node may be required for certain diagnostic tools. For example, a multichannel sensor node is used for EEG signals for brain-computer interface applications [5]. Multichannel signal

detection will increase the data rate requirement. As an example, if we use 200 Hz sampling frequency for 10 channel EEG signal, the required data rate is calculated as 200 sample/s per channel $\times$ 10 channels $\times$ 8–10 bits/sample = 16–20 Kbit/s.

One of the requirements of body area network (BAN) is to have individual wireless sensor nodes. Even if we integrate a multichannel EEG signal into a BAN system and considering the additional preamble bits in a data package, the required data rate for a WBAN-based physiological monitoring system is still sufficiently low. A lot of available wireless transceiver will provide enough bandwidth to handle such data rates. When the number of sensor nodes increases, the required data rate will depend on the multi-access communication used. In case of TDMA (Time Division Multiple Access) and CSMA (Carrier Sense Multiple Access), the bandwidth requirement is low. For frequency division multiplexing techniques (e.g., FDM, FHSS, OFDMA) and CDMA schemes, a wideband will be required for data transmission when the number of users (here sensors) is increased. Probably this is one of the main reasons why the WPAN (wireless personal area network) systems such as ZigBee use CSMA as a multi-access communication. It can have a higher number of nodes with available low bandwidth. For more information about multi-access communication techniques in WBAN, refer to the related chapters of the book.

6.2.2 *Wireless Systems and Platforms*

In addition to the sensing front end, a sensor node and the BCU require a microcontroller and a wireless transceiver to coordinate the transfer of data. Numerous frequency bands can be used in medical monitoring system. So far there is no available standard to define operation frequencies specifically targeting a WBAN. It is important to select a proper and safe (interference free) wireless band. Especially for medical data transmission, it is crucial for the patient‘s safety to monitor accurate information. Table 6.2 presents the unlicensed frequency bands that can be used for WBAN applications.

Low ISM bands, especially the 13.56 MHz frequency, are widely used for radio-frequency identification (RFID) applications,

Table 6.2. Available frequency bands

Model	Country	Frequency	BW	RF power (dBm)
UWB	Worldwide	3.1–10.6 GHz	>500 MHz	−41
MICS	US, Australia Europe, Japan Worldwide	402–405 MHz	300 kHz, 10 channels	$-16(25\ \mu W)$
High ISM	Worldwide	2.4–2.5 GHz, 5.725–5.875 GHz	20 MHz, 40 MHz	> 0
Mid ISM	Europe US Canada, Australia	433.05–434.79 MHz 865– 868 MHz 902–928 MHz	kHz range , 200–500 kHz 10–15 channels MHz	Up to 15
Low ISM	Worldwide	6.765–6.795 MHz 13.55–13.567 26.95–27.283 40.66–40.70	kHz range, 14 kHz for 13 MHz	0
WMTS	US, Canada	608–614 1395–1400 1427–1432	1.5 MHz 5–6 MHz	>10

inductive links for implantable systems, and smart cards for security systems [6, 7]. Most probably designers will continue to use these low-frequency ISM bands for inductive link based implantable systems as they present better performance at low frequencies. For medium ISM (Mid-ISM) range, countries in Europe, New Zeeland, and Honk Kong use 865–868 MHz. Australia, Korea, Taiwan, Hong Kong, and Singapore use a frequency range within and the US and Canada use the whole band between 902–928 MHz. Japan has 950–956 MHz ISM band frequencies. These frequencies have widely been used for cordless headphones and microphones.

In addition to unlicensed ISM bands, there are medical bands such as MICS and WMTS, which are specifically regulated for medical monitoring by communication commissions around the world. The MICS is an ultra-low power, unlicensed, mobile radio service for transmitting data to support diagnostic or therapeutic functions associated with implanted medical devices [8]. In order to monitor medical implant devices and status of inner organs, a frequency around 400 MHz have been a popular transmission band. In fact this frequency is an optimal frequency to provide a fully

integrated circuit approach for a wireless transceiver design and causes relatively insignificant penetration loss (10 dB with 10 mm penetration) [9]. Using a higher frequency causes higher penetration loss. Meantime high-level integration becomes difficult at lower frequency. In addition, a small antenna design is difficult at lower frequency (less than 400 MHz).

In addition to medical implants, metrological aid service has primary allocation at 402–405 MHz band and the Earth exploration-satellite service together with metrological-satellite service has secondary allocation at 402–403 MHz. Thus transmission in the MICS has some regulated parameters in terms of channel spacing and transmission power level. At the moment in some countries, the MICS is being extended from 402–405 to 401–406 MHz, introducing additional 2 MHz wider band, which can increase the population of monitoring patients in hospital environment.

WMTS is used in the United States and Canada but not in Europe. In Japan, WMTS frequencies are 420–429 MHz and 440–449 MHz. WMTS has long been used for wireless patient monitoring system in the United States and Japan [10].

The most common wireless systems such as ZigBee (IEEE 802.15.4), WLANs, and Bluetooth (IEEE 802.15.1) operate at 2.4 GHz ISM band. The technologies operating at 2.4 GHz ISM band may suffer from interference issues when they are located in the same environment. In addition, there may be a variety of other sources such as microwave and cordless phones operating in 2.4 GHz band. Latency sensitive WBAN nodes like an ECG node can suffer significance performance loss from this mutual radio-frequency interference as a correct submission of a sensor will be delayed.

The electromagnetic interference is another source of interference that may limit the use of wireless in certain environments, especially in medical applications. Electromagnetic energy from a device can interfere with another when they are operating in the same environment. There have been already incidents where telemetry devices have affected the available medical systems in the hospitals [11].

In addition to the above wireless bands, the ultra-wide band (UWB) can also be used for monitoring of physiological signals. High data rate transmission, as commonly known, is not the only

unique property of an UWB-based monitoring system. Some other advantages of a wide band technology are its low transmitter power, the physical size which can be extremely small because of the design at GHz range, the simplicity of transmitter design, and the band is not crowded as compared to other available bands [12]. The maximum transmission power is regulated as -41 dBm. Such a low-signal level will have insignificant RFI/EMI (radio frequency interference/electromagnetic interference) effect on medical equipment. The current drawback of UWB technology is that not enough devices available in the market that can be used as a complete solution.

The MICS band has also low emission power (25 μW, comparable to UWB) and lower power consumption, and will thus provide one of the most suitable medical sensor nodes. It is envisioned that the sensor nodes of a WBAN will use a specified wireless link, which will most likely be a narrow ISM band considering the current wireless technology developments. The UWB band can be used when interference and EMI are an issue for the environment. For implantable body area networks, the MICS band may still continue to be the preferable choice.

6.2.2.1 Wireless transceivers and microcontrollers

Most common wireless chips used in low power sensor network applications are listed in Table 6.3. The chips that exhibit low power and have small size are Zarlink's MICS chip, Nordic's nRF24E1 device, and CC2420 of TI. Zarlink provides one of the lowest power wireless chips available today. The low power is achieved by reducing the supply voltage to a value as low as 1.2 V, while most of the other transceiver chips operate with a nominal voltage around 3 V. The power figures shown in Table 6.3 are for the maximum transmission power levels and a nominal supply voltage, which is 3 V. Although these chips are advised to operate at 3 V, their supply voltage in practice can be reduced to as low as 2 V. This way the power consumption will be lower than what is shown in the table. The Zarlink chip has been designed for implantable sensor nodes. The Nordic device nRF24E1 consumes a transmit current of 10.5 mA for an output signal level of −5 dBm and 18 mA receiver current for

Table 6.3. Some suitable wireless chips for potential use as a wireless medical sensor node

						Power consumption	
Model	Company	Frequency	Data rate	RF power (dBm)	Physical dimension	**Tx**	**Rx**
CC1010	TI[1]	300 to 1000 MHz	76.8 Kbps	−20 to +10	12 × 12 mm^2 (chip)	26.6 mA	9.1 mA
CC24xx	TI[1]	2.4 GHz	1 Mbps	−25 to 0	7.1 × 7.1 mm^2 (chip)	19 mA	17 mA
XE1205	Xemics[2] (Semtech)	433, 868, 915 MHz	304 Kbps	Up to 15	8 × 8 mm^2 (chip)	62 mA	14 mA
CX72303	Conexant[3]	2.4 GHz	1 Mbps	−10 to +2	—	34 mW	43 mW
nRF24E1	Nordic[4]	2.4 GHz	2 Mbps	−20 to 0	6 × 6 mm	11 mA	18 mA
AMIS52100	AMIS[5]	402–405 MHz	16 Kbps	−3 to 12	7.5 × 7.8 mm^2 (chip)	25 mA	7.5 mA
ZL70250	Zarlink[6]	402–405 MHz, 433 MHz ISM	800 Kbps	< 0	7 × 7 mm^2 (chip)	5 mA, TX/ RX	

[1] http://www.ti.com/.
[2] http://www.semtech.com.
[3] http://www.conexant.com.
[4] http://www.nordicsemi.com.
[5] http://www.amis.com.
[6] http://www.zarlink.com/.

a data rate of 250 Kbps. The physical dimensions shown in the table are based on the packages used by the companies.

The Nordic has another transceiver -nRF401 that operates in the 433 MHz ISM frequency band. It uses frequency shift keying (FSK) modulation and presents a data rate up to 20 kbit/s. The current consumptions for both transmitter and receiver are 11 mA and 8 mA, respectively.

The CC1010 transceiver chip from TI (Chipcon) has the capability to transmit anywhere within 300 and 1000 MHz. It can be used to generate signals for MICS, Mid-ISM bands, and WMTS frequencies. The AMIS52100 chip from AMI Semiconductor requires a crystal oscillator at 12.56 MHz to generate MICS band. A crystal with any frequency can be used with CC1010 to generate medical and ISM band frequencies. The effective frequency of the device is arranged by the external VCO inductor in addition to the crystal oscillator. For example, an inductor value of 12 nH gives a frequency range of 565–730 MHz. The PLL in chip is able to quickly lock onto WMTS frequency of 610 MHz. The frequency registers of the device allow for jumps of 250 Hz, making this device suitable for multiple channel selection and taking advantage of the available bandwidth by using FDMA or frequency hopping.

The Semtech's XE1205 chip can be used for the 433, 868, and 915 MHz license-free ISM frequencies. Similar to CC1010, it can also operate in other frequency bands in the 180–1000 MHz range. CX72303 from Conexant operates at 2.4 GHz. This technology is specifically designed for Bluetooth system solutions

Another Chipcon's chip CC2420 is a 2.4 GHz IEEE 802.15.4/ ZigBee compliant RF transceiver. It is based on digital direct sequence spread spectrum (DSSS) baseband modem providing a spreading with data rate of 250 Kbps. This chip has been widely used in sensor nodes because of its low-power design and its operation for ZigBee and Bluetooth applications.

AMIS52100 and TI's cc10xx chip series can provide MICS and WMTS signals. Both chips' output can go as low as −20 dBm meeting the requirement of −16 dBm transmission power for the MICS band. Zarlink's ZL70250, CC1010, and Semtech XE1205 uses FSK data modulation, AMIS52100 amplitude shift key/on-off key (ASK/OOK) modulation, while CC2420 uses offset quadrature

phase- shift keying (O-QPSK) with half-sine chip shaping, which is equivalent to MSK modulation. The newer version transceiver from AMI Semiconductor (AMIS53000) can operate using one of the following modulation schemes: OOK, FSK, or GFSK. The nRF24E1 operates at 2.4 GHz with GFSK modulation. The transceivers can work based on both Manchester and NRZ bit coding schemes; however, the data rate is half in the case of Manchester coding.

6.2.2.2 Existing sensor boards

The unit responsible for processing data, controlling the functionality of the components of the sensor node, and coding the sensor data for the wireless transceiver is the microcontroller. The task of a microcontroller for a sensor node in WBAN applications is relatively simple due to the low frequency of biological signals. Thus a less complex and small size microcontroller can usually be utilized. The commercially available microcontrollers have a 10-bit and 8-bit ADC built-in, which eliminates the need for an external off-shelf ADC.

Considering that the sensor node board is required to be light and small in order to be wearable, a wireless transceiver chip containing a microcontroller would be advantageous. As an example, CC1010 from TI has a microcontroller builtin which has a memory of 2048 + 128, 10-bit ADC, and 22.7 kHz sampling frequency. A small board can easily be designed, similar to that of Mica2DOT shown in Fig. 6.6. The Nordic's nRF24LE1 chip also contains a microcontroller unit and an ADC. The microcontroller is an 8051 compatible microcontroller, and the ADC is 10 bit with 100 Kbps.

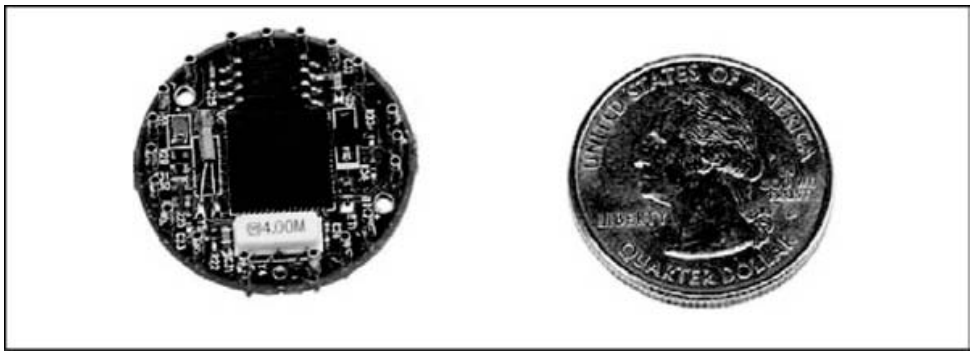

Figure 6.6. A Mica2DOT board (taken from www.xbow.com). See also Color Insert.

The sensor board with these devices will require only a few external components: the needed sensing front end given in Fig. 6.3, regulator IC for power supply arrangement and matching network together with antenna.

Some of the commonly used wireless sensor platforms (as a complete sensor boards) are shown in Table 6.4. Crossbow's Mica2DOT and T-node are the smallest sensor nodes available in commercial domain. Another widely used sensor node is Tmote Sky node [13]. It uses 250 Kbps 2.4 GHz IEEE 802.15.4 Chipcon Wireless Transceiver (CC2420) and a separate 16-bit 8 MHz Texas InstrumentsMSP430 microcontroller (10 K RAM, 48 K Flash).

MicaZ node also uses CC2420 transceiver and 10-bit ATmega 128L microcontroller, which has 4 KB RAM and 128 KB FLASH memories. The MicaZ is a 2.4 GHz mote module used for enabling low-power wireless sensor networks. TinyNode584 is another ultra-low power wireless sensor node, which uses Xemics XE1205 for wireless communication and TI MSP430 microcontroller (10 K RAM, 48 K Flash) as a processing unit [14]. The physical dimension of this board is 30×40 mm^2.

The Crossbow's Mica2 sensor node works at 868 and 916 MHz ISM frequencies. Like MicaZ it uses a separate microcontroller — ATmega128L (4 K SRAM, 128 K Flash, 8 MHz). The total power consumption of this board at 3.3 supply voltage, including the radio and microcontroller, is 148. 5 mW (= (27 + 10 + 8)*3.3). During sleep mode, the power consumption is at μW levels.

The Mica2DOT mote is a third-generation mote module wireless platform designed for smart sensors similar to the Mica2. Its quarter-sized (25 mm) form factor makes it suitable for sensor network applications requiring low size. Mica2DOT is one of the smallest sensor nodes available in commercial domain (Fig. 6.6). The power consumption of this node is similar to Mica2 (MPR400). Mica motes run on TinyOS (TOS) distributed software operating system v1.0 [15]. They can operate on the frequencies such as 868/916 MHz, 433 MHz, or 315 MHz multichannel radio transceiver. The Mica2DOT is Mica2 compatible and uses the same microcontroller.

Another small node for sensors is T-nodes working in the 868 MHz ISM frequency band. The board uses a separate chip for

Table 6.4. Various hardware sensor nodes configurations

Model	Company	Frequency	Data rate	Trans. power (dBm)	Physical dimension	Power consumption†	
						Tx	Rx
Mica2 (MPR400)	Crossbow[1]	868/916 MHz	38.4 Kbps	−24 to +5	58 × 32 × 7 18 g (board)	27 mA @ 3.3 V	10 mA @ 3.3 V
MicaZ	Crossbow[1]	2400 MHz to 2483.5 MHz (IEEE 802.15.4)	250 Kbps	−24 to 0	58 × 32 × 7 18 g (board)	17.4 mA @ 3.3 V	19.7 mA @ 3.3 V
Mica2DOT	Crossbow[1]	868/916 433 MHz	38.4 Kbps	−20to +10	25 × 6 mm^2 3 g (board)	25 mA @ 3.3 ×	8 mA @ 3.3 V
Tmote Sky node	Moteiv	2.4 GHz (IEEE 802.15.4)	250 Kbps	−25 to 0	66 × 32.6 × 7 mm	19.5 mA @ 3 V	21. 8 mA @ 3 V
T-node	SOWNet	868, 433, 915, or 315 MHz	52.2 Kbps	−20 to −5	Diameter of 23 mm	25 mA @ 3 V	13 mA @ 3 V
Sensium™	Toumaz	868/915 MHz	50 Kbps	−23 to − 7	90 × 45 × 10 mm	3 mA @ 1 V	2.7 mA @ 1 V
Wibree	Nokia	2.4 GHz (Bluetooth)	200 Kbps	−6	—	—	—

[1]http://www.xbow.com.

†Transmitter (Tx) power values are usually for the maximum transmission power level. When the transmission power level is configured to lower values, transmitters will consume a power lower than the values in this Table.

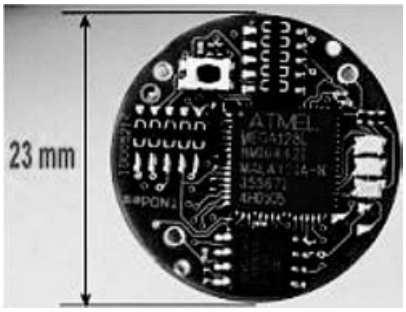

Figure 6.7. A T-node sensor node [16]. See also Color Insert.

microcontroller with 10-bit ADC, memory of 128 K flash memory and 4 Kbyte SRAM [16]. It consumes only 20 μA during sleep mode. It has a similar size to that of Mica2DOT (23 mm), shown in Fig. 6.7.

The Sensium™ sensor node uses the chip TZ1030, which uses a wireless transceiver operating at 868/915 MHz and the 8051 processor for digital processing and with 10-bit ADC. It provides 50 Kbps of data rate [17]. The low power consumption of this node is resulted from the low-supply voltage of 1 V. The node samples input signals within a dc to 250 Hz bandwidth.

Another popular node is BTnode [18], which consists of a Chipcon CC1000 radio (it is CC1010 without a microcontroller built-in) operating at 433–915 MHz, Atmel AVR microcontroller, and a Bluetooth radio (Zeevo ZV4002). In other words, a BTnode is made of a Crossbow Mica2 Mote with SRAM (256 K) and an additional Bluetooth radio. This node's power consumption is high due to the operation of two radios (∼200 mW). However, it gives the advantage of connecting to another device using the Bluetooth technology. This node can be used to interface with mobile phones and the Internet using the Bluetooth link. Its microcontroller is from Atmel (ATmega 128L), having 64 + 180 Kbyte RAM, 128 Kbyte FLASH ROM, and 4 Kbyte EEPROM.

The Conexant is another node based on Bluetooth wireless technology. It uses CX72303 RF transceiver and CX81400 baseband controller to establish a Bluetooth communication link [19]. The CX81400 integrates an RISC processor ARM7TDMI having 192 KB ROM and 192 KB RAM.

Among the available Bluetooth modules Wibree is probably the most suitable node for a lowpower sensor network application.

The device has been designed by Nokia to have similar power consumption and battery life as ZigBee. This device similar to ZigBee applications, because of its small form factor, can be used in health care, fitness, security, wrist watches and home entertainment industries. It operates on coin cell batteries. Wibree operates in 2.4 GHz band with a data rate up to 1 Mbps with a 10 m distance similar to any other Bluetooth technologies.

In addition to these commercially available sensor nodes, there are also nodes that have been developed specifically for medical monitoring. In reference [20], a very compact system has been developed for a wearable ECG sensor node that can communicate wirelessly with a base station. The node uses Nordics nRF24E1, a 2.4 GHz RF transceiver together with an embedded 8051-compatible microcontroller (DW8051) with 512 byte ROM, 4 K RAM, and 9-bit ADC. The board has the size of 26 (L) $\times$ 15 (W) $\times$ 7 (H) mm^3.

BSN nodes developed by Imperial College [21] are TinyOS-based sensor nodes The node also uses CC2420 from TI and MSP430 microcontroller families with 2 KB RAM, 60 KB flash, and 12-bit ADCs. The node has a size of 26 mm. The power consumption of these nodes is similar to the power consumption of CC2420 transceiver given in Table 6.3. The sensor board in reference [22] uses the Nordic nRF905 transceiver however operating at 915 MHz ISM with 0 dBm and 10 Kbps. This sensor node includes 3-axis accelerometer SCA3000 and has active power of 7.8 mW and 8.2 mW for transmitter and receiver respectively. Its dimension is as small as a one dollar coin.

Another sensor node [23] developed for a medical sensor network uses the medical bands MICS and WMTS for applications in the hospital environment. The board uses AMIS and CC1010 transceivers for the radio system and PIC16F785 microcontroller having 10-bit, 52 kHz sampling clock , and 368 + 256 RAM. The board has a dimension of 30 mm $\times$ 80 mm.

The power consumption given Table 6.4 defines the life time of a sensor node. For example, a continuously active sensor node using the CC24XX family (this chip family is used for ZigBee and also for Bluetooth) can last about seven hours when using a battery with a capacity of 300 mAh, assuming the transmitter and receiver working with the same amount of time (the nodes are always active either

there is transmission (the transmitter is active) or the receiving (the receiver is active)). For monitoring patients in emergency and disaster events, sensors measuring critical vital signals are required to be active (like ECG signal) as these vital signals are crucial for the patient's life. However, there may be some sensors information needed to be monitored once a while. The life time of such a sensor will be similar to current cellular phones we use in our daily life. It is important to note that the power consumption values given in Table 6.4 is for the maximum transmitter power. When the distance between the control unit and the sensor nodes is short, which is likely the case for the targeted medical applications, a lower transmission power can be configured in the transceiver of the sensor nodes to increase the battery life.

6.2.3 *Design of Implanted Sensors Nodes for WBAN*

Electrocardiogram (ECG) and temperature recording have been used for more than 50 years in medical diagnosis to understand biological activities [24] The early implantable devices are constructed with simple electronic structures to make the devices small enough so that they can be inserted in the body. A simple transmitter connected to a sensor is used to send the signal from inside the body to external devices for tracking certain organs' physiological parameters. Recent implantable systems have focused on more complex microelectronics systems with the use of the advanced integrated circuit technology. Some milestones of implantable devices are given below:

- **1957** — First wearable **pacemaker** (in 1958 fully implant)
- **1984** — **The Australian cochlear implant** approved by FDA
- **2000** — First clinical trial **wireless endoscope** (electronic pill)
- Study of **Bionic eye** since 1990

In addition to these projects, there is a vast area of different implantable systems, being designed by designers, such as cardioverter defibrillators, micoelectrode arrays for detecting and

stimulating brain functions, and electronic pills for drug delivery systems. Moreover, there are implantable biosensors developments to conduct animal studies.

Electronics for implantable sensors are designed taking into account very specific requirements for a given wireless telemetry application. Wireless technologies such as ZigBee, WLANs, and Bluetooth (IEEE 802.15.1) developed in the commercial domain cannot be used directly in medical implants because of the following reasons: (1) they have been optimized for general use; (2) the device size exceeds the required size limitation of the current implant technology, (3) their frequency bands are very crowded, and (4) they do not meet the safety-related radiation. The existing advanced wireless systems operate at 2.4 GHz ISM band and suffer from strong interference from each other when they are located in the same environment [25]. Thus an implant system should have a different transmission band for an interference-free wireless link as the transmitted information could be related to patients' critical conditions.

In implantable telemetry systems, to optimize the power and data telemetry links independently, the dual-band (i.e., two-inductive links) has been used [26]. The power and data signals are carried on two wireless links. For implantable systems like the cochlear implant and bionic eye, one wireless data link (i.e., forward data link) is used to transmit data from the external unit to inside the skin to stimulate the nerves in order to help the patient restore hearing and sight. These devices also require the transmitting of status information regarding the operation of the device, which is done based on a third link-back telemetry. There are also systems such as pacemakers, electronic pill, and biosensors that send physiological data such as ECG, pressure, or video images from inside the body to the external unit and then to the monitoring station in order to track a patient's condition. The latter implantable systems may or may not require the forward data link depending on whether data or a control signal is required from the external unit to control the implantable system.

Figure 6.8 shows the basic building blocks of implant systems. The power signal is received and then regulated to provide supply for the wireless data links, the sensors, and the signal

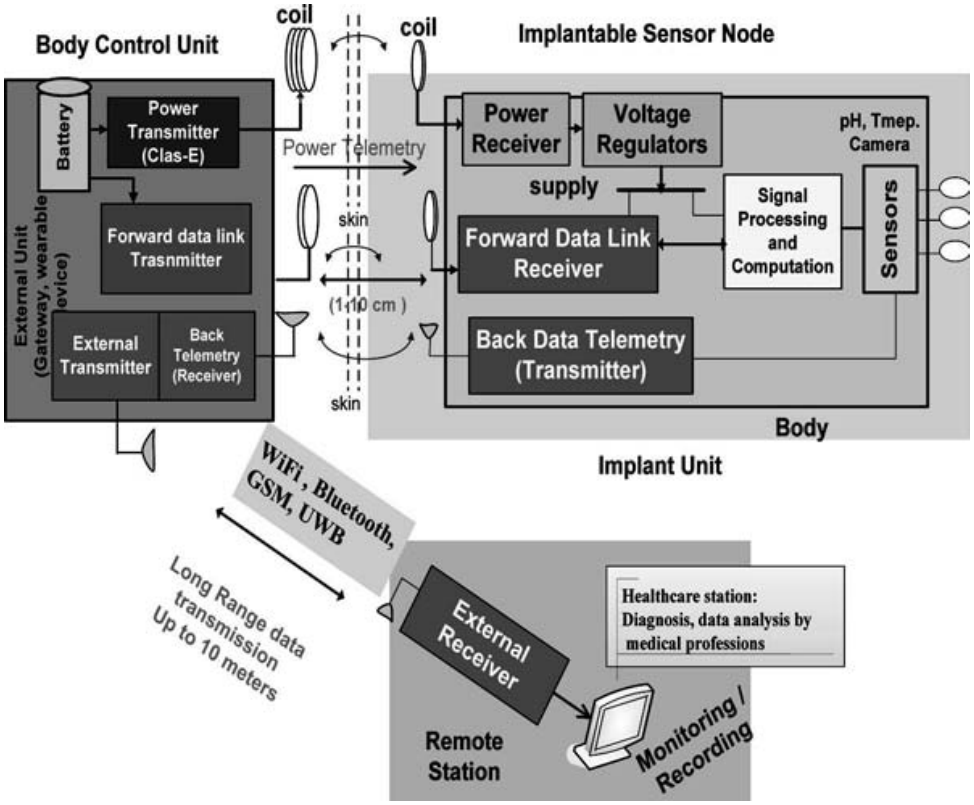

Figure 6.8. An implanted sensor node with the external unit and wireless data links. See also Color Insert.

acquisition unit, which processes and amplifies the senor data. The external unit may contain another wireless link that will control the communication between the implant devices and the remote monitoring station. The patient will wear the external unit, which will be on the surface of the body close to the implanted device. A remote wireless receiver will be used to receive data from the external unit for monitoring and analyzing the data. As the required specifications are not restricted for this link, commercial wireless devices can be used to undertake this duty. This additional wireless link will provide patient free in a room in the hospital environment.

Implantable systems have been constructed using inductive links between the external and implanted units with a distance of a few centimeters. The main reason behind the short distance and the inductive link is the need of wireless powering. Inductive links are mainly used to power implants to eliminate the use of batteries. The wireless module is designed with a very simple

communication scheme such as binary ASK (amplitude-shift keying), FSK (frequency-shift keying), and PSK (phase-shift keying) modulators and demodulators [26].

The 13.56 MHz ISM band is usually the most common frequency for such telemetry systems and is also used for RFID applications. A low transmission frequency usually less than 20 MHz is utilized mainly because of the simplicity in the design and to avoid the use of power-hungry blocks such as mixer, oscillators to maintain the miniature size of the implant. For example in reference [27], PSK is used at 20 MHz carrier frequency for the wireless data link for a retina prosthesis. ASK is used for a bionic eye system in reference [28] with 1–10 MHz frequencies and for a recent cochlear implant in reference [29] at 2.5 MHz transmission frequency. In addition, there are some attempts for general implants and neural prostheses systems employing FSK [30, 31] operating at 480 kHz and 5/10 MHz frequencies, respectively. The most suitable frequency for such implantable system requiring low frequency forward data transmission would be the ISM band 13.56 MHz as given in Table 6.2. Otherwise, designers would have to obtain permissions from communication authorities (e.g., FCC) to use a frequency rather than ISM. In addition to the wireless power link, utilizing a low frequency transmission has been attractive to eliminate the absorption of more energy [32].

There are some issues with the communication schemes of implantable systems for forward data telemetry and back data telemetry. For example, when many similar types of implantable systems are used in the same environment or for the same patient, the simple communication systems mentioned above will face the problem of interference and lack the multiuser (i.e., multi-access) capability. For a frequency less than 20 MHz, you are only allowed to use a few kHz bandwidths, which limit the use of the multi-access (also known as multiuser) communication techniques to allow several implantable devices work in the same environment. For example, allowable bandwidth for 13.56 MHz ISM (the industrial, scientific, and medical) band is regulated with 14 kHz. Thus a more advanced wireless technology will be required in the future to accommodate better radio links for medical implants enabling safe and reliable communication links [33].

The above issue has become more evident in practice when more advanced medical implants such as wireless implantable cardioverter defibrillators and electronic pills (i.e., wireless endoscopes) started to appear in clinical environments. These modern devices need a much longer range for the wireless telemetry in addition to a higher bandwidth. Moving to higher operation frequencies was the only way to increase the range and dedicate enough spectrums for a reliable communication. Thus, in order to alleviate some of the issues mentioned above, international authorities have allocated a band at 402–405 MHz with 300 kHz channels (MICS band). With the use of this band, it is aimed to deliver high level of comfort, better mobility, and better patient care [34, 8].

The MICS band has been proposed to permit individuals and medical practitioners to utilize ultra-low power medical implant devices such as cardiac pacemakers and defibrillators, particularly without causing interference to other users of the electromagnetic radio spectrum. However, unlike the low-frequency inductive links, at high frequencies like 400 MHZ a wireless transceiver requires the use of radio-frequency (RF) blocks such as voltage-controlled oscillators (VCOs), mixer and phase-locked loops (PLLs) to down convert (or up convert for the transmitter case) the frequency signal in order to process it using the integrated circuit technology. These blocks are constructed using inductors and capacitors on chip or off chip, which increase the physical size of the wireless chip [9, 35]. Medical implants have a physical limitation for the electronics of the wireless telemetry and cannot afford to accommodate such blocks. Thus high-level of integration, which results in miniaturization and low power consumption, should be met for wireless designs at MICS band. So far only one company, Zarlink, designed a transceiver for implantable applications. Zarlink's transceiver still requires some external components for its full functions [35]. Although with an MICS link a data could be transferred from or to the implant within a distance of a few meters, when the implant system requires the use of a wireless power or wirelessly charging the battery, the external unit still will need to be attached to the body close or adjacent to the implant system for an efficient power transfer as indicated in Fig. 6.8. It is still necessary to utilize the power signal at a lower

frequency, which also eliminates the possible interference issue from the power signal to the data signals [27].

Medical implant telemetry can be categorized into two groups: high data rate and low data rate systems. As an example, the wireless capsule endoscope and the retina prosthesis are the recent implanted systems requiring a large amount of data delivered to or outside the body. Implantable multichannel neural recording systems and multichannel monitoring of continuous signals electroencephalogram (EEG) also necessitate a high data rate communication. As an example, scientists aim to achieve the recording of more than 100 channels in order to simultaneously record brain functions; a data rate more than 20 Mbps is required. A similar figure is also useful for a wireless endoscope implant to obtain higher resolution and detailed real-time video images. MICS has been divided into channels with 300 kHz bandwidth and thus cannot provide such data rates. Thus for these types of implantable systems requiring high data rate, UWB will be the technology to investigate [12].

6.3 WBAN Systems

The early telemedicine systems have used the WMTS for patient monitoring at hospitals. As an example, the LX-5160, which is a WMTS telemetry transmitter (608∼614 MHz WMTS Band), has been developed by Fukuda Denshi USA [36]. It transmits ECG and respiration parameters to a central telemetry receiver, which can be displayed on a remote computer. This device has a dimension of 5.4 (W) × 2.2 (D) × 8.6 (H) cm and a weight of 80 gram. Transceiver-608 telemetry device developed by Mindray [10] also uses a WMTS transmitter for patient monitoring. This telemetry uses a 12-lead ECG and has a dimension of (13.0 × 7.5 × 3.1 cm). Its weight is 181.4 g. The wireless telemetry is based on channelized WMTS frequency meaning uses different frequency for transmit and receive signals. For example, 608–614 MHz (transmit) WMTS channelized 1395–1400 MHz and 1427–1429.5 MHz (receive) WMTS are used. Welch Allyn is another company developing patient monitoring system for vital signs monitoring

for hospital and sportive applications [37]. They have developed micropaq® Wearable Monitor that displays heart rate, one or two ECG leads, motion-tolerant SpO_2 and pulse bar. The device can also connect wirelessly to a central monitoring station. This device has a large dimension similar to a mobile phone.

Comparing to the wireless module discussed before, these devices are bulky and are not appropriate sensor node when considering a WBAN application. Thus new telemedicine systems are currently being developed using new small size sensor nodes described earlier.

Recently Corventis, Inc. has developed a small sensor node called PiiX™ for wireless cardiovascular solutions [38]. It uses a wireless gateway device named zLink™ to communicate with the monitoring center. The device has some limitations. For example, PiiX is intended for single patient use and cannot be used for patients with implantable devices. The unique features of this device are leadless and water-resistant. It eliminates the cumbersome leads and wires, and can still operate during showering or sleeping. Piix sensor is quite small and can easily be attached to the body like a plaster. Figure 6.9 shows a picture of PiiX sensor node from Corventis and micropaq® Wearable Monitor from WelchAllyn.

A UK-based company Toumaz [17, 39] is developing a digital plaster where the sensor node can be attached to the human

Figure 6.9. Figure PiiX sensor node from Corventis [38] and micropaq® Wearable Monitor from WelchAllyn [37]. See also Color Insert.

body with a plaster. The wireless sensor node is based on ECG and temperature data. The data received from the plaster can be displayed on a PDA device. It can also be transferred to a monitoring station via WLAN link using the PDA as a gateway device. The digital plaster can communicate with PDA up to 3 meter distance. The plaster is based on the chip TZ1030 which uses the 8051 processor for digital processing a wireless transceiver.

The Fitbit has developed a wireless sensor node that a tracks motion of a human body. The Fitbit sensor contains a 3D motion sensor that tracks the motion in three dimensions and converts to useful information such as calories burned, steps taken, distance traveled, sleep quality, etc. It can be worn on the waist, in pocket or on undergarments. Nike and adidas have produced similar body-worn devices Nike+iPod and miCoach Pacer, respectively, for sport activities [40].

Here in we will discuss some of ongoing projects for WBAN applications. These projects have mainly used the sensor nodes provided in Table 6.4. Some have designed their own sensor nodes by using the wireless transceivers in Table 6.3 together with one of famous microcontroller — ATMega128L, MSP430, and/or 88051. There have been a number of different developments for WBAN systems in the literature. The goal here is to compare the existing systems in terms of their suitability for a large scale implementation for WBAN applications. We will discuss whether the available systems demonstrate a multi-patient or a single-patient monitoring. A comparison of some of current implemented WBAN systems is given in Table 6.5.

The project in reference [41] presents the AID-N triage system for disaster applications. It uses the MicaZ or TmoteSky platform from Crossbow Technology (2.4 GHz Radios (802.15.4) with CC2420 transceiver chip) in the sensor node for data collection. The sensor node communicates with another ZigBee device that is attached to a personal server, which is a laptop and PDA. Software programs have been developed to gather vital signs from a disaster scene. This system requires WLAN connections with an IEEE 802.11 link for transmission of patients' data to a remote server in a medical centre. If there is no network connection, the data will be stored in a device or can be monitored on a PDA in an emergency vehicle until patients are taken to a hospital.

Table 6.5. WBAN-based telemedicine systems

Existing systems	Wireless device	Sensors	Comments
CodeBlue [42]	802.15.4 (2.4 GHz)	Pulse oximeter, EKG, motion-activity	It uses MicaZ/T-mote sensor nodes.
WiiSARD [43]	802.11	Pulse oximeter	It uses PDA device as a sensor in order to use Wi-Fi link to connect the Internet.
(Gao, 2007) [41]	ZigBee (2.4 GHz)	SpO_2 , ECG, BP	It uses mesh networking for multi-patient, and WLAN for remote destinations.
(Park, 2006)	nRF24E1 radio (2.4 GHz)	ECG	The ECG sensor communicates to a computer wirelessly or a base station with the Wi-Fi link. No multi-patient scenario.
(Espina, 2008) [44]	IEEE 802.15.4 (2.4 GHz)	ECG, PPG, blood pressure	Single-user data is presented.
(Chen, 2009) [1]	IEEE 802.15.4 (ZigBee)	8–Channel EEG	Single patient. Internet data transmission is provided. No wireless gateways.
(Zhang, 2009) [2]	Bluetooth (2.4 GHz)	ECG	Although it mentions it is done for two persons ECG, one continuous ECG monitoring data is shown. The control device is directly connected to a home computer via USB (no wireless gateways). No data transmission through the Internet.
(Anliker, 2004) [45]	GSM	Blood pressure, SpO_2, 1-lead ECG	Multiple sensors have been integrated in one hand-held device.

(*Contd.*)

Table 6.5. (*Continued*)

Existing systems	Wireless device	Sensors	Comments
(Yuce, 2008) [23]	MICS, WMTS	Temperature, pulse rate, single lead ECG/EEG	he design targets monitoring of physiological ameters for multi-patient. It uses multi-hoping technique. Long-range data transmission through the Internet. Several wireless gateways to increase mobility.
TZ1038 Sensium [17,39]	868/915 MHz	Single lead ECG, temperature	Data received and displayed on a PDA device. Also transferred to a monitoring station via WLAN link using the PDA as a gateway device.
(Jovanov, 2005) [1]	ZigBee (2.4 GHz)	Activity sensor	The control device connects with a computer for data display directly or wirelessly using a Wi-Fi link. It is a multi-hopping system with multi-sensors; however, one patient data has been implemented. No Internet transmission has been indicated.
BSN Node [21]	IEEE 802.15.4 (2.4 GHz)	3-lead ECG, 2-lead ECG, and SpO_2 sensors	Multichannel sensor node. Sensor signals can be gathered, displayed, and analysed on a PDA. The PDA works as a wireless gateway for remote destinations.

(Wang , 2009)	nRF905 (915 MHz)	3-D acceleration	The sensor nodes communicate directly to a base-station board that includes an aMSP430F149 microprocessor and an nRF905. Data from single body is tested.
(Yuce, 2009) [12]	UWB	Multichannel EEG/ECG	The design targets monitoring of multichannel continuous physiological ameters for implantable and wearable systems. No wireless gateways.
Human++ [48]	nRF24E1 radio (2.4 GHz)	Single-lead ECG, EEG	An ECG node is designed using flexible polyimide material. No wireless gateways.
HeatlhGear [46]	Bluetooth (2.4 GHz)	Oximeter	The sensor communicates with a cell phone using the Bluetooth link. No wireless gateways. Individual use.

The CodeBlue project uses sensor nodes based on the popular MicaZ and T-mote designs [42] for a multi-patient monitoring system. The WiiSARD team [43] developed a prototype system for pulse oximeter sensor. It operates with the Wi-Fi link to enable a medical response through the Internet. It uses a PDA device as a senor which has a large size which is not attractive for a medical sensor node.

In reference [44], Espina et al. presented an IEEE 802.15.4-based wearable telemedicine system that monitors continuous cuff-less blood pressure and ECG signals. The sensor data was measured on a single user. Date is displayed from the sensor to a PDA or a wristwatch device. Anliker and his colleagues [45] designed a wrist-worn device to measure multiple physiological parameters from one person. Sensors like blood pressure, SpO_2, one lead ECG all have been integrated in one handheld device. The data is then transmitted using a GSM data link to a computer similar to Fig. 6.1. The device acts the same as a regular cellular phone since it operates with the GSM network. However, measurements more than one patient at the same time have not been provided. HealthGear project uses a cell phone as a central processing unit that receives signals from body sensors [46]. It uses the Bluetooth technology to connect a Bluetooth-enabled cell phone. The sensor is a Nonin's flex oximeter used to measure a single user's blood oxygen level (SpO_2). The Berkeley Tricorder sensor node is another Bluetooth-based WBAN system developed at Berkley [47] for ambulatory health monitoring systems. The system utilizes a multichannel wireless sensor node, including parameters such as ECG, EMG, blood oxygenation, respiration, and motion all on one board. The data are received and stored on a PC via a Bluetooth link.

Another system in reference [20] designs very small, wearable (probably one of the smallest custom-made sensor nodes available at the present time) ECG sensor that communicates wirelessly with a base station connected to a computer. The system works similar to a multi-hopping network by using the Wi-Fi link. Although a multi-patient data monitoring is not presented, this system can be used for measurements and monitoring of vital signs from multiple patients.

A wireless patient monitoring system based on an ECG patch has been developed for cardiac monitoring by IMEC Belgium. IMEC's Human++ program develops wearable wireless devices [48]. The current ECG node electronic is assembled on flexible polyimide substrate that can easily be integrated in textile.

There are also ongoing projects to develop sensor platforms operating at UWB (3–10 GHz) [12], MICS, and WMTS bands [49]. A WBAN system for multi-patient medical monitoring is presented in reference [23]. It uses a multi-hoping technique through wireless gateways to transfer data from sensors on several human bodies to remote locations. It uses the Internet to allow access at any location. In reference [12], a low-power WBAN system has been developed using UWB technology for implantable multichannel neural recording for brain–computer interface applications and 8-channel ECG for patient monitoring. The ECG data is monitored at a remote station.

Table 6.5 shows the current progress in WBAN applications. Real-time and simultaneous monitoring is required from multi-sensors on multi-bodies for future WBAN systems. System should take the advantage of the Internet for data transmission to remote locations, which will provide an access to a person's data anywhere in a city. Future WBAN systems should also develop small-size sensor boards to meet the size and power constraints. Most of the current systems use the commercially available ZigBee (IEEE 802.15.4) devices and boards, which are designed for many other applications and, thus, are not entirely wearable.

For longer range communications, the wireless nodes should be able to communicate to remote stations through a wireless, portable gateway (it could be a watch, PALM, iPhone, mobile phone, etc.). The wireless transmission technique between the gateway device and remote monitoring stations could be done using one of wireless protocols such as ZigBee, Bluetooth, or Wi-Fi for using the Internet.

The implanted device will most likely use the MICS band or a frequency around 400 MHz. The wearable nodes in a WBAN system will use an ISM band for low data rate communication and UWB when a high data rate transmission is required.

6.4 A WBAN-Based Multi-Patient Monitoring System

A WBAN system that has been designed for health care applications is presented in this section. The system is based on a multi-hopping network technique that can be used in medical environments for remote monitoring of physiological parameters from multiple patient bodies [52]. The system is depicted in Fig. 6.10. The data is transferred to remote stations through the local area network or the Internet already available in medical centers.

An example of sensor node design for medical monitoring is depicted in Fig. 6.11. The analog front-end of the sensor node for EEC, EEG, and EMG uses the circuit given in Fig. 6.3. The pulse rate sensor consists of an infrared emitter (SFH487-880nm) and a phototransistor (SFH309FA). Light is shone through the tissues, and the variation in blood volume alters the amount of light falling on the detector. When the heart beats, a pressure wave moves out along the arteries at a few meters per second. This pressure wave can be felt at the wrist, but it also causes an increase in the blood volume, which can be detected by a plethysmograph. Human heartbeat ranges between 50 bpm and 200 bpm. These figures indicate that the frequency range of human heartbeat is between 0.83 Hz and 3.33 Hz: A high-pass filter and a low-pass filter are used to form a band-pass

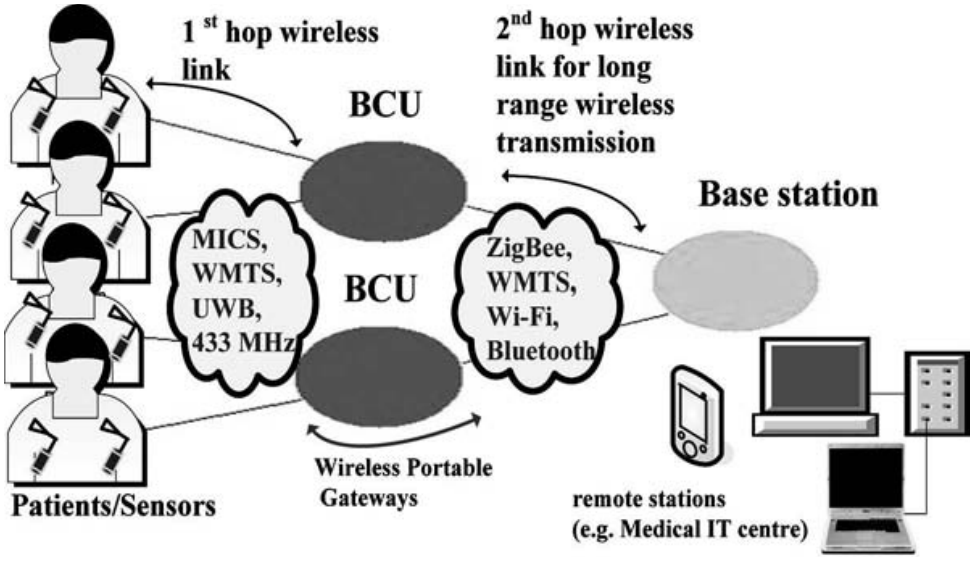

Figure 6.10. Multi-hopping WBAN-based multi-patient monitoring.

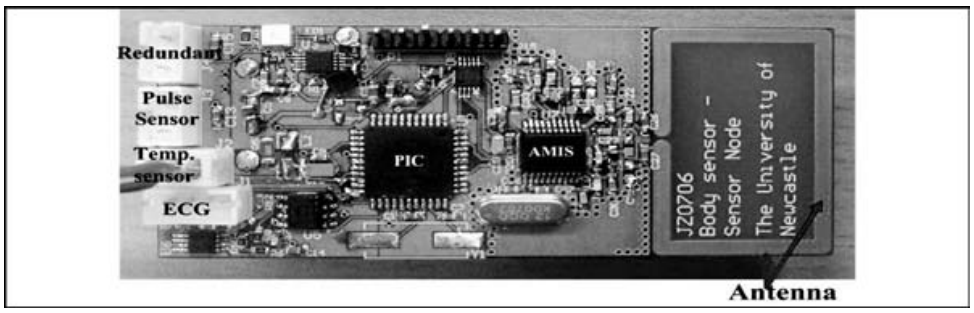

Figure 6.11. A 4-channel sensor node. See also Color Insert.

filter to remove unwanted environment signals. The optical part of the pulse sensor consumes quite large power [49]. It is also possible to detect the pulse rate from the ECG signal as explained later in Fig. 6.16. The temperature sensor uses the IC LM 35 for temperature measurement. The IC produces an analog voltage with respect to temperature. The ADC in the microcontroller samples the voltage and converts it to a digital/data for RF wireless transmission.

The primary function of BCUs is to collect data from sensor nodes via the first wireless link and forward these data to a remote PC (i.e., control station) for further analysis. Two types of BCU devices are needed in order to provide a complete WBAN transmission coverage in a medical center. One BCU is designed to be connected to a computer (Fig. 6.12a) via the USB port, while the other BCU is used to function as an intermediate device (Fig. 6.12b) that presents a second wireless link for a longer range wireless sensor network. The latter case is more suitable for large medical centers and functions as a portable gateway device. Although both BCUs can be used for multi-patient monitoring, the first BCU type (BCU-1) can also be useful for private usage at home or in a room of a hospital for single-patient monitoring.

The sensor nodes/BCU hardware requires a microcontroller and a wireless transceiver to coordinate all activities. The BCU-1/sensor nodes consist of a microcontroller PIC16F87 and a wireless transceiver (AMIS52100 IC and CC1000). Both AMIS and CC1000 can generate MICS band frequencies. Especially when CC100 is used, the operation frequency can be configured to 433 MHz ISM, WMTS bands as well as MICS.

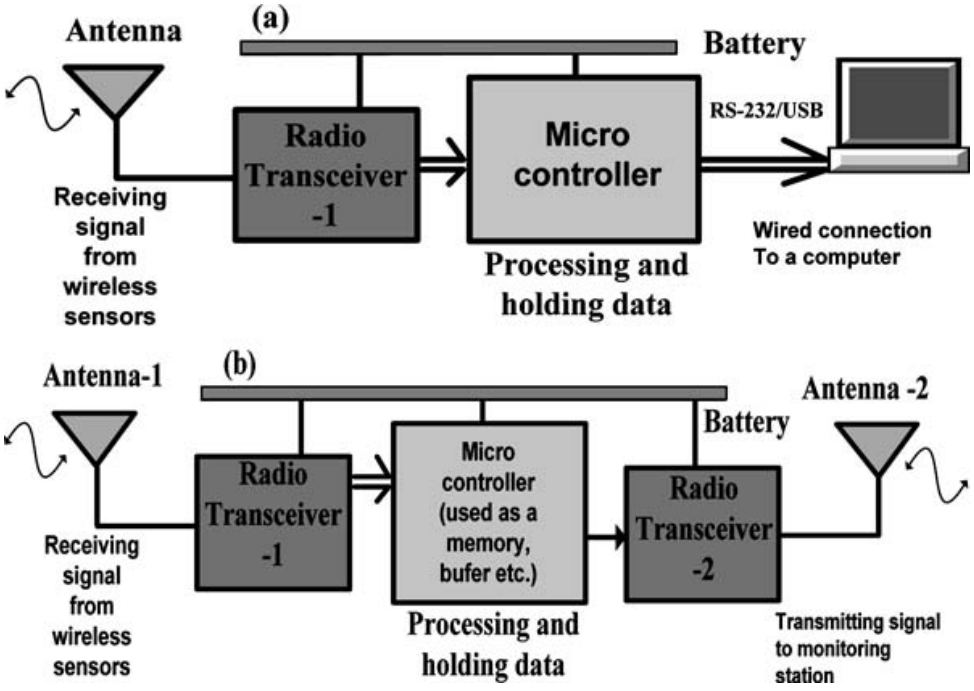

Figure 6.12. Block diagram of BCUs: (a) wired BCU, (b) portable BCU. See also Color Insert.

In addition to these chips, we use another transceiver, the CC1010 chip from TI (this chip contains CC1000 and a microcontroller built in), on the intermediate BCU (BCU-2) board to develop a wireless transmission and networking between BCUs and the remote base station. The CC1010 and CC1000 transceiver chips have the capability to transmit anywhere within 300 and 1000 MHz (It was tuned to WMTS band for the second wireless link in our prototype system). The AMIS IC has a data rate capability of 19 Kbps, while CC1010 provides 76 Kbps. The BCU-2 device in a WBAN can also be composed of standards such as ZigBee and the 802.11 Wi-Fi standards to accommodate and interface with different wireless platforms and to connect to the Internet for remote monitoring. A summary of devices used in BCUs and sensor node boards is given in Table 6.6. The hardware implementations of BCU-1 and BCU-2 are given in Figs. 6.13 and 6.14.

The modulation technique used in CC10xx chips is FSK with a frequency step of 64 kHz, which is acquired by loading the crystal. FSK has better interference rejection and causes less spectrum splatter normally seen in ASK systems. The picture in Fig. 6.15

Table 6.6. Summary of devices used in sensor nodes and BCUs

Device features	AMIS (52100)	CC1000	CC1010*	PIC16F887
Size (mm)	7.5×7.8	9.7×6.4	12.9×12.9	17.53×17.53
Modulation	ASK/OOK	FSK/OOK	FSK	—
Sensitivity	-117 dBm	-109 dBm	-107 dBm	—
Power: Transmitter	TX: 25 mA	Tx: 26.7 mA	Tx: 26.6 mA	< 0.6 mA (active)
Receiver	Rx: 7.5 mA	Rx: 7.4 mA	Rx: 9.1 mA	
Data Rate	19 Kbps	76.8 Kbps	76.9 Kbps	—
Sniffing**	500 nA	200 nA	~ 0 mA	—
Memory (RAM)	—	—	$2048 + 128$	$368 + 256$
Additional Features	—	—	10-bit, 22.7 kHz sampling frequency	10-bit 52 kHz sampling frequency

*Note: CC1010 has a microcontroller built-in.
** Sniff mode enables the receiver to wake up or operates at times to "sniff" received RF signals and then return to "sleep" or "wait" mode if a signal is not detected.

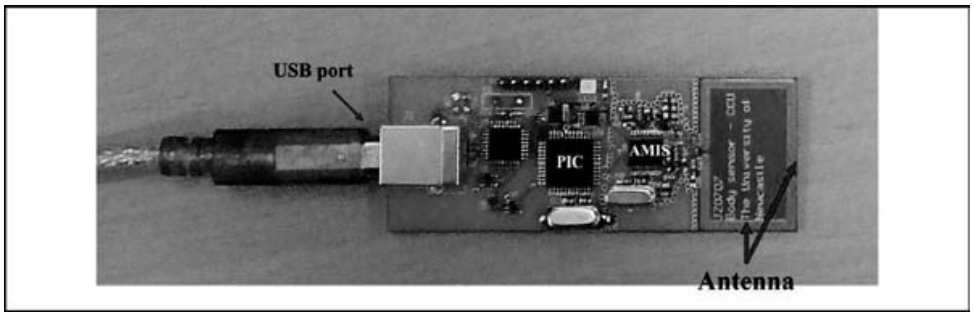

Figure 6.13. A wired BCU (BCU-1). See also Color Insert.

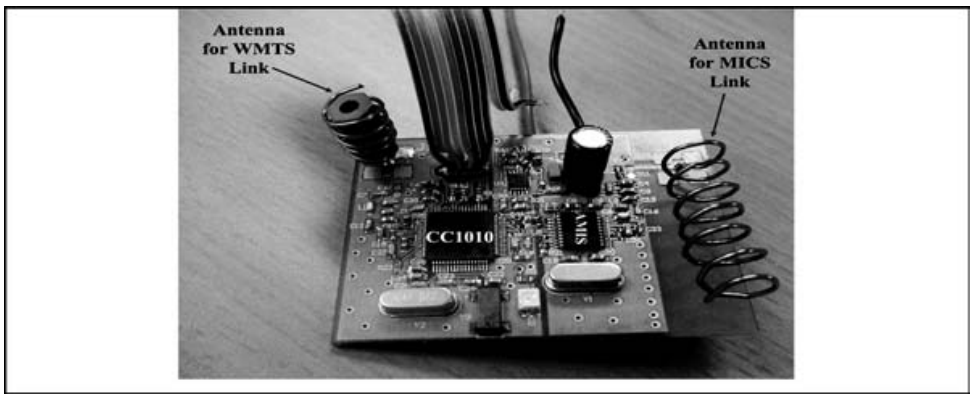

Figure 6.14. Intermediate body control unit (BCU-2). This device is shared by more than one patient and is portable. It contains dual wireless transceiver to support two directional wireless links. See also Color Insert.

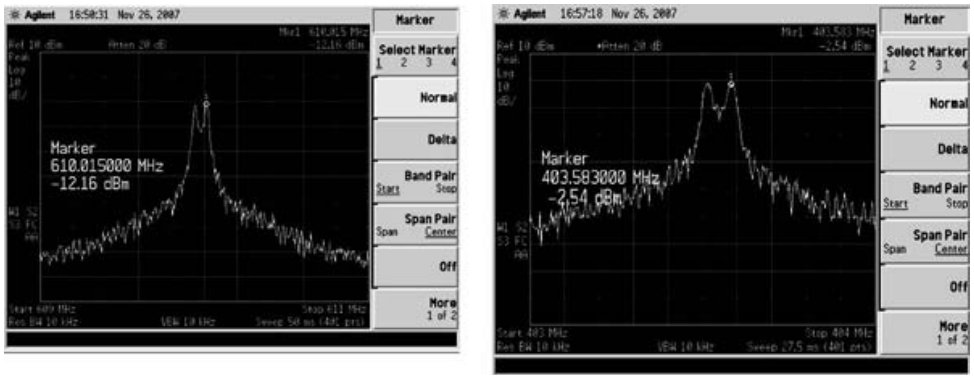

Figure 6.15. Spectrums generated for MICS and WMTS frequencies with Chipcon CC1010.

demonstrates the FSK modulation for MICS and WMTS bands. What is necessary to realize from this picture is that the bandwidth of the signal is well within the bandwidth of the WMTS band (608–615 MHz).

In order to provide communication from sensors to a personal computer, a wired serial port interface, such as RS-232 standard, should be used to connect the base station to monitor the received body signals. The interface system here uses RS-232 serial interface and USB connections.

Figure 6.16 is an ECG signal obtained from our set up. The ECG signal is transmitted from a sensor node to the computer. Each sensor node representing only one patient can only have one ECG. In order to eliminate the DC noise (50 Hz/60 Hz interference), a recursive filter has been software implemented to obtain an accurate ECG signal (see appendix for notch filter implementation). As shown in Fig. 6.10, by clicking on 50 Hz filter, the recursive notch filter operates on the received ECG signal.

High computation programs like MATLAB can further be used to analyze data automatically and to warn medical professionals when the value of a critical data goes outside the safe margin. A warning signal could be easily generated by the program at the PC to warn health professionals to track the sensor node generating a warning signal. This feature will strengthen the reliability and safety in implementation, which would be useful for patients' lives.

Figure 6.16. A wireless ECG monitoring showing pulse rate as well.

A medical data from a single human body can be monitored within 300 ms for a distance of 1 m when the WBAN system is implemented in a four–patient scenario. When the active patient is doing all sort of activities, e.g., sitting standing, turning around the other patients, the average delay is 1 s up to 5 m and 2 s at the distance of 10 m. These values show that the WBAN system exhibits a correct, timely, and reliable communication performance up to 10 m with a time performance less than 2 s for a multi-patient scenario [52].

6.4.1 *Software Programs and Monitoring*

In order to monitor data in body area network applications, several computer programs should be developed. The necessary software programs have been identified in Fig. 6.17 for this specific application. A software called GATEWAY should be developed at the monitoring PC to control the communication with the BCU to get readings from sensors and then forward them through another network/Internet to an application on a remote PC (at a remote location). While performing this task, the GATEWAY will also verify the data integrity and schedules retransmission, if required. Another software program is developed at the remote PC (called BSN),

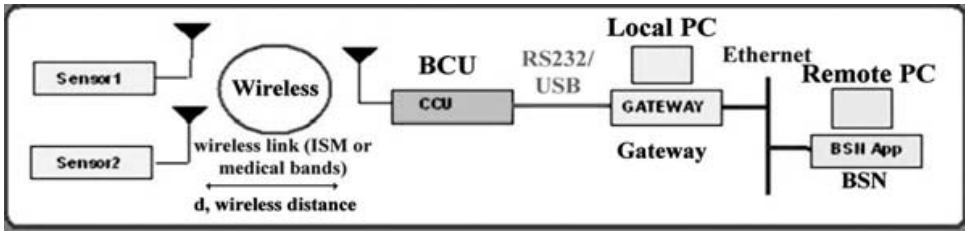

Figure 6.17. Software programs for the proposed WBAN application. See also Color Insert.

which gets readings from GATEWAY via the network/Internet. These readings are stored in the remote PC for analysis. A graphical user interface (GUI) at the local PC as well as at remote PCs should be designed to display the human body data. Both the data received from the BCU and the data sent to the BSN can also been shown by the GUI in text or graphical formats. In case of medical application, the physiological signals of patients can be accessed by medical staff anywhere in the medical center as long as their computers are connected to the local area network in the building.

The BSN application is designed to collect and store readings automatically so that no person is required to be stationed at the application. It gets sensor information and readings from the GATEAWAY and will ask retransmission if error is detected. It undertakes the administration of patients' particulars such as assigning new sensor ID to patients, segregating sensor readings from different patients, and storing them into the data base. The GUI at the monitoring PCs allows medical personnel to enter patients' information. It can also display live monitoring graphs on the screen (Fig. 6.18). Every sensor device has a unique sensor ID and must be registered under a patient name before they are used. In the event that an unregistered sensor node is used, all its readings received will be discarded by the BSN application

Since all sensor nodes of a body are communicating with the same BCU, the data is prefixed with an identifier, which is used to identify the source of the data. As mentioned earlier, to reduce collisions further between data sent, a firmware (medium access control (MAC) protocol) is written to control data transmissions. The communication between the sensors and the BCU is bi-directional as to support a multiuser (i.e., multi-patient) communications.

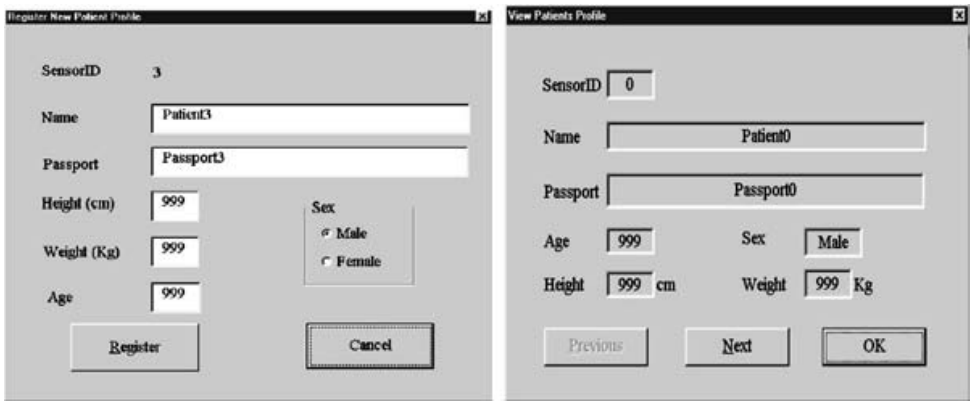

Figure 6.18. Example of a graphical menu registering and viewing patients.

The GATEAWAY menu shows a GUI at the local PC, which is designed to configure the source and destination socket and port numbers for data transfer on the Ethernet (See Fig. 6.19). This GUI ensures portability if the BSN application or the GATEWAY need to be relocated, it can be configured to work without additional changes in the codes. Both the data received from the BCU and the data sent to the BSN can also been shown here in text format. The physiological signals of patients can be accessed by medical

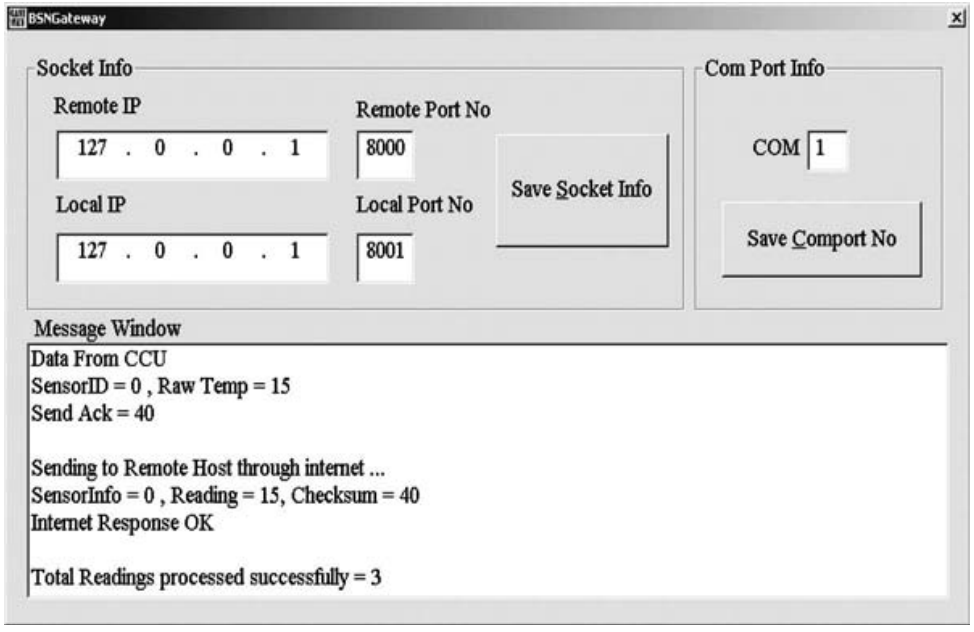

Figure 6.19. The GATEWAY menu.

staff anywhere in the medical center as long as their computers are connected to the local area network in the building.

The software packages used for monitoring and storing data (in the database) should be user friendly so that medical professionals utilize them efficiently. The programs should allow a medical professional to easily set up sensors. When needed, one or more sensors should be removed without affecting the operating of the other sensors in the system. Software programs at the monitoring PC can be designed in such a way that when a sensor stops working, the data from the remaining sensors should still be received and monitored. Before a new sensor is deployed for a particular person, a new sensor ID (i.e., user ID) should be assigned at the monitoring PC so that the MAC protocol used for the data communication will enable a communication from that sensor. The MAC protocols mentioned above can integrate an error-checking mechanism to allow the monitoring of correct data only and discard when a data is faulty.

A database server is developed to maintain data integrity, which is necessary for big medical centers. Monitoring of ECG for an individual patient is shown in Fig. 6.20. In this GUI, more detailed patient's particulars can be seen from the database. Clicking on

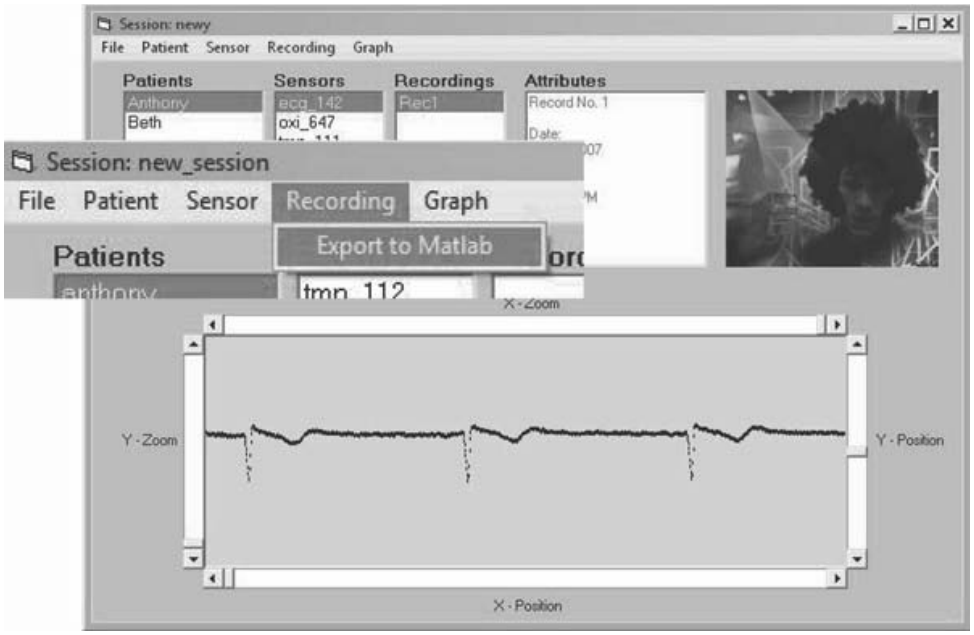

Figure 6.20. An example of ECG Monitoring. See also Color Insert.

a patient shows the sensors attached to them and their personal information/picture. Clicking on a sensor displays the sensor's information (e.g., interval). It also brings up how many recordings are available. Single clicking a record shows when the record was made. Double clicking displays the record on the graph. In the following figure, it is arranged for an ECG monitoring. It is very handy to have a data file compatible with a computation software program like MATLAB for signal analysis as shown in the window.

6.5 Conclusion

We have discussed implementation issues and presented details of techniques for design of wireless sensors in WBAN applications. Portable and wireless gateway nodes are used to connect the sensor nodes to the local area network or the Internet already available for long-range access points. Wireless standards such as ZigBee (IEEE 802.15.4) and Bluetooth (IEEE 802.15.1) are popular low-power technologies for communication between sensors and the control device. New wireless devices specifically targeting at WBAN application can be designed based on MICS, WMTS, 433 MHz ISM as well as UWB bands. Miniaturization of the sensor node electronics, especially the sizes of the microcontroller, the wireless chip, the battery, and low-power consumption are current hardware related issues for small sensor nodes. TI's CC2420 and CC1010 transceivers and Nordic's transceivers like nRF24E1 are current popular choices for wireless module in a sensor node. The successful implementation of a WBAN system should operate and coexists with other network devices and should provide wearable, wireless (no wire connections), easy to remove, and attach sensor nodes, leading to increased mobility of patients and flexibility.

Any future projects based on WBAN should take under consideration the co-existence of other network devices operating in similar frequency bands. The majority of WBAN systems cover only wearable sensor nodes. There is very limited information on integration of wearable and implantable systems together. Implanted or wearable sensor nodes should be able to work together in a WBAN system without any data collisions.

Acknowledgements

I would like to thank Anthony Bott and Ng Peng Choong for their help in developing software programs and boards.

Appendix

Digital Notch Filter Designs

A digital notch filter can be designed to filter out the 50/60 Hz noise for continuous physiological parameters. We used the website in [53] as a reference. Two parameters should be defined: f, the center frequency, and BW, the bandwidth. Finding the notch filter coefficients:

$$
\begin{aligned}
R &= 1 - 3 \times \mathrm{BW} \\
\mathrm{BW} &= 0.033 = 13.2 \text{ Hz} \\
\therefore \quad R &= 0.901 \\
f &= \frac{50}{400} = 0.125 \\
K &= \frac{1 - 2 \times 0.901 \times \cos(2\pi f) + 0.901^2}{2 - 2 \times \cos(2\pi f)} \\
\therefore \quad K &= 0.917731353 \\
a_0 &= K,\, a_1 = -2K\cos(2\pi f) = -1.297868126,\, a_2 = K \\
b_1 &= 2R\cos(2\pi f) = 1.27420642,\, b_2 = -R^2 = -0.811801
\end{aligned}
$$

These are used in the equation

$$
\begin{aligned}
y[n] = a_0 x[n] + a_1 x[n-1] + a_2 x[n-2] \\
+ \cdots + b_1 y[n-1] + b_2 [n-2]
\end{aligned}
$$

Note that BW and f are fractions of the sampling frequency. All calculations are done in radians. The bandwidth 13.2 Hz, which could be wide for the application, can easily be decreased to a nominal value.

The system requires that three previous inputs and the last two outputs are stored. Whenever a new value is calculated, the array

is shifted so that $x[n-1] = x[n]$, etc. It is possible to increase the number of coefficients but at the expense of CPU resources and the increased risk of instability. Decreasing the bandwidth of the filter also has limits and will cause problems if it becomes too small.

References

1. Jovanov, E., Milenkovic, A., Otto, C., and de Groen, P. C. (March 2005) A Wireless Body Area Network of Intelligent Motion Sensors for Computer-Assisted Physical Rehabilitation, *Journal of NeuroEngineering and Rehabilitation*, **2(6)**, doi:10.1186/1743-0003-2-6.
2. http://focus.ti.com/lit/ds/symlink/ina321.pdf, 2010.
3. http://www.analog.com/static/imported-files/data_sheets/AD620.pdf.
4. E. Company-Bosch and E. Hartmann , ECG Front-End Design is Simplified with Micro-Converter® " Analog Dialogue 37-11, November (2003).
5. P. A. Pour, T. Gulrez, O. AlZoubi, G. Gargiulo, and R. A. Calvo (15–18 December 2008) Brain-Computer Interface: Next Generation Thought Controlled Distributed Video Game Development Platform, *IEEE Symposium on Computational Intelligence and Games,* pp. 251–257.
6. S. Hanna (2009) Regulations and Standards for Wireless Medical Applications, *ISMICT* 2009.
7. K. Finkenzeller (April 2003), *RFID Handbook*, 2nd edn, John Wiley and Sons, New York, USA.
8. FCC Rules and Regulations (January 2003) MICS Band Plan, *Table of Frequency Allocations*, Part 95.
9. A. Tekin, M. R. Yuce, and W. Liu (2008) Integrated VCOs for Medical Implant Transceivers, *VLSI Design*, 2008, Article ID 912536, 10 pages, doi:10.1155/2008/912536.
10. http://www.na.mindray.com/pdf/panorama_WMTS_specifications_us.pdf.
11. http://www.fda.gov/MedicalDevices/Safety/MedSunMedicalProductSafetyNetwork/ucm127778.htm, 2010.
12. M. R. Yuce, H. C. Keong, M. Chae (October 2009) Wideband Communication for Implantable and Wearable Systems, *IEEE Transactions on Microwave Theory and Techniques*, **57(2)**, pp. 2597–2604.

13. Moteiv Corporation (2010) http://sentilla.com/files/pdf/eol/tmote-sky-datasheet.pdf.
14. http://www.tinynode.com. Ref: Tinynode.
15. http://webs.cs.berkeley.edu/tos/.
16. http://www.snm.ethz.ch/Projects/T-Nodes.
17. A. Wong, G. Kathiresan, C. Chan, O. Eljamaly, O. Omeni, D. McDonagh, A. Burdett, and C. Toumazou (2008) A 1 V Wireless Transceiver for an Ultra-Low-Power SoC for Biotelemetry Applications, *IEEE Journal of Solid-State Circuits,* **43**, pp 1511–1521.
18. http://www.btnode.ethz.ch/Documentation/BTnodeRev3Sensor Guide.
19. http://www.palowireless.com/database/conexant/101685b.pdf.
20. C. Park, P. H. Chou, Y. Bai, R. Matthews, and A. Hibbs (2006) An Ultra-Wearable, Wireless, Low Power ECG Monitoring System, in *Proceedings of IEEE BioCAS*, pp. 241–244.
21. G. Z. Yang (2006) *Body Sensor Networks*, Springer-Verlag London.
22. B. Wang, et al. (11–13 June 2009) A Body Sensor Networks Development Platform for Pervasive Healthcare, *in Proceedings of the 3*rd *International Conference on Bioinformatics and Biomedical Engineering,* pp. 1–4.
23. M. R. Yuce, and C. K. Ho (August 2008) Implementation of Body Area Networks Based on MICS/WMTS Medical Bands for Healthcare Systems, *IEEE Engineering in Medicine and Biology Society Conference (IEEE EMBC08),* pp. 3417–3421.
24. R. S Mackay, B Jacobson (1961) Radio Telemetering From Within the Human Body, *Science*, **134**, pp. 1196–1202
25. S. Y. Shin, H. S. Park, and W. H. Kwon (August 2007) Mutual Interference Analysis of IEEE 802.15.4 and IEEE 802.11b, *Computer Networks*, **51**, pp. 3338–3353.
26. W. Liu, et al. (September–October 2005) Implantable Biomimetic Microelectronic Systems Design, *IEEE Engineering in Medicine and Biology Magazine*, **24**, pp. 66.
27. M. Zhou, M. R. Yuce, and W. Liu (September 2008) A Non-Coherent DPSK Data Receiver With Interference Cancellation for Dual-Band Transcutaneous Telemetries, *IEEE Journal of Solid-State Circuits*, **43**, pp. 2203–2012.
28. W. Liu, et al. (October 2001) A Neuro-Stimulus Chip With Telemetry Unit for Retinal Prosthetic Device, *IEEE Journal of Solid-State Circuits*, **35**, pp. 1487–1497.

29. S. K. An, et al. (June 2007) Design for a Simplified Cochlear Implant System, *IEEE Transactions on Biomedical Engineering*, part 1, 54, pp. 973.
30. P. R. Troyk, and G. A. DeMichele (September 2003) Inductively-Coupled Power and Data Link for Neural Prostheses Using a Class-E Oscillator and FSK Modulation, in *Proceedings of the IEEE International Conference on Engineering in Medicine and Biology Society*, pp. 3376–3379.
31. M. Ghovanloo, and K. Najafi (December 2004) A Wideband Frequency Shift Keying Wireless Link for Biomedical Implants, *IEEE Transactions on Circuits Systems II*, **51**, pp. 2374–2383,.
32. M. A. Stuchly, A. Krazewski, S. S. Stuchly, and A. M. Smith (1982) Dielectric Properties of Animal Tissues in Vivo at Radio and Microwave Frequency: Comparison Between Species, *Physics in Medicine and Biology*, **27**, pp. 927–936.
33. D. Halperin, et al. (March 2008) Security and Privacy for Implantable Medical Devices, *IEEE Pervasive Computing*, **7(1)**, pp. 30–39.
34. Australian Communications Authority, Radio Frequency Planning Group (October 2003) Planning for Medical Implant Communications Systems and Related Devices, *Proposals Paper*, http://www.acma.gov.au/.
35. P. D. Bradley (December 2006) An Ultra-Low Power, High-Performance Medical Implant Communication System (MICS) Transceiver for Implantable Devices, in *Proceedings of the IEEE Biomedical Circuits and Systems Conference (BioCAS 2006)*, pp. 158–161, also at http://www.zarlink.com/zarlink/hs/4889.htm.
36. http://www.fukuda.com/fukuda_usa/lx-5160.html, 2010.
37. http://www.welchallyn.com, Micropaq® Monitor.
38. http://www.corventis.com/AP/nuvant.asp, 2010.
39. A. Burdett (2006) Low Power Device Communication, *IET Seminar on Biocompatible Materials and Devices*, http://www.toumaz.com/.
40. www.micoach.com.
41. T. Gao, et al. (September 2007) The Advanced Health and Disaster Aid Network: A Light-Weight Wireless Medical System for Triage, *IEEE Transactions on Biomedical Circuits and Systems*, **1(3)**, pp. 203–2007.
42. V. Shnayder, B. Chen, K. Lorincz, T. R. F. F. Jones, and M Welsh (2005) Sensor Network for Medical Care, *Technical Report TR-08-05*, Division of Engineering and Applied Sciences, Harvard University.
43. https://wiisard.org.

44. J. Espina, T. Falck, J. Muehlsteff, Y. Jin, M. A. Adán, and X. Aubert (June 2008) Wearable Body Sensor Network Towards Continuous Cuffless Blood Pressure Monitoring, in *Proceedings of the 5th International Workshop on Wearable and Implantable Body Sensor Networks*, pp. 28–32.
45. U. Anliker, et al. (2004) AMON: A Wearable Multiparameter Medical Monitoring and Alert System, *IEEE Transactions on Information Technology in Biomedicine*, **8**, pp. 415–427.
46. N. Oliver, and F. Flores-Mangas (2006) HelathGear: A Real-Time Wearable System for Monitoring and Analysing Physiological Signals, in *Proceedings of the IEEE International Workshop on Wearable and Implantable Body Sensor Networks (BSN 2006)*, pp. 1–5.
47. R. Naima, and J. Canny (June 2009) The Berkeley Tricorder: Ambulatory Health Monitoring, in *Proceedings of the 2009 6th International Workshop on Wearable and Implantable Body Sensor Networks*, pp. 53–58.
48. J. Penders, at al. (December 2008) Human++: From Technology to Emerging Health Monitoring Concepts, in *Proceedings of the 5th International Summer School and Symposium on Medical Devices and Biosensors (ISSS-MDBS 2008)*, pp. 94–98.
49. M. R. Yuce, et al. (December 2007) Wireless Body Sensor Network Using Medical Implant Band, *Journal of Medical Systems*, **31**, pp. 467–474.
50. H. Chen, W. Wu, and J. Lee (March 2009) A WBAN-Based Real-Time Electroencephalogram Monitoring System: Design and Implementation, *Journal of Medical Systems.*, **34**, pp. 303–311.
51. Y. Zhang, and H. Xiao (November 2009) Bluetooth-Based Sensor Networks for Remotely Monitoring the Physiological Signals of a Patient, *IEEE Transactions on Information Technology in Biomedicine*, **13(6)**, pp. 1040–1048.
52. 52**.** M. R. Yuce (July 2010), "Implementation of Wireless Body Area Networks for Healthcare Systems," *Sensors & Actuators: A. Physical*, **162**, pp. 116-129.
53. http://www.dspguide.com/ch19/3.htm.

Chapter 7

Wireless Body Area Network Implementations for Ambulatory Health Monitoring

Reza Naima[a] and John Canny[b]

[a] *Department of Bioengineering, University of California, Berkeley, 306 Stanley Hall #1762, Berkeley, CA 94720-1762*
[b] *Electrical Engineering and Computer Sciences, University of California, Berkeley, 387 Soda Hall, MC1776,Berkeley, CA 94720-1776*
reza@reza.net; jfc@cs.berkeley.edu

The design and implementation of an ambulatory health monitoring device is a process of matching the medical need to available technology. The process starts with an understanding of the requirements, which leads to the design of sensors, filters, amplifiers, etc. There are a number of additional decisions to be made that range from the battery chemistry to the wireless technology that must also match the underlying requirements. Finally, some existing implementations will be reviewed.

7.1 Design Process

The first step in developing a device is to understand the medical need in detail. It is not sufficient to simply have an understanding

Wireless Body Area Networks: Technology, Implementation, and Applications
Edited by Mehmet R. Yuce and Jamil Y. Khan

ISBN 978-981-4316-71-2 (Hardcover), ISBN 978-981-4241-57-1 (eBook)
www.panstanford.com

of the physiology, pathology, etc., and to build a device accordingly. From the physician's perspective, the device might be too complex to use, the data might be too verbose to analyze, or the physician might not trust the data compared to the existing standards. From the patients' perspective, the device might be too cumbersome or irritating to wear, the battery might die too quickly, the device might require too much maintenance, or they might not see sufficient value in the device to comply with the doctor's instructions. There are many other stakeholders that must also be considered through the design process: nurses or other caregivers, insurance companies or other sources of reimbursement. There is a great book that discusses the design process for medical devices in detail [1], and is highly recommended.

Once the high-level application, set of sensing modalities, data storage, and wireless telemetry mechanism are determined, the requirements of the individual components need to be flushed out. It isn't sufficient to "record ECG"; rather, the application will result in requirements that need to be satisfied by the design. For example, many ECG circuits will bandwidth limit the signal to 40 Hz, and thus only require a sampling rate around 80 Hz (based on Nyquist–Shannon sampling theorem). However, if the data is to be used to measure heart-rate variability, then a sampling rate of 1 kHz is required to have the required resolution. It is easy to miss this step and to start designing a circuit based on a number of assumptions which might not be valid — only to find out months later and have to spend considerably more time and effort trying to fix the design or work around the flaws. This is a lesson the author has learned the hard way — spend the time understanding the application and the requirements, and the interdependence of requirements between the various components.

To help understand the design process, we will give examples involving an ambulatory health monitor developed at the Berkeley Institute of Design, named the Tricorder (Fig. 7.1). The original goal for the Tricorder was a small and highly integrated device, which records a number of parameters that can be used to assess the wellness-state of the user. The data was intended to be used by health care providers to better monitor the health state of the user, to help in the treatment of any chronic condition, and to provide

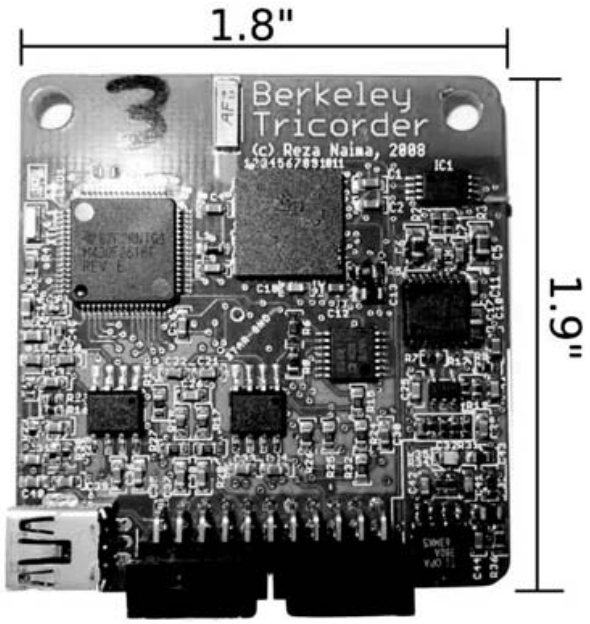

Figure 7.1. The Berkeley Tricorder. See also Color Insert.

advanced notice of any possible health problems. Based on our application, we developed the following high-level design goals:

- A means of data storage for at least 24 h and a mechanism for offloading said data.
- Remote telemetry for real-time data viewing.
- A comfortable means of wearing the device.
- As many relevant sensing modalities as possible in a single highly integrated form factor.

Based on these design goals, we decided on Bluetooth for the wireless telemetry, microSD card for the data storage, and a number of sensing modalities, detailed in Table 7.1. Examples involving the Tricorder will be presented in the various sections of this chapter.

7.2 Existing WBAN Implementations

There are a large number of existing WBAN (wireless body area network) implementations for an array of applications. Any attempt at categorizing implementations is artificial, and the distinctions

Table 7.1. Device parameter summary

Modality	Sampling rate	Bits/sample	Comment
ECG	256 Hz	12	2-Stage HPF; RFI filer; single channel
EMG	256 Hz	12	1-Stage HPF; RFI filter
Respiration (bioimpedance)	256 Hz	12 Phase; 12 Mag.	4-Electrode configuration; 350 μA current at 50 kHz
Acceleration (3-Axis)	256 Hz	8/Axis	
Blood oxygenation	256 Hz	15	Reflective forehead sensor; 2-stage amp with DC-offset subtraction

between different deployments can be very different from the perspective of two different users. We will attempt to group together various common characteristics between some of the different implementations used in the noninvasive health/medical space based on my experiences and research, and present it as a starting point.

Other sections in the chapter are dedicated to the implementation of sensing modalities at a low level — this section will focus on the differences at a higher level: the hardware design paradigm, the firmware implementation, and mechanism by which data is handled.

7.2.1 *Hardware Paradigms*

There is a big tradeoff between implementations that are designed and built from the ground up, and designs which use OEM (original equipment manufacturer) components to accelerate development. Fully custom designs will generally take longer to develop, test, and debug — but they will provide the smallest form factor, lowest power consumption, and best fit for your application. These implementations might have higher up front costs associated with all the required development tools, but will cost lower to produce in volume.

Examples of highly integrated circuits include a non-contact ECG electrode with an integrated amplifier [2]. In this case, the electrode form factor requires a highly integrated device, which is not possible with OEM options. The same is true with another group that has developed a button-sized wireless pulse oximeter [3]. Even greater levels of integration can be achieved by fabricating

an application-specific integrated circuit (ASIC) containing all the required components for a WBAN system on a single chip [4], or just a portion [5].

A majority of WBAN devices utilize at least one OEM component — ranging from small PCBs that implement the wireless link to fully integrated sensing devices such as a pulse oximeter, which provides the blood oxygen saturation percentage data over a serial stream [6]. The use of OEM components can greatly accelerate the design cycle; however, each module often implements redundant components such as the power stage and microcontroller's which consume more power, take up more space, might not provide an ideal form factor, and have higher costs.

The most common OEM modules are ZigBee-based motes. Motes[1] are a class of devices that are conform to the 802.15.4 communications standard and allow for a data transfer and relay between motes in a mesh configuration. Motes can include an ADC (analog-to-digital converter) and serial ports to interface with custom sensing boards, such as the MICAz mote from Crossbow. The Telos moteiv also includes temperature, humidity, and light intensity sensors. Their popularity is based on their low levels of power consumption, a well-established networking interface, and the ability to relay data between motes.

There are many mote-based implementations, such as the group at the University of Alabama, which has a built a custom ECG module to interface with a Telos Mote [7, 8].

Another group has proposed a system that utilizes a number of OEM modules, including a Nonin ipod pulse oximeter, a belt-based respiration rate sensor, and MICA based motes [6]. A joint effort between Stanford University and NASA has resulted in the Lifeguard [9], a platform that utilizes a number of OEM components such as the Nonin Xpod pulse oximeter and the Accutracker II blood pressure monitor.

7.2.2 *Firmware*

There are two main camps in terms of how the firmware operates — either as a single application, or as an operating system that

[1] Dr. Kris Pister, inventor of motes, defines a mote as a single dust particle

runs the application. As with the hardware example, writing a stand-alone application provides the greatest flexibility in how to access the hardware and utilize its resources, whereas implementing an operating system, such as TinyOS[2], can help accelerate the development cycle and provide a large set of built-in tools but introduces overhead into the application and imposes some limits in terms of how the application is structured.

TinyOS is the primary operating system running in most of the motes to handle network communications, and is used by a number of projects. The CodeBlue group at Harvard University have developed a number of sensors that use TinyOS motes for data acquisition and telemetry [10] and evaluated their use for triage [11].

A group at the Imperial College London has utilized a TinyOS-based sensor module developed at the University of California, Berkeley to accelerate the development cycle of a number of biosensors. These include an ECG module and a pulse oximeter module, each of which can relay data directly to a PDA [12].

7.2.3 *The Data*

Once data is collected, it can be stored, processed, transmitted, or any combination thereof. For data storage, the predominant mechanism is by the use of a secure digital card, especially the microSD form factor, which is 15 mm $\times$ 11 mm $\times$ 1 mm. These devices require standard Serial Peripheral Interface (SPI), present on most microcontrollers. Their use is further promoted by the availability of numerous royalty-free interface libraries and the availability of multi-gigabyte cards. This is especially important for devices such as the Berkeley Tricorder, which can generate up to 823 MB of data in 24 h [13]. It should be noted that during a write cycle, SD cards use considerable bursts of current, which can introduce noise to your system. For the Berkeley Tricorder, we found this noise was coupled onto the LED current, which produced noise from the pulse oximeter signal (visible in Fig. 7.15). A redesigned current source is expected to correct this.

[2] http://www.tinyos.net/

Processing of data can involve digital filtration to remove signal noise, or calculating the percentage oxygen saturation from the output of the pulse oximeter photodiode and lookup tables. Processing of data consumes limited CPU cycles and increases the power consumption of the microcontroller. Hence, as much data processing as possible should be performed on more powerful devices (i.e., a cell phone or a personal computer).

In terms of telemetry, there are a large number of possible implementations that depend on: the desired telemetry range, requirements of data relaying, the operating frequency, and the requried bandwidth. As a general rule of thumb, the technology that meets all the requiremets while minimizing the power consumption and PCB real-estate will provide the best option.

7.3 Signal Acquisition

The number of possible sensing modalities is very large — a discussion of all the possible modalities is beyond the scope of this chapter. Instead, we will discuss some common strategies used in interfacing analog and digital components, with examples in the modalities used in the medical space.

The strategy for any sensing modality is to start with a characterization of the signal of interest in the context of how that data is to be used. The parameters of interest include the frequency bandwidth, the required dynamic range, and source impedance. It is always critical to start with signal source and design the rest of the system from that point; otherwise you might find yourself in the position of being forced to redesigning portions of your circuit at the expense of extra time and cost.

In addition to designing the circuit based on the signal of interest, it must also be designed to be immune to noise coupled from the power supply, from radio-frequency interference (RFI), or from other components on the circuit board while adhering to various safety requirements.

A similar strategy exists for sensing modalities that do not require any analog interface, such as an accelerometer that communicates through a digital interface. In this situation, it's

important to understand data's application and to design around those requirements. For example, an accelerometer that is used for fall detection might require a high sampling rate, but not many bits of resolution, whereas an accelerometer used to measure cardiac output (i.e., balistocardiograph) would require significantly higher resolution but a lower sampling rate.

7.3.1 *Frequency Bandwidth of Interest*

An understanding of the frequency bandwidth ($f_{\min} - f_{\max}$) of interest (FOI) for any particular sensing modality is perhaps the single most important characteristic to understand. For analog-based signals, it will determine how the front-end interface is designed, will influence the choice of the amplifier, and determine the sampling requirements for the ADC. The FOIs are best determined by doing research on the modality of interest, especially for any biologically originating signals as most of them have been well characterized.

The FOI is often derived by an examination of the power spectrum of the modality of interest. For example, consider the power spectrum of an ECG signal sampled at 256 Hz (Fig. 7.2). By 40 Hz, we can see a 15 dB drop in the power of the signal, which means that the importance of the 40 Hz frequency is $10^{\frac{-15}{10}} =$

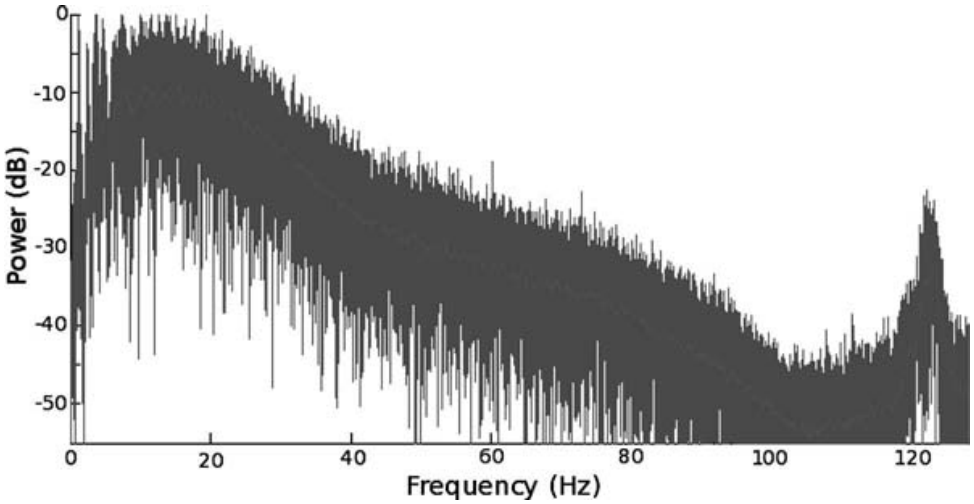

Figure 7.2. Power spectrum of ECG signal. The peak at 120 Hz is a harmonic of the 60 Hz power-line interference. See also Color Insert.

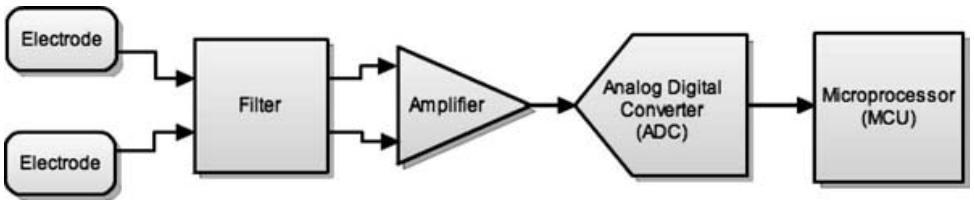

Figure 7.3. Biopotential signal transduction pathway

3.1% that of the dominant frequency. The importance continues to drop down to -40 dB, or $10^{\frac{-40}{10}} = 0.01\%$. Depending on the application, this data can help determine what range of frequencies are of interest.

7.3.2 *Measuring Surface Biopotentials*

There are a number of sensing modalities that are based on detecting and amplifying biopotentials from the skin. These include the electromyogram (EMG) for detecting the activity of muscle fibers, the electrocardiogram (ECG) for detecting the electrical activity of the heart, the electroencephalogram (EEG) for detecting the electrical activity of the brain, the electroretinogram (ERG) for measuring the activity associated with eye movement, among others. All these modalities operate under the same basic mechanism (Fig. 7.3).

7.3.2.1 The electrode

The first site of signal transduction occurs at the skin-electrode interface, where ionic potentials are converted into electrical potentials through reduction/oxidation reactions that follow the basic form

$$C \rightleftharpoons C^{n+} + ne^{-} \tag{7.1}$$

$$A^{m-} \rightleftharpoons A + me^{-} \tag{7.2}$$

where C and A represent the cation and the anion, respectively, and m and n represent their respective valencies. These reactions are reversible for most electrode/electrolyte combinations, but not all. As a result, it is wise to not be too creative with electrode

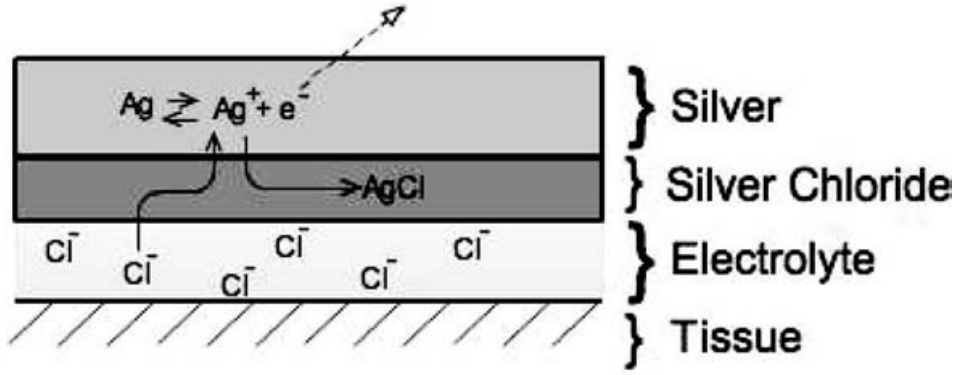

Figure 7.4. Silver-silver chloride electrode redox reaction.

choices. There are many electrode/electrolyte combinations that have various advantages and disadvantages, but we will focus on the most commonly used one: the silver-silver chloride (Ag-AgCl) electrode. Among other benefits, the electrode chemistry will help minimize the effects of motion artifacts [14].

The Ag-AgCl electrode consists of a layer of silver surrounded by a very thin layer of silver chloride. A gel containing a high concentration of Cl^- ions and saturated with AgCl is often used in conjunction with the Ag-AgCl electrodes (Fig. 7.4).

The interface of the Ag-AgCl electrode, the electrolyte, and the skin form a equilibrium, which is governed by the following equations:

$$Ag \rightleftharpoons Ag^+ + e^- \tag{7.3}$$

$$Ag^+ + Cl^- \rightleftharpoons AgCl \tag{7.4}$$

Metallic sliver will give up electrons and spontaneously combine with free chloride ions to form silver chloride, which due to its limited solubility, will precipitate out of solution adding to the silver chloride layer. These reactions occur constantly and reversibly, but the concentrations of the various constituents remain the same averaged over time resulting in no net current. However, if the potential of the tissue at the location of the electrode changes, then the reactions will be driven in one direction or another causing a net flow of electrons into or out of the electrode, which can be measured.

It is also possible to measure the electrical potential differences using capacitative electrodes that do not have a galvanic connection [15]. These electrodes can be fabricated with a thin layer of nonconducting dielectric material and offer benefits, including being able to sense potential differences though clothes, but suffer from a very high sensitivity to external noise and an attenuation in the low-frequency components of the signal.

7.3.2.2 Filtering

As mentioned in Section 7.3.1, different biological processes exhibit electrical activity at different frequencies, and should be filtered accordingly. Beyond filtering for unwanted noise, a low-pass filter is always required to avoid aliasing, while a high-pass filter is required to bias the signal. Furthermore, it is always a wise idea to add an RFI filter [16] to prevent output offset errors due to RF rectification inside the amplifier.

7.3.2.3 Amplifier

Picking an optimal operational amplifier (OpAmp) for the application is a critical step in the design in a biopotential measurement device. Care must be taken that the amplifier does not contribute additional noise to the system, that its input impedance is sufficiently greater than the source impedance of the signal to prevent distorting the signal, and that it can provide sufficient gain at the frequencies of interest. A number of other issues exist, such as verifying that the amplifier is able to operate at the supply voltage of the PCB or that the quiescent current consumption is sufficiently low, but these issues are more obvious and do not require as much attention.

As most biosignals are based on the difference in potential from two different sites, the use of an instrumentation amplifier (InAmp) is highly recommended. An InAmp is designed to provide balanced, high input-impedance (typically 10^9 Ω) inputs with low bias currents, and a low impedance output with low DC-offset error. An InAmp can be constructed with two or three OpAmps; however, using a monolithic single-package InAmp has the advantage of

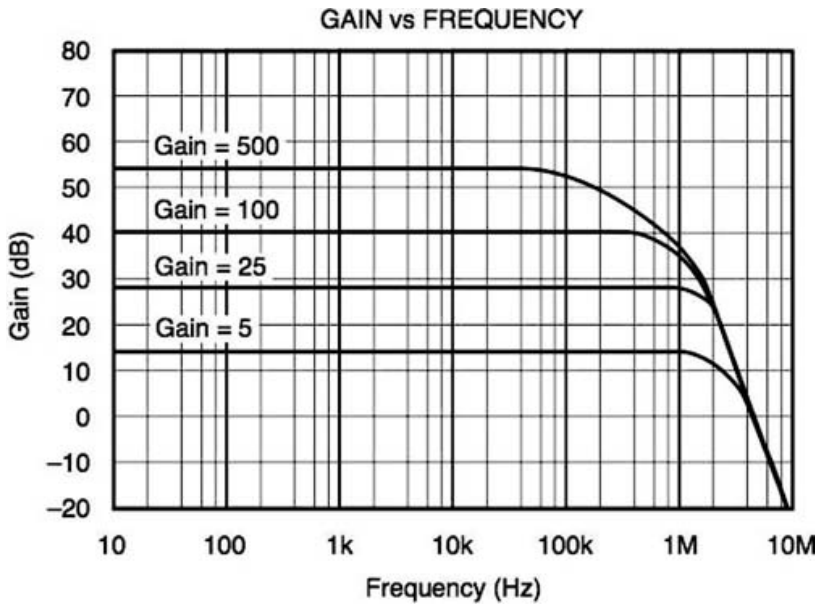

Figure 7.5. Texas Instruments INA331 Instrumentation Amplifier Gain-Frequency Bode Plot.

having highly matching passive components that are often trimmed to provide lower errors and very high common-mode rejection. Additionally, a monolithic InAmp will use less PCB space to help reduce the WBAN size. There are a number of free online references that help explain OpAmps [17] and InAmps [18].

The first step in picking the right amplifier is to see if it's able to provide a flat gain response over the range of frequencies of interest (Section 7.3.1) by examining the Bode plot, or the gain-frequency response of the amplifier on a log-log plot (Fig. 7.5).

Although most passive components can generate noise, referred to as thermal noise, the noise from active components (i.e., OpAmps/InAmps, transistors, etc.) usually dominates the signal. There are a number of noise sources in OpAmps and InAmps, but the main ones to be concerned with are input bias currents and input-referenced voltage noise. For biopotentials, the source impedance is often very high (upward of 10^5 Ω), where the bias-current noise will dominate. Only by understanding the characteristics of the signal requiring amplification can you determine what amplifier requirements exist for your implementation.

7.3.2.4 Analog Digital Converter and Microcontroller

The number of low power microcontrollers (MCU) is ever increasing with certain applications allowing a device to remain operational for years with a single battery. Most contemporary MCUs include ADC and digital to analog converter (DAC), which greatly simplify the design; however, do not feel restricted to using the provided peripherals if they do not satisfy your design requirements.

For the design of the Berkeley Tricorder, we required an MCU that provided us with multiple fast, high-precision ADC inputs for data acquisition as well as a DAC for our SpO_2 implementation. We needed multiple serial (UART, SPI, I^2C) interfaces, a DSP for digital filtering, and low power consumption for extended battery life. We found the Texas Instruments MSP430 MCU a perfect fit for our needs. Our current design utilizes the MSP430F2618, which is fast (16 Mhz), and has large RAM (8 kb). The built-in ADC is capable of 200 k samples per second with a 12-bit resolution and is multiplexed across eight channels.

7.3.3 *Electrocardiograph*

The electrocardiograph is a device that measures the electrical activity of the heart. The heart can be thought of as four distinct pumps, which are synchronized to beat in a specific order. Blood from the body first fills the right atrium, which is essentially a low-pressure pump that fills the right ventricle. The right ventricle is a higher pressure pump that pumps blood into the lungs. When blood returns from the lungs, it similarly fills the left atrium, which fills the left ventricle whose job is to pump blood at high pressure throughout the body.

The timing of these pumps is coordinated by means of the heart tissue itself. A region known as the sino-atrial node, known as the pacemake of the heart, initiates an electrical depolarization that causes muscle tissue nearby to start contracting. A healthy heart is able to direct the wave of electrical depolarization in such a way to cause a highly orchestrated series of contractions resulting in a synchronized pumping action.

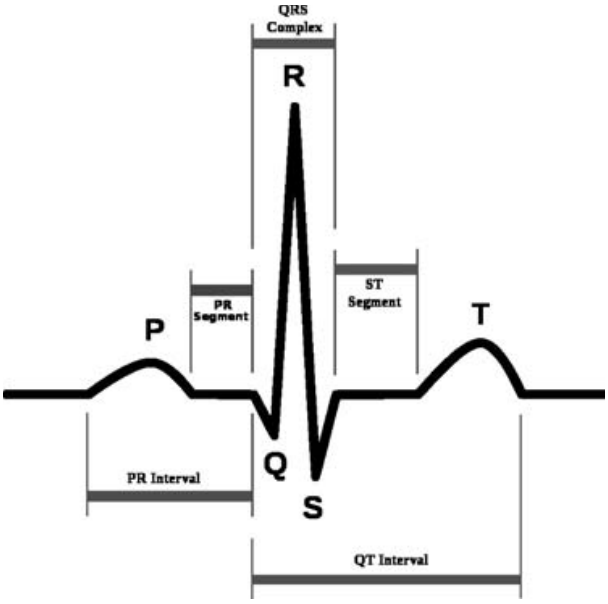

Figure 7.6. ECG waveform. See also Color Insert.

When the heart initiates a contraction, a potential difference forms between different regions of the heart and follows the wave of depolarization as it progresses though the heart. The potential difference can be treated like a dipole that moves through a volume conductor, generating potential differences on the surface of the body. This potential difference is what the ECG detects, and the placement of the electrodes provides different views of the heart's electrical activity (Fig. 7.6).

A damaged heart, as is the case after a heart attack, can result in problems with the propagation of the wave of electrical depolarization resulting in a number of chronic conditions. By utilizing an ECG to detect how the electrical activity of a heart has been altered, a cardiologist can determine how the heart has been damaged.

There are many additional uses for an ECG. The simplest use is to measure the heart rate, which is performed by measuring the main left-ventricular contraction, which appears as the strong positive deflection known the R-peak.

ECGs are described by either the number of channels or the number of electrodes. A channel refers to the number of different differential pairs, whereas the number of electrodes simply refers

to the number of electrodes. The same electrode can be used as a reference for multiple differential pairs, but when people speak about 5- or 12-electrode ECGs, standard known configurations are used. At a minimum, two electrodes are required to generate an ECG trace, but 3-electrode, 5-electrode, and 12-electrode configurations can provide additional views of the heart's electrical activity to aid in monitoring and diagnosis. In this section, we will detail the implementation of a single-channel ECG, which can be extrapolated out to configurations requiring additional channels.

The range of frequencies of interest for an ECG depends on the application. Often, the distinction is made between monitoring-ECG and diagnostic-ECG. Monitoring-ECG is used for routine examination of the ECG waveform, and is more heavily filtered to remove noise artifacts with a pass-band of 0.5 Hz to 40 Hz. Diagnostic-ECG is filtered less to provide a more detailed waveform for diagnosing cardiac problems, and typically ranges from 0.05–150 Hz. You can see the relative contributions at the various frequencies in the power spectrum in Fig. 7.2. The peak at 120 Hz results from the first harmonic of the 60 Hz power-line noise; the 60 Hz peak is not noticeable due to the high signal-to-noise ratio at that frequency.

The heart is a large muscle capable of generating a strong signal on the surface of the skin, in the range of several millivolts in amplitude, which makes it a fairly easy signal to detect. For a two-electrode configuration, placing an electrode on either side of the chest will work; however, it will be useful to understand the logic behind some standard ECG configurations in determining where to place the electrodes.

The first electrode configuration proposed was by Einthoven (Fig. 7.7), and uses two channels and three electrodes. The electrodes are placed on the left arm, right arm, and the left leg, and forms a triangle with the heart in the center. The differential voltage between any two electrode locations defines a view from the lead defined by electrodes, denoted as I, II, and III. Given the symmetry of the triangle, only two differential pairs are required to be measured, and the third lead can be determined from the sum or difference of the two differential measurements [19]. For example, if both positive electrodes are placed on the right foot (V_F), and the negative lead from one channel is placed on the left arm (V_L) and the

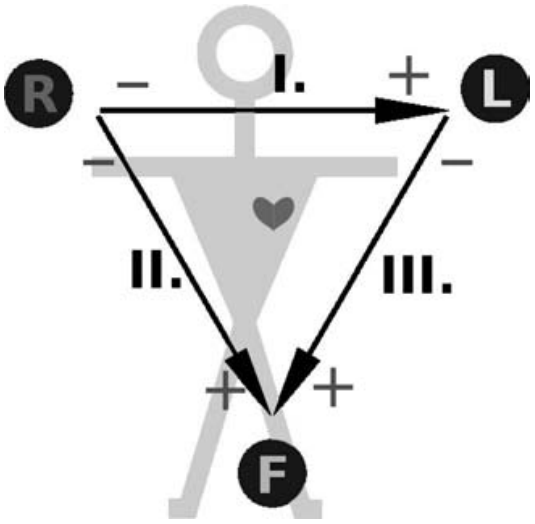

Figure 7.7. Einthoven ECG lead locations (from wikiCommons). See also Color Insert.

other is placed on the right arm (V_R), then you have the following relationships:

$$V_{\text{II}} = V_F - V_R \tag{7.5}$$

$$V_{\text{III}} = V_F - V_L \tag{7.6}$$

It can then be shown that the difference of equation 7.6 from 7.5 will yield V_I.

$$V_{\text{II}} - V_{\text{III}} = (V_F - V_R) - (V_F - V_L)$$

$$V_{\text{II}} - V_{\text{III}} = V_L - V_R = V_{\text{I}} \tag{7.7}$$

There are a number of other electrode configurations worth considering [20–22], but it's important to note that differential surface potentials can be arithmetically combined to form different electrical views as long as more than one channel is being used.

If the electrodes are close to any other large muscles, such as the pectorals, then they can also pick up the electrical activity associated with the muscle activity. It is possible to build a device known as an electromyogram (EMG) to measure the activity of arbitrary muscles, which will be discussed in Section 7.3.4.

After deciding where the electrode, are to be placed, leads must be attached connecting the electrodes to the amplification circuitry. The leads should be kept as close to one another, and ideally

be twisted together to prevent picking up electromagnetic noise differentially. The instrumentation amplifier can do a very good job of rejecting common-mode noise, which appears on both wires; however, the further the wires are from each other, the greater the probability that noise can be coupled onto just one wire, which will show up as a differential signal and amplified by the InAmp.

7.3.3.1 Berkeley Tricorder

The Berkeley Tricorder was designed to have a monitoring-ECG rather than a diagnostic-ECG as our use-case required any detected abnormalities to be escalated to a cardiologist for a workup. The design utilizes a second-order high-pass filter biased at the mid-supply voltage followed by radio-frequency interference filter and an instrumentation amplifier with a gain of 1000. A second-order high pass filter was required to minimize the DC bias drift resulting from motion artifacts while maintaining a low -3 dB corner frequency (0.79 Hz). A low-pass filter was not required as the instrumentation amplifier has a natural roll-off starting at 200 Hz at a gain of 1000. Although this frequency is higher than required, it simplified the design to use the built-in low-pass filter than to add an additional one.

The output of the instrumentation amplifier is biased to mid-rail $\left(\frac{3.3\text{ V}}{2} = 1.65\text{ V}\right)$, and the ADC has a positive/negative reference voltage of 3.3V/0V, respectively. Thus, the output of the amplifier can swing ± 1.65 V before saturating. For a gain of 1000, this translates to an input voltage of $\left(\frac{\pm 1.65\text{ V}}{1000} = \pm 1.65\text{ mV}\right)$ from the skin surface potential.

7.3.4 *Electromyogram*

The focus of this section will be on surface EMG measurements. Although transcutaneous ("needle") EMG electrodes are useful for a number of applications [23], it is not likely that a WBAN implementation will have this requirement and the safety concerns associated with placing electrodes under the skin is beyond the scope of this chapter.

A lot of the same methodologies apply to EMG as it does to ECG, after all, the ECG is a specialized case where the electrical activity of the myocardium is being measured. As with the ECG, the EMG measures surface potentials generated by muscle fibers during contraction. There are a large number of muscles that can be measured, all with different applications ranging from kinesiology studies [25] of motion to stress detection [26].

Unlike ECG, the EMG signal has higher frequency components as noted in its power spectrum (Fig. 7.8) and thus require high sampling rates. It is typically accepted that the EMG signal has a bandwidth of 500 Hz, thus minimum a sampling rate of 1 kHz is typically used due the Nyquist sampling theorem. Given the shape of the power spectrum, a bandpass filter between 5–10 Hz and 500 Hz is typical. The band-pass filter is created by placing a low-pass filter of 500 Hz in series with a high-pass filter at 5–10 Hz. However, if only the envelope of the signal is required, rather than the individual peaks, the signal can be rectified, low-pass filtered at 50 Hz, and sampled at 100 Hz [27] (Fig. 7.9). EMG surface potentials can range from 0–6 mV peak to peak, depending on the muscle being

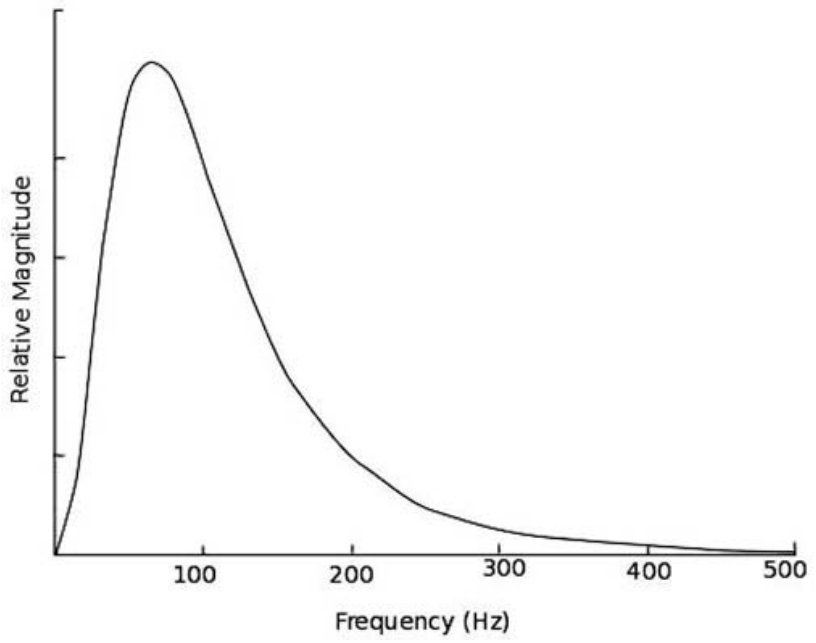

Figure 7.8. EMG power spectrum (redrawn from [24]).

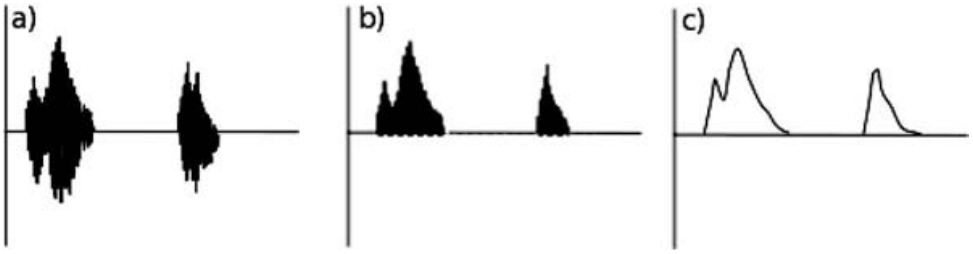

Figure 7.9. (a) Raw EMG signal, (b) rectified EMG signal, (c) low pass filtered.

investigated. Hence, the amplifier should provide sufficient gain to utilize the full dynamic range of the ADC without saturating.

For a more detailed examination of the requirements associated with EMG measurements, the reader is directed to reference [24].

7.3.4.1 The Berkeley Tricorder

Our initial interest in an EMG sensor was to measure back tension by measuring muscle activity as a proxy for stress. For this, we did not require a very fast input stage and reused the bulk of the ECG design. Given that the bandwidth of the EMG signal is in the range of 20–500 Hz, we could be more aggressive with the HPF. A single stage with a a -3 dB of 7.9 Hz was chosen and found to be effective. The amplifier we chose demonstrates a gain roll-off starting at 300 Hz, and allows us to sample the signal at a slower rate. This is sufficient to measure a general level of muscle activity. However, for a more diagnostically relevant EMG implementation, we are considering migrating to a faster amplifier and higher sample rates.

7.3.5 *Pulse Oximetry (SpO_2)*

Blood oxygenation is a critical parameter that can help diagnose conditions of pulmonary distress, hypovolemia [28], vascular perfusion, among other. Blood oxygenation has a secondary benefit in that it can be used to compute pulse transit time (PTT), or the amount of time between the ejection of blood from the heart to the pulse arrival time at a peripheral location. It has been shown that there is a direct correlation between PTT and arterial blood pressure [29].

Pulse oximetry is a method by which the variation in the absorption of light by tissue is used to determine the percentage saturation of blood hemoglobin by oxygen. The modern technique was invented by Takuo Aoyagi, and works based on the following two principles. The first involves the macromolecule responsible for oxygen transport, hemoglobin. The iron containing macromolecule found inside blood cells binds to oxygen molecules and helps transport them at much higher concentrations than possible with freely dissolved oxygen in the blood. Deoxygenated hemoglobin (Hb) absorbs red light more than oxygenated hemoglobin (HbO_2), giving HbO_2 a brighter red color. The opposite is true for infrared light, where HbO_2 absorbs infrared light more than Hb (Fig. 7.10). This means that by measuring the ratio of absorption of red versus infrared light, the percentage oxygenation of the hemoglobin can be determined in samples of blood. However, there are many other types of tissues found in the body that also absorb varying levels of red and infrared light, so the simple technique cannot be applied to blood in the body.

The second principle, which was the key to Takuo's discovery, was that it is possible to measure the variation in amplitude of light being absorbed due to the pulsatile nature of blood. As the

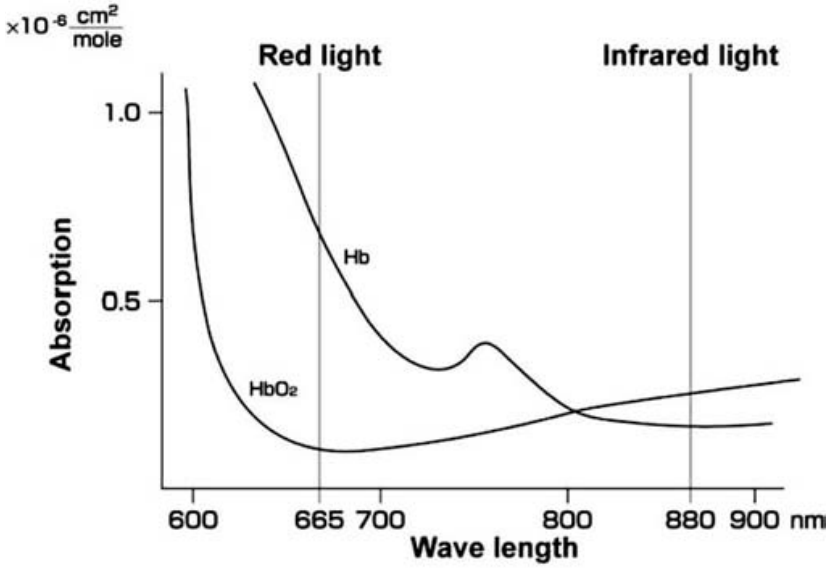

Figure 7.10. Hemoglobin light absorption curves.

heart beats, a pressure wave travels through the arteries to the capillaries, which change in volume as they fill and empty with blood. By examining the ratio of absorption for just the pulsatile portion of the signal, you are able to compare red and infrared light absorption by the portion of blood that is changing, allowing for a direct measurement of a component of blood rather than that of any other tissue components.

The implementation of this technique is simple: measure the ratio of the pulsatile portion of red to infrared light as it passes and is absorbed by tissue, multiplied by a calibration value. Both these steps are performed by shining alternating red and infrared light from closely mounted (ideally on the same die) LEDs through tissue (i.e., finger, ear) and measure intensity of transmitted light by a PIN photodiode. A PIN photodiode is sensitive light detector. The resulting waveform will resemble Fig. 7.11. Next, in software, the amplitude of the waveform is measured for both light frequencies (AC_{RED}, AC_{IR}) as well as the DC bias of the waveforms (DC_{RED}, DC_{IR}). The ratio $\frac{AC_{RED}}{AC_{IR}}$ needs to be corrected for variations in light intensity from the differed LEDs, the difference in absorption of the different frequencies of light by the tissue, as well as the varying sensitivity of the photodiode to the different frequencies of light. The ratio of DC biases $\left(\frac{DC_{IR}}{DC_{RED}}\right)$ takes into account all of these variables,

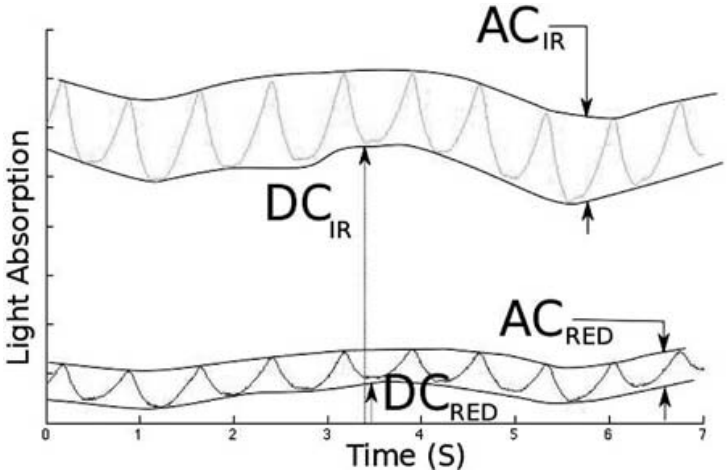

Figure 7.11. Light absorption through tissue by infrared (top curve) and red (bottom curve) light.

and the product of the $\frac{AC_{RED}}{AC_{IR}}$ and the correction factor $\frac{DC_{IR}}{DC_{RED}}$ will result in a ratio $\left(R = \frac{DC_{IR}}{DC_{RED}}\frac{AC_{RED}}{AC_{IR}}\right)$ which directly corresponds to the percentage saturation of hemoglobin by oxygen (SpO_2).

Note that most literature defines R as $\frac{\log_{10}\left(\frac{AC_{RED}}{DC_{RED}}\right)}{\log_{10}\left(\frac{AC_{IR}}{DC_{IR}}\right)}$. However, as the ratio R is an arbitrary number used in conjunction with an empirically derived mapping, there is no need to take the logarithms. This simplified explanation of the process does not explain the underlying theory; for more information, the reader is directed to reference [30].

As contemporary amplifiers are very fast compared to the rate of the heart beat, it is possible to only have the LEDs on for a very short period of time, take a measurement, then shut off the LEDs to conserve power for some period of time. An additional light intensity measurement should be taken while the LEDs are off in order to subtract out any background light from both the infrared and red light signals. The duration of the LEDs on time to the off time is referred to as the duty cycle, and the lower the duty cycle, the less power the circuit consumes, which is an important consideration for a battery-powered device.

Although a theoretical correlation between R and the percentage SpO_2 exists, sufficient deviation exists to necessitate use of an empirically derived mapping of R and percentage SpO_2. The empirical mapping is made by simultaneous measurements of R through pulse oximetry and blood oxygen though samples drawn from a subject while the subject is being deprived oxygen. Based on these measurements, a conversion factor that maps R values to SpO_2 percentages can be determined, which is valid for the device and LED/photodiode configuration. A new empirically derived mapping will have to be made if the circuit or any of the components change. Also, the mapping is only valid down to approximately 80% blood saturation as depriving oxygen to the test subjects below that point is dangerous. This is the case with all commercially available monitors. However, given that there are number of commercially available and calibrated pulse oximeters, it is sufficient to use one of these devices to derive an R-SpO_2 mapping, rather than drawing and analyzing blood from test subjects.

The description thus far has been for a transmissive pulse oximeter that works by measuring the levels of light absorbed by blood as light passes through tissue. There exists another type referred to as a reflective pulse oximeter that works by measuring the levels of light absorbed by blood as the light travels through tissue and backscatters back to the same side of the tissue where the LEDs are. The most prominent placement for such a sensor is the forehead, but other locations have also been evaluated in reference [31].

There are a number of tradeoffs that should be considered early in the design process:

- The SNR is proportional to the volume of blood in the tissue being measured, thus; tissues that suffer from poor blood flow or vasoconstriction due to cold temperatures will result in a poor signal.
- The greater the SNR, the further the LEDs and photodiode are from each other, as the light travels through and is affected by more tissue, but additional LED current is required (and LEDs that can handle higher currents) which decreases battery life.
- The faster the amplifier and ADC circuitry, the shorter the duty cycle of the LEDs, which results in lower power consumption at the expense of additional noise due to higher cutoff frequency for the low-pass filters

There are many different SpO_2 circuit implemetnations, such as this one by Texas Instruments [32]. However, the basic building blocks consist of noise-free current source to drive either a RED or IR LED, a PIN photodiode to pick up the light transmitted, a transimpedance amplifier to convert the current from the photodiode to a voltage, and a DC subtraction and amplification stage to remove the DC bias and further amplify the signal.

7.3.5.1 The Berkeley Tricorder

In order to derive blood oxygen saturation, determine pulse arrival time, and keep costs low, we needed to record the SpO_2 waveform rather than to use an OEM device, which only computes the oxygen

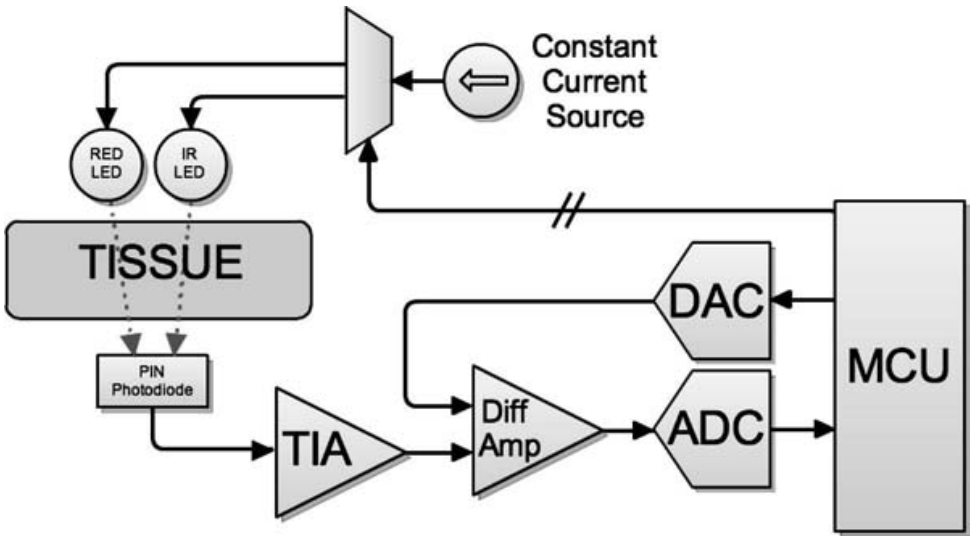

Figure 7.12. Block diagram of pulse oximeter.

saturation percentage. Being able to visually inspect the SpO_2 waveform is also important to the physician as a figure of merit for the SpO_2 calculation. Poor perfusion or poor SpO_2 placement can lead to erroneous oxygenation.

Our design (Fig. 7.12) called for a circuit capable of illuminating one of the two LEDs with a constant current and measuring the amount of light picked up from a nearby PIN photodiode. We decided to do our initial development and testing using a commercial reflective SpO_2 sensor manufactured by Nellcor (Max-Fast, Nellcor/Tyco, Pleasanton, CA). Nellcor produces a series of disposable and reusable sensors, which utilize a DB-9 connector with identical pinouts allowing for the ability to quickly test different devices and configurations.

The output stage of our device consists of a constant-current H-Bridge LED driver. The LEDs on the Nellcor sensor have their anode and cathodes connected. By driving one side high and the other low, one can choose which LED to illuminate. It is critical to drive the LEDs at a constant current to avoid coupling supply noise onto the received signal.

The input stage consists of a transimpedance amplifier (TIA) connected to a PIN photodiode in the sensor followed by a differential amplifier used to subtract out the dc-offset of the signal

and add additional gain. The offset subtraction signal is generated from the MSP430's on-board DAC. A feedback loop keeps the SpO_2 signal from saturating by adjusting the DAC output. The DAC value is also stored and used for the blood oxygenation computation.

The system also measures background levels by repeating the measurements with both LEDs are turned off. These values are also used in the blood oxygenation calculation. All the data is then stored and/or transmitted for further processing to extract the relevant features.

7.3.6 *Respiration*

Monitoring respiration is important in a large number of cases. It's critical to monitor respiration in patients with cardiopulmonary issues such as congestive heart failure and patients who are on medication that suppresses breathing. It's also useful in diagnosing a number of conditions such as systemic inflammatory response syndrome (SIRS).

7.3.6.1 The Berkeley Tricorder

Our original attempt at respiration rate detection relied on acoustic pickup with a microphone, but we found bioimpedance to be a much more reliable indicator of respiration rate. Bioimpedance also allows us to measure relative breathing tidal volumes and to detect coughs. Bioimpedance can also be used for a number of other diagnostic measurements beyond respiration such as measuring cardiac output [33] and body fat [34], although we have not investigated these applications.

A high frequency sinusoidal signal (50 kHz) is used so that the effects of the skin impedance are minimized through capacitative coupling. We chose a 350 μA current at 50 kHz in order to provide us with a good signal, while being significantly lower than the maximum safe current as defined by IEC60601-1-2005. Using a pair of electrodes connected to a high impedance differential amplifier, we can accurately measure the voltage difference between the electrodes, which is directly related to the impedance between those points.

We originally planned on building a fully analog impedance measurement system; however, we were able to significantly reduce the system complexity by utilizing Analog Device's AD5933 impedance analysis IC. The AD5933 has previously been shown effective in bioimpedance measurements [35]. Our output stage consisted of a voltage-to-current circuit followed by a 3.3 nF DC blocking capacitor. The input stage utilizes the ECG electrodes, passes the signal through an RFI filter to a programmable differential amplifier which feeds the amplified signal back to the AD5933. Although the AD5933 should be very effective at filtering out any high-frequency noise, we felt it would be prudent to add an RFI filter to the input stage — given its importance in ECG measurements. The IC then computes the real and imaginary components of the signal, which we convert to a magnitude and phase. The magnitude of the impedance is proportional to the chest volume, and breathing can easily be seen as a variation of the impedance (Fig. 7.15, bottom trace). From this signal, we can determine respiration rate and approximate tidal volume.

7.3.7 *Accelerometry*

Most health monitors incorporate an accelerometer. With this, one can determine body orientation, activity levels, and perform fall detection. With additional processing, it is possible to deduce what activity the subject is engaded in [36, 37–39]. Furthermore, it is very easy to implement — hence its prevalence.

7.3.7.1 The Berkeley Tricorder

Our first implementation utilized a 3-axis analog accelerometer, which was connected to the MSP430 by means of three analog input lines. Although this approach worked well, it used too many ADC channels of the MSP430. We later switched to the LIS302DL manufactured by STmicroelectronics. Not only does it provide a digital serial interface, but it also has built-in hardware fall detection. Although initially designed to detect the fall of a portable electronic device, the IC can be used to detect if the patient falls down without taxing the microcontroller.

7.4 Wireless Interface

The number of wireless options is ever changing and evolving with no clear dominant player at this point. One must consider all the requirements based on the end application to determine the right technology. Issues to consider include transmission range, data rate, interoperability, and operating frequency. It is also insufficient to simply present a table with the comparison of the various features as many of the values will differ based on the manufacturer and operating environment.

We will discuss the requirements for the Berkeley Tricorder and the rational behind the choice of its wireless technology, followed by a discussion on some of the issues that are important to consider in making a decision for the wireless data link. Additionally, Table 7.2 at the end of this section provides a general summary for a number of wireless technologies. The complied data should not be considered concrete as there are many different implementations of the various technologies that it should only be considered a starting point.

7.4.1 *The Berkeley Tricorder*

Telemetry is an important requirement for a medical device as it provides a means for the diagnostic data to be viewed in real-time, or to be transmitted to caregiver or a more powerful system to perform computational analysis of the data. We chose Bluetooth to satisfy our telemetry needs for a number of reasons.

Table 7.2. Comparison of wireless technology standards

	ZigBee	Bluetooth	ANT	Wi-Fi	Wi-Fi
IEEE Standard	802.15.4	802.15.1	Propriatary	802.11b	802.11g
Frequency	868 Mhz/915 Mhz/ 2.4 Ghz	2.4 Ghz	2.4 Ghz	2.4 Ghz	2.4 Ghz
Max Rate Over Air	20/40/250 Kbps	1−24 Mbps	1 Mbps	11 Mbps	54 Mbps
Max Achievable Rate	10/20/125 Kbps	–	20 Kbps	6.3 Mbps	31.4 Mbps
Range (meters)	10−75 (1500 for Pro)	1−100	10	10−100	10−100
Current (mA)	1−50	1−35	1−22	100−350	100−350

- High level of penetration in consumer devices such as cell phones and laptops.
- Standardized profiles (serial, audio, object transfer, dial-up networking, etc) requiring no additional development effort.
- High-speed wireless (v1.2 Bluetooth is rated at 1 Mbit/s).
- Lower power consumption per bit than competing devices.
- Single IC implementation.
- Multiple built-in interfaces peripherals to help simplify device design such as an ADC/DAC/USB interface

Rather than using a monolithic serial to Bluetooth module, we have incorporated the CSR plug'n'go BlueCore3 chipset directly. Not only does this give us full access to many peripheral interfaces, but it also significantly reduces the device cost. The BlueCore3 IC provides audio input/output, a USB interface, 16 general-purpose I/O lines, which can be used for I^2C or SPI communication, ADC, DAC, and a serial interface. The firmware can be configured to provide many different profiles including object exchange (OBEX) to facilitate bulk data transfer, and more importantly, dial-up networking (DUN) to allow telemetry without the need for any custom phone software. Our current implementation utilizes Bluetooth as a serial device and interfaces with the MSP430 at up to 1 Mbps.

7.4.2 *Power Consumption*

Of primary importance to many WBAN projects is the power consumption of the wireless data link, which in most cases is the dominant power consumer for the device. As we stated earlier, it's almost impossible to put together a table that's capable of comparing, apples to apples, the power consumption of the various radio technologies. This is because it's impossible to separate the radio technology from an implementation of that technology. Consider a radio transceiver that generates the RF signal. There are many transceivers to choose from which all have different power consumption characteristics, even if they operate at the same frequency, have identical output power, and modulation. For example, both Texas Instruments CC2500 IC and Nordic

Semiconductor's nRF2401A IC operate at 2.4 Ghz and can support Gaussian Frequency-Shift Keying (GFSK) modulation, which is used for Bluetooth. However, the nRF2401A datasheet specifies 13 mA at 0 dBm (1 mW) output power while the CC2500 specifies 21.2 mA. Even this comparison is unfair as there are many other differences between the feature set of the components, but it demonstrate the difficulty in comparing power consumption between technologies.

Newer implementations of a protocol can vary the power consumption of a device — depending on the feature set. For example, Bluetooth version 4.0 defines Bluetooth low energy technology, which trades off bandwidth for a decrease in power consumption (50% to 99% reduction based on use case) while doubling the maximum range.

The duty cycle of the radio will have a huge impact in regards to power consumption. If your wireless technology allows for a maximum bandwidth of 1 Mbps, but your application only requires a 10 Kbps stream to be transmitted, then you should be able to shut down the radio 99% of the time to save on power consumption. This is just a very rough approximation, and it's never so so clear cut. There is additional time required for the radio to exit low power, it needs to power on at regular intervals to see if some other transmitter is sending it data, it needs to deal with the protocol overhead, and if there is a problem with the data link, then the radio will need to retransmit data.

7.4.3 *Data Range and Transmit Power*

The range of a wireless data link is dependent on the power of the transmitter, the quality and orientation of the antennas (TX & RX), the frequency of the transmitter, and the surrounding material. Let's first discuss how the power from the radio is sent to the antenna, through space, and to the receiver and the various points of power loss along the path.

The transmit power plays a very large role in the range of a wireless link, and how much of this signal makes it to the receiver will determine the range of the link. RF power is measured in dBm which decibel value in reference to 1 mW of transmit power, and is

defined as

$$P = \frac{10^{(x/10)}}{1000} \tag{7.8}$$

where P is the transmit power in watts and x is the dBm. Note that 0 dBm is equal to 1 mW, and the power doubles for every 3 dBm, or is halved for every -3 dBm. The RF transceiver will generate this power, and it will be sent to an antenna; however, impedance mismatches between the transmitter, the PCB trace(s) (or coax cable(s)), and the antenna can reduce the amount of transmitted power.

The type of antenna and its radiation pattern will also play a role in how efficiently the power is transmitted. The simplest antenna is formed on the PCB by a specially designed trace pattern. These are the simplest and cheapest solutions, but not necessarily the best. The use of a chip antenna is a good compromise with generally improved performance while utilizing minimal board space at a low cost.

The radiation pattern of the antenna determines how the antenna can focus energy in a particular direction. The ability of an antenna to direct its energy is measured in dBi, or the decibels of radiated power for a particular radiation geometry as compared to an isotropic antenna, which radiates equally in all directions. Antennas exist that can focus the transmission energy giving significant gain in one orientation, but at the expense of being significantly weaker in other orientations. If the body-worn RF device is to be consistently oriented in reference to a remote receiver, then the transmit range can be extended by using a directional antenna with a high dBi. However, for most applications, the relative antenna orientations cannot be guaranteed and thus an omnidirectional antenna will be preferred to maximize transmit power independent of the subject's orientation.

Once the RF power hits the antenna and is transmitted in free space, the RF energy degrades with the square of the distance between the transmitter and receiver. Furthermore, the ability for the receiving antenna to pick up a signal also degrades with the square of the frequency. The loss attributed to these two factors determines the free-space path loss (FSPL) and is defined as the ratio of transmit power (P_t) to receive power (P_r). For an isotropic

antenna,

$$P_t = 4\pi d^2 S \tag{7.9}$$

and

$$P_r = \frac{S\lambda^2}{4\pi} \tag{7.10}$$

where S is power per unit area, λ is the wavelength, and d is the distance between the transmitter and receiver. Considering the ratio of Eqs. 7.9 and 7.10

$$FSPL = \frac{P_t}{P_r} = \frac{4\pi S d^2}{S\lambda^2/4\pi} = 16\pi^2 \frac{d^2}{\lambda^2} = \left(4\pi \frac{d}{\lambda}\right)^2$$

Substituting in $\lambda = c/f$, where f is the frequency and c is the speed of light,

$$FSPL = \left(\frac{4\pi}{c} df\right)^2 \tag{7.11}$$

Expressed in dB,

$$FSPL(dB) = 10 \log \left(\frac{4\pi}{c} df\right)^2 \tag{7.12}$$

For a 2.4 Ghz transmitter with a receiver 10 m away, the free space path loss will be in the order of $10 \log((4\pi/3 \times 10^8)(10 \times 2.4 \times 10^9)) \approx 30$ dB.

However, the losses will be greatly increased if there is no clear line of sight between the transmitter and receiver. This loss is dependent on both the frequency as well as the blocking material, such as the building walls or the human body. Consider 2.4 Ghz radiation — it is used by microwave ovens to heat water in foods. Likewise, given that the human body consists mostly of water, the energy of a 2.4 Ghz RF link (about 1,000,000 weaker than a microwave) is absorbed and heavily attenuated by the human body. This is a huge problem with many of the technologies that operate at 2.4 Ghz, such as certain ZigBee and Wi-Fi implementations, and Bluetooth. If the body-worn device is on the front of the subject's chest, and the receiver unit is located behind the subject, severe signal degradation will occur.

7.4.4 *Data Rate*

The maximum data rate is determined by the operating frequency and the modulation technique of the technology in question. This (often sited) theoretic upper limit does not include the protocol overhead and assumes a high quality RF link. One should consider the maximum required data rate for the application at hand, determine the location of any bottlenecks in the system, and verify that the chosen technology can satisfy that data link given real values, not the ones found in datasheets.

For example, consider the case of two ZigBee-based sensors, each sampling with a resolution of 12 bits at 4,000 samples per second (sps) with the data being received by a PDA mounted with a ZigBee receiver. If every sample is to be sent as a 16-bit word, then each sensor will generate 64,000 bits per second of data (bps). This means that the receiver must be able to handle 128 Kbps. ZigBee is rated to handle 250 Kbps according to the spec sheet, but this doesn't include all the protocol overheads or any retransmissions due to loss. A good rule of thumb for ZigBee is that you should expect about half specified transmission rate with a good data link, or 125 Kbps. In this case, a reduction in the sampling rate or some other technique to lower the data rate would be required — or using a different technology that can handle the higher data rates.

7.4.5 *Human Safety*

As discussed in Section 7.4.3, the human body is capable of absorbing RF energy and converting it to heat. Although a radio transmitter is orders of magnitude less powerful than a microwave oven, it is important to consider how the energy can affect the body or implants such as pacemakers, and so as to minimize any potential health hazards. There are a number of different regulatory bodies that have established safety guidelines for the use of RF transmitters that should be referenced. In the United States, the FCC guidelines were derived from the recommendations of the National Council on Radiation Protection and Measurements (NCRP) and the Institute of Electrical and Electronics Engineers (IEEE). Many European countries use the guidelines established by the

International Commission on Non-Ionizing Radiation Protection (ICNIRP). The NCRP, IEEE, and ICNIRP guidelines specify different permissible energy levels based on the frequency and on whether part of the body or the whole body is exposed.

The FCC's guidelines can be found in OET bulletins 56 [3] and 65[4], and are highly recommended readings. As far as RF emissions are concerned, the FCC differentiates between whole-body exposure from partial-body exposure from a smaller device, such as a cellphone or WBAN device. The FCC limits for partial-body exposure, defined as a radiating source operating within 20 cm of the user, are based on the specific absorption rate (SAR) of a particular frequency of energy per unit mass of tissue. For the general public, 1.6 W/kg averaged over 1 g of tissue are permissible, though less restrictive limits are defined by the regulatory agencies in other countries. For example, the CENELEC-imposed limit in the United Kingdom is 2 W/kg averaged over 10 g of tissue[5].

The shielding in pacemakers and other implantable devices should prevent most interference from a WBAN device; however, contemporary implantable devices are designed for bidirectional RF communication and thus a risk interfering with the operation of the device exists. As a result of a study performed in 1997 [38], the FCC recommends that the transmitter should be at least 6 inches away from the pacemaker.

7.4.6 *Security*

For most WBAN-type applications, especially if health-related information is being gathered, then data security is a must. Depending on the country the device is to operate in, various government regulations apply, such as the Health Insurance Portability and Accountability Act (HIPAA) in the United States. Violations of these requirements can result in incarceration, so care must be taken in the implementation of the authentication of peers and encryption of data to be transmitted.

---

[3] http://www.fcc.gov/oet/info/documents/bulletins/#56
[4] http://www.fcc.gov/oet/info/documents/bulletins/#65
[5] http://webstore.iec.ch/webstore/webstore.nsf/artnum/033746

Many of the wireless technologies support some level of encryption, but as security expert Bruce Schneier often states, it's not the encryption that fails, but the implementation of the encryption. Consider the WEP encryption used by many Wi-Fi routers. The encryption used is RC4, which is still secure. However, the implementation of the encryption is faulty, and as a result a WEP password can be determined within minutes using standard tools. In the case of WEP, this is because the encryption vectors are reused often if there is sufficient traffic allowing for cryptographic attacks. This is a fundamental flaw in WEP, and similar flaws might exist in the implementation of the security of your wireless technology — or in your particular implementation of a technology.

If you are required to use a particular technology and you need to comply with regulations such as HIPPA, but the security provided by your particular technology is insufficient, there is no reason you can't implement your own additional layer of authentication or security. Bruce Schneier's book *Applied Cryptography* is a great resource in understanding the fundamentals of encryption and authentication if you plan on implementing your own. Some encryption schemes are simple to implement and can be done using spare clock cycles in a microprocessor — others might require more power computational power on a complex programmable logic device (CPLD) or digital signal processor (DSP). However, care must be taken if a multi-IC solution is used where a secret key might be transmitted from one IC to another in an unencrypted fashion.

7.5 Batteries

In choosing what type of battery to use to power a WBAN device, one must consider the battery size, capacity/power density, nominal operating voltage, internal resistance, and safety. The right battery for a WBAN implementation is the result of weighing all the options relative to the design requirements and making an informed decision.

Size is important in such that it helps determine the minimum physical dimensions of the WBAN device — though this often at the expense of capacity. The smallest battery options include

coin-cells, which can be as small as 4.8 mm in diameter and 1.2 mm in height, and lithium-polymer ion (LiPo) batteries, which can be manufactured to any specified size. Coin-cell batteries are convenient that they can be mounted directly to the PCB; however, it also means that the end user needs to have access to the PCB to change the battery. And although rechargeable coin-cell batteries are available, they suffer from higher level of self-discharge and lower charge densities than other rechargeable technologies, making them less practical.

Capacity is measured in ampere hours (Ah), or milliampere hours (mAh) for smaller batteries. The runtime can be determined by examining the discharge graph for the battery chemistry you are interested in. If you are using a linear regulator, then you must maintain the battery voltage above the sum of the operating voltage of your device and the dropout voltage from the linear regulator. Consider the case of a lithium-ion battery in Fig. 7.13. If your microcontroller requires 3.3 V to operate at, and your linear regulator has a 150 mV dropout voltage, then the minimum battery voltage required is 3.45 V. The point at which the discharge curve intersects with the minimum required voltage will indicate your

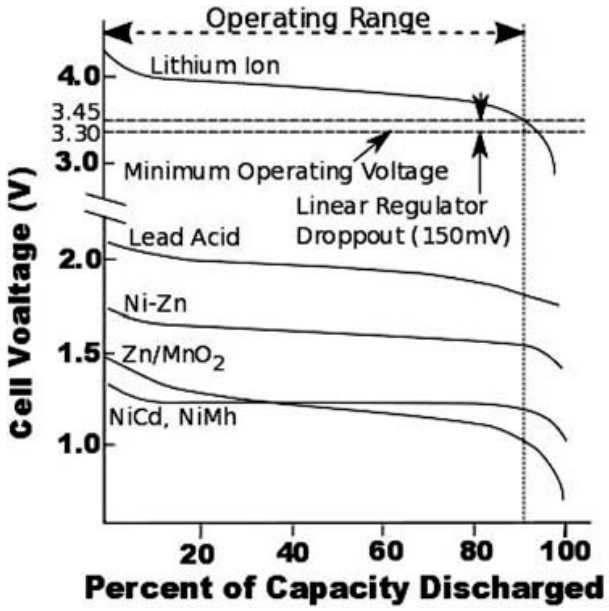

Figure 7.13. Discharge graph for various battery chemistries (adapted with permission from mpoweruk.com).

runtime. For a single-cell lithium-ion battery, you can operate down to 90% of your battery's capacity, which means 10% of the capacity is wasted. By lowering the required voltage, you can decrease this wasted capacity.

If your device uses a switching mode power supply (SMPS), you will be limited by whichever voltage is higher: the minimum safe operating voltage of the battery or the minimum operating voltage of the switching mode supply. However, an SMPS will introduce noise onto your supply lines, and possibly onto any analog signals in your device, unless great care is taken in its implementation.

The nominal voltage is the characteristic operating voltage of the battery, and if the required voltage is greater than the nominal voltage of a single cell, then putting additional cells in series will increase the voltage. For example, a LiPo battery has a nominal voltage of 3.7 V. Two batteries in series will produce a voltage of 7.4 V.

The discharge rate of batteries often normalized and presented as the discharge rate in ampere hours divided by the capacity of the battery in ampere hours and is presented as fractions of C. $1C$ represents fully discharging a battery in one hour, $2C$ in half an hour, and $0.5C$ in 2 hours. The discharge curve of a battery will be depressed as the battery ages, at higher discharge currents, and at lower operating temperatures. For example, in the case of Fig. 7.14, operating a LiPo battery at 0°C will decrease its capacity by 17% versus at 25°C.

The internal resistance of a battery limits the maximum available current that the WBAN device will consume. Although the WBAN device might be designed with a low average current requirement, various components on the device can consume high current in bursts, especially the wireless transmitter. For example, if your wireless transceiver is a GSM cell module, then you can expect bursts of power consumption in the range of 2 amps while your WBAN device averages less than 100 mA of current. If the battery has a high internal resistance, then the voltage provided by the battery can dip below the required levels, causing the digital components on your device to latch up, and/or result in erroneous data on the analog side. The use of large-capacitance low effective serial resistance (ESR) capacitors can help buffer the power usage and minimize these effects.

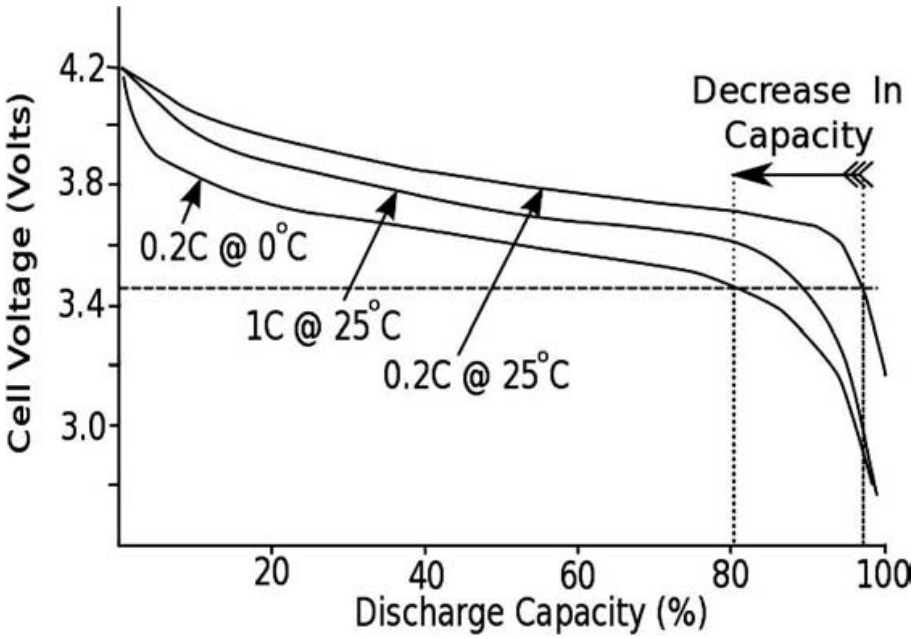

Figure 7.14. Discharge graph for lithium-ion at various temperatures and currents.

Of the various battery options, LiPo batteries have very low internal resistance and can provide many amps of current if required making them an ideal choice. However, it is important to provide a low-resistance path to the ICs that will be consuming the bursts of power or else there will be little benefit in using a battery with low internal resistance. This is often accomplished by the use of dedicated supply and ground planes on the PCB. This technique will also help minimize potential supply voltage differences in the circuit, which can result in unexpected behaviour in analog circuits. Another advantage to LiPo batteries is that they can be manufactured in to fit any required shape, though the size is directly proportional to the amount of charge the battery can store.

If the end user is expected to replace the batteries often, then the use of a standard battery should be considered. In the United States, they include sizes denoted as AAA, AA, or 9-Volt. These batteries are easily found in both rechargeable and nonrechargeable flavors. The main advantage in using these types of batteries is their availability.

In terms of safety, it is important to design the WBAN device to prevent the battery, or the cables attached to the battery, from contacting an unintentional part of the device. For example, if the

WBAN device includes ECG electrodes, and the battery accidentally contacts the electrode leads, then sufficient current can flow through the heart to cause fibrillation and kill the user. Furthermore, some battery chemistries, such as LiPo, are flammable/explosive if the enclosure is punctured and can result in sever burns. Thus, it is important to provide an adequate enclosure for the battery to guarantee that the user or some other component cannot damage the battery.

7.6 Final Thoughts and the Berkeley Tricorder

The Berkeley Tricorder, currently in its 7th version, has been used in a number of studies. These include two to evaluate its ability to record ambulatory data, one on evaluating activities of daily living, and to evaluate sports training. A sample of the data acquired from the ambulatory study can be found in Fig. 7.15. The EMG signal was derived from electrodes placed over the latissimus dorsi muscle on the back. A reflective SpO_2 sensor manufactured by Nellcor (Max-Fast, Nellcor/Tyco, Pleasanton, CA) was placed on the forehead as it minimized motion artifacts. The system performed well with

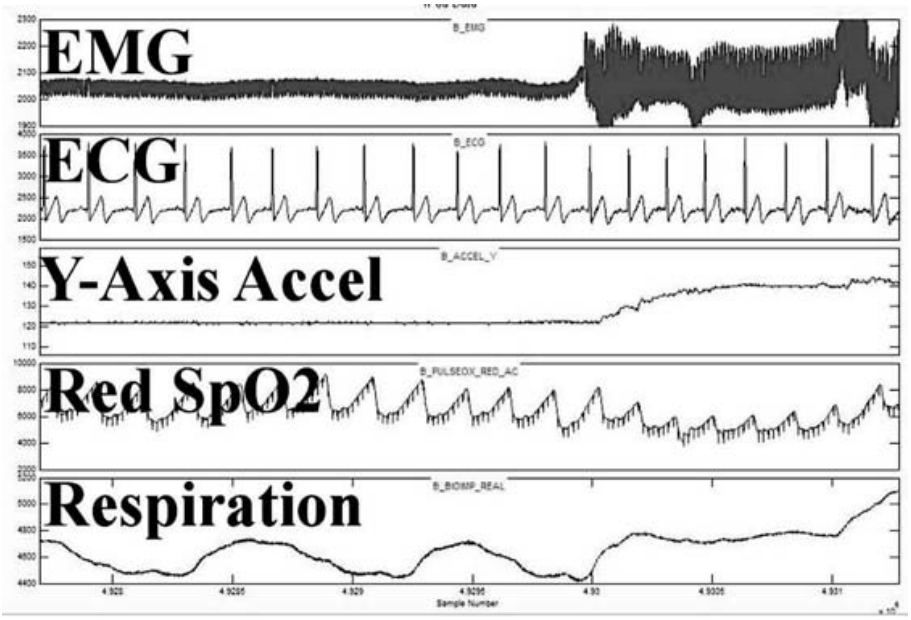

Figure 7.15. Sample data from the Berkeley Tricorder. See also Color Insert.

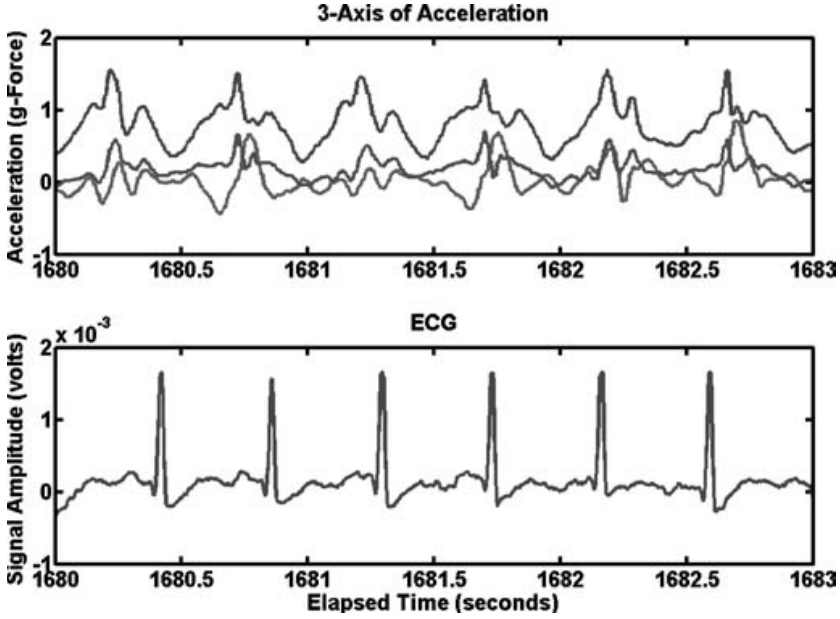

Figure 7.16. ECG signal (lower plot) captured while subject in motion (upper plot). See also Color Insert.

minimal motion artifacts. Fig. 7.16 shows the ECG signal while the subject was walking.

Many lessons have been learned through the process of designing the Berkely Tricorder, and this chaper has tried to convey some of those learned lessons and expereiences. There is no cookbook methodology of desinging a WBAN device; rather, the need to understand the problem and formulate a solution while understanding the various trade-offs. This same theme has been reitterated in many sections of this chapter and is perhaps the single most important lesson this author has learned.

References

1. S. Zenios, J. Makower, P. Yock, T. J. Brinton, U. N. Kumar, L. Denend, and T. M. Krummel (January 2009) *Biodesign: The Process of Innovating Medical Technologies*, New York, Cambridge University Press.
2. Y. Chi, S. Deiss, and G. Cauwenberghs (2009) Non-contact low power EEG/ECG electrode for high density wearable biopotential sensor networks, in *Proceedings of the 2009 Sixth International Workshop on Wearable and Implantable Body Sensor Networks*, **00**, pp. 246–250.

3. Y. Mendelson, R. J. Duckworth, and G. Comtois (July 2006) A wearable reflectance pulse oximeter for remote physiological monitoring in *Proceedings of the International Conference of IEEE Engineering in Medicine and Biology Society 2006*, **1**, pp. 912–915.
4. T. H. Teo, G. K. Lim, D. S. David, K. H. Tan, P. K. Gopalakrishnan, and R. Singh (2007) Ultralow power sensor node for wireless health monitoring system in *Proceedings of ISCAS 2007*, pp. 2363–2366.
5. L. Wang, J. Y. Zhang, J. Huang, L. K. Chen, L. Yu, Y. T. Zhang, and G. Z. Yang (April 2009) A field programmable analogue ASIC towards low power processing-on-node BSNs, in *Proceedings of the Sixth International Workshop on Wearable and Implantable Body Sensor Networks*, pp. 1–4 doi: 10.1109/P3644.54.
6. E. Teaw, G. Hou, M. Gouzman, K. W. Tang, A. Kesluk, M. Kane, and J. Farrell (August 2005) A wireless health monitoring system, in *Proceedings of the 2005 IEEE International Conference on Information Acquisition*, pp. 247–252.
7. C. Otto, A. Milenkovic, C. Sanders, and E. Jovanov (January 2006) System architecture of a wireless body area sensor network for ubiquitous health monitoring, *Journal of Mobile Multimedia* **1(4)**, pp. 307–326.
8. E. Jovanov, A. Milenkovic, C. Otto, and P. C. de Groen (March 2005) A wireless body area network of intelligent motion sensors for computer assisted physical rehabilitation, pp. 1–10.
9. K. Montgomery, C. Mundt, G. Thonier, A. Tellier, U. U. Barker, R. Ricks, L. Giovangrandi, P. Davies, Y. Cagle, J. Swain, J. Hines, and G. Kovacs (April 2004) Lifeguard — A personal physiological monitor for extreme environments, pp. 1–4.
10. D. Malan, T. Fulford-Jones, M. Welsh, and S. Moulton (2004) CodeBlue: An ad hoc sensor network infrastructure for emergency medical care, in *International Workshop on Wearable and Implantable Body Sensor Networks*, **5** pp.
11. T. Gao, D. Greenspan, and M. Welsh (December 2005) Improving patient monitoring and tracking in emergency response, pp. 1–6.
12. B. P. Lo, S. Thiemjarus, R. King, and G. -Z. Yang (May 2009) Body sensor network — A wireless sensor platform for pervasive healthcare monitoring, pp. 77–80.
13. R. Naima and J. Canny (April 2009) The Berkeley tricorder: Ambulatory health monitoring, *2009 Sixth International Workshop on Wearable and Implantable Body Sensor Networks*, pp. 53–58 doi: 10.1109/P3644.57.

14. R. WEBSTER, Medical instrumentation sm 3e, *lavoisier.fr* (January 1997) URL http:// www.lavoisier.fr/notice/frLWO6A2LARRWLKO.html.
15. M. Oehler, V. Ling, K. Melhorn, and M. Schilling (2008) A multichannel portable ECG system with capacitive sensors, *Physiological Measurement*, **29**, pp. 783–793.
16. C. Kitchin, L. Counts, and M. Gerstenhaber Reducing RFI rectification errors in in-amp circuits, Analog Devices Inc, Application Note (AN-671).
17. B. Carter and T. Brown (2001) *Handbook of Operational Amplifier Applications*, Texas Instruments Application Report, *SBOA092A*.
18. C. Kitchin and L. Counts (January 2000) A designer's guide to instrumentation amplifiers, *school.mech.uwa.edu.au* URL http://school.mech.uwa.edu.au/mechatronics/El-resources/Kitchin-Op-Amplifiers%2520Guide.pdf.
19. F. Wilson, A. Macleod, and P. Barker (December 1931) The potential variations produced by the heart beat at the apices of Einthoven's triangle, *American Heart Journal*, **7(2)**, pp. 207–211, URL http://linkinghub.elsevier.com/retrieve/pii/S0002870331904110.
20. E. Goldberger (1942) A simple, indifferent, electrocardiographic electrode of zero potential and a technique of obtaining augmented, unipolar, extremity leads, *American Heart Journal*, **23(4)**, pp. 483–492.
21. H. Burger and J. V. Milaan (1948) Heart-vector and leads, *British Heart Journal*, **10(4)**, pp. 229.
22. J. Malmivuo, R. Plonsey, and J. Cameron (January 1995) Bioelectromagnetism: Principles and applications of bioelectric and biomagnetic fields, *Informa Pharma Science* URL http://www.informapharmascience.com/doi/abs/10.3109/03091909609009004.
23. G. Rau, E. Schulte, and C. Disselhorst-Klug (2004) From cell to movement: To what answers does EMG really contribute? *Journal of Electromyography and Kinesiology*, **14(5)**, pp. 611–617.
24. B. Gerdle, S. Karlsson, S. Day, and M. Djupsjobacka (1999) Acquisition, processing and analysis of the surface electromyogram, in *Modern Techniques in Neuroscience* (ed. U. Windhorst and H. Johansson), Berlin, Springer Verlag, pp. 705–755.
25. J. Ahlgren (1967) Kinesiology of the mandible an EMG study, *Acta Odontologica*, **25(6)**, pp. 593–612.
26. U. Lundberg, R. Kadefors, B. Melin, G. Palmerud, P. Hassmen, M. Engstrom, and I. E. Dohns (1994) Psychophysiological stress and EMG

activity of the trapezius muscle, *International Journal of Behavioral Medicine*, **1(4)**, pp. 354–370.

27. R. Merletti (1999) Standards for reporting EMG data, *Journal of Electromyography and Kinesiology*, **9(1)**, pp. 3–4.
28. M. Shamir and C. Weissman (January 2003) Plethysmographic waveform variation as an indicator to hypovolemia, *Anesthesia and Analgesia* URL http://www.anesthesia-analgesia.org/content/97/2/602.2.full.
29. L. Geddes, M. Voelz, and C. Babbs (January 2007) Pulse transit time as an indicator of arterial blood pressure, *Psychophysiology* DOI: 10.1111/j.1469-8986.1981.tb01545.x, URL http://www3.interscience.wiley.com/journal/119574157/abstract.
30. T. Rusch, R. Sankar, and J. Scharf (1996) Signal processing methods for pulse oximetry, *Computers in Biology and Medicine*, **26(2)**, pp. 143–159.
31. A. Tobola and C. Douniama (June 2007) Evaluation of alternative derivation areas for plethysmography and pulse oximetry, in *Proceedings of SENSATION Second International Conference, Monitoring Sleep and Sleepiness with New Sensors Within Medical and Industrial Applications* pp. 1–2.
32. V. Markandey (June 2009) Pulse oximeter implementation on the tms320vc5505 DSP medical development kit (MDK), Texas Instruments Application Report SPRAB37 pp. 1–28 URL http://focus.ti.com/lit/an/sprab37/sprab37.pdf.
33. G. Cotter, Y. Moshkovitz, E. Kaluski, A. Cohen, and H. Miller (January 2004) Accurate, noninvasive continuous monitoring of cardiac output by whole-body electrical bioimpedance, *Chest* URL http://www.ncbi.nlm.nih.gov/pubmed/15078756.
34. R. Sung, P. Lau, C. Yu, and P. Lam (January 2001) Measurement of body fat using leg to leg bioimpedance, *Archives of Disease in Childhood* URL http://www.fetalneonatal.com/content/85/3/263.full.
35. F. Seoane, J. Ferreira, and J. Sanch'ez (January 2008) An analog front-end enables electrical impedance spectroscopy system on-chip for biomedical applications, *Physiological Measurement* URL http://iopscience.iop.org/0967-3334/29/6/S23/pdf/0967-3334_29_6_S23.pdf.
36. U. Maurer, A. Smailagic, D. Siewiorek, and M. Deisher (2006) Activity recognition and monitoring using multiple sensors on different body positions, in *Proceedings of the International Workshop on Wearable and Implantable Body Sensor Networks (BSN'06)* URL http://www.ece.cmu.edu/~bfrench/ewatch_files/papers/ewatch%2520papers/01612909.pdf.

37. S. Patterson, D. Krantz, L. Montgomery, P. Deuster, S. Hedges, and L. Nebel (2007) Automated physical activity monitoring: validation and comparison with physiological and self-report measures, *Psychophysiology*, **30(3)**, pp. 296–305.
38. D. Hayes, P. Wang, and D. Reynolds (January 1997) Interference with cardiac pacemakers by cellular telephones, *The New England Journal of Medicine* URL http://content.nejm.org/cgi/content/abstract/336/21/1473.
39. M. J. Mathie, B. G. Celler, N. H. Lovell, and A. C. F. Coster (2004) Classification of basic daily movements using a triaxial accelerometer, *Medical and Biological Engineering and Computing*, 42 (5), 679–687, DOI: 10.1007/BF0234755,URL: http://www.springerlink.com/content/0140-0118/42/5/.

This page intentionally left blank

Chapter 8

Ambulatory Recording of Biopotential Signals: Constraints and Challenges for Analog Design

Refet Firat Yazicioglu,[a] Sunyoung Kim,[a] Tom Torfs,[a] Julien Penders,[b] Buxi Singh Dilpreet,[b] Inaki Romero,[b] and Chris Van Hoof[a, b]

[a] *IMEC, Kapeldreef 75, Leuven, 3001, Belgium*
[b] *IMEC-nl/Holst Centre, High Tech Campus 48, 5656 AE Eindhoven, The Netherlands*
firat@imec.be

The monitoring of biopotential signals such as EEG, ECG, and EMG is a common procedure in modern clinical practice. The instruments that can monitor these signals are traditionally realized by combining precision building blocks with powerful DSP modules. The growing interest toward the improvement of patients' quality of life and the use of biopotential signals in nonmedical applications such as entertainment, sports, and brain-computer interfaces requires the implementation of miniaturized and wireless biopotential acquisition systems with ultra-low power dissipation. This has dramatically changed the way of developing instruments for the extraction of biopotential signals, placing stringent constraints on the design of analog front-end circuits that can be used in

Wireless Body Area Networks: Technology, Implementation, and Applications
Edited by Mehmet R. Yuce and Jamil Y. Khan

ISBN 978-981-4316-71-2 (Hardcover), ISBN 978-981-4241-57-1 (eBook)
www.panstanford.com

ambulatory biopotential monitoring applications. In addition, the ambulatory monitoring of patients has introduced new challenges that can jeopardize the signal integrity.

This chapter will focus on the design of analog-integrated circuits that can be used in ambulatory biopotential monitoring applications. Several constraints in terms of power dissipation and signal-to-noise ratio will be addressed. Later, an important challenge in ambulatory biomedical signal monitoring, namely motion artifacts, will be introduced and different strategies to tackle this problem will be explained.

8.1 Introduction: The Need for Portable Medical Electronics Systems

The need for portable medical electronics stems from the fact that the current health care routine is very much centralized by heavily focusing on the hospitalization of patients. This requires that people adapt to this data-centric approach, which is indeed very efficient for curative care delivery but, on the other hand, very expensive. Keeping this in mind, demographical changes indicate that the continuously aging population is leading to significant rise in chronic diseases, resulting in ever-increasing health care costs as shown in Fig. 8.1 [1]. Such increase in costs not only creates a significant burden on the economical system, but also reduces the efficiency of health care delivery.

Therefore, there is a strong interest to introduce the parts of health care cycle into the daily routine of people. It is expected that this will significantly reduce hospitalization costs and also help in increasing the efficiency of health care delivery. The initial interest is to introduce the practice of signal monitoring and analysis into people's daily routine through ambulatory and continuous monitoring systems with miniature size and wearable form factor. This can significantly reduce the hospitalization requirements of people and assist health care professionals in data analysis, significantly reducing the time and the cost of long-term patient monitoring. In the long run, such monitoring systems will evolve to

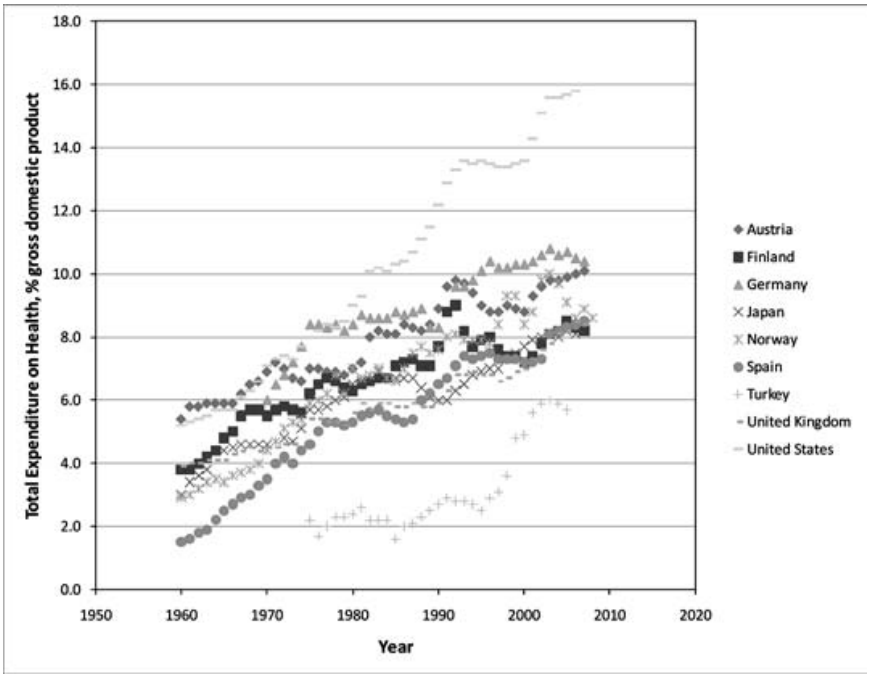

Figure 8.1. Change of total expenditure on health (percentage of gross domestic product) over years. See also Color Insert.

smarter systems capable of performing reliable diagnostics based on acquired medical signals, and even perform partial treatment and/or suppression of the disorder through drug delivery and/or electrical/visual stimulation systems.

The key for the realization of such a vision is a technology platform that can enable the collection of data from patients and communicate these to medical professionals in a reliable manner. The e-Health project, "The use, in the health sector, of digital data — transmitted, stored, and retrieved electronically — in support of health care, both at the local site and at a distance." as defined by WHO, can be the platform for the support and the diagnostics of patients. E-health is claiming to offer the potential to reduce medical cost, enable personalized health care, deliver remote health services, and increase the delivery efficiency in real-time. Therefore, the gathering of fast, reliable, and continuous medical information from patients lies in the center of the e-Health project further addressing the necessity for the realization of miniature and smart systems for medical signal monitoring.

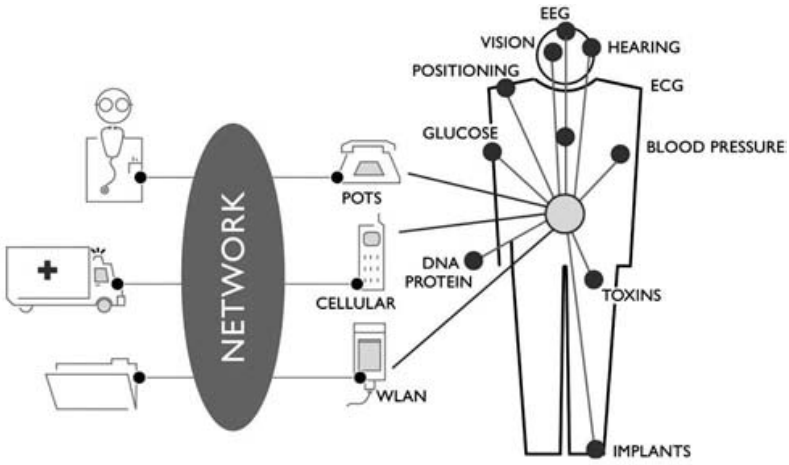

Figure 8.2. Technology vision for future medical monitoring and diagnostics systems [2]. People will be carrying their personalized sensor nodes, collecting medical information from the patient and their surroundings, analyze it, and communicate the results to medical professionals with wireless communication.

This requirement is being addressed by body area networks (BAN) [2], which consist of smart and miniaturized sensor nodes collecting information from patients and its environment, processing this information, and wirelessly communicating the results to medical professionals. The main challenge behind the realization of these sensor nodes is the fact that the available power budget for performing these functionalities is strictly limited due to the small form factor of these sensor nodes. Hence, research focuses on the realization of power-efficient implementation for each and every building block of this smart system.

Therefore, this chapter will focus on the analog front-end part of these miniature sensor nodes and how to implement low-power analog front-end circuits, which not only extract biomedical signals with high signal quality, but also provide a method to monitor signal integrity problems in ambulatory monitoring systems.

The outline of the chapter is as follows: Section 8.2 will present the basics of biopotential signal acquisition. Section 8.3 will address constrains and challenges in analog circuit design for the monitoring of biopotential signals in portable/ambulatory biopotential recording systems. Section 8.4 will describe how to design power efficient instrumentation amplifiers extracting

biopotential signals in a power-efficient manner. Last but not the least, Section 8.5 will describe signal integrity problems in ambulatory measurement systems.

8.2 Basics of Biopotential Signal Acquisition

Figure 8.3 shows the characteristics of biopotential signals as presented in reference [3]. These signals can be grouped in two categories. The signals in the first group are electrocardiogram (ECG) and electromyogram (EMG) signals, which are due to muscular activity, i.e., activity due to the cardiac muscles and the skeletal muscles, respectively. On the other hand, the signals in the second group are due to neural activity within the brain, and the naming convention changes according to the measurement invasiveness and the focus of the measurement. The action potential (AP) measurements are invasive measurements and refer to the signals' single neurons. Similarly, local field potential (LFP) measurements are also invasive, but the signal of interest is the average activity of group of neurons. It should be noted that since these two measurements are invasive, large biopotential signals can be picked up. On the other hand, as the measurements move toward noninvasive methods such as electrocorticogram (ECoG),

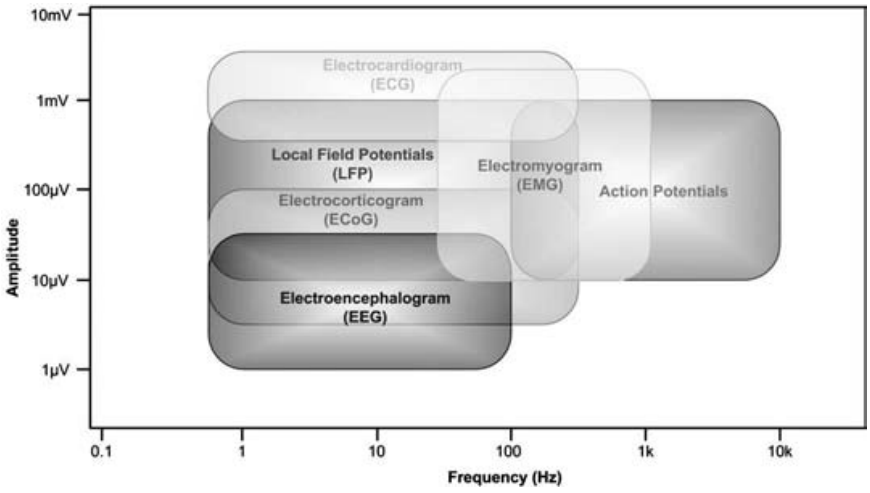

Figure 8.3. Frequency and amplitude characteristics of biopotential signals — most commonly monitored signals in medical practice [3]. See also Color Insert.

where the signals are measured on the surface of the cortex, and electroencephalogram (EEG), where the signals are measured above the skull, the signal amplitudes decrease significantly, requiring higher performance analog building blocks for signal acquisition.

The acquisition of biopotential signals requires two main elements: 1) biopotential electrodes and 2) an instrumentation amplifier. The purpose of the electrodes is to convert the ionic current within the body into electronic current so that the instrumentation amplifier can process this signal for amplification [3]. The measurement of biopotential signals can be grouped into three categories according to the electrode configurations as:

- Type I: Bipolar measurement with third electrode biasing
- Type II: Bipolar measurement with lead biasing
- Type III: Unipolar measurement

Type I measurement configuration is intended for precision measurements, where the common-mode signals need to be rejected from the measurement. However, this measurement needs the use of a third electrode for setting the DC potential of the patient. On the other hand, Type II enables the bipolar measurement of signals without using the third biasing electrode. This is generally the preferred measurement method for applications requiring the use of minimum number of electrodes, where the common-mode signals need to be rejected. The third, and the last measurement method, is the unipolar measurement method. This method is generally used, where the signal amplitudes are sufficiently large, or the common-mode signals are sufficient low, such that it is not required, by the application, to reject the common-mode signals.

Similar to the measurement configuration, the design of an instrumentation amplifier also depends on the application. For applications where the signal levels are very small, together with Type I measurement a high-performance instrumentation amplifier is required. On the other hand, an instrumentation amplifier with lower performance specifications may be sufficient for measurements with larger signals enabling the implementation of a lower power instrumentation amplifier.

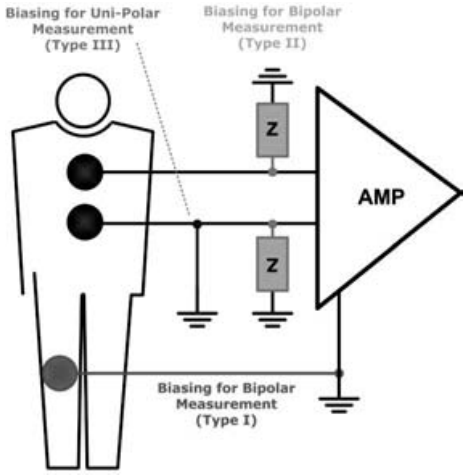

Figure 8.4. Different measurement and biasing methods for biopotential signal acquisition. See also Color Insert.

8.3 Constrains and Challanges

The previous section has given a brief introduction to the measurement of biopotential signals. Of course, such an ideal model indicates that the implementation of an analog front-end can be a straightforward process and that simple amplifier architectures can be used to achieve very low-power analog front-end circuits. However, this is unfortunately not the case for biopotential measurements. There are significant aggressors and error sources that create challenges and constrains for instrumentation amplifier design. This section will summarize these constrains and challenges, which will enable the analog designer to select the best amplifier topology to be used in different applications of biopotential measurements.
The nonidealities in biopotential measurements can be due to:

i. Electrostatic Interference
ii. Biopotential Electrodes
iii. Instrumentation Amplifier

These three main groups of nonidealities are shown in Fig. 8.5 for a Type I measurement. The first nonideality comes from the interference to human body appearing due to the electrostatic coupling to surrounding mains, which results in a displacement current flowing through the human body [4] leading to the

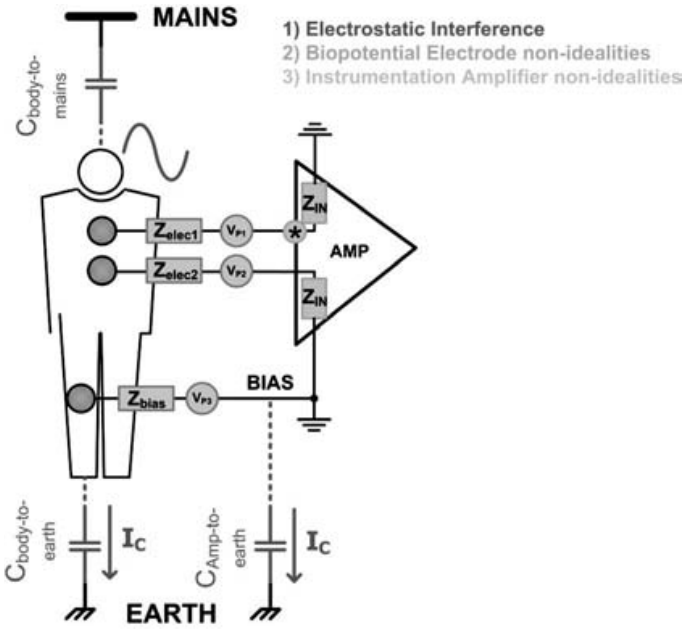

Figure 8.5. Measurement of biopotential signals (Type I measurement) introducing the nonidealities from different sources. See also Color Insert.

generation of an AC potential over the body. This potential appears as a common-mode signal to the instrumentation amplifier and requires sufficiently large common-mode rejection ratio (CMRR) so that we can reject the large common-mode signals and extract the weak biopotential signals.

The second nonideality is due to the electrodes. An electrode sitting on a skin, or on a tissue, results in complex impedance and a polarization voltage between the signal source and the input of the instrumentation amplifier [3]. The latter leads to a net DC input to the instrumentation amplifier, which can be rejected by introducing AC coupling prior to amplification. On the other hand, the prior, combined with the finite input impedance of the instrumentation amplifier, leads to the conversion of the common-mode signals into differential mode according to:

$$\frac{V_{\mathrm{DM}}}{V_{\mathrm{CM}}} = \frac{\Delta Z_{\mathrm{ELEC}}}{Z_{\mathrm{IN}}} \tag{8.1}$$

where V_{DM} is the differential mode signal at the input of the amplifier, V_{CM} is the common-mode signal on the human body, ΔZ_{ELEC} is the mismatch of the impedances between two recording electrodes, and Z_{IN} is the input impedance of the instrumentation

amplifier. Therefore, it can be seen that even if we can implement an instrumentation amplifier with infinitely large CMRR, the finite input impedance and the mismatch of electrode impedance lead to the conversion of the common-mode signal into differential mode. This means that the affective CMRR is significantly reduced by the finite input impedance of the amplifier.

Last but not the least, the nonidealities from the instrumentation amplifier can affect the accuracy of the biopotential recordings. Two major nonidealities with significant impact on the quality of recordings are the noise and the finite input impedance of the instrumentation amplifier. The latter, unless sufficiently large, may load the electrodes, as well as, leading to the conversion of common-mode signals into differential mode. The prior, on the other hand, significantly reduces the signal-to-noise ratio of biopotential recordings due to the fact that biopotential signals have very low frequency behavior [5].

As a result of this discussion, we can divide the main performance specifications of instrumentation amplifiers into four groups:

i. DC Headroom
ii. Common-Mode Rejection Ratio
iii. Input Impedance
iv. Noise Performance

It should be noted that the quantitative specifications for these requirements will be defined by the application, and the choice of the instrumentation amplifier should be able to meet these specifications. A very good example on how application defines the instrumentation amplifier specifications can be seen from different brain activity measurement methods as shown in Fig. 8.6.

During EEG measurements, the electrodes are placed above the skull. This leads to biopotential signals with very weak amplitudes, which make them very sensitive to various aggressors. On the other hand, due to the less strict material choice, the electrodes are more stable leading to more relaxed DC headroom requirements. This means that instrumentation amplifiers addressing EEG applications should realize very high performance, i.e., high CMRR, very high input impedance, and very low noise, whereas, the DC headroom specifications are not very strict.

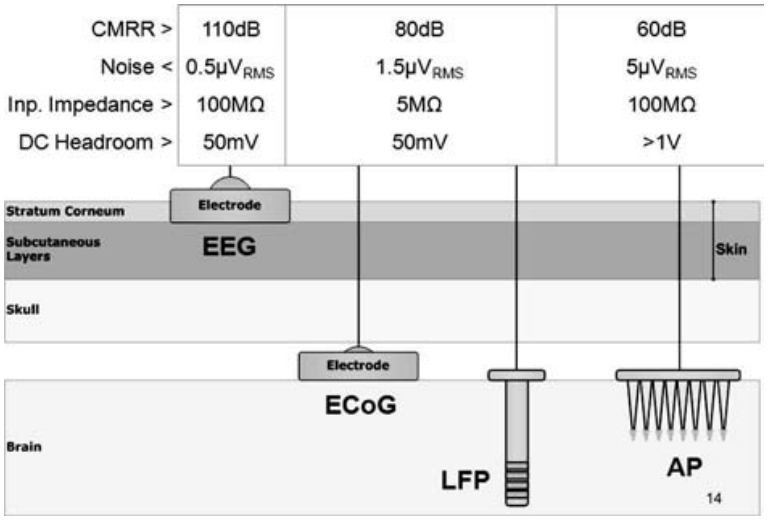

Figure 8.6. Different measurement methods of brain activity showing how the application defines the instrumentation amplifier specifications.

On the other hand, if we have a look at more invasive measurements, for instance ECoG measurements, the signal amplitudes are larger, relaxing noise, CMRR, and input impedance specifications. This means that circuits targeting these applications may be more aggressive on low-power consumption rather than the noninvasive measurements of biopotential signals.

Finally, if we have a look at more invasive measurements such as AP measurements, the signal amplitudes even further increase, which means that the noise and CMRR requirements can be more relaxed. On the other hand, the size of the electrodes is significantly reduced, which leads to a very large electrode impedance. In addition to that, very strict biocompatibility requirements limit the choice of electrode material. Hence, even larger polarization voltages can be seen while recording biopotential signals from such electrodes. Hence, instrumentation amplifiers implementing very large input impedance and incorporating large DC headroom are required.

Therefore, the conclusion is that the design of instrumentation amplifiers for different biopotential recording applications targets different specifications. The next section will review these different instrumentation amplifier architectures and why they suit very well for specific applications.

8.4 Design of Instrumentation Amplifiers for Biopotential Recordings

The most common instrumentation amplifiers that are being used for biopotential recordings can be grouped into two main categories:

i. Uncompensated Instrumentation Amplifiers
ii. Compensated Instrumentation Amplifiers

The name compensation represents the use of circuit techniques that reduce the effects of flicker noise in CMOS transistors and mismatch related errors. Therefore, the amplifiers utilizing compensation are being used in applications requiring very high performance instrumentation amplifiers. On the other hand, the uncompensated amplifiers focus on aggressively improving the power efficiency of the instrumentation amplifiers, which is one of the most important criterions in implantable applications. Therefore, this section will describe the most commonly used instrumentation amplifiers for the extraction of biopotential signals. Their key advantages and disadvantages will be reviewed.

8.4.1 *Uncompensated Instrumentation Amplifiers*

There are two main types of instrumentation amplifiers that do not use any compensation for the amplifier nonidealities. These instrumentation amplifiers differ in the sense that the first type uses the ratio of resistors to define the gain of the instrumentation amplifier, or namely resistive instrumentation amplifiers, whereas the second type uses the ratio of capacitors, or so called capacitive instrumentation amplifiers.

The typical architecture of the resistive instrumentation amplifiers is shown in Fig. 8.7 [6]. The instrumentation amplifier consists of an input transconductance stage and an output transimpedance stage. The input stage converts the differential input voltage into a current over the resistor R_1. This current is converted into a voltage at the transimpedance stage. Hence, the voltage gain of the architecture is defined by:

$$A_V = \frac{R_2}{R_1} \tag{8.2}$$

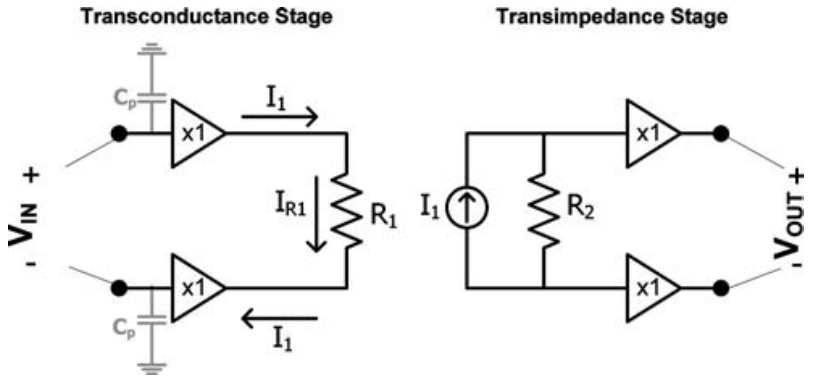

Figure 8.7. Simplified architecture of the resistive instrumentation amplifier topology [6] that does not make use of any compensation technique for improving CMRR and reducing noise.

If we analyze the important characteristics of this instrumentation amplifier topology, the critical performance specifications can be summarized as:

i. **DC Headroom:** The lack of AC coupling significantly reduces the DC headroom of this instrumentation amplifier. Additional circuitry is required for the introduction of AC coupling.
ii. **CMRR:** It is defined by components mismatches. Especially, the gain mismatch of the input buffers will lead to the conversion of the common-mode voltage into differential current over the input resistor R_1. As a result, the CMRR of this amplifier topology will be in the moderate-low range.
iii. **Input Impedance:** One of the key advantages of this architecture is its input impedance, which is solely defined by the parasitic capacitances at the inputs of the transconductance stage. This simply means that the input impedance of this architecture is the maximum possible value for a given instrumentation amplifier topology.
iv. **Noise Performance:** The input-referred noise of this instrumentation amplifier architecture is defined by:

$$\overline{v_{\mathrm{IA}}^2} = 2 \times \overline{v_{\mathrm{BUF}}^2} + \overline{v_{R_1}^2} + \frac{\overline{v_{R_2}^2}}{A_{\mathrm{v}}^2} \tag{8.3}$$

This shows that the noise of the instrumentation amplifier is defined by the noise of the input buffers together with the resistors defining the transconductance of the input stage. It

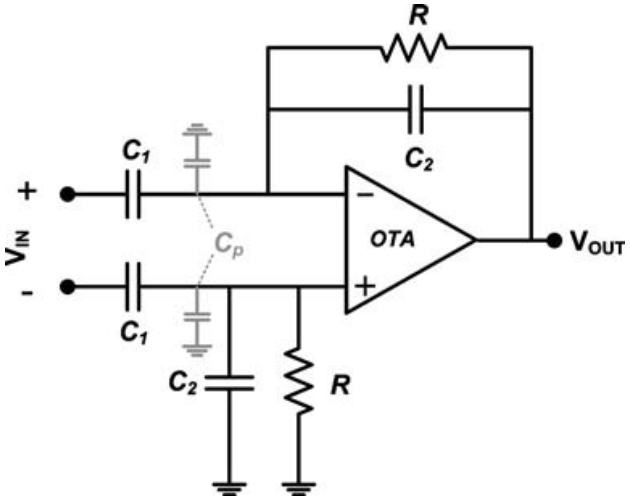

Figure 8.8. Simplified architecture of the capacitive instrumentation amplifier topology [8].

should be noted that the noise of the buffers will be dominated by flicker noise, significantly reducing the signal-to-noise ratio of the measurements at low frequencies, i.e., the range of biopotential signals.

As an alternative to the resistive instrumentation amplifier, the architecture of the capacitive instrumentation amplifier is shown in Fig. 8.8 [7, 8]. It is similar to a differential resistive feedback amplifier, but resistors are replaced with capacitors, hence the gain is defined as:

$$A_V = \frac{c_1}{c_2} \tag{8.4}$$

In such a configuration, the DC voltages at high impedance nodes are defined by the resistors. Note that these resistors are implemented using transistors operating in weak inversion, implementing very large values on-chip by using a very small area [8]. The critical performance specifications can be summarized as:

i. **DC Headroom:** This architecture is inherently AC coupled. Supply level DC voltages can be rejected by this instrumentation amplifier.
ii. **CMRR:** It is defined by the components mismatches. Hence, the expected CMRR is also in the moderate-low range.

iii. **Input Impedance:** The input impedance is defined by the input capacitances C_1 and can be given as:

$$Z_{\text{IN}} = \frac{1}{jwC_1} \tag{8.5}$$

Hence, the input impedance of this architecture is also very large considering the fact that biopotential signals have very low frequency behavior.

iv. **Noise Performance:** The total input referred noise of the instrumentation amplifier is mainly dominated by the noise of the core operational transconductance amplifier (OTA) as represented in Eq. 8.6. The only nonideal effect that elevates the instrumentation amplifier noise above the core OTA noise level is the presence of the parasitic capacitance C_p. The value of this parasitic capacitance appears at the numerator of the noise equation. Hence, the capacitors C_1 and C_2 should be sized properly to minimize the effect of C_p. In addition, the core OTA also suffers from flicker noise. This significantly increases the noise of the OTA for low-frequency applications.

$$\overline{v_{\text{IA}}^2} = \left(\frac{C_1 + C_2 + C_{\text{p}}}{c_1}\right)^2 \times \overline{v_{\text{OTA}}^2} \tag{8.6}$$

As a conclusion, if we compare the two uncompensated instrumentation amplifier topologies, both of the architectures suffer from large 1/f noise and limited CMRR, but the capacitive one presents a clear advantage of having maximal DC headroom, which is an important requirement for the extraction of AP and LFP signals.

On the other hand, neither of the instrumentation amplifiers has sufficient performance for the recording of weaker biopotential signals, where the 1/f noise and limited CMRR are important error sources. Hence, compensated instrumentation amplifiers are used for applications requiring very low noise levels.

8.4.2 *Compensated Instrumentation Amplifiers*

A well-known technique that reduces flicker noise and improves the CMRR of amplifier is called chopper modulation (Fig. 8.9) [9]. This technique works on the principle that the input signal can be modulated to a frequency location, where flicker noise and

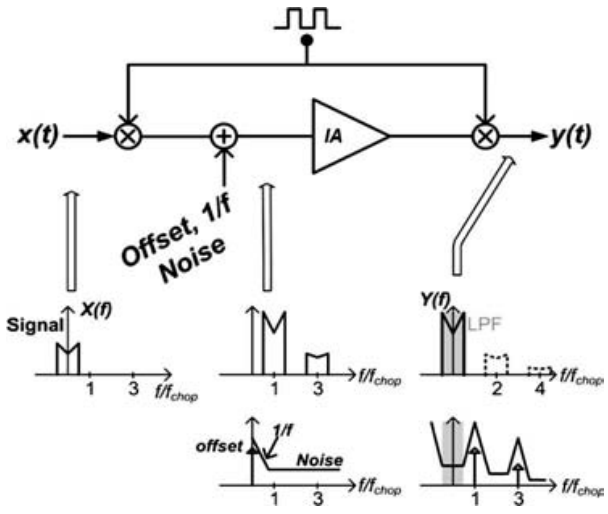

Figure 8.9. Operating principle of chopper modulation. Signal aggressors are modulated to out of the signal band.

other DC errors are not present, passed through the amplifier and demodulated back. In such an implementation, square-wave modulation is used, where the modulators are implemented using cross-coupled switches toggling at alternating clock phases. These modulators only modulate the differential input signal, but they are transparent to common-mode signals. Therefore, not only the flicker noise of CMOS transistors can be pushed out of the signal band, but also the CMRR can be increased.

The only problem that prevents the use of chopper-modulated instrumentation amplifiers for biopotential measurements is the fact that this technique inherently leads to the implementation of DC-coupled instrumentation amplifiers. A simple solution to this problem can be the use of off-chip passives implementing high-pass filter characteristics. However, this can lead to the use of large number of external components, especially important for multichannel EEG recording applications with high channel count.

As an alternative to off-chip passives, a recently proposed technique utilizes a DC servo to implement AC coupling (Fig. 8.10) [10]. In this architecture, the input of the DC servo input is connected to the output of the amplifier after the demodulator. It checks the

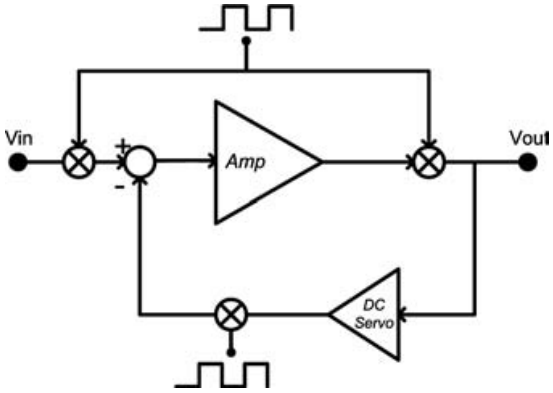

Figure 8.10. Implementation of an AC-coupled chopper-modulated instrumentation amplifier. The DC servo loop regulates the input of the core amplifier to reject the differential input impedance to chopper-modulated instrumentation amplifiers [10].

DC level of the output signal and regulates the input voltage of the amplifier to reject the input DC voltage.

Similar to uncompensated instrumentation amplifiers, there are two different instrumentation amplifier architectures, which use chopper modulation. The first architecture is called resistive compensated instrumentation amplifiers. Figure 8.11 shows the actual implementation of an AC-coupled chopper modulated instrumentation amplifier relying on resistors as the gain elements [10, 11].

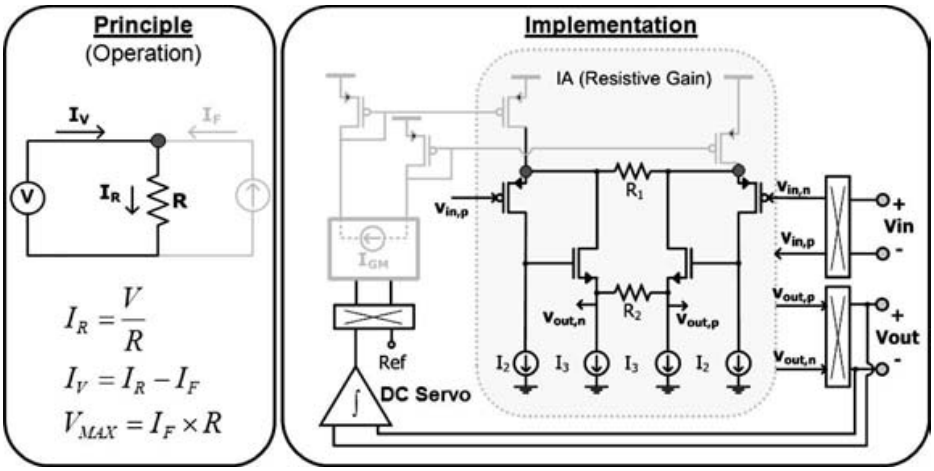

Figure 8.11. The complete architecture of a compensated instrumentation amplifier using a DC servo loop for implementing high-pass filtering characteristics [10, 11]. See also Color Insert.

The core of the instrumentation amplifier is an uncompensated resistive instrumentation amplifier, whose simplified architecture is shown in Fig. 8.7. The modulators and demodulators are located at the input and output of the resistive instrumentation amplifier. The input of the DC servo is sensing the DC level of the output and subtracts it from the input of the amplifier. This subtraction takes places at the terminals of the resistor R_1, which is actually based on the principle shown in the inset figure. This principle simply indicates that applying a voltage over a resistor leads to a current I_R, flowing through R. However, the source of this current will depend on the presence of other current sources forcing current trough R. For instance, if a current source forces a current I_F through resistor R, the voltage source only needs to supply I_R-I_F through the resistor R. This is the exact operating principle of DC servo loop presented in Fig. 8.11. The input transconductance only supplies the rest of the current due to I_{GM}. DC servo ensures that I_{GM} equals to the input DC voltage divided by R, so that our transimpedance will not receive this current to convert it into voltage.

The critical performance specifications can be summarized as follows:

i. **DC Headroom:** The DC servo loop introduces AC coupling to the chopper-modulated instrumentation amplifier. However, the maximum current that can be supplied from the DC servo limits the DC headroom to:

$$\text{DC Headroom} = I_{\text{GM,max}} \times R_1 \tag{8.7}$$

ii. **CMRR:** Chopper modulation eliminates the errors related to component mismatches. Therefore, the CMRR of instrumentation amplifiers can reach more than 120 dB.

iii. **Input Impedance:** The input impedance of this architecture is slightly reduced compared with the input impedance of an uncompensated resistive instrumentation amplifier due to the up modulation of the input signal.

iv. **Noise Performance:** The main advantage of chopper-modulated architecture is the removal of flicker noise. Hence, this architecture can implement very low noise at low frequencies.

The second compensated instrumentation amplifier architecture uses capacitive instrumentation amplifier as the core and introduces

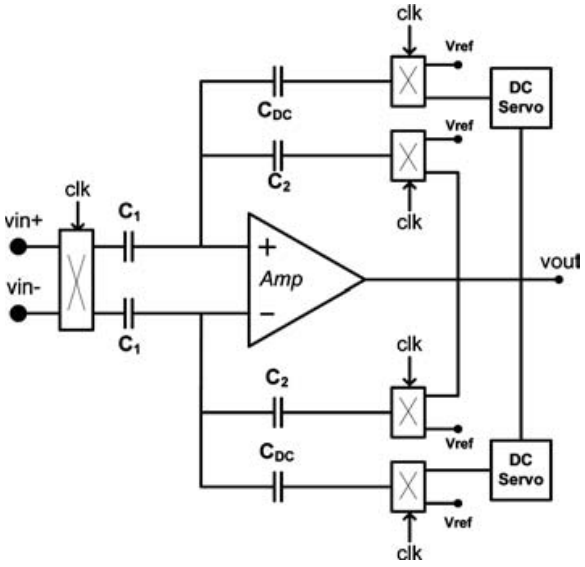

Figure 8.12. The complete architecture of a compensated capacitive instrumentation amplifier using a DC servo loop for implementing high-pass filtering characteristics [12].

chopper modulation. Figure 8.12 shows the architecture of the instrumentation amplifier [12]. Similar to the resistive instrumentation amplifier, a DC servo loop is used for the introduction of AC coupling. Different from the resistive instrumentation amplifier, the DC servo is implemented through capacitive coupling. Again, the current through the input capacitor C_1 can be seen as the addition of DC and AC input signals. In order to prevent its amplification, the current due to the DC input is subtracted through the DC servo path from the amplification signal path leading to AC coupling characteristics.

The basic specifications of this instrumentation amplifier can be summarized as:

i. **DC Headroom:** The DC servo introduces AC coupling. The DC headroom is again defined by the limitations of the DC servo as:

$$\text{DC Headroom} = \frac{C_{\text{DC}}}{C_1} \times \frac{V_{\text{DD}}}{2} \tag{8.8}$$

ii. **CMRR:** Chopper modulation increases the CMRR of the architecture.

iii. **Input Impedance:** One of the main drawbacks of this architecture is the input impedance. The modulation of the input signal

reduces the equivalent input impedance. This is due to the fact that input impedance is defined by the capacitance C_1. Therefore, the input impedance of the architecture can be given as:

$$Z_{\text{IN}} = \frac{1}{j(w_{\text{in}}c_1 \pm n \times c_1)} \tag{8.9}$$

where w_{in} is the frequency of the input signal and n is defined by the harmonics of the square-wave modulation as:

$$n = \frac{4}{\pi}\sum_{k-1,3\ldots}^{\propto} \frac{1}{k} \times k \times w_{\text{clk}} = \frac{4}{\pi}\sum_{k=1,3\ldots}^{\propto} w_{\text{clk}} \tag{8.10}$$

The first scaling factor within the summation formula comes from the odd harmonics of a square wave, and the second scaling factor comes from the increasing frequency of the odd harmonics. These two factors cancel each other leading to a pure summation of the clock frequency as the scaling factor of C_1. Note that the effective range of C_1 is defined by the resistance of the chopping switches and the capacitance of the instrumentation amplifier.

iv. **Noise Performance:** Chopper modulation eliminates the flicker noise of the core amplifier. This means that the noise equation of this architecture can be written as Eq. 8.6, with the key improvement that the core amplifier noise is only defined by the thermal noise.

8.4.3 *Summary and Comparison of Instrumentation Amplifier Topologies*

In this section, we have presented four different instrumentation amplifier architectures, which are commonly used in biopotential measurement applications. These architectures are categorized according to their gain elements as resistive or capacitive and according to the use of compensation techniques.

It should be noted that the correct amplifier choice for a given application should combine the lowest possible power with sufficiently good performance. In addition to the discussion on amplifier specifications, Fig. 8.13 compares the power efficiencies of the instrumentation amplifiers presented in this section. It is interesting to see that the best efficiency is achieved by

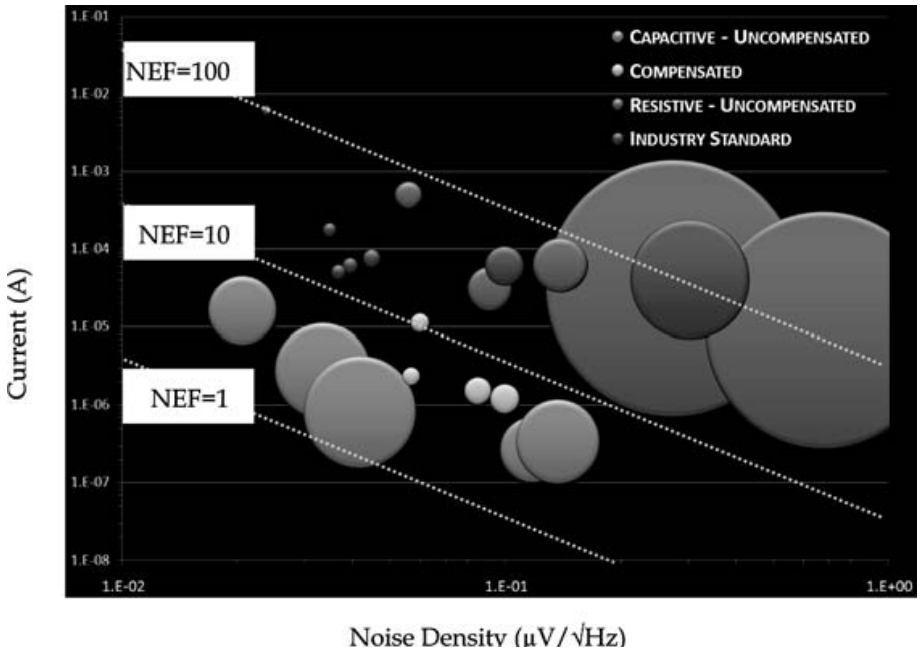

Figure 8.13. Comparison of different instrumentation amplifiers in terms of their power efficiency. Y-axis indicates the current consumption of the instrumentation amplifier and x-axis indicates the noise density of the instrumentation amplifier. Dashed lines indicate the constant contours of noise efficiency factor (NEF) lines [8]. The diameter of a circle indicates the total integrated noise of the instrumentation amplifier. See also Color Insert.

capacitive uncompensated amplifiers. This is due to the fact that this instrumentation amplifier topology uses only a single active circuit, which is the core OTA. Unfortunately, the implementations using the capacitive uncompensated instrumentation amplifier topology achieve relatively large total integrated noise. On the other hand, due to the presence of the servo loop, compensated amplifiers have slightly worse efficiency, but they have very much lower total integrated noise compared with capacitive uncompensated instrumentation amplifiers. Finally, uncompensated resistive and industry standard three opamp [13–15] instrumentation amplifiers have simply much worse power efficiencies preventing their use in ambulatory biopotential measurement applications.

It can be concluded from this discussion that capacitive uncompensated instrumentation amplifiers can be the preferred choice for applications that can live with relatively large circuit noise level.

Table 8.1. Comparison of different instrumentation amplifier architectures

	Figure 8.7 Resistive uncompensated	Figure 8.8 Capacitive uncompensated	Figure 8.11 Resistive compensated	Figure 8.12 Capacitive compensated
DC Headroom	Limited	Maximum	Limited	Limited
CMRR	Low to Moderate	Low to Moderate	High	High
Input Impedances	High	High	High	Moderate
Noise Performance	Large 1/f noise	Large 1/f noise	Low Noise	Low Noise

Last but not the least, Table 8.1 summarizes the properties of instrumentation amplifiers presented in this section and presents the comparison of their key characteristics. Not only due to their bad power efficiency but also due to their lower performance specifications, resistive uncompensated instrumentation amplifiers are not the preferred choice for portable biopotential monitoring systems. On other hand, the rest of other three instrumentation amplifier topologies are very attractive in terms of their power efficiencies as well as their performance specifications.

In addition to having the best power efficiency, uncompensated capacitive amplifiers have very large input impedance and maximal DC headroom. If we refer to Fig. 8.6, these characteristics match very well with the requirements of AP and LFP measurements.

The compensated version of this amplifier, i.e., compensated capacitive instrumentation amplifiers, additionally removes flicker noise and improves the CMRR of the instrumentation amplifier. On the other hand, the equivalent input impedance is reduced due to the capacitive nature of the input impedance. Hence, this architecture is generally used for ECoG applications where lower noise and higher CMRR performance are expected from the instrumentation amplifier, but lower input impedance values can be allowed by the application due to the use of invasive electrodes with large surface area.

Finally, resistive compensated instrumentation amplifiers have very high input impedance, low noise, and high CMRR. Therefore, their characteristics match very well with noninvasive biopotential measurements, where a high performance instrumentation amplifier is required.

8.5 Signal Integrity Problems in Ambulatory Measurements

In addition to the noise sources such as circuit noise, interference to measurement setup, and irrelevant biological signals that correlate the biopotential measurements, another important noise source in ambulatory measurements is motion artifact signals. These potentials occur in the electrode cables, in the skin, and at the electrode/electrolyte interface. While artifacts coming from cables can be reduced by appropriate electrode cables, artifacts from the skin and electrode/electrolyte interface are difficult to reduce by design.

The main source of the motion artifacts, as the name implies, is the motion present in ambulatory measurements. During ambulatory measurements, the subject/patient is continuously moving. The relative movement of electrode and tissue leads to significant voltage fluctuations called motion artifact signal. It is assumed that the source of the motion artifact signal is the fluctuations in the polarization generated at the electrode-tissue interface and within the tissue [16].

These motion artifact signals may have large amplitudes, and also they may have similar frequency spectrum as biopotential signals. Hence, amplitude-based or frequency-based algorithms, or the algorithms combining both methods, can significantly suffer from these motion artifacts reducing the reliability of biopotential measurements in ambulatory conditions. Therefore, there is a strong need for the methods and circuits that can enable the differentiation between the medically irrelevant motion artifact signals and the biopotential signals.

8.5.1 *Methods Focusing on Motion Artifact Reduction in Biopotential Recordings*

There have been several proposals in the literature trying to tackle the motion artifact problem in ambulatory biopotential recordings. Time synchronous averaging or median is one of them [16]. This is a classic technique widely used for cleaning of signals like ECG. However, these methods require the use of several ECG beats in

order to obtain one single clean beat, and, therefore, beat-to-beat variations are removed.

Another technique is the use of fixed filters [17]. This technique could give the information about beat-to-beat variations. However, it does not adapt to the time-variant properties of noise and requires some previous knowledge of the noise. Furthermore, the design of linear phase band-pass filters is critical in preventing distortion of the ECG. Wavelets have also interesting filtering properties [18]. Wavelet de-noising based on a decomposition of the signal using wavelets that are highly adapted to the ECG gives a higher resolution in lower frequencies and, therefore, could lead to better removal of noise. However, wavelet processing is computationally heavy for ultra-low power ambulatory biopotential recording systems.

An alternative technique called adaptive filtering was introduced in the 60's as a new tool for ECG de-noising [19]. Since then it has become more and more popular, and several approaches have been implemented. For noise removal, the input of an additional reference signal is required, which should be highly correlated with the noise. Several reference signals have been investigated with successful results such as motion measured by accelerometers [20], skin-electrode impedance [21], and skin stretch measured by optical sensors [22].

Finally, independent component analysis (ICA), which contains beat-to-beat information and requires no reference signal, aims to reconstruct the ECG and motion artifact signals [23]. This method is, however, also computationally expensive and requires more than one ECG lead. Table 8.2 gives a summary of existing methods that are trying to reduce the effect of motion artifact signals on biopotential recording applications.

Among these methods, adaptive filtering is gaining more and more attention since it focuses on removing motion artifacts from biopotential signals without affecting ECG signal parameters. Also another advantage of adaptive filtering is the fact that it is computationally less heavy compared with ICA analysis.

8.5.2 *Readout Circuits for Adaptive Filtering*

Compared with other methods, adaptive filtering presents several advantages. First of all it can be implemented using a single-lead

Table 8.2. Summary of methods found in the literature for artifact reduction in biopotential recordings (ECG)

	Advantages	Disadvantages
Time Synchronous Averaging	Low computational complexity	Nonstationary information removed, require fiducial point demarcation.
Filter Banks	Beat-to-beat information	No adaptation to time-varying noise
Adaptive Filtering	Adapts to time-varying noise, no previous knowledge of noise required	Choice of reference signal is critical, implying complexity in reliable noise measurement
Independent Component Analysis	No reference signal required	Multiple leads required. Computationally heavy.

biopotential measurement (unlike ICA analysis), it does not require the history of the signal (unlike time synchronous averaging), and it can successfully eliminate noise from biopotential recordings even though the noise source looks exactly similar to the biopotential signal of interest (unlike filter banks). Therefore, there has been a specific attention on adaptive filtering over the last years. However, a critical requirement for adaptive filters is the extraction of a signal from the biopotential measurement system that is correlated with the motion artifact but uncorrelated with ECG signals.

A possible approach to tackle this problem is to collect data from other sensors that have maximum correlation with motion artifact signals and minimal correlation with biopotential signals. Several approaches has been tried in the literature, such as using accelerometers to sense the subjects' movement, electrode bend sensors to detect the motion of electrodes, skin stretch sensors to sense the movement of skin, and electrode impedance measurement circuits to correlate electrode impedance measurement with the motion artifact [22, 24–27].

Among these possibilities, the use of electrode-tissue impedance as the reference signal input to adaptive filters is gaining even more attention, since it does not require the use of an additional sensor and also since the characteristics of the electrode-tissue interface is actually responsible for motion artifact signals. Therefore, different circuit topologies that focus on the simultaneous measurement of biopotential signals with the electrode-tissue impedance have

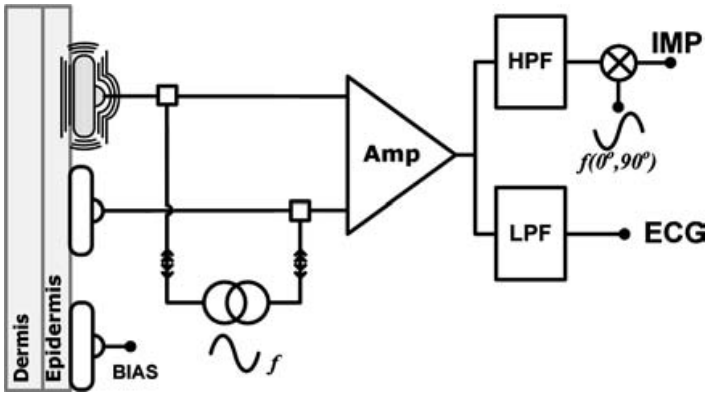

Figure 8.14. A circuit topology proposed by [26] to monitor biopotential signals simultaneously with the electrode-tissue impedance.

been proposed. Figure 8.14 shows the most common circuit topology for the measurement of biopotential signals with the electrode-tissue impedance [26]. A sinusoidal stimulation current is injected differentially to the measurement electrodes. The AC current frequency is selected such that it is out of the frequency band of biopotential signals. Hence, the low-pass filtering of the instrumentation amplifier output can extract biopotential signals, whereas the demodulation of the output with the AC current frequency can extract the electrode-tissue interface impedance. Although this technique can be very effective for extracting the required information, it requires the use of sinusoidal current generation blocks, which can be very power consuming in CMOS technology.

An alternative measurement method focuses on using the bias electrode for extracting the electrode-tissue impedance simultaneously with biopotential signals [27], Fig. 8.15. Instead of using a fixed bias voltage for the human body, an AC bias voltage is used. Under ideal conditions, this bias voltage appears as a common-mode signal to the instrumentation amplifier. However, as stated in Eq. 8.1, the finite input impedance of the instrumentation amplifier combined with the mismatch of the electrode impedances converts the common-mode signal into differential mode. Hence, the electrode-tissue impedance can be extracted using the formula:

$$V_{\mathrm{IMP}} = \frac{|\delta Z_{\mathrm{ELEC}}|}{Z_{\mathrm{IN}}} \times V_{\mathrm{BIAS}} \tag{8.11}$$

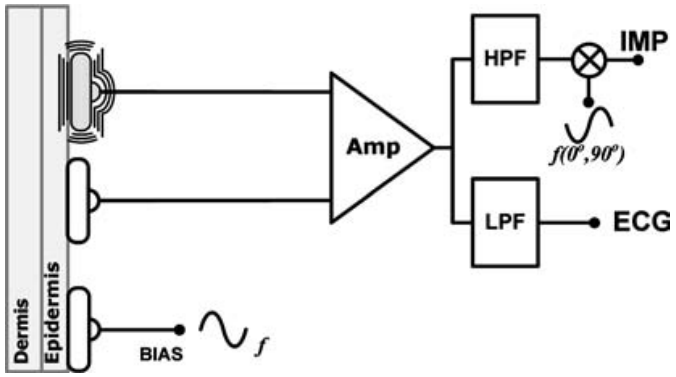

Figure 8.15. Another circuit topology proposed by [27] to monitor biopotential signals simultaneously with the electrode-tissue impedance. The method modulates the bias voltage of the patient to extract the electrode-tissue impedance.

However, it can be seen from the measurement method that this principle relies on the finite input impedance of the instrumentation amplifier, which simply contradicts with the requirements from biopotential measurement systems, i.e., as large as possible input impedance.

Last but not the least, a recent circuit topology that focuses on the measurement of electrode-tissue impedance with low-power dissipation has been proposed by [28], Fig. 8.16. This circuit uses square wave current stimulation rather than sinusoidal current stimulation. This way an integrated circuit with much lower power

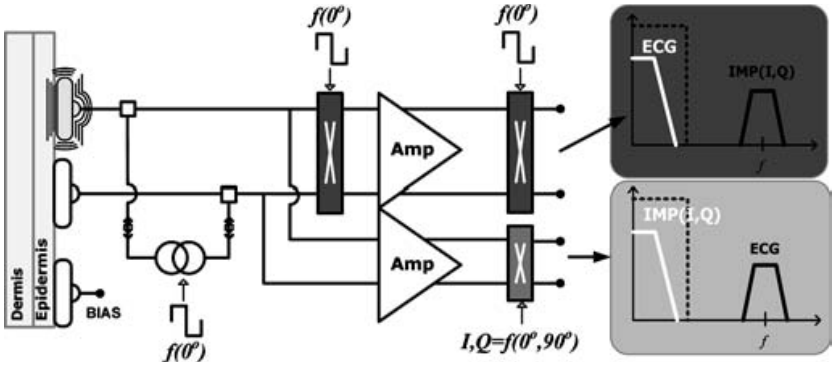

Figure 8.16. The implementation of electrode-tissue impedance measurement circuit operating simultaneously with the biopotential measurement circuit [28]. Instead of sinusoidal current sources and analog modulators/demodulators, chopper-modulation technique has been employed. See also Color Insert.

dissipation can be realized. This is due to the fact that the development of sinusoidal currents and their demodulation only relies on the use of chopper modulators leading to a significantly lower power dissipation compared with the methods using sinusoidal currents and analog modulators/demodulators.

8.6 Conclusion

As the cost of health care is increasing, the remote monitoring of people is gaining more and more attention. This leads to a strong urge for portable medical signal monitoring systems that can be integrated into people's daily lifestyle. It is expected from these systems that they can collect data, analyze these, and communicate the results to medical professionals.

One of the most important building blocks for this system is the realization of the analog front-end circuit that can consume minimal power and can still meet the challenging requirements of medical monitoring systems. In this chapter, we have reviewed the most commonly used instrumentation amplifier topologies for different medical signal acquisition. It can be seen from this review that there is not a single instrumentation amplifier topology ideal for different biomedical signal acquisition applications; rather, it is more important to consider the requirements of the application and select the instrumentation amplifier topology accordingly.

In addition to instrumentation amplifier design, an important challenge in ambulatory medical signal measurement systems is motion artifacts. These signals, though do not have any medical relevance, appear together with biomedical signals and reduce the reliability of signal analysis software. Several methods that address this problem have been presented in this chapter. The advantages and disadvantages of these different techniques have been reviewed. In particular, adaptive filtering approach has been favored due to its advantages over other methods. Last but not the least, the implementation of analog circuits that can generate the reference signal of an adaptive filter is described, and low-power techniques for such circuits have been presented.

References

1. OECD health data 2009.
2. B. Gyselinckx, R. Vullers, C. Hoof, J. Ryckaert, R. Yazicioglu, P. Fiorini, and V. Leonov (October 2006) Human++: Emerging Technology for Body Area Networks, in *2006 IFIP International Conference on Very Large Scale Integration*, pp. 175–180.
3. J. G. Webster (1992) *Medical Instrumentation: Application and Design*, 2nd edn, Houghton Mifflin, Boston (Mass.).
4. J. C. Huhta, and J. G. Webster (March 1973) 60-Hz Interference in Electrocardiography, *IEEE Transactions on Biomedical Engineering*, **20(2)**, pp. 91–101.
5. B. Razavi (2001) *Design of Analog CMOS Integrated Circuits*, McGraw-Hill.
6. C. Toumazou, et al. (1989) Novel Current-Mode Instrumentation Amplifier, *IEEE Electronics Letters*, **25(3)**, pp. 228–230.
7. R. Olsson, A. Gulari, and K. Wise (20–22 March 2003) A Fully Integrated Band-Pass Amplifier for Extracellular Neural Recording, in *Proceedings of the 1st International IEEE EMBS Conference on Neural Engineering*, pp. 165–168.
8. R. Harrison, and C. Charles (June 2003) A Low-Power Low-Noise CMOS Amplifier for Neural Recording Applications, *IEEE Journal of Solid-State Circuits*, **38(6)**, pp. 958–965.
9. C. Enz, E. Vittoz, and F. Krummenacher (June 1987) A CMOS Chopper Amplifier, *IEEE Journal of Solid-State Circuits*, **22(3)**, pp. 335–342.
10. R. F. Yazicioglu, P. Merken, R. Puers, and C. Van Hoof (6–9 February 2006) A 60 μW 60 nV/$\sqrt{}$Hz Readout Front-End for Portable Biopotential Acquisition Systems, *IEEE International Solid-State Circuits Conference Digest of Technical Papers*, pp. 109–118.
11. R. F. Yazicioglu, P. Merken, R. Puers, and C. Van Hoof (3–7 February 2008) A 200 μW Eight-Channel Acquisition ASIC for Ambulatory EEG Systems, *IEEE International Solid-State Circuits Conference Digest of Technical Papers*, pp. 164–165.
12. T. Denison, K. Consoer, A. Kelly, A. Hachenburg, and W. Santa (2007) 2.2 μW 97nV/$\sqrt{}$Hz, Chopper Stabilized Instrumentation Amplifier for EEG Detection in Chronic Implants, *IEEE International Solid-State Circuits Conference Digest of Technical Papers*, pp. 162–163.

13. M. A. Smither, D. R. Pugh, and L. M. Woolard (September 1977) CMRR Analysis of the 3-op-amp Instrumentation Amplifier, *IET Electronics Letters,* **13**, pp. 594.
14. A. C. Metting van Rijn, A. Peper, and C. A. Grimbergen (1990) High-Quality Recording of Bioelectric Events; Part 1: Interference Reduction, Theory and Practice, *Medical and Biological Engineering and Computing*, **28**, pp. 389–397.
15. M. Burke, and D. Gleeson (February 2000) A Micropower Dry-Electrode ECG Preamplifier, *IEEE Transactions on Biomedical Engineering*, **47(2)**, pp. 155–162.
16. H. Tam, and J. G. Webster (1977) Minimizing Electrode Motion Artifact by Skin Abrasion, *IEEE Journal on Biomedical Engineering*, **24**, pp. 134–139.
17. V. Afonso, W. Tompkins, T. Nguyen, K. Michler, and S. Luo (1996) Comparing Stress ECG Enhancement Algorithms, *IEEE Engineering in Medicine and Biology Magazine*, **15**, pp. 37–44.
18. P. Augustyniak (2007) Separating Cardiac And Muscular ECG Components Using Adaptive Modeling in Time-Frequency Domain, in *Proceedings of the WACBE World Congress on Bioengineering*.
19. B. Widrow, J. Glover, J. R. J. McCool, J. Kaunitz, C. Williams, R. Hearn, J. Zeidler, J. Eugene Dong, and R. Goodlin (1975) Adaptive Noise Cancelling: Principles and Applications, *IEEE Journal Proceedings*, **63**, pp. 1692–1716.
20. D. Tong, K. Bartels, and K. Honeyager (2002) Adaptive Reduction of Motion Artifact in the Electrocardiogram, in *Proceedings of the 2nd Joint EMBS/BMES Conference*, **2**, pp. 1403–1404.
21. P. H. Devlin, R. G. Mark, and J. W. Ketchum (1984) Detecting Electrode Motion Noise in ECG Signals by Monitoring Electrode Impedance, in *Proceedings of Computers in Cardiology* pp. 51–56, Los Angeles.
22. P. Hamilton, M. Curley, R. Aimi, and C. Sae-Hau (2000) Comparison of Methods for Adaptive Removal of Motion Artifact, *Computers in Cardiology*, **27**, pp. 383–386.
23. M. Milanesi, N. Martini, N. Vanello, V. Positano, M. Santarelli, R. Paradiso, D. De Rossi, and L. Landini (2006) Multichannel Techniques for Motion Artifacts Removal From Electrocardiographic Signals, in *Proceedings of the 28th Annual International Conference of the IEEE Engineering in Medicine and Biology Society*, pp. 3391–3394.
24. P. T. Gibbs, L. B. Wood, and H. H. Asada (2005) Active Motion Artifact Cancellation for Wearable Health Monitoring Sensors Using Collocated

MEMS Accelerometers, in *Proceedings of the Society of Photo-Optical Instrumentation Engineers*.

25. P. S. Hamilton, and M. G. Curley (1997) Adaptive Removal of Motion Artifact, in *Proceedings of the 19th Annual International Conference of the IEEE Engineering in Medicine and Biology Society*, pp. 297–299.
26. J. Ottenbacher, M. Kirst, L. Jatobá, U. Großmann, and W. Stork (2007) An Approach to Reliable Motion Artifact Detection for Mobile Long-Term ECG Monitoring Systems Using Dry Electrodes, in *Proceedings of the IV Latin American Congress on Biomedical Engineering*.
27. T. Degen, and T. Loeliger (August 2007) An Improved Method to Continuously Monitor the Electrode-Skin Impedance During Bioelectric Measurements, in proceedings of 29th Annual International Conference of the IEEE *Engineering in Medicine and Biology Society*, pp. 6294–6297.
28. R. F. Yazicioglu, P. Merken, R. Puers, and C. Van Hoof (February 2010) A 30 μW Analog Signal Processor ASIC for Biomedical Signal Monitoring, in *Proceedings of IEEE International Solid-State Circuits Conference Digest of Techical Papers*, pp. 124–125.

Chapter 9

Network and Medium Access Control Protocol Design for Wireless Body Area Networks

Jamil Y. Khan
School of Electrical Engineering and Computer Science,
The University of Newcastle, Callaghan,
NSW, 2308 Australia
Jamil.Khan@newcastle.edu.au

Wireless body area network (WBAN) is considered a special-purpose sensor network designed to collect and transmit physiological data within a short distance. Physiological sensors could be either implanted or placed external to a human body. A WBAN will generally operate either as a stand-alone personal area network (PAN) or as an interconnected network in telemedicine applications. The network configuration of a WBAN will depend on medical applications. In a WBAN design, the MAC protocol plays a very important role, which determines the QoS (Quality of Service) performance, energy efficiency, and reliability of a network. This chapter introduces the WBAN architecture, MAC protocols, and network design techniques for medical applications. The chapter initially introduces different network topologies followed by fundamental description of MAC protocols and its classifications,

Wireless Body Area Networks: Technology, Implementation, and Applications
Edited by Mehmet R. Yuce and Jamil Y. Khan

ISBN 978-981-4316-71-2 (Hardcover), ISBN 978-981-4241-57-1 (eBook)
www.panstanford.com

and then reviews several WBAN-specific MAC protocols. Following the MAC protocol discussions, the chapter introduces energy management techniques and patient monitoring design techniques. Some simulation results of a WBAN are presented to analyze the performance of a CSMA/CA MAC-based WBAN networks.

9.1 Introduction

The WBAN is becoming a key component of future telemedicine-based health care systems [1, 11]. Applications of WBAN in future can bring a number of key benefits to the health care system. Major benefits include collection of medical data of patients from their home or workplaces, collection of transient medical data in a cost-effective manner, patient's mobility, reduction of health care cost, improved patient care based on the availability of timely information, etc. On some occasions, collection of transient data for different diagnostic purposes could be difficult. In many cases, patients need to be kept under observation in hospitals or clinics for an extended period to detect certain medical conditions, which is quite resource intensive. Applications of WBAN could reduce the cost of patient observation and treatments because health care professionals can access those data from anywhere anytime.

A WBAN is a special-purpose wireless sensor network with specific QoS requirements [21]. Key requirements of a WBAN are low packet transmission delay, low to medium data transmission rate, near zero packet loss, minimum delay jitter, and low energy usage. Performance of a WBAN system will depend on a number of factors, which include the hardware design, applications characteristics, and network design.

In a patient monitoring system, data transmission reliability and latency is extremely important. The reliability and latency of a WBAN will largely depend on the design of physical (PHY) and medium access control (MAC) layers. For optimum network efficiency and data transmission reliability, the MAC layer needs to be designed to suit specific needs of specialized applications. Considering the importance of WBAN applications, an IEEE standard group (IEEE802.15.6 working group) is working on the

development of a body area network architecture [22]. The new standard will define the PHY and MAC layer management issues, which could be used to develop a low cost, ultra-low power and highly reliable wireless network. Reliability of a medical network can be defined in terms of its main QoS parameters such as delay profile, delay jitter, and information loss rate. Performance and reliability of a WBAN will depend on the PHY and MAC layer procedures as well as on the network topology used. Following sections examine network architecture and MAC protocol design issues for a WBAN-based patient monitoring system. Before moving into the discussion of design issues, first we examine the network and MAC protocol design requirements of a WBAN. Listed below are some of the main requirements of a WBAN.

- A WBAN should be able to support a range of medical applications, which includes acquiring data samples from periodic and nonperiodic sources and transmitting information to a service node within a maximum fixed delay without any loss of critical information [2]. Also, the system should be able to support exchange of nonmedical and control information with various remotely controlled appliances.
- A WBAN should be able to operate in a power-constrained environment where power sources such as battery should operate for a reasonably longer period of time. Power savings for implantable nodes are more critical than other nodes. Power savings can be achieved by combining PHY and MAC layer procedures [3].
- A WBAN should be self-healing, secure, and reliable.
- A WBAN should support data rates between few tens of kbs to several Mbps to host a range of applications such as images and video clips.
- A WBAN should support QoS management features to offer priority services. Particularly when a critical patient is monitored, the system must guarantee the delivery of critical information to a service node. For medical data, the main QoS features will be the transmission delay and the packet loss.

- A WBAN may incorporate a narrow transmission band (400 MHz or 2.4 GHz) together with the UWB (ultra-wide band) technology to cover different environments.
- A WBAN should operate and coexists with other network devices operating in similar frequency bands. Also, a WBAN should be able to operate in a heterogeneous networking environment, where networks of different standards may cooperate with each other to acquire information from different sensors.

In this chapter, we concentrate on the network design techniques, mainly concentrating on the MAC and energy management issues. The MAC protocol implements a set of rules, which are used to coordinate packet transmissions in a shared transmission channel environment. Numerous MAC protocols have been designed to support applications in different types of networks. In this chapter, we review several MAC protocols that could be used for WBAN applications. This chapter also introduces an interconnected WBAN architecture, which can be used to support remote patient monitoring applications. Rest of the chapter is organized as follows. Section 9.2 introduces the network topology and configurations used in wireless sensor networks. Section 9.3 introduces the basic properties and classifications of MAC protocol. Section 9.4 discusses scheduled and polling MAC protocols and their design features. Section 9.5 discusses the random access protocols and their design features. Section 9.6 presents a hybrid MAC protocol design proposed by the IEEE 802.15.4 standard. Section 9.7 discusses the energy management issues in a WBAN. Section 9.8 presents the design of several patient monitoring networks. Section 9.9 presents some simulation results of a ZigBee-based patient monitoring system. Conclusions are presented in Section 9.10.

9.2 Network Topologies and Configurations

A communication network can be designed using a number of different topologies that define the geometrical position of communication nodes [12]. A network topology is generally selected

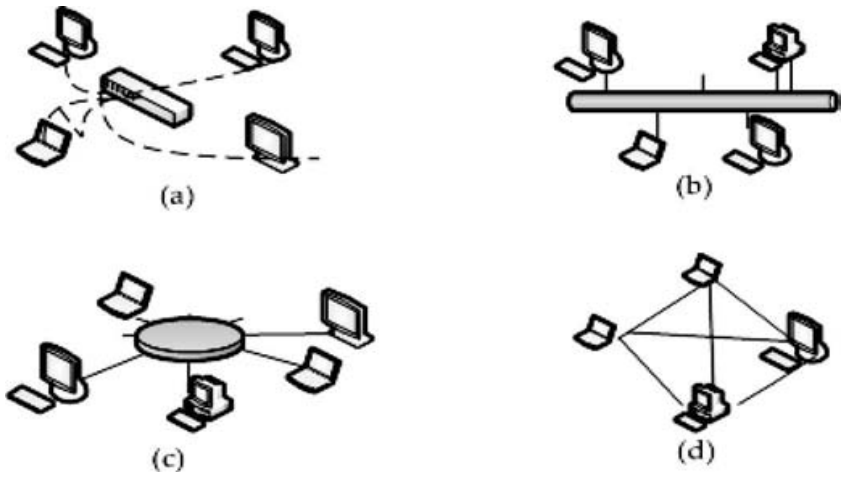

Figure 9.1. Network topologies: (a) centralized star topology; (b) distributed bus topology; (c) ring topology, and (d) fully connected mesh topology.

based on application scenarios. There are five standard topologies generally used: *star, bus, tree, ring, and mesh*. Figure 9.1 shows commonly used four network topologies. The star topology consists of a centralized controller where all nodes communicate directly with the central controller to exchange information. Information between nodes is also exchanged via the central controller. The star configuration is suitable for WBAN applications where a central controller can collect and aggregate all physiological data from different sensors. The bus structure supports communication among various nodes in a decentralized manner. The topology has been developed to support operation of random access protocols with minimum protocol control overhead. Bus structure could be used for wired body area network applications. The ring topology is used to transmit packets in a contention free mode using a token, which is a form of distributed polling network. In the ring topology, nodes are connected in a serial closed-loop fashion where a control packet, known as the *token*, schedules the transmission of packets. A ring network may not be suitable in a WBAN due to longer transmission delay and maintenance of token overhead. A ring network is generally more suitable for high data rate networks with high volume of traffic. The mesh topology is used to provide full connectivity between all nodes. The topology provides many redundant transmission links, thus offering higher reliability in a

large network. The mesh network topology is quite often used in large sensor networks to provide full connectivity. For a WBAN application, the mesh topology is not very useful because each body area network will generally consists of limited number of nodes. However, a mesh topology could be used in a large hospital network for multi-patient monitoring systems.

The star topology in a wireless sensor network is organized as a cluster tree topology where the star network controller becomes the cluster head. A cluster-based network forms a PAN; in case of a wireless clustered network, it is referred to as the WPAN (Wireless PAN) where the cluster head becomes the PAN coordinator [14]. All data communication in a cluster network goes through the cluster head or in case of a PAN/WPAN, through the PAN coordinator. The PAN coordinator is also responsible for resource allocation, synchronization, allocation of a PAN ID. Each node in a cluster has a unique cluster ID, which is controlled by the cluster head. The cluster head/PAN coordinator is a more computationally powerful data processing device, which collects information from all its sensor nodes. In WPAN, nodes are generally classified into two types: full functional device (FFD) and reduced functional device (RFD). The FFD can operate in three modes serving as PAN coordinator, a coordinator, or as a network node. The RFD can only act as a simple node, which forward information to a coordinator or to a PAN coordinator. RFDs can exchange information only through the PAN coordinator. To operate a cluster-based WPAN, it is necessary to activate a star configuration. In a cluster-based WPAN, a FFD is activated first, which may establish its own network and become the PAN coordinator. All devices in a PAN are identified by the PAN identifier. Once the PAN identifier is chosen, the PAN coordinator allows other nodes to join the network. WPAN network devices generally do not implement the full seven-layer protocol stack; rather, it implements only the lower two layers of the protocol stack, i.e., the physical layer (PHY) and the data link layer (DLL).

9.3 Basics of Medium Access Control Protocols

A sensor node is designed using the standard OSI (open system interconnection) model to exchange data using communication links.

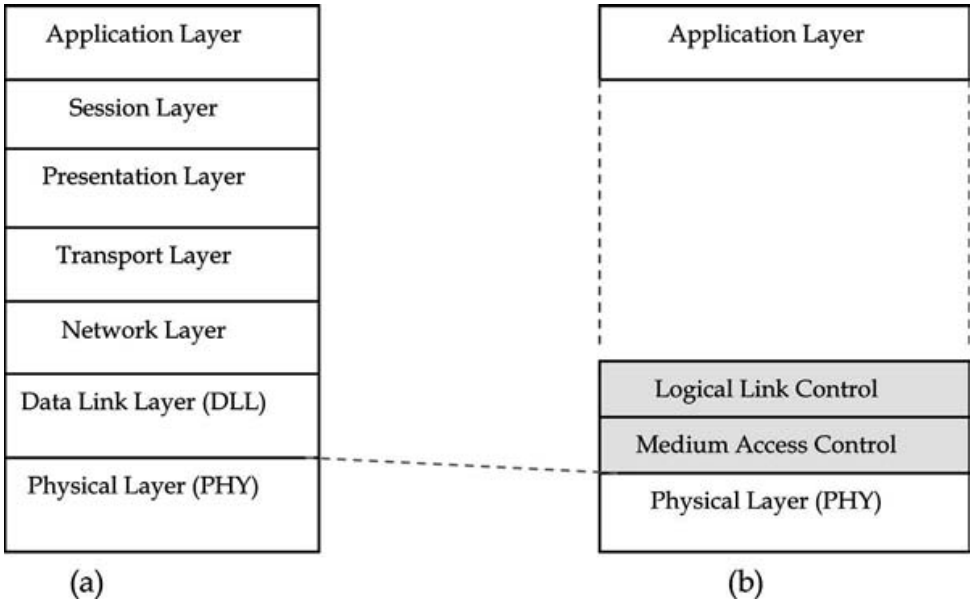

Figure 9.2. Protocol stack (a) standard OSI model, (b) three-layer WPAN model.

The basic seven-layer OSI model and the corresponding WPAN protocol stacks are shown in Fig. 9.2. A WPAN device will only implement two and half or three layers of the OSI model, which includes PHY, mostly a sublayer of the DLL, and an application layer [14]. The physical layer is responsible for the transmission and reception of physical signals using the hardware resources. The PHY layer is also responsible for conditioning of transmitted and received signals suitable for the transmission channel. A WPAN will generally only use the MAC sublayer of the DLL. The MAC protocols are used in multiuser communication networks to transmit packets in a contention-free mode. The MAC protocol allow users to transmit packets in an interference free mode while maintaining high network throughput and low delay, thus supporting QoS of different types of traffic. MAC protocols can also control transmission power of a node by optimizing packet transmission and scheduling processes. MAC protocols have been evolving over the last few decades to support different type of networks and applications. MAC protocols can be classified into two broad categories: fixed assignment- and dynamic assignment-based protocols as shown in Fig. 9.3. Fixed assignment-based protocols use the basic properties

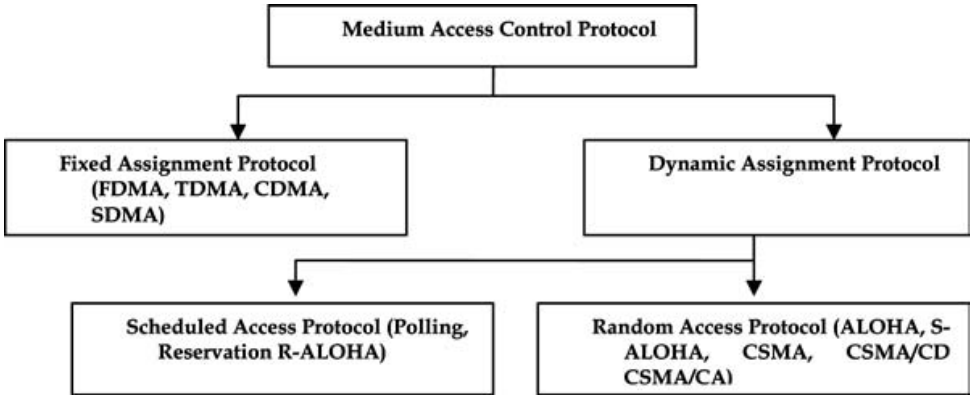

Figure 9.3. MAC protocol classifications.

(time, frequency, and code) of a transmission channel to divide transmission resources and use the allocated resources to transmit their information in an interference-free mode. Fixed allocation-based MAC protocols generally do not alter allocated transmission resources during the length of a data session. Fixed assignment protocols can also be viewed as scheduled protocols. Some of the commonly used fixed resource assignment-based protocols are: FDMA (frequency-division multiple access), TDMA (time-division multiple access), CDMA (code-division multiple access), and SDMA (space-division multiple access) [13, 14]. For WBAN applications, some of the systems use the TDMA technique to accommodate multiple sensor nodes.

Dynamic assignment-based protocols are generally known as ON demand-based protocols where transmission resources are allocated to transmitters only when an actual transmission takes place. ON demand protocols are more suitable for bursty non-periodic traffic sources. The dynamic access protocols are again divided into two subclasses: scheduled access protocol and random access protocol. A scheduled access protocol allocates transmission resources in a dynamic manner, but it coordinates transmission either in a centralized or in a distributed manner to avoid any interference or collisions. The random access protocols are also ON demand-based transmission system where transmitters may use some channel state information to transmit a packet. The channel sensing mechanism is used to reduce the probability of collisions. A random access protocol generally requires less

control signaling compared to the scheduled access protocols. Transmission of control signaling has implications on a network. Large control overheads could reduce the information transmission capacity of a WBAN; also control signaling could increase the power requirements of a node or a network.

One of the key issues of a WBAN MAC protocol design is power management. Power requirements of a WBAN will be jointly determined by PHY and MAC layers. The MAC protocol can also control the physical layer of a node to control the sleep cycle of a node, which can affect the energy requirements of a node. The MAC protocol can determine sleep, wakeup, and listening periods depending on the application. Most of the medical applications will generate low duty cycle data. The MAC protocol can synchronize various application duty cycle data and intelligently control the sleep cycle of a transceiver [13, 4]. Further discussion on MAC energy management is provided in Section 9.7.

QoS requirements of a WBAN protocol are simple and straightforward. Most of the nodes will transmit information in a periodic manner using fixed size packets. It is necessary for a WBAN that packets can be transmitted in a contention-free mode with high guarantee of delivery and low packet transmission delay. For WBAN applications, most cases packet retransmission needs to be avoided because generally the sensor nodes will have little buffer and processing capabilities. Also, retransmission of packets will reduce the life of the WBAN energy source. Some of the specialized WBAN nodes connected with a tiny camera may require higher transmission bandwidth to transmit images. A WBAN can prioritize its transmission by assigning different priority value to different traffic sources. QoS requirements of WBAN applications have not been strictly defined yet. With the further development of the IEEE 802.15.6 standard, it is expected that QoS profiles for medical data will be developed for future applications.

9.3.1 *WBAN Traffic Characteristics*

Traffic sources in a WBAN are mostly medical sensors which generate data depending on the properties of physiological signals. Table 9.1 lists some of the common diagnostic medial signal

Table 9.1. Physiological signal characteristics

Parameter	Value	Frequency (Hz)	Data Rate (bits/sec)[1]
ECG Signal (single lead)	0.5–4 mV	0.01–250	4,000
Respiratory rate	2–50 breaths	0.1–10	160
Blood pressure	10–400 mm Hg	0–50	800
EEG	3–300 μV	0.5–60	960
Body temperature	32–40°C	0–0.1	1.6
EMG (Electromyogram)	10 μV–15 mV	10–500	8,000
GSR (Galvanic Skin Reflex)	30 μV–3 mV	0.03–20	320

[1] Assuming an 8 bit A/D converter is used.

properties. Data rate presented in the fourth column is calculated based on the Nyquist frequency and an 8 bit/sample A/D converter. The table shows that signal data rate and interarrival time vary quite significantly. All the traffic generated by various sensors is periodic in nature because of constant sampling rate. For patient monitoring applications, it is also possible that sensors could transmit data on demand basis, i.e., a sensor transmit data only when a sensor is being queried by a medical device. In addition to following medical data, a WBAN may also support image or video transmission from either an implanted or an on-body camera. Data rate for imaging devices will depend on application and image/video resolution and frame size. A WBAN also needs to cater for irregular events such as irregular heart beat when a patient may enter into a critical stage. WBAN can be used in an ambulatory environment where a critical patient could be monitored over a communication network. Hence, it is apparent from this discussion that a WBAN generally needs to cater for periodic data, but on occasions it may be necessary to cater for nonperiodic bursty data. Besides these signals, a WBAN may need to transmit/receive control signals from specialized medical devices. In future for specialized applications, a WBAN will probably consist of sensor nodes as well as diagnostic medical appliances.

9.4 Scheduled Protocols

Packet transmissions in a WBAN will be controlled by the MAC protocol. A scheduled MAC protocol will allocate transmission

resources to all nodes in an orderly manner using either a fixed or a dynamic channel assignment technique. In a WBAN transmission resource is the radio channel. In communication networks many other scheduled protocols are used in various systems; however, for WBAN applications we focus on TDMA and polling protocols because they are most likely to be used for medical applications. For certain applications, fixed assignment protocols can be modified into adaptive assignment protocol such as ATDMA (advanced TDMA) protocol.

9.4.1 *TDMA Protocol*

Time-division multiple access (TDMA) is one of the simplest fixed assignment protocols [14]. TDMA protocol allows multiple users to share a transmission channel by dividing the transmission time among users. The TDMA protocol operates using a frame and slot structure where a frame consists of a numbers of time slots with a fixed frame length. The time slots are allocated to each transceiver that can transmit or receive information using their allocated time slots. The TDMA frame is synchronous in nature, which repeats at a constant rate. For a WBAN, TDMA links can be configured either in a full duplex or in a half duplex manner. Duplex links could be frequency-division duplex (FDD) or a time-division duplex (TDD). The implementation of FDD links is more costly because each node needs to use a duplex filter, whereas a TDD link can be easily implemented using a software scheduler on a node. For WBAN applications, most of the time traffic will be transmitted in one direction, i.e., sensor to the coordinator; hence, either a full duplex or a TDD link will be suitable. A TDMA-based WBAN can be designed using both star and bus network topology. TDMA, being a synchronous packet transmission system, can handle periodic traffic more efficiently than nonperiodic traffic. A TDMA link can provide fixed packet transmission delay, which is one of the key requirements of a WBAN. Another benefit of the protocol is the use of minimum number of overhead bits to support information transmission due to the fixed channel allocation technique. The main disadvantages of a TDMA-based system are scalability and efficient support of nonperiodic traffic sources. The energy efficiency of

a TDMA-based system can be enhanced by synchronizing the transmission frame/slots with the sleep cycle of a node [5]. Energy efficiency issues are discussed in Section 9.7.

9.4.2 *Polling Protocol*

Polling is one of the dynamic scheduled access mechanisms that can be used to support packet transmission in any size network [6]. A polling network is a centralized network architecture where a central network node controls the transmission of packets, avoiding any collisions of packets. Unlike the TDMA protocol, polling protocols generally do not require any fixed allocation of resources but require higher level of signaling to transmit information. Figure 9.4 shows a typical wireless polling network and its polling sequence operating in star topology. This figure shows that all nodes in the network are polled by the central controller in a round-robin manner to receive data from these nodes. The controller sends a poll message to a specific node, which in reply can send either a data packet or a NACK (negative acknowledgement) specifying that it has no data to send. To minimize packet transmission, the controller could include the acknowledgement of the pervious transmission with the current poll message. Since a poll message is a broadcast message, all nodes in the network can receive the message. However,

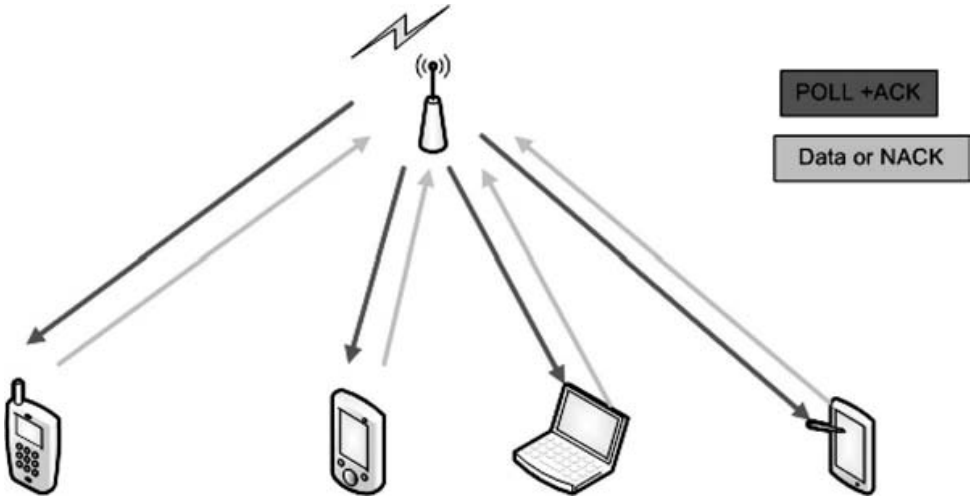

Figure 9.4. A wireless polling network showing the polling sequence. See also Color Insert.

the controller specifies in the poll message which node should reply. A polling system is more flexible than a TDMA-based system due to direct interaction between the controller and a node. In this case, each node can be polled based on its transmission requirements. For example, Table 9.1 shows that an ECG sample is produced after every 2 ms whereas an EMG sample is produced every 0.2 ms. If we assume 10 signal samples are transmitted in a packet, then the ECG node needs to be polled after every 20 ms whereas the EMG node needs to be polled every 2 ms. This flexibility is not available in a TDMA-based system. Also, in polling networks, nodes can transmit different size data packets depending on the application. These flexibilities are achieved at the expense of extra signaling and the processing capability of the central controller. Polling sequence and rate can be tailored for different applications.

Packet transmission delay in a polling network will depend on the polling cycle time [12]. As shown in Fig. 9.4, nodes are polled in a sequential manner where a node can transmit a packet after it has been polled. So the packet transmission delay will be the sum of packet queuing time and the packet transmission time. In a WBAN, propagation delay is extremely small, which can be neglected. In a network if the controller is polling all the nodes at a constant rate, then the polling cycle will be the sum of polling time and packet transmission time. For example, if the poll and acknowledgement packet transmission time is 1 ms and the data packet transmission time is 2.5 ms, then each node in Fig. 9.4 will be polled after every 14 ms assuming that all nodes always have data to transmit when polled. In this case, if the first node generates data in the middle of a polling cycle, then it must wait 8 ms before a poll message is received and then it will take another 2.5 ms to transmit the data packet to the controller, incurring a 10.5 ms delay for the transmission. For a WBAN application, if the nodes are polled by matching their data generation rate, then the polling cycle length will vary due to the number of active nodes in each polling cycle. A polling system can be tailored to cater for data with different priorities and data generation rates. A high priority node can be polled more frequently compared to lower priority nodes. Polling networks are easily scalable, particularly when the controller finds a new node it can include the new node in its polling list or delete a node from

the list if a node does not respond to subsequent polls. The energy requirements of a polling network can be variable depending on the system design. Polling networks can be implemented using star, bus, and ring topologies. For WBAN application, a star topology-based polling network will be most suitable because the bus and ring topologies introduce higher polling and message transmission delay.

9.5 Random Access Protocols

Random access protocols are generally used in distributed networks without the presence of any central coordinator [12, 13, 14]. Nodes using random access protocols coordinate the transmission of packets to minimize collisions. Nodes using this class of protocols will use the transmission channels only when they have data to transmit. Random access protocols are more complex than scheduled access protocols; hence, careful approach is required to design the protocol and the network. Random access protocols are in use in local area networks for many years. This class of protocol is also becoming popular for wireless sensor network applications. The IEEE 802.15.x standard defines a number of random access protocols for a number of short-range wireless networks [7]. Bluetooth was the first short-range low-to-medium data rate MAC protocol developed for WPAN applications. Later the Bluetooth protocol was modified to develop the IEEE 802.1.5.1 standard. Subsequently, a low-power low data rate standard, the IEEE 802.15.4 MAC protocol, was developed for the wireless sensor network applications. In the IEEE 802.15.4 standard, which consists of PHY and MAC layers, functionalities have been merged with application layer protocols to develop the ZigBee standard. The IEEE 802.15.x family of protocols is becoming one of the major wireless sensor networking standards. The IEEE 8021.5.6 protocol is currently under development to support WBAN applications. It is most likely that the new WBAN standard will be based on the CSMA/CA (carrier sense multiple access/collision avoidance) standard [22].

One of the first random access protocols used in computer networks is the ALOHA protocol. Since the development of the

ALOHA protocol, many other random access protocols have been developed by further enhancing the features of the protocol. A more efficient random access protocol known as the CSMA protocol was developed from the ALOHA/S-ALOHA (slotted ALOHA) protocols [12]. Using the CSMA protocol, each transmitting node checks the status of the transmission channel to decide whether to transmit a packet or not. The philosophy of the CSMA protocol is *listen before transmit*. The CSMA protocol can operate either in persistent or in a nonpersistent mode. In the persistent mode, a node constantly monitors the status of the transmission channel and starts transmitting as soon as the channel becomes free. Using the nonpersistent mode, a node constantly monitors the status of a transmission channel. When the channel becomes free, the node then can either immediately transmit or backoff for a certain period of time to check the channel again. The decision whether to transmit a packet or to defer a packet transmission depends on the transmission probability value generated by a random number generator at the MAC layer. The nonpersistent protocol has been developed to minimize the probability of collisions by randomizing packet transmission times. The persistent protocol may offer a low transmission delay at the expense of higher level of packet collisions, whereas the nonpersistent CSMA protocol offers network stability at the expense of higher average packet transmission delays. A compromised version of the CSMA protocol is quite widely used and is known as the p-persistent protocol, where the probability of a transmission or a deferment can be adjusted by selecting appropriate value of p, which is the packet transmission probability [15]. In a CSMA/CA network, an ACK packet is used to inform the transmitter about the status of a transmission. A receiver transmits an ACK packet when a packet is successfully received. A transmitter may not receive an ACK packet if either the transmitted packet is incorrectly received due to channel errors or packet transmission is unsuccessful due to collisions. A transmitter can successfully transmit a packet if all other transmitter remains silent for a period of maximum propagation delay, t_p, of the network. After the propagation delay, all nodes of a network become aware of the transmission and will not attempt to transmit any packet while the current transmission continues.

Channel sensing and *p* persistent techniques are combined to improve the performance of a network by trying to avoid collisions. CSMA/CA-based protocols also use another collision avoidance technique particularly to reduce the *hidden* user problem [13]. A wireless terminal is considered to be a *hidden* terminal if the terminal is unable to receive transmitted signal(s) from its neighboring terminals because that particular terminal could in a RF (radio frequency) shadow region compared to its neighboring terminals. In such case, a hidden terminal could increase the packet-collision level in a network. A *hidden* terminal may be unaware of other transmission or transmission attempts and inadvertently interfere with other transmissions. The CSMA/CA protocol uses the RTS/CTS (ready to send/clear to send) signaling to reduce the *hidden* terminal problem. However, for a WBAN application, the *hidden* terminal will not be a problem due to the size of the network and the proximity of terminals.

Random access protocols can offer several advantages for WBAN applications. The first advantage is the support of periodic and nonperiodic traffic with equal efficiencies. Using a random access protocol, a transmitter can initiate a packet transmission on its own only when a packet is generated at the node. Unlike the scheduled access protocol, the transmitter does not need to wait for a time slot or a poll message to initiate a transmission. In a WBAN when periodic and nonperiodic traffic are mixed, the problem of collision reduces due to randomization of packet generation rate. Second, the main advantage of the random access protocol is the energy consumption [16]. A node using the random access protocol can stay in the sleep state most of the time, waking up only when transmitting a packet. Another key advantage of a random access protocol is the scalability. The networking size can easily be increased or decreased without the need for any software or hardware upgrade. The main disadvantage of the random access protocol is variable packet delay due to collisions at the higher traffic load. However, this issue is not a problem for WBAN applications if the volume of traffic is kept relatively lower compared to the network transmission capacity. Random access protocols have been widely accepted for sensor network applications. Industrial standards such as ZigBee, Bluetooth, etc are quite widely used in sensor network applications.

Both ZigBee and Bluetooth standards are based on the CSMA/CA-based MAC standards, which can be successfully used in WBAN applications.

9.6 Hybrid MAC Protocol

Previous sections discussed scheduling and random access protocols, which are used in different wireless sensor networks. For sensor network applications, the IEEE 802.15.4 standard defines a hybrid packet transmission structure, which allows transmitters to use both contention and guaranteed transmission modes [14, 17, 18]. The hybrid transmission structure has been developed to efficiently support periodic, intermittent, and repetitive low latency data. The IEEE 802.15.4 standard supports the hybrid transmission mode using the super frame structure as shown in Fig. 9.5. The super frame structure is controlled by the PAN coordinator. The coordinator periodically sends beacons that identify the PAN. The PAN is identified by a 16 bit PAN identifier. The beacon frame also contains information, a list of outstanding frames, and other system-related parameters. The time interval between beacon signals is constant, and users can select a value which is a multiple of 15.38 ms. The maximum beacon interval time could go up to 252 ms. Two consecutive beacon signals form a *super frame* separated by 16 equally sized time slots as shown in Fig. 9.5. The super frame is subdivided into active and inactive periods. All nodes, including the coordinator, can turn off their transceivers and go into a sleep

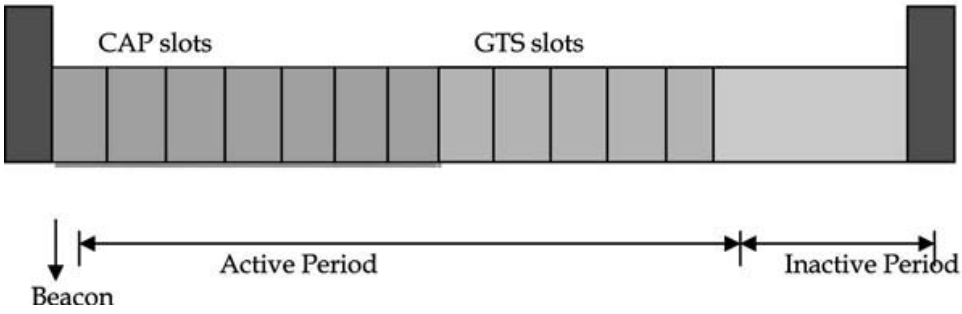

Figure 9.5. IEEE 802.15.4 MAC super frame structure. See also Color Insert.

state during the inactive period of a super frame. The active period consists of 16 timeslots, where each timeslot is divided into two groups. One set of slots forms the *contention access period* (CAP) and the rest of the slots become part of the *guaranteed time slots* (GTS). The length of the active and inactive periods is configurable, hence allowing system design flexibility to accommodate different types of applications. The CAP slots can be accessed using the standard CSMA/CA procedure, whereas the GTS slots are allocated by the coordinator when a request is made by a node. The flag in the request packet indicates whether the slot will be used to transmit or receive. Upon receiving a slot request, the coordinator will allocate a slot when appropriate resources are available. GTS slots are organized in the same way as the TDMA slots. When GTS slots are used for transmission, a node can schedule its sleep cycle and wake up just before the time slot starts and send the packet. On the other hand, when a CAP slot is used, the node must wake up in advance and perform carrier sensing or other collision avoidance procedures before it can initiate a transmission.

The super frame structure based on the hybrid MAC protocols could be well suited for WBAN applications where medical data with different QoS requirements will be transmitted. Sensors of lower priority data could be transmitted using CAP slots, whereas high priority data could be transmitted using GTS slots. The super frame structure is configurable where the active and inactive periods can also be adjusted.

9.7 Energy Management in a WBAN

Energy management of nodes is one of the crucial requirements of WBAN deployments [19]. WBAN's could be deployed for patient monitoring continuously for several days. In such deployments, it is important that nodes are designed properly so that the battery lasts for the duration of the deployment. Energy requirements of a node will depend of a number of factors, which includes the PHY layer and hardware design, MAC layer-controlled sleep cycle, MAC packet scheduling, and the application requirements. Source of energy of WBAN nodes will be a battery whose life cycle will

depend on the way a node will drain the energy. There are a number of battery phenomena that could affect both charge and discharge outcomes. Two important phenomena are the rate-capacity effect and the recovery effect. The rate-capacity effect of a battery is the idea that drawing a large, continuous current from a battery will lead to it depleting faster than expected. In an ideal battery, it is assumed that the voltage stays constant for the entire life of the battery, and then drops to zero. In the real world, however, voltage is not constant over the entire life of the battery; instead it drops during the discharge. This drop in voltage during the discharge varies in severity from battery to battery. In all cases though, it leads to a perceived drop in battery capacity. Figure 9.6 shows the typical rate capacity characteristics of a battery for a continuous and an intermittent load situation [6]. An intermittent transmission is a typically ON/OFF scenario when a transmitter sends data for a brief period and then moves into an inactive state. When a transmitter moves to an inactive state, the battery load will be low, allowing the battery to recover. Figure 9.6 shows that an intermittent application could prolong the life of a battery due to the recovery effect. For a continuous discharge, the slope remains fairly constant as expected. For an intermittent discharge, however, the battery is able to recover some of the lost charge, resulting in a piecewise-continuous discharge slope. This results in the battery having a longer lifetime.

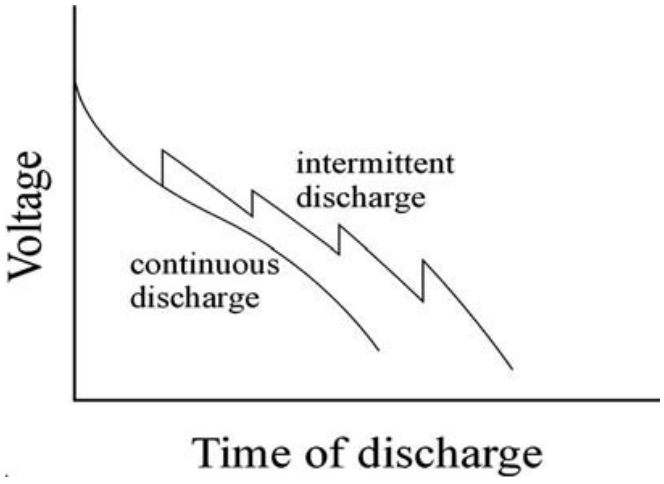

Figure 9.6. Battery charging and discharging phenomena.

As shown in Fig. 9.6, the battery lifetime of WBAN node can be sufficiently extended by appropriately designing the packet transmission schedule in a network. It is possible to optimize the power requirements of a sensor node by using the following techniques.

- Lower data transmission frequency by the use of data aggregation technique.
- Reduction of proportional frame overhead by selecting appropriate payload size.
- Appropriate use of power management algorithms to coordinate the sleep cycle.
- Placement of nodes in a WBAN to avoid poor transmission channel conditions.

To achieve significant advantages, each of the above techniques needs to be carefully designed and integrated with the MAC protocol. Lower the data transmission frequency can reduce the power requirements of a sensor node. Average current consumed by a sensor node is described by Eq. 9.1. The equation clearly shows that transmission duration and average transmitter current requirement will increase with more frequent transmission of data. In addition to power requirement for data transmission, there are other power requirements. For example, for a CSMA/CA-based network for every packet transmission the node needs to listen to the channel when the node acts as a receiver. On the basis of channel sensing result, it either transmits or backoff for a certain duration. It is necessary for reduced power consumption that during the backoff period, the transmitter goes to the standby mode. The transmitter could be switched ON by a timer for further channel sensing and transmission decision-making. This intermittent ON/OFF process of the transmitter will help to prolong the battery. Data aggregation technique will lower frequency of data transmission as well as reduce the frame overhead [10]. For example, EEG data samples are generated at a rate of 60 Hz, i.e., samples are generated after every 16.66 ms. If we use 8 or 12 bit A/D converter and transmit each sample individually, then the payload size will be very small. Instead of a single sample if a number of EEG samples are combined and transmitted every second, then the payload size becomes

480 bits or 720 bits depending on the chosen A/D converter word size. In this case the transmitter will use far more less power to transmit without introducing unnecessary delays. Similarly the data aggregation technique can be applied for a multichannel sensor networks as described in Chapter 5. In case of a multichannel WBAN, samples from different channels will be aggregated and encapsulated in a single packet. The use of data aggregation technique has another advantage for a random access network. The data aggregation technique will reduce the number of packet transmission attempts for a CSMA/CA network, thus reducing the packet collision probability and increasing the QoS of a WBAN. In a random access network such as ZigBee or Bluetooth network, transmission of fewer large packets will reduce the collision level as well as the transmission power requirements.

$$I_{\text{avg}} = T_{\text{txon}} \times I_{\text{txon}} + T_{\text{rxon}} \times I_{\text{rxon}} + (1 - T_{\text{txon}} - T_{\text{rxon}}) \times I_{\text{stb}} \quad (9.1)$$

T_{txon} is the transmission duration including packet transmission and other time necessary to support the transmission.
T_{rxon} is the packet reception time.
I_{txon} is the average current consumed by the transmitter.
I_{rxon} is the average current consumed by the receiver.
I_{stb} is the current consumed by the transceiver module in the standby mode.

The coordination of sleep cycle is important for the node power management. On the transmitter side, sleep cycle can be easily managed because the transmitter blocks can be turned ON or OFF by the MAC layer depending on a node's transmission requirements. The transmitter circuit will only be turned ON when the MAC layer receives packet from its higher layer. Switching the receiver block between ON/OFF modes is a critical issue. A node needs to know when it is expecting a packet or a control packet. For a TDMA or a poll-based system, the receiver can easily work out the packet reception time. In this case, the receiver can be left in the standby or sleep mode until the packet reception time. However, using the CSMA/CA protocol the packet reception time is not fixed until the transmitter and receiver work out the packet transmission schedule. In case of WBAN applications, sensor nodes will be mostly

transmitting information packets. Sensor nodes will only receive acknowledgement packets or occasional control packets. On the other hand, the coordinator or the PAN coordinator will receive information and control packets from different sensor nodes; hence, it may be necessary for the coordinator the keep the receiver circuit ON for the duration of its operation. A receiver can save more power when receiving data from periodic sources. However, a WBAN node should be able to receive data from different type of sources, i.e., periodic and nonperiodic sources.

Power transmission requirement of a node is also influenced by transmission channel conditions. Although a WBAN will operate within a small area, it is possible that the receive signal will be corrupted when transmission loss increases due to the placement of a node or a posture of a body. Most of the modern transmitters will transmit at a minimum power level, which will allow the receiver to correctly receive the transmitted information. For a multi-patient monitoring system, it is important that mutual interference should be minimum; hence, all transmitters must transmit at their optimum power level. An optimum power level is defined as the minimum power level at which a receiver can receive packets with zero bit error rate (BER). The transmitter power level requirement will increase with increasing transmission losses. A transmitter can adjust its transmission power level based on the feedback from the receiver, which informs the link condition. A receiver can send a feedback using a positive ACK when a packet is received correctly or a NACK (negative acknowledgement) in case a packet is received incorrectly. For a WBAN, transmission of ACK or NACK could introduce additional traffic load. It may be possible that ACK or NACK mechanism can be used only for critical data leaving other nodes to transmit data at a predetermined power level. In this case, a receiver may occasionally send explicit instruction to the transmitter to change its power level to maintain zero BER level.

To examine the effect of sensor node power management issues, we use the CC2420 chip parameters for sample calculations. The receiver module of the chip operates on a fixed power level, which consumes 18.8 mA current. The transmitter power requirement depends on the transmitted RF (radio frequency) signal power. Transmitter current values are listed in Table 9.2 for different

Table 9.2. CC2420 IC current consumptions

RF signal Power Level (dBm)	Transmitter Current (mA)
−25	8.5
−15	9.9
−10	11
−5	14
0	17.4

transmitted RF signal powers. The table shows that the chip can operate at six different power levels. Strongest RF signal will consume an average current of 17.4 mA, whereas the weakest RF signal will consume 8.4 mA of current. The standby current of the IC is 1 μA. The required RF signal power level will be determined by the transmission loss value. The transmission loss value can be calculated using the Eq. 9.2. For WBAN applications, additional losses can add with the transmission loss. Major additional loss component value is the tissue absorption particularly for implanted nodes. The received signal strength should be at least equal to or greater than the receiver sensitivity. The receiver sensitivity of the CC2420 IC is -95 dBm. If a transmitter is generating a RF signal at −25 dBm, then the total transmission loss should be lower than 70 dBm.

$$PL\ (d)\ \text{dB} = PL\ (d_0) + 10\gamma \log_{10}\left(\frac{d}{d_0}\right) + X_\sigma, \qquad (9.2)$$

where $PL(d_0)$ is the path loss at the reference distance, $d_0$is the reference distance, and X_σ is the shadowing variance.

Let's now analyze the power requirements of a CSMA/CA-based transmitter. The CSMA/CA protocol uses a series of procedures before a node can transmit a packet. Figure 9.7 shows the packet transmission sequence of the CSMA/CA protocol. When the transmitter senses a channel and initially it finds busy, then it waits until the channel is idle for the DIFS (distributed intra-frame spacing) duration. After the DIFS waits the transmitter enters

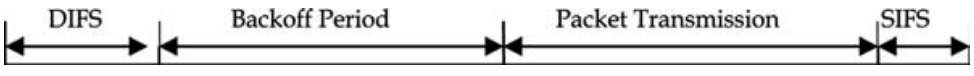

Figure 9.7. Packet transmission sequence of the CSMA/CA protocol.

into a backoff period. Following the backoff, the transmitter could transmit in a contention mode, i.e., transmit a packet with a risk of collision. After the transmission of a packet, the terminal will wait for a period known as SIFS (short IFS) [12]. After the SIFS, the transmitter is expected to receive an ACK packet. Typical CSMA/CA timing parameters are as follows. The DIFS length is 50 μs, minimum back period is 140 μs, and the SIFS value is 10 μs. The packet transmission time will depend on the packet size. The IEEE 802.15.4 CSMA/CA packet will consist of PHY layer header of 6 byte, MAC layer header 5 byte assuming a 2 byte address field and a 2 byte FCS (frame check sequence). Total transmission time of a packet can be calculated using Eq. 9.3 neglecting the propagation delay. For a 40 byte/320 bit payload, the packet length will be 51 byte, and the packet transmission time of the CC2420 transmitter will be 1.63 ms. Table 9.3 lists current consumption values of different CSMA/CA parameters for different RF signal levels. Values listed Table 9.3 is calculated based on the assumptions that a packet can be transmitted in the first attempt; hence, these are best case values. For example, when the channel is sensed and found to be busy, the transmitter will backoff and resense the channel after the backoff period. A node senses the channel after each backoff period until it finds the channel free for a DIFS period when it could initiate a packet transmission. In this case power transmission requirements of packet can significantly increase. If we assume that a WBAN node is using two 900 mAH AA batteries, then a node can transmit 30,706 packets at 0 dBm RF signal level. The same node can transmit 60,851 packets at -25 dBm RF signal level effectively doubling the lifetime of a battery for the best transmission case condition. In a

Table 9.3. Current consumption values for different CSMA/CA parameters

				Packet transmission	
RF Signal (dBm)	DIFS (μA)	SIFS (nA)	Backoff (nA)	(μA)	Total (μA)
0	0.94	0.01	0.14	28.36	29.31
-5	0.94	0.01	0.14	22.82	23.76
-10	0.94	0.01	0.14	17.93	18.87
-15	0.94	0.01	0.14	16.13	17.07
-25	0.94	0.01	0.14	13.85	14.79

WBAN node, if one packet is transmitted per second, then the battery can potentially last up to 17 h for the −25 dBm RF signal level. Packet retransmissions can affect the life of a battery. However, in the best transmission case, the battery can last slightly longer than the above value due to the battery recharging phenomena as shown in Fig. 9.6.

$$T_{\text{packet}} = T_{\text{DIFS}} + T_{\text{BO}} + \frac{L}{R} + T_{\text{SIFS}} \tag{9.3}$$

where T_{DIFS} is the DIFS period, T_{BO} is the backoff period, L is the packet length in bits, R is the transmission rate in bits/s, and T_{SIFS} is the short interframe spacing.

Discussions in this section clearly show that the battery lifetime of WBAN will depend on selected MAC parameters and traffic characteristics. Data aggregation and packet scheduling technique will significantly influence the power requirements of a node. For a polling network node, transmission power requirements will depend on the design of polling message and cycle.

9.8 Patient Monitoring Network Design

In this section, we will introduce the general rules and techniques of WBAN design. As mentioned earlier, WBAN is a special-purpose, low-to-medium rate sensor network with a typical operating diameter of about 1 m. The number of nodes in a typical WBAN is expected to be around 2 to 5 with each node connected to a number of sensors. So the data rate requirements per node will not be significantly high unless a node is connected to a camera or supporting multichannel ECG data. Main QoS requirements of a WBAN are low latency, no or very minimum packet loss, and low power transmission to avoid any tissue heating or damage. Two main networking requirements of a WBAN are low power consumption and the network should be a scalable one. The size of WBAN could range from a single-body network to an interconnected multi-body network operating as a multi-hop network as shown in Fig. 9.8. To design a WBAN, the following design issues need to be considered.

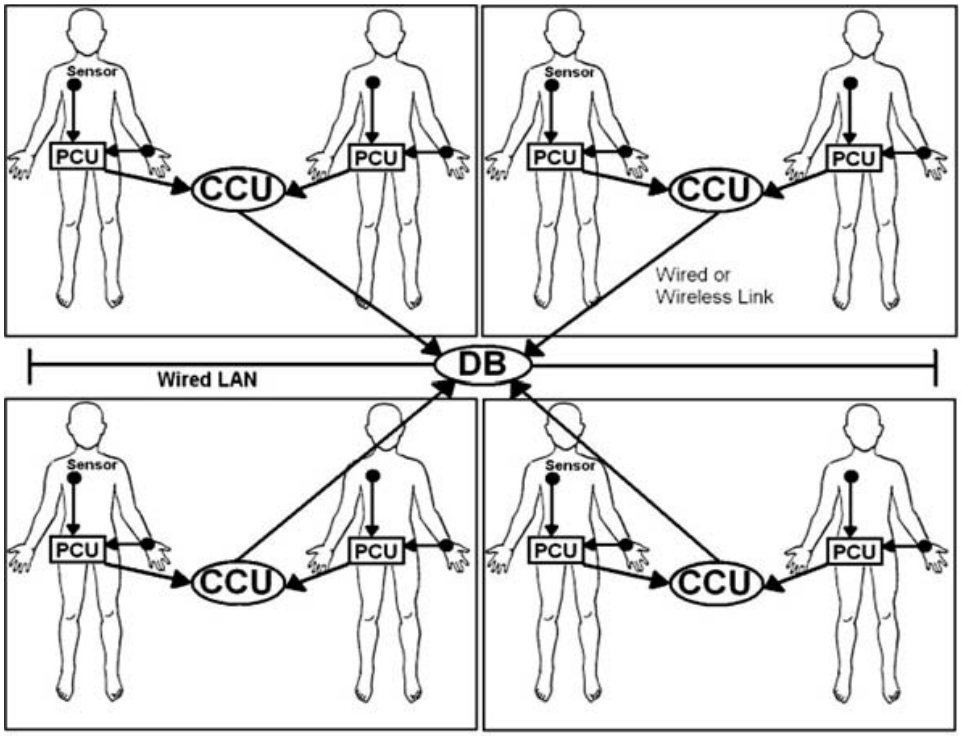

Figure 9.8. A WBAN-based multi-patient monitoring system. Each patient's body forms a PAN and consists of sensor nodes and the PCU.

9.8.1 *Transmission Capacity Requirements*

It is necessary to develop the data profile of a network. Most of the data will be generated from physiological sensors. It is important to examine all physiological signal characteristics and calculate the minimum and maximum transmission data requirements of each signal. Data must be characterized in terms of their interarrival rate, which is related to the sampling rate and the data burst size. The designer should also consider the dynamic range of signals and select the sampling rate and A/D converters appropriately. Next, the aggregate data volume should also be considered. The aggregate data rate is important for the selection of the networking standard and the MAC protocol. The total aggregate data rate of a network should not exceed 85–90% capacity of a scheduled access network. In case of a random access network, the aggregate data rate should be below 75% of the maximum capacity of the network. Performance of a network could be significantly affected by the

aggregate data rate of a network. It is also important to work out the peak-to-average data transmission rate of a network. In a WBAN, most of the time data rate will be steady, but monitoring a critical patient may occasionally generate peak traffic. If the peak-to-average traffic rate is high, then occasional data loss can happen due to congestions or buffer overflow.

9.8.2 *PHY and MAC Layer Parameter Selection*

It is important to select PHY and MAC parameters appropriately to satisfy the requirements of a WBAN [8]. Although PHY layer parameter selections are difficult because in most cases PHY parameters are decided by the hardware design. Important PHY layer parameters include the modulation and coding techniques that can influence the performance of a sensor node. The modulation and coding parameters determine the receiver sensitivity and effective packet error rate (PER) based on the channel BER. Selection of MAC parameters is very crucial in determining performance of a network. Sections 9.4–9.7 have discussed various features of various MAC protocols. MAC protocol selection will influence the power consumption, QoS values, and scalability issues. Scalability could be an important issue for the WBAN deployment. A WBAN should offer flexibility to health care professionals so that they either increase or decrease the number of nodes on a body without any major change in software or hardware. It will be useful if the MAC protocol can adaptively accommodate varying number of sensor nodes. The TDMA protocol will not be very scalable unless software modifications are done on the network controller side. Using a polling network, it is possible to add or remove sensor nodes without major changes [11]. From the scalability point of view, the CSMA/CA protocol offers the best advantage. In case of CSMA/CA protocol, since there are no central coordination necessary, any new sensor node will read the broadcast message of its PAN coordinator and will register with PAN coordinator for data exchange within a WBAN.

Most of the sensor networking standards such as code blue, Wibree, Mica2, etc. have selected the CSMA/CA MAC protocol to develop medical applications [21]. As mentioned above, a CSMA/

CA-based system is adaptive in nature, requires minimum control signaling, and supports required QoS for a WBAN. Also, the CSMA/CA protocol can be optimized for different application scenario by appropriate selecting transmission and priority parameters. The IEEE 802.15.4-based hybrid protocol could be a good choice for future systems where low priority nodes can transmit packet using the contention mode, whereas the GTS mode could be used for high priority nodes. Hybrid protocol will also offer excellent scalability feature.

9.8.3 *Network Configuration*

The network configuration of a WBAN depends on the deployment scenario. A WBAN can be deployed either in a stand-alone mode or in an interconnected mode [20]. A stand-alone mode could be used for a single-patient monitoring system, whereas an interconnected mode could be used for either monitoring multiple patients or monitoring a patient remotely. A stand-alone mode will simply form a PAN with a CCU (central coordination unit) as the PAN coordinator. In this mode, the CCU will collect all sensor data and store them for further processing [9]. The protocol architecture will be very simple where application layer can directly communicate with the MAC layer for transmitting and receiving information. In this mode, we don't need to consider mobility because it is most likely that all nodes will be attached to a single human body and the CCU will also be located either on the body or close to the body in a fixed location.

Multi-patient or remote monitoring system will require a complex networking configuration where we need to construct a multi-hop network as shown in Fig. 9.8. In this case, each body will form a single PAN and all PANs need to be connected to a PCU (patient coordinator unit — a wearable device that can be carried, wearable by the patient). Each CCU will act as a router for their PAN and transmit all its sensor data to the PCU. The PCU could be connected to a hospital LAN (local area network) or to the Internet. All CCU's can transmit their packets in the broadcast mode with PCU address in the MAC address field. The multi-hop network needs to introduce some form of packet scheduler to minimize the contention if the CSMA/CA protocol is used. In the multi-hop

networking scenario, all sensor nodes, CCUs, and PCU will transmit packets in the contention mode; hence, it is necessary that some form of power control and packet scheduling need to be introduced. For example, sensor nodes in each PAN should transmit their packets with a minimum power sufficient for their CCU to receive packets with zero BER. If sensor nodes transmit at a higher power level than necessary, then it may be possible packet transmissions in other PANs will be affected. It is also necessary that CCUs should introduce some form of pseudo synchronized packet scheduling so that all of them should not try to send their packets at the same time. Each CCU will individually adjust its transmitter's power based on its PCU link characteristics.

A multi-patient or a stand-alone patient monitoring system could be converted to a remote patient monitoring system by introducing the TCP/IP (transmission control protocol/Internet protocol) stacks either at the CCU or at the PCU. The TCP/IP protocol stack will allow these nodes to communicate with external networks. In this case no modifications will be necessary for the sensor nodes because they still will be sending their data within their PAN.

Some deployment scenario of WBANs may require the network to support mobility. For example, mobility support is necessary when a patient is monitored while they are carrying out their day-to-day activities either at home or at workplace. Mobility can introduce two additional problems: the variation of link characteristics and routing data to the appropriate node. If a mobile patient is supported within an indoor area, then it is most likely an access point will be used within the home or work area, which can connect it with the CCU to exchange data. In that case, we might use a Wi-Fi access point to connect with the CCU. It is preferable to use a Wi-Fi access point because it can support a larger cell size — up to 300 m link distance and relatively cheaper to implement. In this case, we need to develop a CCU with dual protocol stack. If we assume a ZigBee-based PAN and a Wi-Fi-based access point, then CCU will act as a router and it will have vertically split protocol stack supporting the ZigBee protocol on the PAN side and Wi-Fi on the CCU to access point link. Basically in this case, the CCU will be built using dual radio IEEE 802.15.4 and IEEE 802.11. If a WBAN requires mobility at a higher speed for sports training applications, then wireless standards such

as GSM or UMTS or WiMAX should be used because Wi-Fi can only support mobility up to 5 km/h.

9.9 Performance Analysis of a WBAN

In this section, we will analyze the performance of a ZigBee-based patient monitoring system. Figure 9.8 shows a typical WBAN network architecture for mult-patient monitoring applications. The data from each sensor are transmitted to a PCU. The PCU aggregates sensor data and transmit them to a CCU located at a short distance. The PCU can gather data from both implant and external nodes. The CCU acts as an intermediate network device that forward the collected medical data to a patient database (DB) where remote monitoring devices can retrieve patient's data for health care professionals. Each patient body forms a PAN where a PCU acts as the PAN coordinator. In this WBAN application, the CCU acts as the PAN coordinator for all PCUs, which can be considered a second-tier network. The network operates in a multi-hop fashion where each link transmits data using the CSMA/CA protocol. Relay nodes such as the PCU and the CCU can be configured in two ways. One of the configurations is that these nodes simply act as forwarding node, i.e., it receives a packet and simply forwards the packet to the next link. Other configuration is that these nodes receive multiple packets from sensor nodes and then encapsulates multiple packets and forwards a larger packet. The former approach can be implemented with nodes with low-processing capability, whereas the latter approach reduces the number of transmission access on the forward link, thus reducing the probability of collisions for a ZigBee-based system.

In this section, we present the performance of the above WBAN for multi-patient monitoring applications using an OPNET simulation model [23]. Using the simulation model, initially we analyze the performance of the data aggregation technique. To analyze the performance of data aggregation technique, we use a single PAN model. Figure 9.9 shows the packet loss and packet generation rate of the simulated WBAN for different payload sizes. Result shows that with the increasing payload size, the throughput

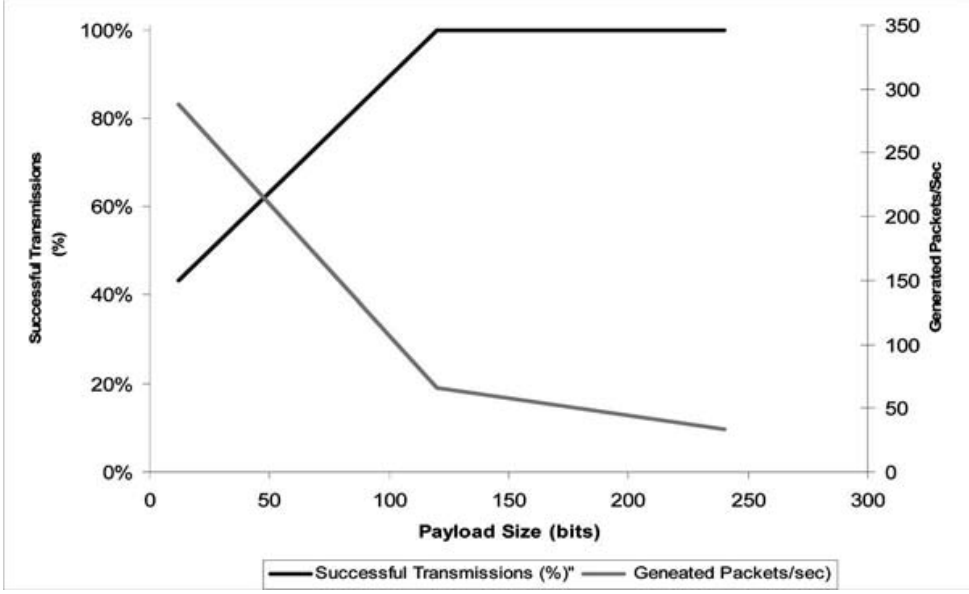

Figure 9.9. WBAN packet loss and packet generation rate for different data aggregation rate/payload size. See also Color Insert.

of WBAN increases due to fewer transmission attempts. The figure shows that with single sample/payload (12 bits), the network only managed to successfully transmit 120 packets, offering a success rate of 40%. When the average payload size is increased to 120 bits/packet, then the number of transmission attempts is dropped to 50 packets/second, offering 100% throughput in the network. The improvement in the efficiency can be achieved due to lower contention level in the network, which resulted fewer packet losses due to the packet dropping threshold. In this simulation, we used five retransmission attempts as the packet dropping threshold, which means if a packet is unable to successfully transmit a packet in five successive attempts, then the packet is dropped from the transmission queue. The delay profile of the WBAN for different payload sizes is also investigated and presented in Fig. 9.10. The plot shows that the average packet delay decreases with the increasing payload size. Both results (Figs. 9.9 and 9.10) show the same trend.

Next we investigate the performance of an interconnected WBAN to analyze the performance of a multi-patient monitoring system. In the proposed scenario, it is assumed that all patients' sensor

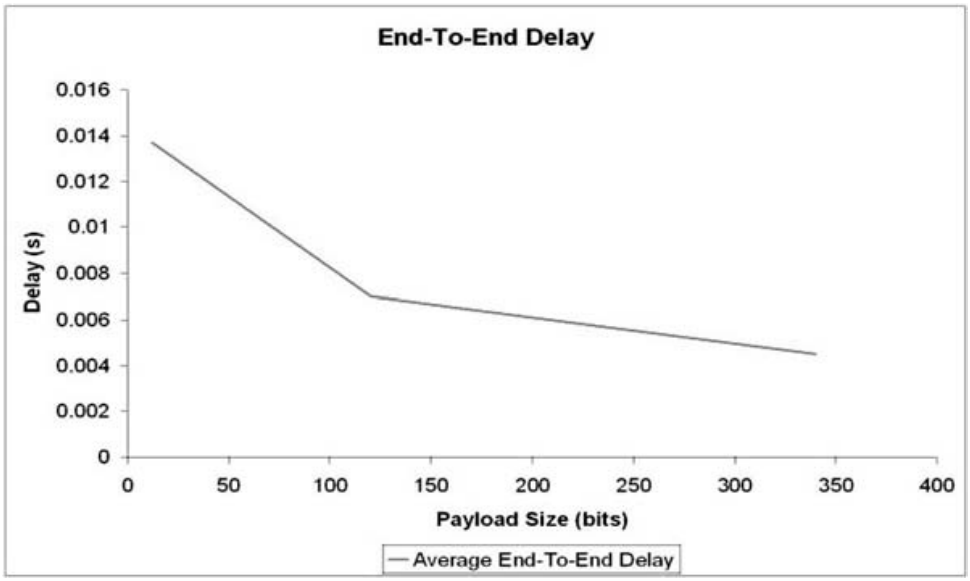

Figure 9.10. WBAN delay profile for different payload sizes.

nodes transmit their data via the PCU and CCU to the database. In this model, PCUs and CCUs are simply acting as a relay node, and forwarding those data to the DB. In order to minimize the number of packets, we use the data aggregation technique at the source node. In this simulation, we connect all sensors on a body using two sensor nodes transmitting data to the PCU. One of the sensor nodes (sensor 1) aggregates ECG, body temperature, and blood pH data and transmits these data after every 145 ms generating 7 packets/second. The other sensor node (sensor 2) aggregates data from the blood flow, blood pressure, and respiratory rate sensors, and transmits these data after every 485 ms generating 3 packets/second. This aggregated packet structure allows 73 data samples with a payload size of 880 bits/packet. Using the aggregation technique, each PAN generates only 10 packets/second. The effective data rate requirement of sensor 1 and sensor 2 becomes 6.05 kbps and 1.92 kbps, respectively.

The delay profile for a multi-patient networking scenario is depicted in Fig. 9.11. The plot shows the average end-to-end delay, which is the total delay over 3 hops (sensor→PCU, PCU→CCU, and CCU→DB). It is observed that the delay increases with increasing number of patients. In this case, the main reason for the increase

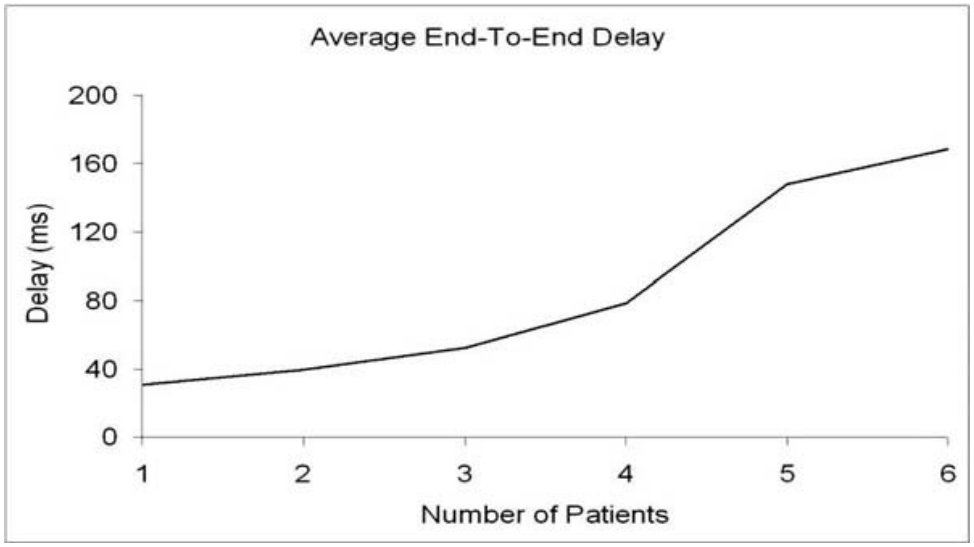

Figure 9.11. Delay profile of the multi-patient monitoring system.

in delay is caused by the contention or interference from different PANs. For an operating ZigBee network, sensor nodes on each patient's body forms a working PAN with the PCU as the coordinator. In a multi-hop networking, collisions can happen either within a PAN or between PANs when simultaneous transmission goes on in different PANs. Also, transmission from the PCU to CCU or from the CCU to DB transmissions can be interfered by the transmissions from other PANs if the IEEE 802.15.4 MAC is used on all the links. In our simulation, all the wireless links used the CSMA/CA protocol. The delay plot shows that the delay profile for up to six patients is quite acceptable where the average packet delay is about 170 ms. A monitoring system will be able to transmit large number of samples within this 170 ms due to the aggregation technique used.

9.10 Conclusions

This chapter presented WBAN network design techniques for various application scenarios. WBAN is currently considered a developing technology, which needs to be standardized for clinical applications. There are many networking techniques that need to be appropriately developed to support medical applications. Since

the MAC protocol is one of the key components of a WBAN design, it is necessary to select appropriate protocol and configure them to achieve optimum performance. This chapter presented theoretical discussions on MAC protocol and network design techniques, which will be useful for medical, IT professionals for future medical application development. Simulation results presented in Section 9.9 can act as a guideline for WBAN design engineers. Section 9.9 also demonstrates the importance of network simulation for the development of an efficient WBAN architecture.

Acknowledgement

Author wishes to acknowledge contributions of Mr. Garrick Bulger and Mr. Benjamin Harding. Mr. Bulger graduated with B.E. Electrical Engineering from the University of Newcastle in 2007. Mr. Harding graduated with B.E. Computer Engineering from the University of Newcastle in 2009.

References

Journals

1. Soomro, A., and Cavalcanti, D. (2007) Opportunities and Challenges in Using WPAN and WLAN Technologies in Medical Environments, *IEEE Communications Magazine*, **45(2)**, pp. 114–122.
2. Golmie, N., Cypher, D., and Rebala, O. (2005) Performance analysis for Low Rate Wireless Technologies for Medical Applications, *Computer Communications*, **28**, pp. 1266–1275.
3. Omeni, O., Wong, A. C. W., Burdett, A. J., and Tomazou, C. (2008) Energy Efficient Medium Access Protocol for Wireless Body Area Networks, *IEEE Transactions on Biomedical Circuits and Systems*, **2(4)**, pp. 251–258.
4. Demirkol, I., Ersoy, C., and Boazici, F. A. (2006) MAC Protocols for Wireless Sensor Networks: A Survey, *IEEE Communications Magazine*, **44(4)**, pp. 115–121.
5. Su, H., and Zhang, Xi. (2009) Battery Dynamics Driven TDMA MAC Protocols for Wireless Body Area Monitoring Networks in Healthcare

Applications, *IEEE Journal on Selected Areas in Communications,* **27(4)**, pp. 424–434.

6. Sharon, O., and Altman, E. (2001) An Efficient Polling MAC for Wireless LANs, *IEEE/ACM Transactions on Networking*, **9(4)**, pp. 439–451.
7. Gutierrez, J. A., Naeve, M., Callaway Ed., Bourgeois, M., Mitter, V., and Heile, B. (2001), IEEE802.15.4: A Developing Standard for Low Power Low Cost Wireless Personal Area Network, *IEEE Network*, **15(5)**, pp. 12–19.
8. Ullah, S., Higgins, H., Islam, S. M. R., Khan, P., and Kwak, K. S. (2009) On PHY and MAC Performance in Body Sensor Networks, *EURASIP Journal on Wireless Communications and Networking*, 2009, pp. 1–7.
9. Yuce, M. R., Ng, P. C., and Khan, J. Y. (2008) Monitoring of Physiological Parameters From Multiple Patients Using Wireless Sensor Network, *Journal of Medical Systems*, **32(5)**, pp. 433–441.
10. Baek, S. J., Veciana, G. de, and Su, X. (2004) Minimizing Energy Consumption in Large Scale Sensor Networks Through Distributed Data Compression and Hierarchical Aggregation, *IEEE Journal on Selected Areas of Communications*, **22(6)**, pp. 1130–1140.

Book

11. Khan, J. Y., and Yuce, M. R. (2010) Wireless Body Area Network (WBAN) for Medical Applications, in *New Developments in Biomedical Engineering,* (ed. Campolo, D.), In-Teh, Croatia, pp. 591–627.
12. Leon-Garcia, A., and Widjaja, I. (2004) *Communication Networks: Fundamental Concepts and Key Architecture*, McGraw Hill, New York.
13. Karl, H., and Willig, A. (2005) *Protocols and Architecture for Wireless Sensor Networks*, John Wiley, England.
14. Ganz, A., Ganz, Z., and Wongthavarawat, K. (2004) IEEE802.15, in *Multimedia Wireless Networks: Technologies, Standards and QoS*, Prentice Hall, New Jersey, pp. 165–185.

Proceedings

15. Chan-Soo , H., Kibeom, S., and Cioffi, J. M. (2006) Opportunistic *p*-persistent CSMA in Wireless Networks, in *Proceedings of the IEEE International Communications Conference,* pp. 183–188.
16. Timmons, N. F., and Scanlon, W. G. (2004) Analysis of the Performance of IEEE 802.15.4 for Medical Sensor Body Area Networking, in *Proceedings of the IEEE SENCON,* pp. 16–24.

17. Zhang, Y., and Dolman, G. (2009) A New Priority-Guaranteed MAC Protocol for Emerging Body Area Networks, in *Proceedings of the IEEE International Conference on Wireless and Mobile Communications,* pp. 140–145.
18. Li, C., Wang, L., Li, J., Zhen, B., Huan-Bang, Li., and Kohno, R. (2009) Scalable and Robust Medium Access Control in Wireless Body Area Networks, in *Proceedings of the 20th IEEE International Symposium on Personal, Indoor and Mobile Radio Communications 2009,* pp. 2127–2131.
19. Khan, J. Y., Yuce, M. R., and Harding, B. (2010) Battery Life Cycle and Transmission Power Profile Analysis of a Wireless Body Area Network With Implanted Nodes, in *Proceedings of the 4th International Symposium on Medical Information and Communication Technology.*
20. Khan, J. Y., Yuce, M. R., and Karami, F. (2008) Performance Evaluation of a Wireless Body Area Sensor Network for Remote Patient Monitoring, in *Proceedings of the 30th Annual International IEEE Engineering in Medicine and Biology Society Conference.*

Technical Report

21. Shnayder, V., Chen, B.-R., Lorincz, K., Fulford-Jones, T. R. F., and Welsh, M. (2005) Sensor Networks for Medical Care, *Technical Report TR-08-05*, Division of Engineering and Applied Sciences, Harvard University.

Website

22. http://www.ieee802.org/15/pub/TG6.html.
23. http://www.opnet.com.

Chapter 10

Power Management in Body Area Networks for Health Care Applications

Vijay Sivaraman,[a] Ashay Dhamdhere,[b] and Alison Burdett[b]

[a] *School of Electrical Engineering and Telecommunications, The University of New South Wales, Sydney, NSW 2052, Australia.*
[b] *Toumaz Technology Limited, 115 Milton Park, Abingdon, OX14 4RZ, United Kingdom.*
{vijay, ashay}@unsw.edu.au; alison.burdett@toumaz.com

For an increasing number of people living with chronic medical conditions, wearable wireless sensor devices can provide nonintrusive yet continuous physiological monitoring, allowing effective clinical management without compromising quality of life. Truly non-intrusive sensor devices will have light weight and small form factor, placing fundamental constraints on the available energy, which necessitates very careful energy management at all layers. This chapter investigates the opportunities and challenges in the use of dynamic radio transmit power control for prolonging the lifetime of such energy-constrained, body-wearable sensor devices.

We first present extensive empirical evidence that the wireless link quality can change rapidly in body area networks (BAN), and a fixed transmit power results in either wasted energy (when the link is good) or low reliability (when the link is bad). We quantify

Wireless Body Area Networks: Technology, Implementation, and Applications
Edited by Mehmet R. Yuce and Jamil Y. Khan

ISBN 978-981-4316-71-2 (Hardcover), ISBN 978-981-4241-57-1 (eBook)
www.panstanford.com

the potential gains of dynamic power control in body-worn devices by benchmarking off-line the energy savings achievable for a given level of reliability. We then propose a class of schemes feasible for practical implementation that adapt transmit power in real time based on feedback information from the receiver. We profile their performance against the off-line benchmark and provide guidelines on how the parameters can be tuned to achieve the desired trade-off between energy savings and reliability within the chosen operating environment. Finally, we implement and profile our scheme on a MicaZ mote-based platform, and also report preliminary results from the ultra-low-power integrated health care monitoring platform we are developing at Toumaz Technology. Our work sets the stage for a holistic approach to power management, incorporating innovations across all layers of BAN design.

10.1 Introduction

Lifestyle changes combined with an aging population and poor diet are contributing to an ever-increasing number of people living with chronic medical conditions requiring ongoing clinical management. This has resulted in a heavy burden on health care systems that are primarily geared toward treating acute conditions. Wireless sensor network technologies have the potential to offer large-scale and cost-effective solutions to this problem. Outfitting patients with tiny, wearable, vital-signs sensors would allow continuous monitoring by caregivers in hospitals and aged-care facilities, and long-term monitoring by individuals in their own homes.

To successfully deploy BANs that can perform long-term and continuous health care monitoring, it is critical that the wearable devices be small and lightweight, lest they would be too intrusive on patient's lifestyle. This places fundamental limitations on the battery energy available to the device over its lifetime. Typical prototype devices in use today, such as MicaZ motes [1] used in Harvard's CodeBlue [2] project, operate on a pair of AA batteries that provide a few watt-hours (a few tens of kilo-joules) of energy. Truly wearable health monitoring devices are emerging that have orders of magnitude lower battery capacity — at Toumaz Technology we

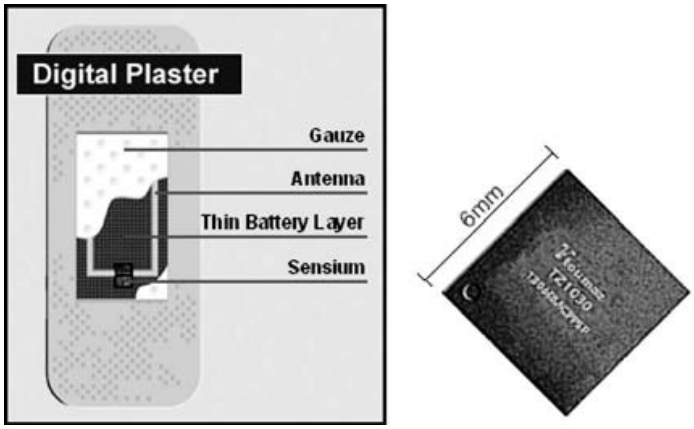

Figure 10.1. Toumaz Sensium^{TM} digital Plaster. See also Color Insert.

are building a new generation of single-chip low-cost disposable "digital plasters" (shown in Fig. 10.1) that provide nonintrusive ultra-low power monitoring of ECG, temperature, blood glucose, and oxygen levels. Our Sensium^{TM} chip operates on a flexible paper-thin printed battery [3] with a capacity of around 20 mW-h (approximately 70 J). Such stringent energy constraints necessitate very careful energy management.

Communication is the most energy-consuming operation that a sensor node performs [4] and can be optimised at multiple layers of the communication stack. At the physical layer, we at Toumaz have innovated an ultra-low-power radio [5] suited to BANs: our radio provides a proprietary 50 Kbps wireless link over a distance of 2–10 m and consumes 2.7 mW at a transmit strength of −7 dBm (compare this to the CC2420 radio [6] in MicaZ motes that consumes 22.5 mW for −7 dBm output). At the data-link layer, energy can be saved by intelligent medium access control (MAC) protocols that duty-cycle the radio, i.e., by turning the radio off whenever packet transmission or receipt is not expected. Several such MAC protocols have been developed in the literature (see [7] for a survey). The B-MAC [8] protocol included in the TinyOS distribution provides versatility to the application in controlling the duty-cycling of the radio, while at Toumaz we have developed our proprietary MAC protocol [9] suited to BANs. However, these MAC protocols only control *when* the radio is switched on, they do not determine the *output power* of the radio when it is on. The focus of this work is to

study the impact of transmission power (for any given transmission schedule) in trading off reliability of the time-varying wireless link for energy efficiency at the transmitting node. We note that the ability to control the transmission power is available on most platforms: the CC2420 radio in Crossbow's MicaZ motes provides 32 transmission levels (ranging from −25 dBm to 0 dBm output) selectable at run-time by configuring a register, while our Sensium™ platform similarly supports eight levels (ranging from −23 dBm to −7 dBm output).

First, we present extensive empirical trace data that profiles the temporal fluctuations in the body area wireless channel. The *large* variations show fixed transmit power to be suboptimal: when link quality is poor, low transmit levels result in reduced reliability, whereas when link quality is good, high transmit levels waste energy. Furthermore, the *rapid* variations render existing schemes (discussed in detail in Section 10.2), that adapt transmit power over long time scales (hours and days), inappropriate for use in BANs. Using trace data we compute off-line the "optimal" power control scheme, i.e., one that minimizes energy usage subject to a given lower bound on reliability. Though infeasible to realize in practise, the optimal gives insight into the potential benefits and fundamental limitations of adaptive power control in BANs, and also provides a benchmark against which practical schemes can be compared.

Second, we develop a class of practical on-line schemes that dynamically adapt transmission power based on receiver feedback. These schemes are easy to implement and can be tuned for desired trade-off between energy savings and communication reliability. We show conservative, balanced, and aggressive adaptations of our scheme that progressively achieve higher energy savings (14–30%) in exchange for higher packet losses (up to 10%). We also provide guidelines on identifying algorithm parameter settings appropriate to application requirements and operating conditions.

Third, we present a real-time implementation of our power control scheme on a MicaZ mote-based platform, demonstrating that energy savings are achievable even with imperfect feedback information. We also present preliminary observations of the efficacy of our scheme in the ultra-low power platform for continuous

health care monitoring being developed at Toumaz Technology. Our work shows adaptive transmit power control as a low-cost way of extending the battery-life of severely energy-constrained body wearable devices and opens the doors to further optimizations customised for specific deployment scenarios.

The rest of this chapter is organised as follows: Section 10.2 briefly discusses prior work in the area of adaptive power control. Section 10.3 presents empirical observations on channel variability in BANs and motivates dynamic power control. Optimal off-line power control is explored in Section 10.4, while practical on-line schemes are proposed and analyzed in Section 10.5. Section 10.6 describes our implementation and experiments on the MicaZ mote and Toumaz Sensium^{TM} platforms, while conclusions and directions for future work are presented in Section 10.7.

10.2 Related Work

Transmit power control has been studied extensively in the literature in several contexts with different objectives. A large number of works, e.g., references [10–15], consider the IEEE 802.11 environment for wireless ad hoc networks and propose adjusting transmit power or transmit rate for data packets based on several factors such as wireless channel conditions (probed via RTS/CTS messages), payload length, etc. In spite of the useful insights from these works, there are significant differences between the IEEE 802.11 WLAN (wireless local area network) environment and a BAN for health care monitoring such as: (a) WLAN devices send sporadic data while BAN devices typically send data periodically, (b) packet sizes are much smaller in BANs than in WLANs, and (c) BAN devices operate on or very near the human body, which makes radio propagation (and hence channel conditions) in BANs markedly different from WLANs. These important differences merit study of power control in the specific context of BANs, which to the best of our knowledge has not been undertaken to date.

A large body of work in power control has also targeted multi-hop networks with the objective of enhancing throughput [16],

increasing connectivity [17, 18] or reliability [19], and reducing delays [20]. Joint routing, scheduling, and power control schemes have also been proposed [21, 22]. Our work considers a single-hop BAN where such issues do not arise. Moreover, the environment presented by a BAN is much more dynamic than the psuedo-static scenarios considered by these works.

More relevant to this work are existing power control schemes that target energy savings in wireless sensor networks. The study in refference [23] proposes two algorithms that adapt transmission power by exchange of information among nodes and based on signal attenuation, while reference [24] proposes a linear prediction model for estimating the optimal transmission power based on measured link quality. However, these studies have targeted static deployments (such as for environmental or structural monitoring applications) wherein variability in wireless link quality has been shown empirically [25, 26] to be slow. In contrast, this work considers wearable mobile devices for which the wireless link quality can change significantly and rapidly since it is very susceptible to position and orientation of the human body [27]. To the best of our knowledge, adaptive power control for body-wearable devices has not been explored by other researchers before.

Two recent papers make interesting observations that are complementary to our work: the authors in reference [28] investigate the number of different power levels that can be effectively leveraged by power control algorithms in an indoor WLAN environment. They show that, due to multipath and fading effects, there is significant overlap between the RSSI distributions for nearby power levels, making them practically indistinguishable at the receiver, and claim that as few as four power levels may suffice to make power control attractive. We leverage this fact when we shift from the MicaZ (32 power levels) to the Sensium^{TM} (8 power levels). Lastly, the study in reference [29] points out that power control by itself does not lead to significant energy savings unless complemented by a good MAC protocol that has low duty-cycling of the radio. We concur with this observation and note that the MAC protocol used in the Sensium^{TM} platform has very low duty cycle.

10.3 The Case for Transmit Power Control in Body Area Networks

We begin by empirically profiling the temporal variations in the quality of the wireless link between a body-worn device and a fixed base-station, as a patient wearing the device performs various activities. The patient was played by the first author. Our experiments in this section use the MicaZ motes from Crossbow Technologies [1], while some preliminary results that use the Toumaz Sensium^{TM} platform are presented in Section 10.6. In each experiment the device was strapped around the patient's chest, simulating continuous monitoring of heartbeat and ECG. We also conducted several experiments in which the device was strapped around the patient's arm (for monitoring blood pH and glucose); the results were qualitatively similar and are omitted here due to lack of space. The experiments were conducted indoors in an office space containing 10 cubicles. The base-station was placed close to one side of the room at an elevation (atop a shelf) to provide better line-of-sight coverage across the office space.

The MicaZ mote operates in the 2.4 GHz frequency band and can support a 250 Kbps data rate. It supports 32 RF output power levels, controllable at run-time via a register; the output power (in dBm) and corresponding energy consumption rate (in mW) for various levels are shown in Table 10.1. Since our goal is to save energy at the body-worn device (which typically has lower energy resources than the base-station), our experiments involve emitting packets periodically from the body-worn device at various power levels,

Table 10.1. Characteristics of the MicaZ CC2420 radio

Transmit level	Output (dBm)	Power (mW)
31	0	31.3
27	−1	29.7
23	−3	27.4
19	−5	25.0
15	−7	22.5
11	−10	20.2
7	−15	17.9
3	−25	15.3

and measuring the link quality at the receiver (base-station). Two metrics of link quality are available on the mote platform: received signal strength indicator (RSSI), which is computed internally in the radio by averaging the signal power over eight symbol periods of the incoming packet, and link quality indicator (LQI) metric, which measures the chip error rate for the first eight symbols of the incoming packet. For a static scenario, previous research [24, 30, 31] has observed LQI readings to suffer from early saturation and be relatively less stable. We conducted experiments to verify this in a BAN scenario. Figure 10.2a,b show the RSSI and LQI as a function of transmit power level for various scenarios of patient distance and orientation relative to the base-station. While the RSSI seems to show a smooth increase with transmit power, the LQI saturates early on for several scenarios and also seems to exhibit a large variance (shown as error-bars), which makes the readings less reliable. Figure 10.2c,d show the RSSI and LQI as a function of

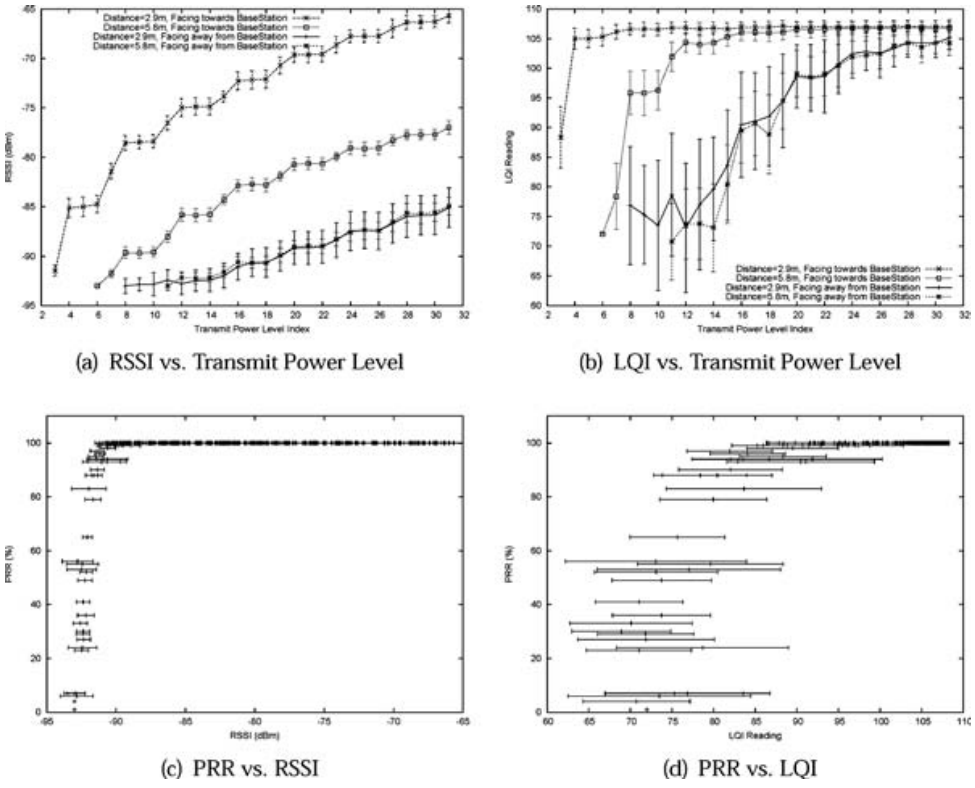

Figure 10.2. Comparison of RSSI and LQI as indicators of channel quality in a BAN.

the packet receive ratio (PRR) observed across several experiments. While the RSSI seems to provide a good estimate of packet loss rates (e.g., RSSI of −90 dBm or larger always corresponds to PRR of 95% or more), the LQI is seen to be a much weaker indicator of PRR due to its high variance. Our subsequent study, therefore, uses RSSI as an indicator of channel quality.

We profile, at different radio transmit levels, the changes in link quality with time as patients perform their routine activities involving resting, moving, turning, etc. To compare link quality at different power levels, we should ideally take *simultaneous* measurements at all power levels, which is infeasible. As an approximation, we make the body-worn device transmit every packet multiple times in quick succession at 16 different transmit levels 31, 29, 27, … 1. The receiver (base-station) can thus record, more-or-less simultaneously, the signal strength corresponding to each transmit level. Measurements for three scenarios are described next.

10.3.1 *Normal Walk*

This scenario has the patient walking back and forth in the room for a few minutes at a normal walking pace; the patient stays between 1 and 8 m from the base-station at all times. The body device, strapped onto the patient's chest, generates a packet every second (which is not entirely unrealistic for a heartbeat/ECG monitor) and transmits it at 16 different output levels. The RSSI is recorded at the base-station for each packet at each transmit level, and plotted in Fig. 10.3a against time for four of the transmit levels. For any fixed transmit power, the received signal strength fluctuates widely: at fixed maximum transmit output (level 31 at 0 dBm), the signal strength at the receiver changes from −64 dBm (at 34 s) to −94 dBm (at 86 s — a change of 30 dBm under a minute. There are nevertheless some discernible trends: for example, in the interval 30–50 s, the received signal is consistently above −72 dBm (at the maximum transmit level) due to the clear line-of-sight presented by the patient walking toward the base-station, while the subsequent interval 50–70 s exhibits RSSI below −75 dBm (again at the maximum transmit level) due to the patient turning and

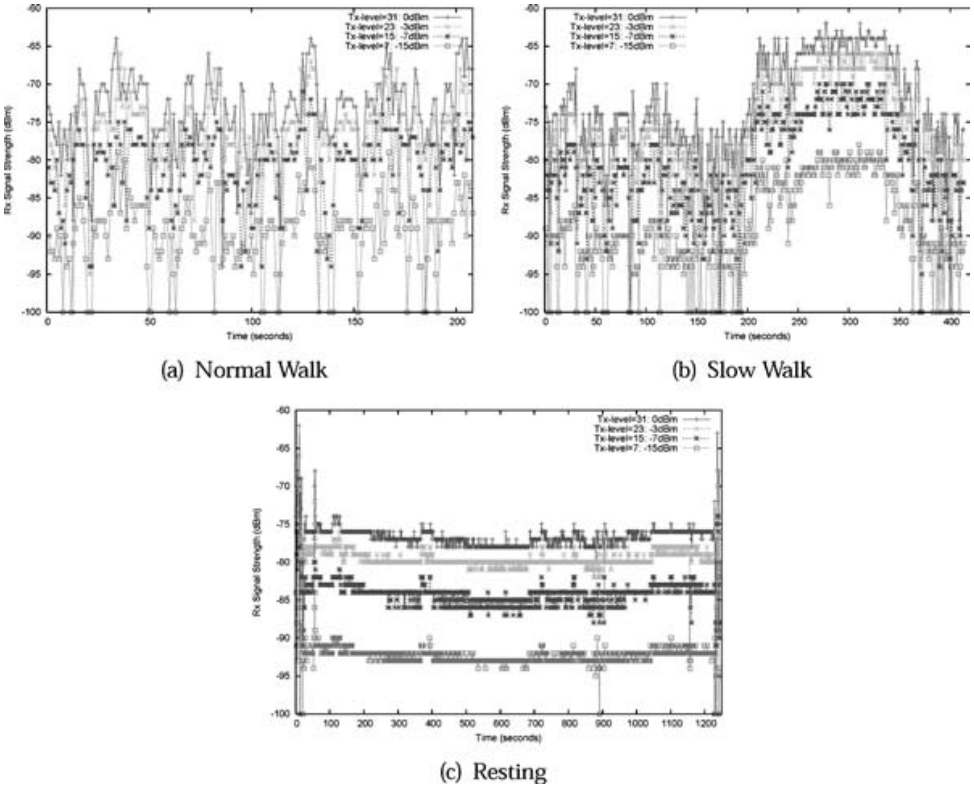

Figure 10.3. RSSI vs. time for various patient scenarios. See also Color Insert.

blocking the line-of-sight with his body. The question of whether these patterns present opportunities for energy savings by adapting transmit power will be tackled in Section 10.4.

10.3.2 *Slow Walk*

In this scenario, we consider a slow-moving person (such as an elderly or a handicapped person with restricted mobility) who takes an exaggeratedly long time (over 6 min) to walk a distance of 3 m and back. As before, packets are transmitted every second at several power levels, and the received signal strength at the base-station is recorded and depicted in Fig. 10.3b. The trend in the plot is very evident: the RSSI is fairly low for the first half, when the patient's body blocks the line-of-sight between the body-worn device and the base-station, and then rises to a perceptibly higher value in the second part of the experiment when the patient is walking facing the base-station (barring the last few seconds when

the patient turns again). This scenario depicts the shortcomings of fixed transmit power: a low transmit level would result in weak signals (and packet loss) during the first half, while a high transmit level would unnecessarily waste energy in the latter half. Such a scenario, therefore, presents opportunities for saving energy by reducing transmit power adaptively when the good channel persists.

10.3.3 *Resting*

In this scenario, the patient sits down to rest for approximately 20 min on a chair at a distance of about 6 m from the base-station. Fig. 10.3c plots the RSSI over the entire period, at several transmit levels. The wireless link is found to be fairly stable when the patient is at rest (in spite of a few other people moving around at several points in the experiment). This is in some sense an "ideal" environment with tremendous potential for energy savings, particularly with patients who are resting for a major part of the day. These energy savings would be unattainable if the transmit level were fixed, since a fixed setting would have to cater to the worst-case scenario of a poor channel.

Having gained an understanding of the wireless channel under various patient activity scenarios, the next section quantifies the potential benefits of adaptive transmit power control.

10.4 Optimal Off-Line Transmit Power Control

To quantify the potential benefits of adaptive transmit power control, we compute what the "optimal" transmission level might be for each of the scenarios considered before. We define the "optimal" as the lowest required transmit power level (as a function of time) to achieve a minimum target RSSI. Based on our studies in Section 10.3 relating packet loss with RSSI for the MicaZ motes in a BAN setting, we choose a conservative target RSSI of -85 dBm. The computation of the optimal transmission level defined thus is done off-line, i.e., using the traces shown in the previous section. For each scenario, at each time instant, we know the RSSI for each transmit power level, and we can, therefore, identify the lowest transmit power at which the signal strength at the receiver is no lower than the threshold

of −85 dBm (if all received signal strengths are below the lower threshold we set the transmit level to be the maximum). We note that such a scheme is not implementable in practice, since it would require the transmitter to have instantaneous knowledge of the RSSI at the receiver for each choice of transmit power level, which is infeasible given that the channel varies with time.

The optimal transmit levels, and their associated RSSI values, for each of the three scenarios are depicted as a function of time in Fig. 10.4. Subplot (a) shows, for the normal walk scenario, that the optimal changes rapidly to track the rapid fluctuations in channel quality, thereby maintaining a fairly stable RSSI as shown in subplot (b): for example, in the time interval 50–75 sec, the optimal transmit level fluctuates multiple times between a high of 29 and a low of 9. Based on the energy draw for each transmit power level (shown in Table 10.1), we can compute the energy savings of optimal power control to be around 34% as compared to using the maximum transmit power. However, as the rapid fluctuations in the optimal level indicates, a practical scheme is unlikely to be able to predict the current optimal transmit level based on prior channel quality.

The optimal transmit power for a slow walk in Fig. 10.4c shows high sensitivity to body orientation, even when the motion is very slow. The rapid changes during the first 200 s arise from minor variations in the patient's body orientation while blocking the line-of-sight between the body-worn device and the base-station (indeed a few packets are lost even at the highest transmit power). But when the patient turns (at approximately 200 s), there is a clear line-of-sight, and the wireless link is relatively stable permitting the optimal transmit power to remain low for a considerable length of time (more than 2 min). This indicates that if the body orientation is favorable, periods of slow activity could be capitalized by a transmit control scheme to save energy without compromising realiability.

When the patient is resting, the link is fairly stable and the optimal transmit power level is near-constant as shown in Fig. 10.4e, which permits an energy savings of over 38% compared to maximum transmit power. It would seem the quiescent wireless channel in this case gives ample opportunity for practical schemes to reduce transmit power without sacrificing reliability. The design of such schemes is discussed next.

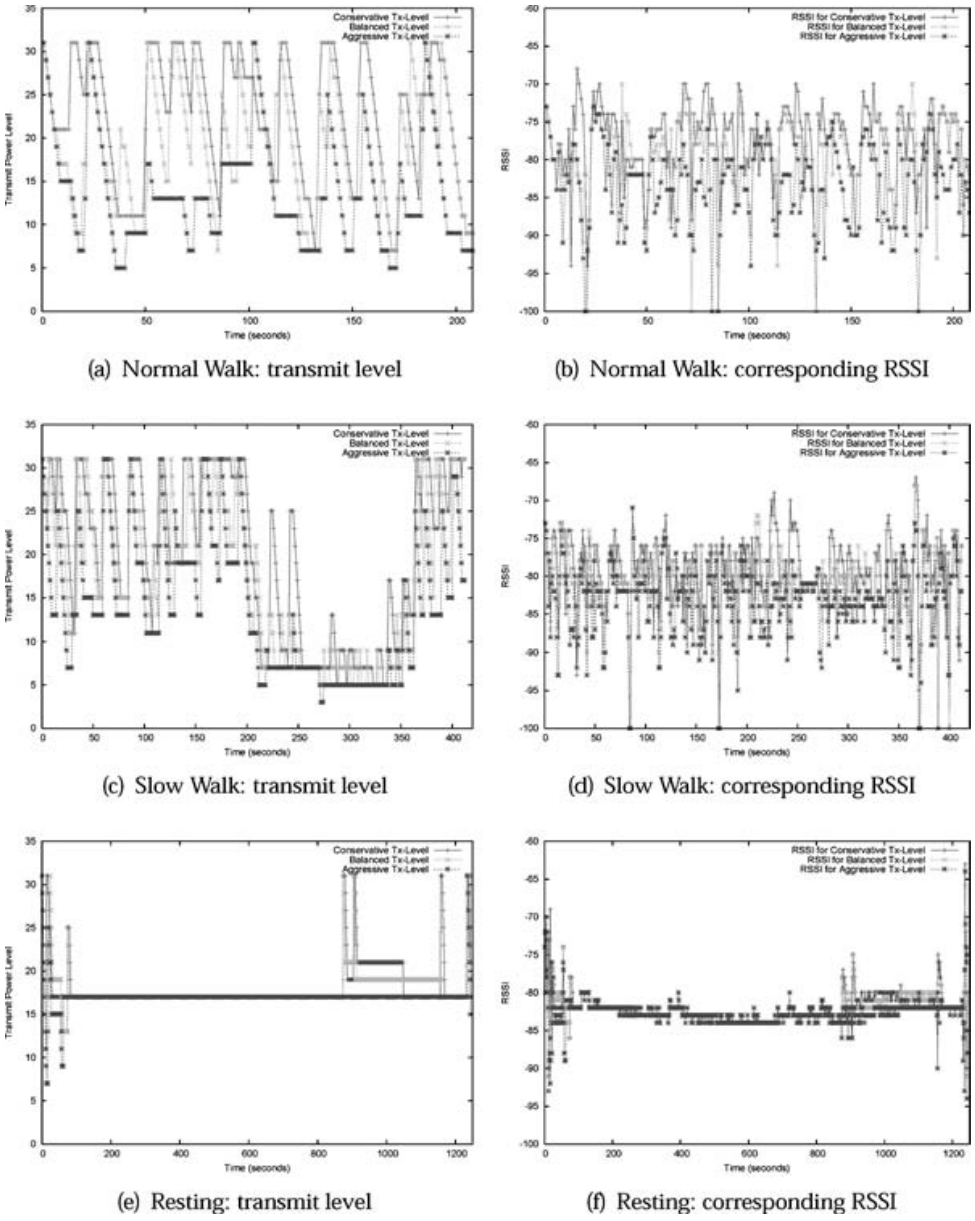

Figure 10.4. Optimal transmit power and associated RSSI for a normal walk, slow walk, and resting position. See also Color Insert.

10.5 Practical On-Line Transmit Power Control

The optimal transmit power control scheme above was performed off-line and required the sender to have *a priori* knowledge of the link quality at the receiver, which is infeasible in reality. This section

develops practical algorithms that are then benchmarked against the optimal.

A *predictive* approach to designing on-line schemes for power control would require a wireless channel model for BANs. Modeling the propagation of electromagnetic waves around the human body, e.g., via "creeping waves" [32], is fairly complex as it needs to account for the permittivity and conductivity of the different layers of bone and tissue in the human anatomy. Additionally, the model has to contend with changes in orientation of the human body, mobility of the patient, and other spatio-temporal aspects (such as room layout, people in the vicinity, etc.). We believe such predictive models are too complex to implement on energy-constrained wearable devices and do not pursue them in our work.

We focus instead on *reactive* schemes that adjust transmit power based on feedback from the receiver (inspired by the way TCP adjusts its transmission rate in reaction to congestion in the Internet). Specifically, the base-station measures the RSSI for each received packet and feeds it back to the body-worn device in the acknowledgment packet. In this section, we assume that the feedback information is perfect (i.e., acknowledgment packets are never lost); this assumption will be relaxed in Section 10.6.1.

10.5.1 *A Simple and Flexible Class of Schemes*

At its core, any reactive power control scheme must ramp up transmit power when the channel quality deteriorates (so as to avoid packet loss) and decrease transmit power when the channel quality improves (in order to save energy). We propose a general class of schemes that allow these operations to be tuned via appropriate parameter settings.

Algorithm 10.1 depicts our class of schemes and is characterized by four parameters: α_u, α_d, T_L, and T_H. The scheme maintains a running average $\bar{R}$ of the RSSI, computed by exponentially weighted averaging (steps 2 and 4) of each newly obtained sample. The averaging weight α_u for a sample representing an improving channel can, in general, be different from the weight α_d used for a sample representing a deteriorating channel; this gives flexibility to a scheme in reacting differently to a perceived increase or decrease

Algorithm 10.1 A class of power control schemes

Require: R {RSSI from the current sample}
Require: $\bar{R}$ {Average RSSI}
1: **if** $R \leq \bar{R}$ **then**
2: $\quad \bar{R} \leftarrow \alpha_d R + (1 - \alpha_d)\bar{R}$
3: **else** $\{R > \bar{R}\}$
4: $\quad \bar{R} \leftarrow \alpha_u R + (1 - \alpha_u)\bar{R}$
5: **end if**
6: **if** $\bar{R} < T_L$ **then**
7: $\quad$ Double the transmit power
8: **else if** $\bar{R} > T_H$ **then**
9: $\quad$ Reduce the transmit power by a constant
10: **else** $\{T_L \leq \bar{R} \leq T_H\}$
11: $\quad$ No action is required
12: **end if**

in channel quality, thereby placing different emphasis on energy savings versus packet loss.

The scheme increases or reduces transmit power by comparing the running RSSI average $\bar{R}$ to lower and upper thresholds T_L and T_H. Based on our previous analysis of RSSI and packet loss (Fig. 10.2c), we believe a lower threshold $T_L = -85$ dbm is appropriate for the MicaZ platform. If $\bar{R}$ falls below this threshold (step 6), the transmit power is immediately doubled (step 7) to avoid imminent packet loss in the deteriorating channel. If, on the other hand, the average RSSI exceeds an upper threshold T_H (step 8), the transmit power is reduced by a small amount (step 9). Our experimental traces indicate that $T_H = -80$ dBm is appropriate for the MicaZ platform; lower values make the target RSSI range $[T_L, T_H]$ too narrow, while larger values lead to higher transmit power (and hence higher energy usage) than required. Readers may note the similarity of our scheme to TCP in that the transmit power increase is multiplicative while the decrease is additive, and thus has a clear bias toward reacting faster to a deteriorating channel than an improving one.

The class of schemes outlined in algorithm 10.1 is fairly easy to implement in platforms with very limited CPU and memory

resources. It is also very flexible, and the parameters α_u and α_d can, in particular, be tuned for appropriate trade-off between energy efficiency and reliability. The performance of the schemes for specific parameter settings is discussed next.

10.5.2 *Example Adaptations of the General Scheme*

A *conservative* approach to energy savings might be warranted in applications where data loss is critical. A relatively high value $\alpha_d = 0.8$ could be used so that a low RSSI value triggers a rapid ramp-up in transmit power, while keeping $\alpha_u = 0.2$ low so that transmit power is reduced cautiously when good channel conditions prevail. Applications in which energy is at a high premium and data loss is not as critical may adopt an *aggressive* strategy with a high $\alpha_u = 0.8$ that reacts quickly to improvements in channel conditions while setting $\alpha_d = 0.2$ so that a transient bad channel is ignored. A *balanced* approach that equally values energy savings and packet loss may place equal emphasis on whether the channel is getting better or worse by setting $\alpha_u = \alpha_d = \alpha = 0.8$.

We tested the efficacy of the conservative, aggressive, and balanced schemes as described above on the trace data for the three scenarios described earlier. The transmitter is assumed to know the RSSI for each transmitted packet via feedback from the receiver; it performs the exponential averaging using the parameters listed for each scheme, and chooses an appropriate transmit power level for the subsequent packet transmission. Figure 10.5 shows the transmit power level and the corresponding RSSI for each of the three schemes for each scenario. The average power draw per packet, as well as packet loss rates, for each of the schemes under the different scenarios is summarized in Table 10.2.

For normal walk, Fig. 10.5a shows that all schemes exhibit considerable fluctuation in their transmit power, since the channel varies quite rapidly. The conservative scheme yields good link reliability (only 1.4% loss) but has high energy usage (30.58% above optimal), while the aggressive scheme yields good energy savings (5.73% within optimal) by sacrificing link quality (9.6% packet loss). As one might expect, the energy usage and packet loss

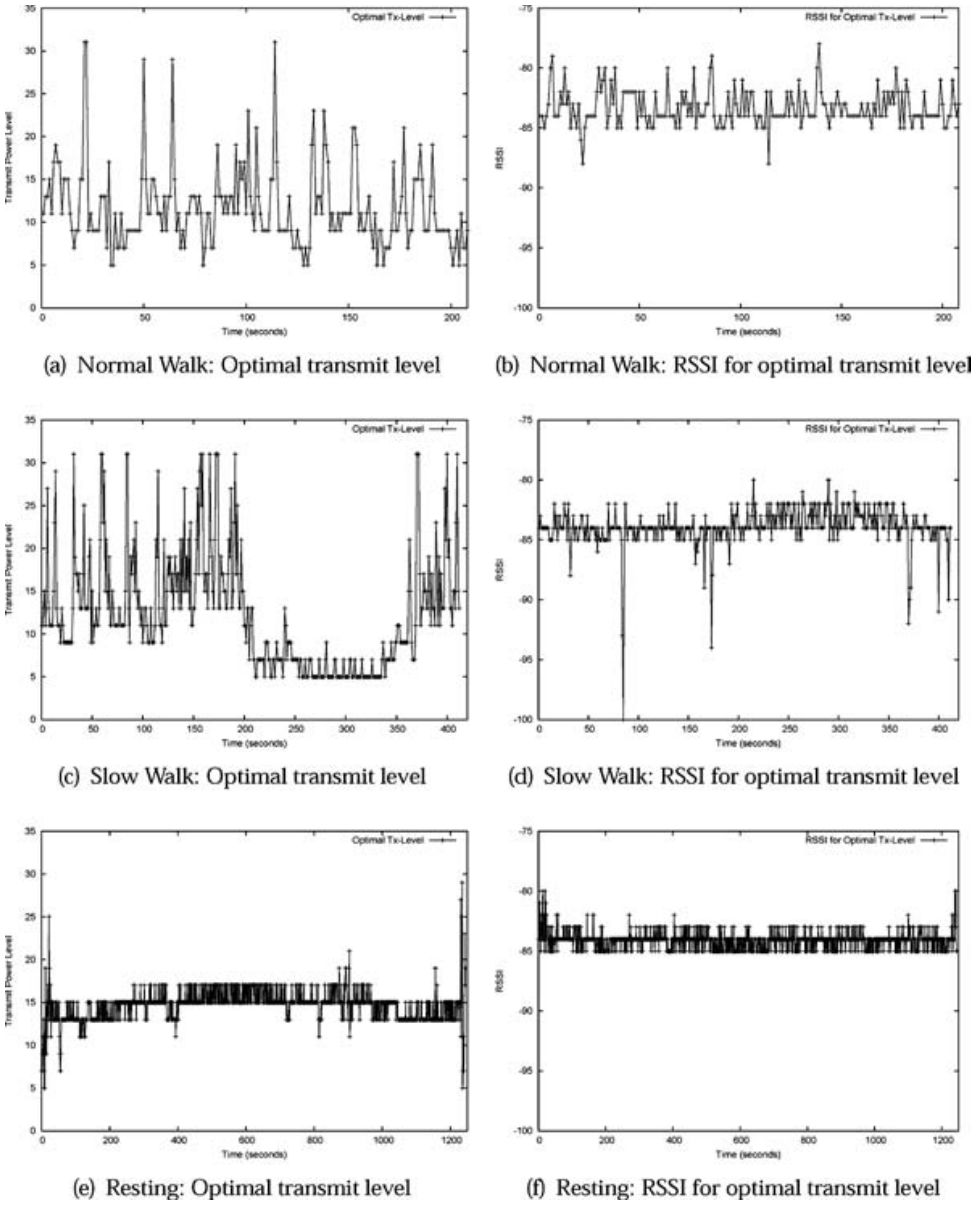

Figure 10.5. Transmit power and RSSI under conservative, balanced, and aggressive schemes for various scenarios.

under the balanced scheme are between those of the conservative and aggressive.

For the slow walk scenario, Fig. 10.5 shows the aggressive scheme to be fairly stable in the interval 210–350 s when the patient is walking slowly facing the base-station, whereas the conservative scheme shows some fluctuations in that region. Again,

Table 10.2. Power draw averaged across packets, and loss rate, for various power control schemes

	Normal Walk		Slow Walk		Resting	
Scheme	power (mW)	loss (%)	power (mW)	loss (%)	power (mW)	loss (%)
Maximum	31.32	0	31.32	1.2	31.32	0
Optimal	20.60	0	20.74	1.2	22.35	0
Conservative	26.90	1.4	25.52	2.18	24.36	0.08
Balanced	25.15	3.85	24.11	3.85	24.22	0.16
Aggressive	21.78	9.6	21.96	7.28	23.74	0.32

the conservative scheme uses 16.21% more energy than the aggressive scheme, but has a packet loss rate much lower than the aggressive scheme, showing that energy and reliability can be traded-off in our schemes by choosing parameters appropriately. As before, the balanced scheme lies between the other two in both its metrics.

The transmit level under the three schemes for the resting scenario, shown in Fig. 10.5e, is fairly stable, barring some rogue glitches in the link quality (e.g., at 905 s) that the conservative scheme over reacts to. The energy savings, as well as the packet loss ratios, are comparable under all three schemes, indicating that under quiescent channel conditions the parameter settings do not influence the algorithm performance significantly.

10.5.3 *Tuning the Parameters*

In this section, we undertake a more detailed study of the impact of the algorithm parameters α_u and α_d on the performance of our class of schemes. We conducted several experiments in which the patient is fairly active, since the parameters have a larger impact on energy and loss under such scenarios. Figure 10.6 plots the energy consumption (left column) and packet loss (right column) of our scheme for various parameters settings for a representative scenario. Figures 10.6a,b show that for any fixed α_d, the energy consumption falls monotonically with α_u: this is because a larger α_u makes the scheme react faster to an improving channel,

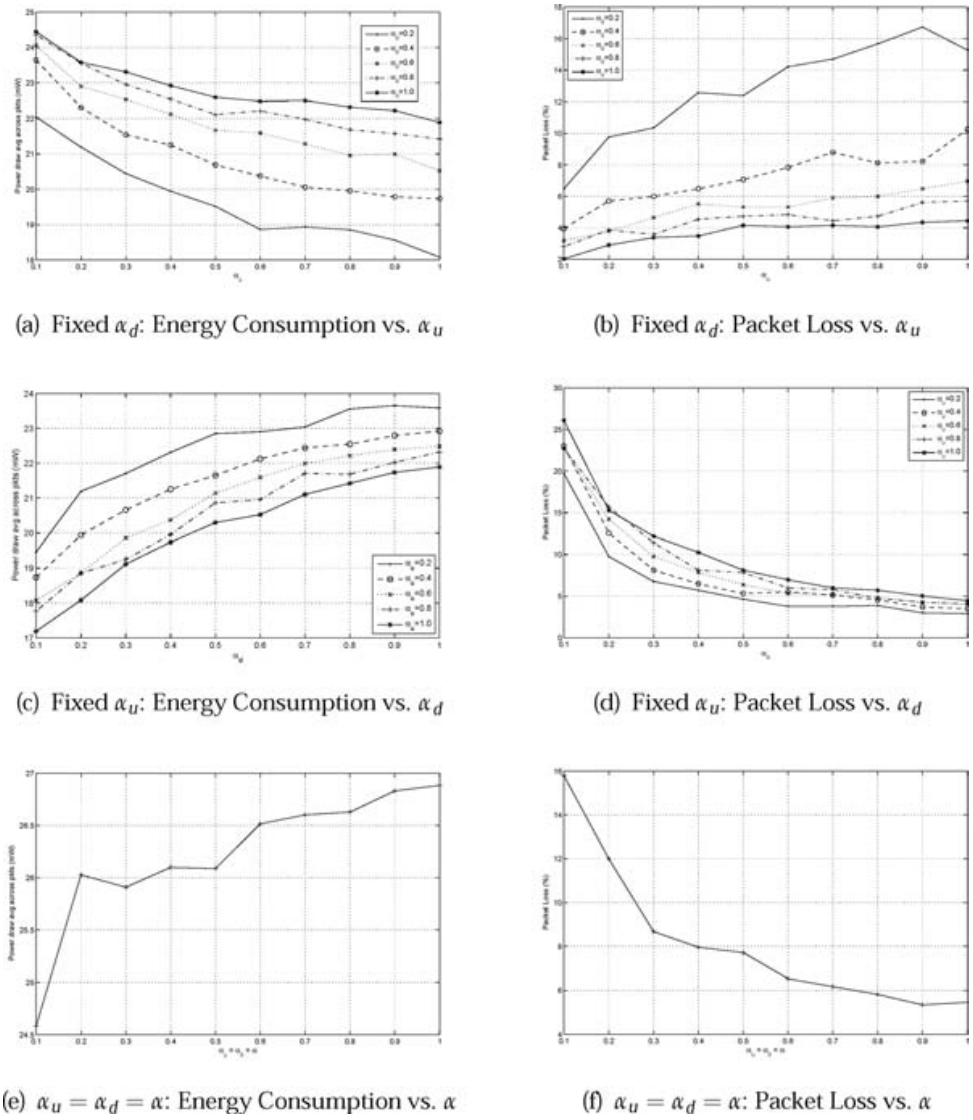

(a) Fixed α_d: Energy Consumption vs. α_u

(b) Fixed α_d: Packet Loss vs. α_u

(c) Fixed α_u: Energy Consumption vs. α_d

(d) Fixed α_u: Packet Loss vs. α_d

(e) $\alpha_u = \alpha_d = \alpha$: Energy Consumption vs. α

(f) $\alpha_u = \alpha_d = \alpha$: Packet Loss vs. α

Figure 10.6. Energy consumption and packet loss for various parameter settings.

thereby reducing transmit power to save energy. When α_u is held constant and α_d increases, the scheme reacts more quickly to a degrading channel, and the packet loss rate diminishes (Fig. 10.6d) at the expense of increased energy consumption (Fig. 10.6c). The plots show clearly that increasing α_u pulls the algorithm in the direction favoring energy savings, while increasing α_d pulls it toward reliability — these opposite trends justifying our decision to devise a scheme with two separate α values. For a balanced scheme that uses

$\alpha_u = \alpha_d = \alpha$, Fig. 10.6e,f show that a scheme that is very reactive to both good and bad channel conditions (i.e., high α) improves loss performance as expected, but incurs a penalty in terms of slightly increased energy usage.

An interesting question concerns the optimization of the parameters for a given operating scenario. For the trace considered in this section, we found that ($\alpha_u = 1.0, \alpha_d = 0.3$) yields maximum energy savings when the loss budget is high at 15%, implying that the ramp-down in transmit power should be immediate while a ramp-up happens slowly over several poor RSSI samples. When the loss margin is stringent at 5%, energy savings are maximized for ($\alpha_u = 0.8, \alpha_d = 1.0$), i.e., the scheme should react immediately to a degrading channel and relatively slowly to an improving channel. Though the optimal settings obtained here do not transfer directly to other scenarios, they provide insight which could conceivably be used by a system to adjust the parameters at run-time based on application requirements and operating conditions.

10.6 Prototyping and Experimentation

This section reports on a real-time implementation of our power control schemes on a MicaZ mote-based testbed, as well as preliminary experiments on the Toumaz Sensium™ platform.

10.6.1 *MicaZ Mote Platform*

The previous section evaluated the performance of the transmit power control schemes using trace data wherein the sender (body-worn device) is assumed to know the RSSI at the receiver (base-station) for each of the packets it has thus far transmitted. In a real operational setting, such feedback information would be contained in acknowledgment packets (from the receiver to the sender), which may also experience loss. This section undertakes a real-time implementation of our scheme on body-worn MicaZ motes to evaluate the efficacy of our power control scheme under imperfect feedback. We note that the base-station is assumed to have abundant energy reserves and does not implement power control, always using the highest power level for transmitting acknowledgments.

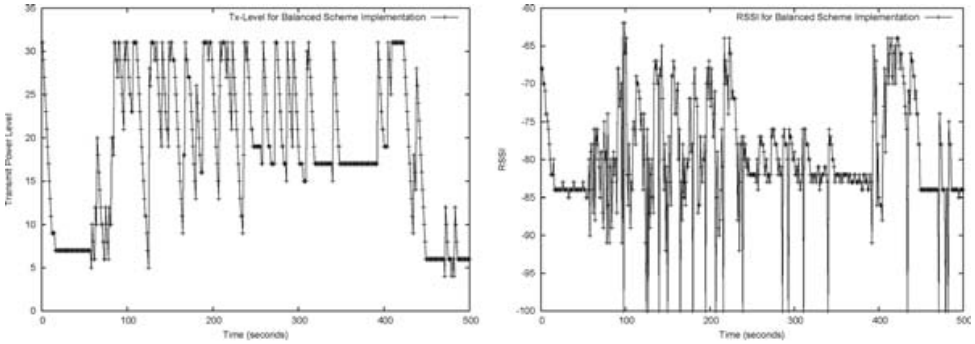

(a) Transmit level (b) RSSI

Figure 10.7. Transmit power and associated RSSI for real-time implementation of balanced scheme on the MicaZ platform.

The implementation performs exactly the steps shown in algorithm 10.1, with the additional step that if an acknowledgment is not received for a transmitted packet, the RSSI for that sample is taken to be -100 dBm (thereby signaling a bad channel to the algorithm). We present results with balanced parameter setting $\alpha_u = \alpha_d = \alpha = 0.8$ for a scenario where the patient undertakes a mix of walking and resting. Figure 10.7a shows the transmit power level under our scheme and Fig. 10.7b the corresponding RSSI. Our scheme performs quite well, yielding average energy consumption rate per packet of 20.23 mW (a 35.4% savings in energy compared to using maximum transmit power), and packet loss rate of 3.8%. Unfortunately, there is no way to benchmark this result (recall that computing the optimal requires a trace that includes the RSSI for all power levels at all times), but a careful look at the plots will show regions where the RSSI is high and yet the transmit power is not reduced, for example in the interval $(410, 420)$ s. It was found that several acknowledgment packets were lost in this interval (the overall acknowledgment loss rate for this scenario was 11.82%), and the absence of feedback information forced our scheme to use a higher transmit power level than would have been necessary with perfect feedback. High acknowledgment loss rates arising from asymmetric link qualities can have a negative impact on the efficacy of feedback-based power control schemes and merit deeper study in future work.

10.6.2 *Toumaz Sensium™ Platform*

A major goal of this project is to evaluate the costs and benefits of adaptive power control in the real-world continuous health monitoring platform being developed by Toumaz Technology. Unfortunately, the digital plaster (which includes the Sensium™ chip, printed battery, etched antenna, and water-protective covering) is still in the packaging process; so we present here preliminary results obtained from using a Sensium™ chip mounted on a development board strapped to the patient's chest, as preliminary indicators on the feasibility and benefits of adaptive transmit power control in the Sensium™ platform.

The hardware-optimized design of the Sensium™ presented several constraints in our experimentation: (i) the radio has only eight transmit power levels (unlike 32 in the MicaZ radio), and the energy savings are upper-bounded at 35% due to the limited transmission power range (Table 10.3a), (ii) the RSSI readout is only 3 bits (compared to 8 bits in the MicaZ), which gives only a coarse estimate of the RSSI (Table 10.3b), (iii) a sleep time of at least 1 s is imposed between successive packet transmissions (for energy efficiency), which restricts our ability to sample the channel at various transmit power levels without substantial change in patient position/orientation, (iv) the RSSI feedback from receiver to sender requires software modification of the acknowledgment packets, which introduces a 1 s lag in the feedback. These limitations not withstanding, we believe there is great value in experimenting

Table 10.3. Sensium™ Radio transmit and receive characteristics (a) Transmit Characteristics (b) Receive Characteristics

Tx level	output (dBm)	power (mW)		
7	−6	2.8	7	> -35
6	−7	2.7	6	−46 to −35
5	−9	2.6	5	−52 to −46
4	−10	2.5	4	−58 to −52
3	−12	2.4	3	−64 to −58
2	−15	2.2	2	−70 to −64
1	−18	2.0	1	−76 to −70
0	−22	1.8	0	< -76

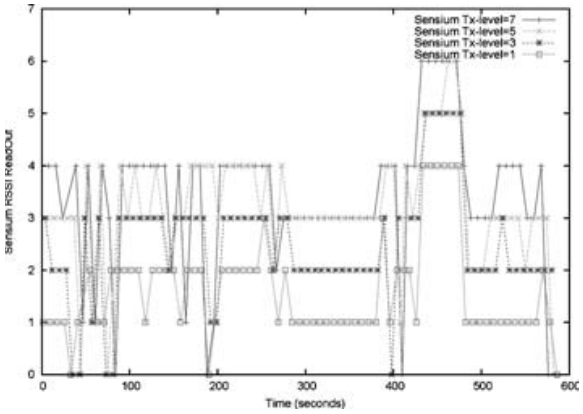

Figure 10.8. RSSI vs. time using the Sensium™ platform. See also Color Insert.

with this real-world wearable device, and these limitations can be addressed in subsequent revisions of the Sensium™ hardware.

As with the motes, we strap the Sensium™ to the patient's chest and make it transmit a packet every second, cycling through the eight available power levels, while the RSSI is recorded at the base-station. A 10 min extract of the recorded RSSI at various transmit power levels is shown in Fig. 10.8; in this scenario, the patient is walking back and forth in the interval 30–80 s, during which period the RSSI fluctuates rapidly, while in the intervals 280–380 s and 420–470 s the patient is stationary (facing away and toward the base-station, respectively) and the RSSI is stable. This confirms that the body area wireless channel presents significant temporal fluctuations in the 862–870 MHz frequency range (much like the 2.4 GHz range of the MicaZ radio), and fixed transmit power is suboptimal.

For the above trace, we compute off-line the optimal transmission power schedule for desired RSSI level of 3 (corresponding to the range -64 to -58 dBm). Figure 10.9 shows the optimal transmit power level (at the sender) and the corresponding RSSI level (at the receiver) and clearly depicts that the transmit power level can be reduced during quiescent periods such as 420–470 s, while preserving reliability during periods when channel conditions are poor. For this scenario, optimal transmit power control uses 14.63% less energy than fixed maximum transmit power, which is a significant saving for this severely energy-constrained device.

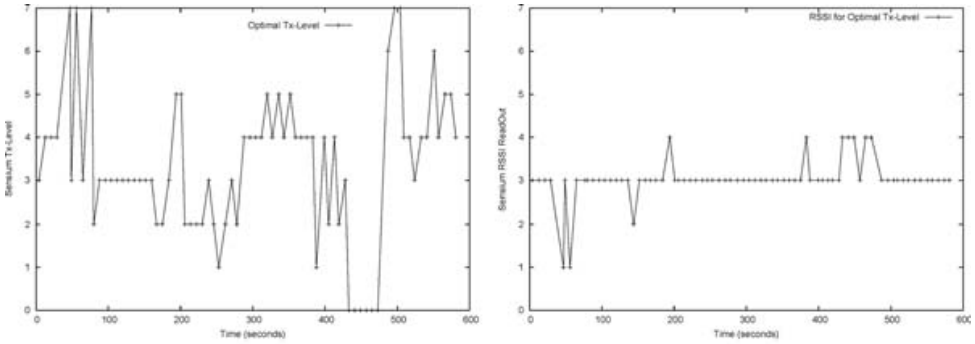

(a) Sensium: Optimal transmit level (b) Sensium: RSSI for optimal transmit level

Figure 10.9. Optimal transmit power and associated RSSI for the Sensium™.

Further results from our testing on the Sensium™ platform are reported in our subsequent work [33].

10.7 Conclusions and Future Work

This chapter outlines the potential benefits and limitations of adaptive radio transmit power control as a means of saving precious energy in body-wearable sensor devices used for medical monitoring. We experimentally profiled the radio channel quality under different scenarios of patient activity and showed that fixed transmit power either wastes energy or sacrifices reliability. We then quantified the theoretical benefits of adaptive transmit power control and showed that across different scenarios it can save nearly 35% energy without compromising reliability. We then developed a general class of practical power control schemes suitable for BANs, and showed specific instances that save 14–30% energy (as compared to using maximum transmit power) in exchange for 1–10% packet losses. We demonstrated that the adjustment of parameters allow our schemes to achieve different trade-offs between energy savings and reliability, making them suitable across diverse applications in different operating conditions. Finally, we demonstrated that a real-time implementation of our scheme on the MicaZ mote-based platform is effective even in the presence of imperfect feedback information and presented preliminary experimental results indicating the potential for saving precious

energy in Toumaz's real-world platform for continuous health care monitoring.

Our work on dynamic power control in BANs, summarized in this chapter from our publications [33–35], can be extended in several ways. There is much further study required in exploring its potential for specific health monitoring environments (e.g., critical care in hospitals, aged care, athlete monitoring, etc.) which have different characteristics in terms of patient mobility, periodicity, and criticality of collected data. There is also scope for more extensive experimentation with truly wearable health monitoring devices used by real patients.

References

1. Crossbow-Technologies, Mica2 and MicaZ motes, URL http://www.xbow.com.
2. V. Schnayder et al. (2005) Sensor Networks for Medical Care, Technical Report TR-08-05, Division of Engineering and Applied Science, Harvard University.
3. Power-Paper, Power Patch Platform, URL http://www.powerpaper.com.
4. D. Culler, D. Estrin, and M. Srivastava (August 2004) Overview of Sensor Networks, *IEEE Computers*, **37(8)**, pp. 41–49.
5. A. Wong, G. Kathiresan, T. Chan, O. Eljamaly, and A. Burdett (September 2007) A 1 V Wireless Transceiver for an Ultra Low Power SoC for Biotelemetry Applications, in *ESSDERC/ESSCIRC*, Munich, Germany.
6. Chipcon, CC2420: 2.4 GHz IEEE 802.15.4 / ZigBee-ready RF Transceiver, URL http://www.chipcon.com.
7. K. Langendoen and G. Halkes (2005) Energy-Efficient Medium Access Control, *Embedded Systems Handbook*, CRC Press.
8. J. Polastre, J. Hill, and D. Culler (November 2004) Versatile Low Power Media Access for Wireless Sensor Networks, in *ACM SenSys*, Baltimore, MD, pp. 95–107.
9. O. Omeni, O. Eljamaly, and A. Burdett (August 2007) Energy Efficient Medium Access Protocol for Wireless Medical Body Area Sensor Networks, in *Proceedings of the IEEE-EMBS Symposium on Medical Devices and Biosensors*, Cambridge, UK, pp. 29–32.

10. S.-L. Wu, Y.-C. Tseng, and J.-P. Sheu (September 2000) Intelligent Medium Access for Mobile Ad Hoc Networks With Busytones and Power Control, *IEEE Journal on Selected Areas in Communications*, **18(9)**, pp. 1647–1657.
11. J.-P. Ebert, B. Stremmel, E. Wiederhold, and A. Wolisz (September 2000) An Energy-Efficient Power Control Approach for WLANs, *Journal of Communications and Network*, **2(3)**, pp. 197–206.
12. J. Monks, V. Bharghavan, and W. Hwu (April 2001) A Power Controlled Multiple Access Protocol for Wireless Packet Networks, in *IEEE Infocom*, Alaska, pp. 219–228.
13. J. Pavon and S. Choi (May 2003) Link Adaptation Strategy for IEEE 802.11 WLAN via Received Signal Strength Measurement, in *IEEE ICC*, Anchorage, AK, pp. 1108–1113.
14. E. -S. Jung and N. Vaidya (January 2005) A Power Controlled MAC Protocol for Ad Hoc Networks, *Wireless Networks*, **11(1–2)**, pp. 55–66.
15. D. Qiao, S. Choi, and K. G. Shin (October 2007) Interference Analysis and Transmit Power Control in IEEE 802.11a/h Wireless LANs, *IEEE/ACM Transactions on Networking*, **15(5)**, pp. 1007–1020.
16. T. ElBatt, S. Krishnamurthy, D. Connors, and S. Dao (June 2000) Power Management for Throughput Enhancement in Wireless Ad Hoc Networks, in *IEEE ICC*, New Orleans, LA, pp. 1506–1513.
17. R. Ramanathan and R. Hain (March 2000) Topology Control of Multihop Wireless Networks Using Transmit Power Adjustment, in *IEEE Infocom*, Tel-Aviv, Israel, pp. 404–413.
18. M. Kubisch, H. Karl, A. Wolisz, et al. (March 2003) Distributed Algorithms for Transmission Power Control in Wireless Sensor Networks, in *IEEE WCNC*, New Orleans, LA.
19. D. Son, B. Krishnamachari, and J. Heidemann (October 2004) Experimental Study of the Effects of Transmission Power Control and Blacklisting in Wireless Sensor Networks, in *IEEE SECON*, Santa Clara, CA, pp. 289–298.
20. O. Chipara, Z. He, G. Xing, Q. Chen, X. Wang, C. Lu, J. Stankovic, and T. Abdelzaher (June 2006) Real-Time Power-Aware Routing in Sensor Networks, in *IEEE IWQoS*, New Haven, CT, pp. 83–92.
21. G. Xing, C. Lu, Y. Zhang, Q. Huang, and R. Pless (May 2005) Minimum Power Configuration in Wireless Sensor Networks, in *ACM MobiHoc*, Urbana-Champaign, IL, USA, pp. 390–401.

22. I. C. Paschalidis, W. Lai, and D. Starobinski (February 2007) Asymptotically Optimal Transmission Policies for Large-Scale Low-Power Wireless Sensor Networks, *IEEE/ACM Transactions on Networking*, **15(1)**, pp. 105–118.
23. L. Correia et al. (October 2005) Transmission Power Control in MAC Protocols for Wireless Sensor Networks, in *ACM/IEEE MSWiM*, Montreal, Canada, pp. 282–289.
24. S. Lin, J. Zhang, G. Zhou, L. Gu, T. He, and J. Stankovic (November 2006) ATPC: Adaptive Transmission Power Control for Wireless Sensor Networks, in *ACM SenSys*, Boulder, CO, pp. 223–236.
25. G. Zhou, T. He, S. Krishnamurthy, and J. Stankovic (June 2004) Impact of Radio Irregularity on Wireless Sensor Networks, in *ACM MobiSys*, Boston, MA, pp. 125–138.
26. J. Zhao and R. Govindan (November 2003) Understanding Packet Delivery Performance in Dense Wireless Sensor Networks, in *ACM SenSys*, Los Angeles, CA.
27. P. S. Hall and Y. Hao (2006) *Antennas and Propagation for Body-Centric Wireless Communications*, Artech House.
28. V. Shrivastava, D. Agrawal, A. Mishra, S. Banerjee, and T. Nadeem (October 2007) Understanding the Limitations of Transmit Power Control for Indoor WLANs, in *ACM/Usenix Internet Measurement Conference (IMC)*, San Diego, CA, pp. 351–364.
29. J. Jeong, D. Culler, and J.-H. Oh (June 2007) Empirical Analysis of Transmission Power Control Algorithms for Wireless Sensor Networks, in *International Conference on Networked Sensing Systems (INSS'07)*, Kanazawa, Japan, pp. 27–34.
30. K. Srinivasan, P. Dutta, A. Tavakoli, and P. Lewis (November 2006) Understanding the Causes of Packet Delivery Success and Failure in Dense Wireless Sensor Networks, in *ACM SenSys*, Boulder, CO, pp. 419–420.
31. K. Srinivasan and P. Lewis (May 2006) RSSI Is Under Appreciated, in *Workshop on Embedded Networked Sensors (EmNets)*, Boston, MA.
32. J. Ryckaert, P. D. Doncker, R. Meys, A. de Le Hoye, and S. Donnay (April 2004) Channel Model for Wireless Communications Around Human Body, *Electronics Letters*, **40(9)**, pp. 543–544.
33. A. Dhamdhere, V. Sivaraman, and A. Burdett (December 2008) Experiments in Adaptive Power Control for Truly Wearable Biomedical Sensor Devices, in *International Workshop on Adaptation in Wireless Sensor Networks (AWSN)*, Sydney, Australia.

34. S. Xiao, A. Dhamdhere, V. Sivaraman, and A. Burdett (January 2009) Transmission Power Control in Body Area Sensor Networks for Healthcare Monitoring, *IEEE Journal on Selected Areas in Communications*, **27(1)**, pp. 37–48.
35. A. Dhamdhere, V. Sivaraman, V. Mathur, and S. Xiao (December 2008) Algorithms for Transmission Power Control in Biomedical Wireless Sensor Networks, in *IEEE Workshop on Wireless Network Algorithms (WiNA)*, Yilan, Taiwan.

Chapter 11

Channel Modeling of Narrowband Body-Centric Wireless Communication Systems

Simon L. Cotton and William G. Scanlon
ECIT Institute, Queen's University Belfast,
Queen's Island, Belfast, United Kingdom
simon.cotton@qub.ac.uk; w.scanlon@qub.ac.uk

The modeling of wireless channels in body-centric communication systems is of paramount importance when designing antennas, protocols, and wireless transceiver hardware. In this chapter, we briefly introduce the concept of *on*-body, *off* -body, and *body*-to-*body* communication channels. We then focus specifically on the modeling of narrowband on-body communication channels, which are an integral part of today's wireless body area networks (WBANs). As well as identifying the factors responsible for shaping fading characteristics in narrowband WBAN systems, we discuss a number of the models commonly used to describe the first- and second-order characteristics of amplitude distribution. The Akaike Information Criterion is introduced as a method of ranking competing channel models, and a worked example is provided to step the reader through the modeling process, as well as providing information on how to simulate the channels. The chapter then concludes with

Wireless Body Area Networks: Technology, Implementation, and Applications
Edited by Mehmet R. Yuce and Jamil Y. Khan

ISBN 978-981-4316-71-2 (Hardcover), ISBN 978-981-4241-57-1 (eBook)
www.panstanford.com

comments on the validity of the analysis presented, especially in the case of non-isotropic signal reception.

11.1 Introduction to Body-Centric Communications

Recent commercial interest in body-centric communications, wireless systems that are designed to operate in close proximity to the human body, has meant that antennas and propagation have become important focal points for research. Study in these areas will help to develop new and innovative solutions and systems geared toward applications in the consumer, medical, and military sectors. For example, requirements for specialist mobile health care have helped to fuel a revolution in body sensor network (BSN) technology, where networks of miniaturized wearable sensors with wireless functionality are attached to the human body and configured to monitor life vital signs such as body temperature, electrocardiography, and motor activity. Other recent popular uses of WBAN technology include data exchange between body-worn cellular devices and wireless headsets, and recreational sports monitoring.

At present, there are two general areas of body-centric communication channel research, broadly categorized as on-body and off-body channels. In on-body channels, such as those found in WBANs, internetworked devices positioned on the human body will typically use over-the-body surface propagation channels to communicate as shown in Fig. 11.1. At ultra-high frequency (UHF) and microwave frequencies, these wireless links are often formed using on-body surface waves and signal components reflected, diffracted, and scattered from other body parts. It should be noted that some links may also utilize free-space propagation (e.g., waist to wrist, etc.) as well as environmental multipath propagation whereby signal transmissions from an on-body node are returned toward the body from the local surroundings. Depending on network topology, some WBAN applications may employ a single body-worn master node for central processing of data and for onward transmission of this information across other wireless networks (e.g., Wi-Fi, Bluetooth, and cellular) using off-body communications

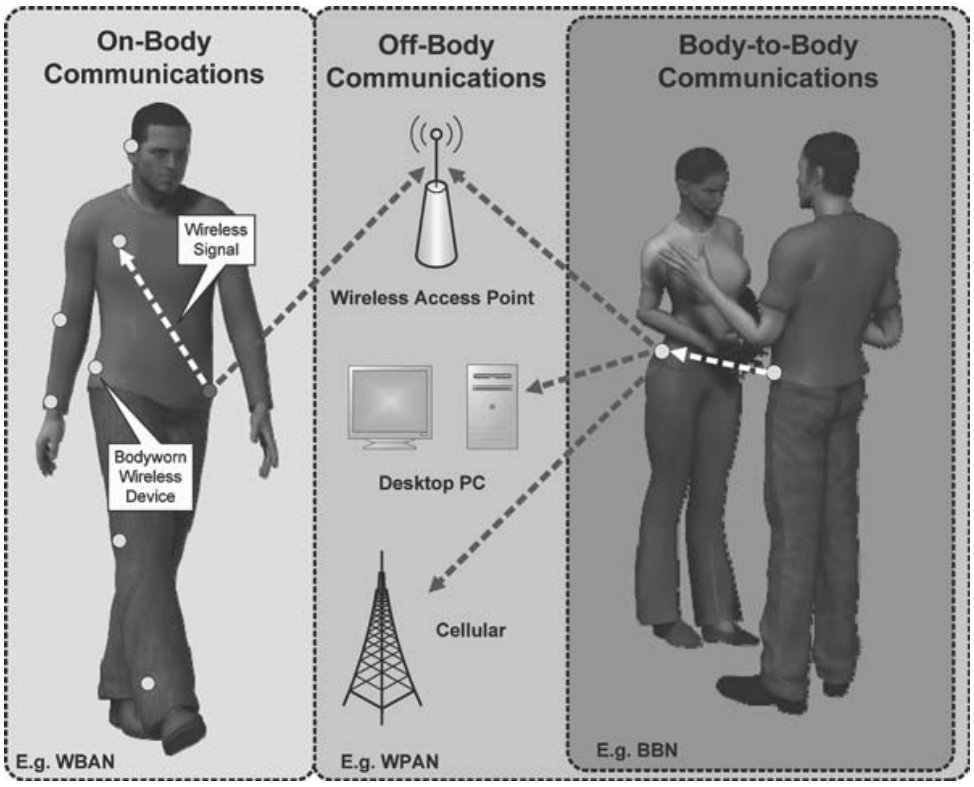

Figure 11.1. Overview of on-body, off-body, and body-to-body communications. See also Color Insert.

(Fig. 11.1). An emerging type of body-centric communications, which also utilizes off-body communications, is body-to-body networking. Body-to-body channels, such as those found in body-to-body networks (BBNs), occur when a wireless device situated on one person is communicating with a wireless device situated on another person.

Much of the current research focus for WBAN applications is centered on the unlicensed industrial, scientific, and medical (ISM) bands at 868 MHz, 915 MHz, and 2.45 GHz. In this chapter, we will focus on narrowband on-body channels at these frequencies. The interested reader is directed to the following references and those contained therein for channel studies on ultra-wideband (UWB) WBANs [1], the use of diversity in WBANs [2–4], and multiple-input multiple-output WBAN systems [5]. Those wishing to learn more about off-body and body-to-body channel characteristics are directed to the following references for narrowband off-body

[6], UWB off-body [7], narrowband and diversity in body-to-body [8] and wideband body-to-body [9]. In the future, millimeter-wave frequencies, such as the world-wide unlicensed spectrum allocations at 60 GHz, will undoubtedly be adopted for high-bandwidth applications. While the propagation characteristics in these bands are difficult with severe blocking by almost all building materials, furniture, and other objects, these same effects can be used to the advantage of the system designer. For example, the limited propagation at millimeter-wave frequencies can be used to mitigate against potential signal-to-interference problems associated with high densities of co-located WBAN users [10]. Other advantages of millimeter-wave operation include the opportunities for device miniaturization and the capacity benefits associated with short-range spatial spectrum reuse.

11.2 Channel Modeling for Wireless Body Area Networks

Wearable wireless devices for WBANs are required to be compact, lightweight, robust, unobtrusive to the user, and usually feature antennas mounted conformal to or in extremely close proximity to the body surface. These requirements must be met while still maintaining a high level of performance, reliability, and efficiency. Clearly, this will introduce design challenges at all layers in the protocol stack, but physical layer characteristics are known to be the limiting factor in the performance of body-centric wireless communication systems.

A key discriminator between body-centric systems and traditional mobile communications is the unique time- and space-varying propagation characteristics encountered. This is in part due to the human body itself, which is an extremely complex operating environment. Body-worn wireless devices are prone to antenna-body interaction effects, which include near-field coupling, radiation pattern distortion, and shifts in antenna impedance, which may degrade the efficiency of the body-worn system and reduce signal reliability [11]. Because the body acts as its own frame of reference, body-centric communication channels are susceptible to time-varying, received signal characteristics, which may range

from quasi-periodic to completely stochastic depending on the person's current physical state. The electromagnetic problem is made even more difficult to analyze as signal reception in body-centric systems may range from isotropic to strongly nonisotropic [12], depending on the degree of body shadowing, attenuation of the on-body creeping wave [13] (if present), and the nature of the local surroundings. Within cluttered multipath environments, inhomogeneous, irregularly spaced dielectric structures, including nearby pedestrians, also cause the signal to undergo reflection, diffraction, scattering, and absorption in varying degrees, creating a spatially distributed electromagnetic field.

To further complicate the analysis of WBAN systems, the magnitude of each of these factors will also be dependent on the geometry of the on-body communication link, i.e., where nodes are positioned on the body relative to one another. This effect is demonstrated by the time series shown in Fig. 11.2, which shows the signal received by nodes positioned on the right ankle and elbow (as shown in Fig. 11.1) while the user was performing walking movements in an anechoic environment. While it may be possible

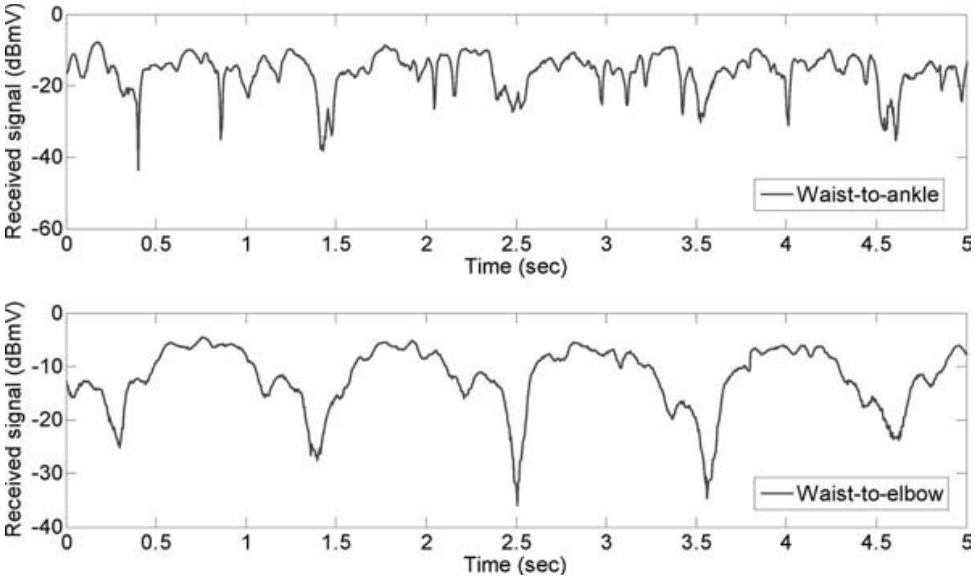

Figure 11.2. Comparison of waist-to-ankle and waist-to-elbow on-body channels at 2.45 GHz while the user was walking within an anechoic environment. The measurement scenario and setup are described in reference [12].